

**THE IMPACT OF THE URBAN ENVIRONMENT  
ON THE ENERGY USED FOR  
COOLING BUILDINGS**

A thesis submitted for the degree of Doctor of Philosophy

by

**Richard Watkins**

**Department of Mechanical Engineering,  
Brunel University**

June 2002

## ABSTRACT

Cities are often warmer than their surroundings, and this can lead to more energy being used to cool buildings. This study looks at one city, London, and assesses the impact of the urban environment on the amount of energy used for air-conditioning.

There are three main strands to the work. First, it was important to determine just how great the variation in air temperature is, and how this varies through time and through the urban space. Eighty measurement stations were established along radiating lines from the centre of London as far as rural areas. These measured the air temperature simultaneously at hourly intervals for over a year. Second, to support the main data acquisition, short-term tests within London looked at specific aspects of the urban environment that affect air temperature: the effects of vegetation in parks, and façade colour in streets. Third, the impact on energy use of the measured temperature variation was then determined by using simulation to model a standard building in different urban contexts.

The mean heat island intensity was found to vary with distance from the centre of London, and with the local degree of urbanization at any given distance. The maximum intensity reached 8°C on occasion but was more usually 1-2°C in the daytime and 3-4°C at night. The proximity of areas of vegetation, such as parks, to a site was associated with cooler daytime temperatures.

The annual cooling load for a standard building at the centre of London was found to be 25% more than at a rural site. However, at the most urban sites over-shadowing reduced the cooling load to 14% more than at a rural site. Heating load decreased towards the centre, but on balance total annual load (for heating and cooling) rose towards the centre to 8.5% more than rural use, and then reduced at the most over-shadowed sites. The balance of the effect of urbanization on heating and cooling load depended on the level of internal gain in the building.

This study makes a significant contribution to understanding the balance of the impact of urban environments on the energy used for cooling and heating buildings.

# CONTENTS

<b>ABSTRACT</b> .....	i
<b>CONTENTS</b> .....	ii
<b>LIST OF FIGURES</b> .....	viii
<b>LIST OF TABLES</b> .....	xii
<b>ACKNOWLEDGEMENTS</b> .....	xiii
<b>CHAPTER 1 Introduction</b> .....	1
1.1 Introduction to the thesis .....	2
1.2 Objectives.....	4
1.3 Original contribution to the body of knowledge .....	4
1.4 Structure of the thesis.....	6
<b>CHAPTER 2 Literature review</b> .....	7
2.1 Introduction .....	8
2.2 The urban heat island .....	9
2.2.1 Historical perspective .....	9
2.2.2 Basic contrasts .....	9
2.2.3 Diurnal pattern.....	10
2.2.4 Seasonal differences .....	11
2.2.5 Spatial differences .....	11
2.2.6 Intensity – characterizing heat islands.....	13
2.2.7 Examples of heat island intensities.....	13
2.2.8 Significance of urban:rural temperature differences .....	15
2.3 The impact of urban development factors affecting the use of cooling energy ...	17
2.3.1 The impact of vegetation .....	17
2.3.2 The impact of albedo .....	23
2.3.3 The impact of urban layout.....	27
2.3.4 The impact of anthropogenic heat .....	32

2.4 The effect of external (or weather) conditions on the efficiency of air conditioning plant .....	35
2.5 Energy demand for cooling in non-domestic buildings in the UK.....	36
2.6 London's heat island .....	39
2.7 Chapter 2 Conclusions.....	41
<b>CHAPTER 3 Measuring the London heat island.....</b>	<b>46</b>
3.1 Measuring the heat island.....	47
3.2 Uncertainties.....	47
3.2.1 Urban temperature measurement.....	47
3.2.2 Reference temperature measurement.....	48
3.2.3 Heat island intensity measurement .....	49
3.3 Field measurement methodology .....	49
3.4 Site selection .....	51
3.4.1 Site surveying .....	51
3.4.2 Local Authority authorization.....	53
3.4.3 Choice of reference site .....	53
3.5 Logging equipment.....	54
3.5.1 Bracket, pole and logger can; design and manufacture .....	54
3.5.1.1 Data loggers.....	54
3.5.1.2 Logger cans .....	54
3.5.1.3 Radiation shielding.....	55
3.5.1.4 Impact of mounting type on temperature .....	56
3.5.1.5 Pole for data collection.....	56
3.5.2 Calibration of loggers .....	57
3.6 Installation.....	57
3.7 Data collection.....	58
3.8 Chapter 3 Conclusions.....	59

<b>CHAPTER 4 The London heat island: measured results for the summers of 1999 and 2000</b> .....	60
4.1 Introduction.....	61
4.2 Intensity.....	61
4.2.1 Mean daily profile.....	61
4.2.2 Frequency distribution.....	63
4.2.3 Percentiles, night and day.....	64
4.2.4 Intensity variation with wind speed.....	66
4.2.5 Intensity variation with temperature.....	67
4.3 Spatial variation.....	69
4.3.1 Variation of mean temperature with distance.....	70
4.3.1.1 All data.....	70
4.3.1.2 Daytime data.....	71
4.3.1.3 Night-time data.....	73
4.3.1.4 Adjusted focus.....	74
4.3.2 Mean thermal centres compared with contours.....	80
4.3.3 Thermal centre movement with wind direction.....	84
4.3.4 Intensity distribution by wind speed.....	84
4.3.5 Mean temperature distribution and prevailing wind directions.....	87
4.4 Chapter 4 Conclusions.....	87
<b>CHAPTER 5 Statistical analysis of factors affecting the London heat island</b> ...	89
5.1 Introduction.....	90
5.2 Banding the data.....	91
5.3 Site categorization.....	92
5.4 Site greenness.....	92
5.5 One-way ANOVA results.....	93
5.6 Upwind greenness.....	99
5.7 Site category and $X_r$ – introduction.....	102
5.8 Site category and $X_r$ – ANOVA results (DAYTIME).....	103
5.9 Site category and $X_r$ – ANOVA results (NIGHT-TIME).....	107
5.10 Anthropogenic impact on temperature.....	112
5.11 Chapter 5 Conclusions.....	114

<b>CHAPTER 6 Field investigation of urban factors – short-term tests</b> .....	116
6.1 Introduction .....	117
6.2 Park test.....	118
6.2.1 Method.....	118
6.2.2 Results.....	119
6.2.2.1 Mean park and streets temperature through time.....	120
6.2.2.2 Variation of temperature with position .....	121
6.2.2.3 Cooling influence beyond the park .....	122
6.3 Gorge tests.....	122
6.3.1 Method.....	123
6.3.2 Results.....	125
6.3.2.1 Variation of surface temperature – overall.....	127
6.3.2.2 Comparison of parallel streets with contrasting façades.....	128
6.3.2.3 Relationship between façade and gorge air temperature.....	129
6.3.2.4 Comparison of air temperature in the street gorges and a park....	132
6.4 Chapter 6 Conclusions.....	133
<b>CHAPTER 7 Modelling the impact of the London heat island</b> .....	136
7.1 Introduction .....	137
7.2 Modelling methodology .....	137
7.2.1 Choice of building .....	138
7.2.1.1 Building description .....	138
7.2.2 Location of modelling sites .....	141
7.2.3 Simulation models .....	143
7.2.3.1 Choice of model .....	143
7.2.3.2 The validity of the predictions of a simulation model .....	143
7.2.3.3 Operation of <i>Tas</i> .....	146
7.2.4 Weather data .....	147
7.2.5 Efficiency.....	148
7.3 Chapter 7 Conclusions.....	149

<b>CHAPTER 8 Modelling results</b> .....	150
8.1 Introduction .....	151
8.2 Pilot modelling results.....	151
8.2.1 Cooling load and site .....	151
8.2.2 Cooling load and mean temperature .....	152
8.2.3 Cooling load and site category.....	153
8.2.4 Cooling load and radial distance.....	154
8.2.5 Conclusions from pilot modelling .....	155
8.3 Main modelling results .....	156
8.3.1 Annual cooling load and site .....	156
8.3.2 Annual cooling load and mean temperature .....	158
8.3.3 Annual cooling load and site category.....	159
8.3.4 Annual cooling load and radial distance.....	159
8.3.5 Annual cooling load and greenness .....	160
8.4 Balance of heating and cooling .....	162
8.4.1 Annual heating and cooling loads.....	162
8.4.2 Annual total load.....	163
8.5 Separation of the temperature and context effects .....	165
8.5.1 The effect of context alone .....	166
8.5.2 The effect of temperature alone.....	169
8.6 Impact on primary energy use .....	171
8.6.1 Conversion to fuel.....	171
8.6.2 Conversion to primary energy .....	172
8.6.3 Primary energy use .....	173
8.7 Impact on carbon dioxide production.....	175
8.7.1 Calculating carbon dioxide production.....	175
8.7.2 Carbon dioxide production .....	175
8.8 Peak energy consumption.....	176
8.8.1 Calculation of peak energy .....	176
8.8.2 Peak energy.....	177
8.9 Conclusions .....	180

<b>CHAPTER 9 Conclusions</b> .....	182
9.1 Main results .....	183
9.2 Conclusions .....	188
9.3 Recommendations for further work .....	191
<b>REFERENCES</b> .....	193
<b>BIBLIOGRAPHY</b> .....	201
<b>APPENDIX 1 – Calibration of loggers</b> .....	210
1.1 Calibration.....	211
1.2 Post-monitoring calibration checks.....	213
<b>APPENDIX 2 – Visualization software</b> .....	215
<b>APPENDIX 3 – Site categorizations of urbanization for all sites</b> .....	218
<b>APPENDIX 4 – Site categorization from aerial photographs</b> .....	220
<b>APPENDIX 5 – Short-term tests</b> .....	223
5.1 Park test pictures .....	224
5.2 Gorge test pictures.....	226
<b>APPENDIX 6 – Building description for model</b> .....	227
6.1 Floor plan .....	228
6.2 Perspective.....	229
6.3 Construction elements .....	229
6.3.1 External walls .....	229
6.3.2 Ground floor .....	230
6.3.3 Intermediate floors.....	230
6.3.4 Roof .....	230
6.3.5 Glazing.....	231
6.4 Internal gains .....	231
6.5 Scheduling.....	232



## LIST OF FIGURES

Figure 2.1	Typical variation of temperature in urban and rural areas.....	10
Figure 2.2	Cross-section of a typical heat island .....	12
Figure 3.1	Illustration of the transects across London .....	51
Figure 3.2	Transect map showing operational stations.....	52
Figure 3.3	<i>Tinytalk</i> logger .....	55
Figure 3.4	Replacement logger cans .....	55
Figure 3.5	Schematic of prototype & picture of a final design of the air temperature measuring device .....	56
Figure 3.6	Number of stations operating, and data collected.....	58
Figure 4.1	London's heat island intensity .....	62
Figure 4.2	Frequency of occurrence of heat island intensities.....	63
Figure 4.3	50 and 90 <sup>th</sup> percentiles for the night-time heat island intensity .....	64
Figure 4.4	50 and 90 <sup>th</sup> percentiles for the daytime heat island intensity .....	65
Figure 4.5	Wind speed and heat island intensity.....	66
Figure 4.6	Urban temperature and heat island intensity.....	68
Figure 4.7	Rural temperature and heat island intensity.....	69
Figure 4.8	The change in mean temperature with distance from London.....	71
Figure 4.9	The change in daytime mean temperature with distance from London .....	72
Figure 4.10	The change in night-time mean temperature with distance from London .....	73
Figure 4.11	The change in mean temperature with distance from London (adjusted focus).....	75
Figure 4.12	The change in daytime mean temperature with distance from London (adjusted focus).....	76
Figure 4.13	The change in night-time mean temperature with distance from London (adjusted focus) .....	77
Figure 4.14	The positions of the optimized origins .....	78
Figure 4.15	Mean temperature Summer (ALL) and effective thermal centre .....	81
Figure 4.16	Mean temperature Summer (DAY) and effective thermal centre .....	82
Figure 4.17	Mean temperature Summer (NIGHT) and effective thermal centre...	83

Figure 4.18	The temperature distribution at 23.50 on 7 August 1999 .....	85
Figure 4.19	The temperature distribution at 23.50 on 8 August 1999 .....	85
Figure 4.20	The intensity distribution on a windy night, at 9pm.....	86
Figure 4.21	The intensity distribution on a relatively calm night, at 9pm.....	86
Figure 4.22	Mean temperature Summer (ALL) and wind direction distribution...	88
Figure 5.1	The distribution of mean daytime local heat island intensity (dT).....	90
Figure 5.2	The distribution of mean night-time local heat island intensity (dT) .	91
Figure 5.3	Mean dT grouped by wind speed (DAYTIME).....	94
Figure 5.4	Mean dT grouped by wind speed (NIGHT-TIME) .....	94
Figure 5.5	Mean dT grouped by solar radiation (DAYTIME).....	94
Figure 5.6	Mean dT grouped by solar radiation (NIGHT-TIME).....	94
Figure 5.7	Mean dT grouped by rainfall (DAYTIME).....	95
Figure 5.8	Mean dT grouped by rainfall (NIGHT-TIME) .....	95
Figure 5.9	Mean dT grouped by cloud cover (DAYTIME).....	96
Figure 5.10	Mean dT grouped by cloud cover (NIGHT-TIME).....	96
Figure 5.11	Mean dT grouped by inner greenness (DAYTIME).....	96
Figure 5.12	Mean dT grouped by inner greenness (NIGHT-TIME).....	97
Figure 5.13	Mean dT grouped by outer greenness (DAYTIME).....	97
Figure 5.14	Mean dT grouped by outer greenness (NIGHT-TIME).....	97
Figure 5.15	Mean dT grouped by radial distance (DAYTIME) .....	98
Figure 5.16	Mean dT grouped by radial distance (NIGHT-TIME) .....	98
Figure 5.17	Mean dT grouped by site category (DAYTIME) .....	98
Figure 5.18	Mean dT grouped by site category (NIGHT-TIME) .....	99
Figure 5.19	Mean dT grouped by inner and outer site greenness (DAY).....	101
Figure 5.20	Mean dT grouped by inner and outer upwind greenness (DAY) .....	101
Figure 5.21	Mean dT when grouped by site category, for $X_r=1$ mile (DAY) .....	104
Figure 5.22	Mean dT when grouped by site category, for $X_r=2$ miles (DAY)....	104
Figure 5.23	Mean dT when grouped by site category, for $X_r=3$ miles (DAY)....	105
Figure 5.24	Mean dT when grouped by site category, for $X_r=4$ miles (DAY)....	105
Figure 5.25	Mean dT when grouped by site category, for $X_r=6$ miles (DAY)....	105
Figure 5.26	Mean dT when grouped by site category, for $X_r=8$ miles (DAY)....	106
Figure 5.27	Mean dT when grouped by site category, for $X_r=10$ miles (DAY)..	106
Figure 5.28	Mean dT when grouped by site category, for $X_r=12$ miles (DAY)..	106
Figure 5.29	Mean dT when grouped by site category, for $X_r=14$ miles (DAY)..	107

Figure 5.30	Mean dT when grouped by site category, for Xr=1 mile (NIGHT) ..	109
Figure 5.31	Mean dT when grouped by site category, for Xr=2 miles (NIGHT).	109
Figure 5.32	Mean dT when grouped by site category, for Xr=3 miles (NIGHT).	109
Figure 5.33	Mean dT when grouped by site category, for Xr=4 miles (NIGHT).	110
Figure 5.34	Mean dT when grouped by site category, for Xr=6 miles (NIGHT).	110
Figure 5.35	Mean dT when grouped by site category, for Xr=8 miles (NIGHT).	110
Figure 5.36	Mean dT when grouped by site category, for Xr=10 miles (NIGHT)	111
Figure 5.37	Mean dT when grouped by site category, for Xr=12 miles (NIGHT)	111
Figure 5.38	Mean dT when grouped by site category, for Xr=14 miles (NIGHT)	111
Figure 5.39	Comparison of the mean temperatures for different mornings at two sites .....	113
Figure 6.1	The positions of the measurement sites at Primrose Hill park .....	119
Figure 6.2	Hourly mean air temperature inside and outside the park .....	121
Figure 6.3	Mean temperature over 13 hours at each site .....	121
Figure 6.4	The positions of the measurement sites around the British Museum	123
Figure 6.5	The variation of gorge surface temperatures .....	126
Figure 6.6	Surface temperature of a re-entrant façade in Montague Place .....	127
Figure 6.7	Surface temperature at ground level & high level different façades .	129
Figure 6.8	Principal dimensions of Montague Street gorge .....	130
Figure 6.9	The hourly variation in gorge air temperature with surface temperature .....	131
Figure 7.1	The ECON 19/3 building as modelled .....	138
Figure 7.2	The ECON 19/3 building in an urban context .....	139
Figure 7.3	A category 7 context modelled in <i>Tas</i> , drawn on a 4m grid .....	140
Figure 7.4	Predicted & measured heating energy used in the double-glazed test room .....	145
Figure 8.1	The cooling load for the ECON 19/3 building in 7 locations .....	152
Figure 8.2	The relationship between mean temperature in August and cooling load .....	153
Figure 8.3	The relationship between site category & cooling load .....	154
Figure 8.4	The relationship between cooling load & distance from the city centre .....	155
Figure 8.5	The annual cooling load for the ECON 19/3 building in 24 locations .....	157

Figure 8.6	The relationship between annual mean temperature & cooling load	158
Figure 8.7	The relationship between site category & annual cooling load.....	159
Figure 8.8	The relationship between annual cooling load & distance from the city.....	160
Figure 8.9	The relationship between annual cooling load & % inner greenness .....	161
Figure 8.10	The relationship between annual cooling load & % outer greenness .....	161
Figure 8.11	The relationship between annual heating & cooling load .....	162
Figure 8.12	Annual heating and cooling load at each site by site category .....	163
Figure 8.13	Annual total load at each site by site category.....	164
Figure 8.14	Annual total load at each site by distance from the city centre .....	164
Figure 8.15	Solar gain received by the ECON 19/3 building for different shading.....	165
Figure 8.16	Percentage change in total annual load with site category & gains..	168
Figure 8.17	Change in total annual load with site category and gains.....	168
Figure 8.18	Percentage change in total annual load with mean temperature and gains.....	170
Figure 8.19	Change in total annual load with mean temperature and gains .....	170
Figure 8.20	Annual primary energy use by distance from the city. BASE gain..	173
Figure 8.21	Annual primary energy use by site category. BASE gain .....	174
Figure 8.22	Change in annual total primary energy use with site category .....	174
Figure 8.23	Change in annual total production of carbon dioxide & site category.....	176
Figure 8.24	Peak electricity demand for cooling and site category .....	178
Figure 8.25	Peak gas demand for heating by site category.....	179
Figure 8.26	Peak gas demand for heating by radial distance.....	179

## LIST OF TABLES

Table 2.1	Reduction in heating days and increase in cooling degree days.....	16
Table 2.2	Albedo of common surfaces .....	23
Table 2.3	Average summer anthropogenic heat release & net radiation input...	32
Table 2.4	Use of electricity for cooling in the service sector .....	37
Table 2.5	Summary of features & evidence of their effects from literature review.....	44
Table 2.6	Quantitative summary of the effects of the urban environment .....	45
Table 3.1	Factors affecting the reference temperature measurement .....	48
Table 4.1	Summary of variance in mean temperature explained by distance of each measurement station from London.....	79
Table 5.1	Banding of data for ANOVA.....	91
Table 5.2	The categorization of the measurement station sites .....	92
Table 5.3	Summary of the effects of various factors on the daytime and night-time temperature differences measured in London .....	93
Table 5.4	Mean summertime temperatures (07.00-12.00) at two main road sites .....	112
Table 6.1	Primrose Hill tests: hourly aligned air temperature data .....	120
Table 6.2	Gorge tests: An example of the surface and air temperature data ....	125
Table 6.3	Reflectivity to daylight of various surfaces in the streets.....	126
Table 6.4	Mean air temperatures over the test period, °C .....	132
Table 7.1	Street contexts used in the model for each site category .....	140
Table 7.2	Criteria used for categorizing sites .....	141
Table 7.3	Pilot modelling: the seven sites and their categorizations .....	142
Table 7.4	Main modelling: the 24 sites and their categorizations .....	142
Table 7.5	Measured and modelled results in a test cell .....	145
Table 8.1	The cooling load for the ECON 19/3 building in 7 locations.....	151
Table 8.2	The annual cooling load for the ECON 19/3 building in 24 locations.....	156
Table 8.3	The internal gains used in the ECON 19/3 building.....	166

## ACKNOWLEDGEMENTS

Such a study as this needs the support, assistance and guidance of many people, and I am very grateful for their generous help – so often given far beyond the call of duty. I would like to thank them all here:

Dr. Maria Kolokotroni has supervised this work from its inception and provided the constant encouragement and insight that has guided it towards its conclusion.

John Palmer of the Building Research Establishment has provided support and guidance throughout the study, and been a strong motivating spirit.

The project was supported by the Building Research Establishment Ltd and I am grateful for access and monitoring equipment without which the project could not have been carried out. At the BRE I would like to thank Dr. Philippa Westbury for her support and inspiration, Dr. Paul Littlefair for his very helpful advice, and Agnes Sheridan, Michael Chandler, David Taylor, David Armitage and Bob Reeboul who were all very helpful.

I'd also like to thank all my fellow student friends from the halcyon days of Mill Hall and Fleming Hall that have at various times provided support, stimulus and a *raison d'être*. My special thanks to Thomas Dewez, Jennifer Turner, Christopher Fullerton, Geneviève Dewez and Suchitra Edussuriya.

This study would not have been possible without the considerable help of the 33 local authorities in London and surrounding areas. Numerous landowners have also been extremely obliging in giving permission for measurement stations to be set up on their land.

# **CHAPTER 1**

## **Introduction**

# **CHAPTER 1 – Introduction**

## **1.1 Introduction to the thesis**

The migration of people into cities and the attendant urbanization of the environment has created both problems and advantages. The distribution of resources (food, water, transport infrastructure, power, employment) is more efficiently achieved in a denser community than in a dispersed one, but the result of the consumption of these resources is a concentration of pollution (waste, waste heat, polluted air) within the city. The resources are of high value and the waste of relatively low value. It is often therefore more difficult to deal with the latter.

The city itself represents a change to the land upon which it was built. To a large extent, a green, living surface is replaced with a synthetic dead one. At the same time, the morphology changes from an open area, whose surfaces absorb and transpire water, to a dry, multi-cavity one that absorbs and stores energy from the sun more strongly. There are many other differences between urban and rural environments and these are discussed in Chapter 2. A net result is that cities tend to be warmer than their surroundings (usually referred to as the urban heat island effect), which in turn leads to a higher demand for energy to cool buildings.

It is difficult to generalize about urban:rural differences as much depends on the particular attributes (climate, topography, etc.) of a location. For example, in Quito, Ecuador, strong heat islands develop in the daytime but are very small at night. In London, the opposite is the case with the largest temperature differences usually developing after sunset. Seasonal differences may also vary for different cities around the world, with maximum differences occurring in the summer, winter, or being independent of season. Overall, the multitude of factors that affect a particular heat island make it difficult to model the climate within the urban areas of a city. Direct measurement is therefore an important method for providing good evidence of the effects of the urban environment on the air temperature around buildings.



This study focuses on one city, London, and assesses the impact of the urban environment on the energy used for cooling buildings. The work concentrates on the increased cooling load associated with warmer temperatures – rather than on the associated reduction in heating load. Energy requirements for air-conditioning are higher than for heating (Landsberg 1981), and research indicates that the elevated urban temperatures impose a net energy penalty for urban areas because of increased cooling requirements. However, the balance of these two effects has been addressed in some detail in Chapter 8.

There are two main elements to the present work. First, it investigates and quantifies the variation in air temperature through time and space. Then, the impact of this is computed by modelling an example building in different environmental contexts. An office building was chosen for this assessment as in the UK, offices are the largest single users of air-conditioning (11 PJ/year) after warehouses (22 PJ/year) (Pout 1998), the latter generally being located away from the city (and heat island) centres. In warmer climates residential air-conditioning is important and studies in other countries have looked at the impact of heat islands on this energy use, but this is not yet appropriate in the UK.

## **1.2 Objectives**

The main objective of the study is to determine the impact of the urban environment on the energy used for cooling. An understanding of the degree to which the urban fabric affects the air temperature around buildings and their energy use provides a basis for deciding on the need for heat island mitigation measures. Associations between different urban site characteristics and temperature help provide guidance on how to achieve such mitigation.

Specific objectives are:

1. Establish a large-scale monitoring array across London to measure the hourly variation of London's urban heat island.
2. Carry out short-term tests in London to examine the effect of vegetation and surface colour on temperature.
3. Model the energy performance of an example building in urban contexts.
4. Determine the factors important to the variation of air temperature and energy used for cooling.
5. Determine the annual balance of the effect of the urban environment on energy used for heating and cooling.

## **1.3 Original contribution to the body of knowledge**

The variation of air temperature in London has been studied before, but not in the level of detail to be described here. The impact of elevated temperatures on cooling energy has also been studied but the majority of work has, understandably, been conducted in warmer climates rather than temperate ones.

The particular facets of the work that are original are listed below:

- A purpose-designed, fixed spaced array of measurement stations was created to measure hourly air temperature at 6m height, simultaneously at 80 sites across a 30 mile diameter circle centred on London.
- The detailed monitoring was long-term, extending to over 12 months to cover winter and two summers.

- The extended data coverage allowed the balance to be determined between the benefit of warmer urban temperatures in the winter and the penalty for cooling in the summer.
- The modelling took into account urban over-shadowing by appropriately reducing the direct solar gain to the example building.

The following publications have resulted from this work:

*Peer-reviewed journals*

1. Watkins, R., J. Palmer, M. Kolokotroni and P. Littlefair (2002). The London heat island – surface and air temperature measurements in a park and street gorges, ASHRAE Transactions, Volume 108, Part 1.
2. Watkins, R., J. Palmer, M. Kolokotroni and P. Littlefair (2002). The London heat island – results from summertime monitoring, Building Services Engineering Research & Technology, to appear.

*Peer-reviewed conferences*

3. Watkins, R., J. Palmer, M. Kolokotroni and P. Littlefair (2002). The balance of the annual heating and cooling demand within the London urban heat island, In Proceedings of Climate change and the built environment, International Conference, CIB Task Group 21, Climate Data for Building Services, Manchester, 8-9 April 2002.

*Professional journal publications and reports*

4. Palmer, J., P. Littlefair, R. Watkins and M. Kolokotroni (2000). Urban heat islands, Building Services Journal, May, pp. 55-56.
5. Graves, H., R. Watkins, P. Westbury and P. Littlefair (2001). Cooling buildings in London - overcoming the heat island, CRC Ltd.

## **1.4 Structure of the thesis**

**Chapter 2** introduces the important differences between urban and rural environments. The basic characteristics of urban heat islands are described and there is a review of the literature on the impact of different environmental factors on cooling energy use. The importance of this study is discussed with reference to the current air-conditioning market and the prospects for its growth.

**Chapter 3** presents the fieldwork carried out to assess the magnitude of the current London heat island. A large array of air temperature measurement stations was set up across the city and the preparation, construction and logistics of this large data acquisition exercise are discussed.

**Chapter 4** looks at the results from the measurement of the London heat island. The temporal and spatial variation of air temperature differences is described.

**Chapter 5** describes the findings of a statistical analysis designed to identify local or site-related factors that are associated with differences in heat island intensity.

**Chapter 6** considers some of the factors that influence local air temperatures: the proximity of green areas; façade colour and form; and the street gorge. These factors have been investigated experimentally through short term measurements in London.

**Chapter 7** introduces the use of simulation modelling. In order to estimate the impact of the variation in temperature profile across London, a thermal simulation model was used to predict the variation in cooling demand. It was necessary to select an air-conditioned building to be notionally positioned at the different sites across the city and subjected to the measured air temperature. The choice and preparation of the model are described.

**Chapter 8** reveals the simulated impact on cooling load and energy consumption of the London heat island. Total and peak cooling load are shown to vary from site to site. The reasons for the variation are investigated. The chapter also considers the impact of the urban environment on the annual balance of heating and cooling.

**Chapter 9** summarizes the main findings of the study and presents the main conclusions.

## **CHAPTER 2**

### **Literature review**

# CHAPTER 2 – Literature review

## 2.1 Introduction

More people are living and working in urban environments than ever before, and the trend has been for this to increase – over half the world’s population were projected to be living in cities by the year 2000 (Yannas 1998). In industrialized countries like the UK, already 80-90% of the population live in urban areas (Taesler 1991). An important implication of this is that the environmental impact of accommodating the needs of the population is concentrated into a relatively small area. This manifests itself most obviously in the close-packing and increased height of buildings, reduced greenscape and - through the concentration of the per capita energy use - the release of large quantities of energy into a dense urban environment.

One net result is that urban air frequently has a different temperature from rural air – sometimes warmer and sometimes cooler – depending on a variety of factors. These urban islands of raised or lowered temperature can be many degrees different from the rural temperature. Higher daytime temperatures in the summer lead to increased energy use for air conditioning. Higher night-time temperatures in the summer reduce the potential for passive cooling.

This literature review gives an introduction to heat islands and then focuses on the effects they have on energy used for cooling buildings. The review is in five sections:

- a review of the characteristics of urban heat islands
- a review of the impact of different environmental factors on cooling energy use
- a note on air conditioning efficiency parameters
- a description of the energy demand for cooling in the UK
- the London heat island

## **2.2 The urban heat island**

### **2.2.1 Historical perspective**

It has long been recognized that urban environments are different from rural ones. Greater air pollution is easily sensed, and it has been noted (Landsberg 1981) that Seneca, writing some 2000 years ago, recorded the contrast he felt between the “heavy air of Rome with its stench from smoky chimneys...” and the air outside Rome.

Less obvious is the way urban temperatures differ from those outside a city. In 1820, Luke Howard published an analysis of ten years of daily temperature measurements which established the existence of London’s heat island, i.e. an area of elevated temperature (Landsberg 1981). These data show a mean 24 hour temperature about 0.6°C higher for July and 1.2°C higher in November in the city than in the country. Howard also noted [in Fahrenheit] that, “Night is 3.70° warmer and day 0.34° cooler in the city than in the country. Thus the latter has 4° more variation.” [2.05°C, 0.18°C and 2.22°C respectively]. Howard’s data provide the first scientific evidence for two important characteristics of temperature anomalies, viz. diurnal and seasonal variation of the size of the anomaly, and possible change in sign of the anomaly (a heat island to a cool island).

Other investigations of temperature followed, particularly by Emilien Renou in Paris in 1868, who wrote that the urban:rural difference “is about 1°C, at the same elevation”. In 1927, Wilhelm Schmidt started using instrumented motor vehicles to facilitate the mapping of isopleths of meteorological parameters (Landsberg 1981). Since that time, and particularly after 1945 with much rebuilding of cities, numerous studies have been made of urban climates.

### **2.2.2 Basic contrasts**

There are many ways in which an urban environment differs from a rural one (Barry 1968; Oke 1982). Some of the parameters are listed below:

- Albedo
- Evaporation and transpiration
- Porosity

- Shade
- Wind speed
- Anthropogenic heat release
- Energy collection and retention efficiency
- Heat capacity
- Air pollution

The combination of these factors determines the way in which heat is absorbed, stored, released and dispersed in the urban environment. The net effect is to differentiate the urban temperature from that of the rural environment. However, this difference is not constant; it varies through time and space.

### 2.2.3 Diurnal pattern

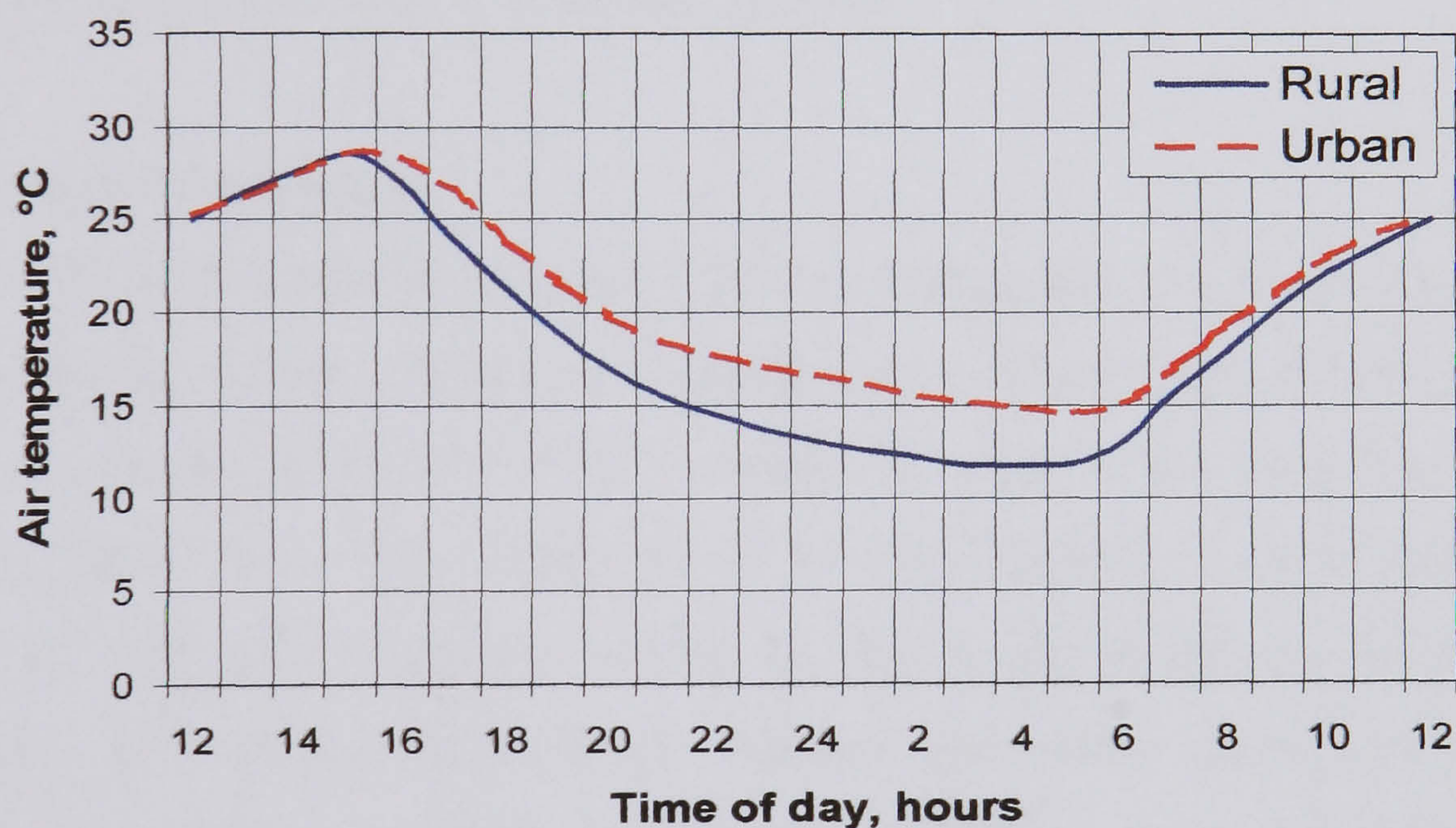


Figure 2.1: Typical variation of temperature in urban and rural areas  
(Based on Oke (Oke 1987))

Typically, urban environments are warmer before sunrise than rural ones, because they have cooled down overnight at a slower rate (primarily through having greater heat capacity and reduced radiative cooling efficiency). As the sun rises, solar energy is used to evaporate dew in rural areas, but starts heating up urban fabric immediately. When the dew has evaporated, the rural surfaces start to warm up more rapidly than the urban ones, because of their lower heat capacity. As the day progresses the urban and rural temperatures converge and cross over in summer months when anthropogenic heat release in cities is small. At, or before sunset, the



rural surfaces rapidly cool, the rate reducing as dew is formed and latent heat released. The city cools more slowly and the urban to rural temperature difference starts to rise. The time of maximum heat island “intensity” varies, but is usually a few hours after sunset, i.e. the nocturnal intensity is greater than the daytime intensity. See Figure 2.1.

This temporal scheme is not universally applicable. Because of the multiplicity of factors that contribute to urban temperature, it is often the case that particular cities have unique characteristics. For example, on average, the daytime temperature in London’s central parks is in fact warmer than around the city for two thirds of the time (Chandler 1976). In Quito, Ecuador, strong heat islands develop in the daytime, but are very small or non-existent at night-time (Hannel 1976). In the city of Athens, exceptionally high daytime temperature elevations have been recorded compared to the surrounding countryside (Santamouris 1998).

#### **2.2.4 Seasonal differences**

The intensity of the urban heat island effect is often greater in the summer than in the winter, because of the greater solar energy input, lower wind speeds, and urban surfaces remaining dry (there is less rainfall) for more of the time than in winter. However, again this is not always true. “In many cities of western Europe, heat islands are strongest in summer whilst in central and northern Europe there is, apparently, little difference between summer and winter intensities. In several Japanese cities, maximum heat island intensities occur in winter” (Chandler 1968).

#### **2.2.5 Spatial differences**

Heat islands are not uniform across a city and their profile, in idealized form, has been described by Oke (Oke 1987). See Figure 2.2. A radial transect across a large city reveals the horizontal profile of air temperature. On clear, calm evenings after sunset, the temperature rises sharply at the outskirts of the urban area (a cliff), broadly plateaus across suburbia, rising more gently to the peak of the urban core. The presence of surface vegetation (e.g. parks), or water (e.g. lakes) along the transect produces a local reduction in temperature.

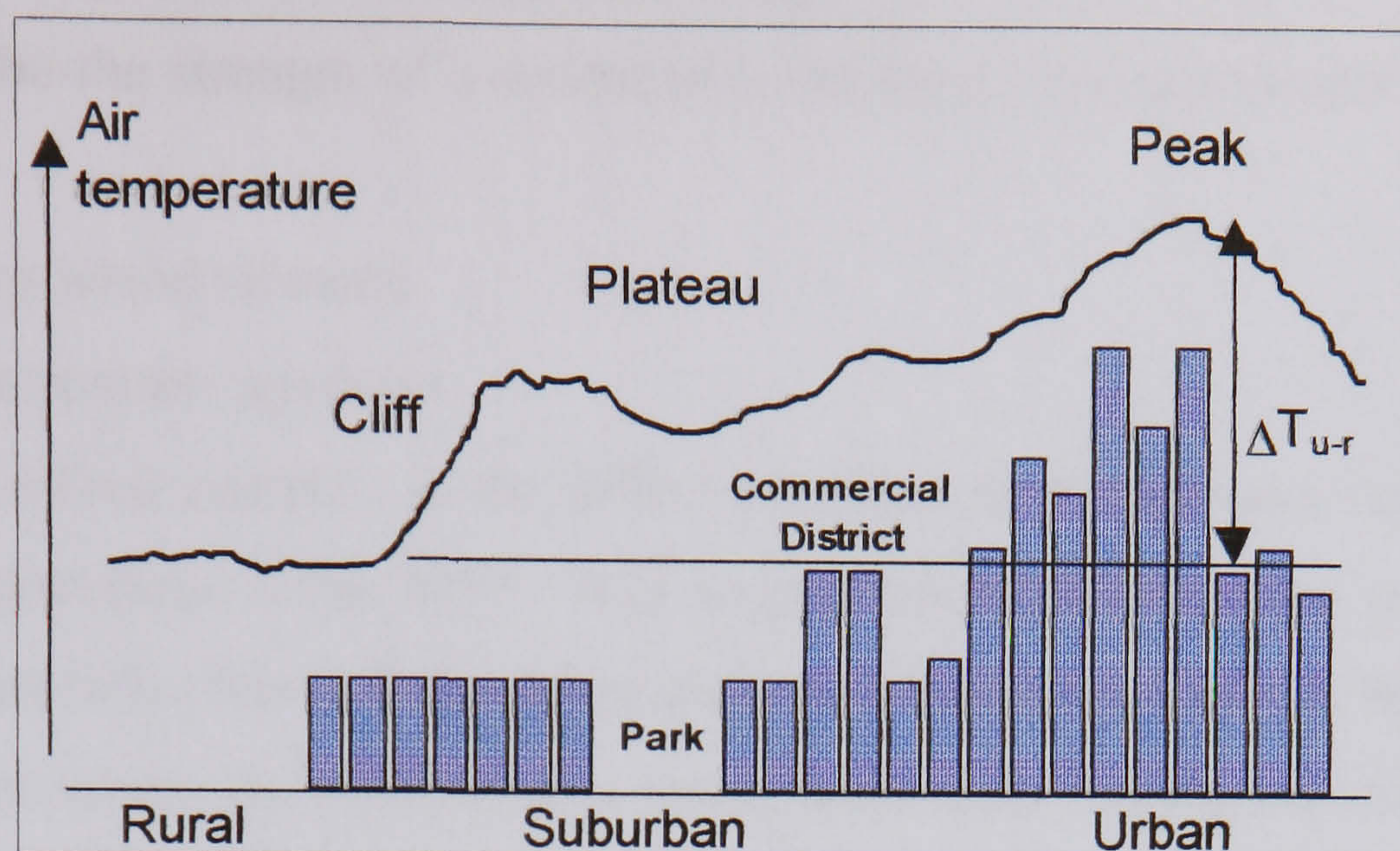


Figure 2.2. Cross-section of a typical heat island (after Oke (Oke 1987))

In practice, this simple visual concept of a sea of cooler isotherms encircling a warmer urban centre belies the reality that temperature “anomalies” are frequently short-range and short-term. An urban environment is more usually made up of a patchwork of micro-climates (Unwin 1980) with pockets of warmer areas scattered across it. There may be a broad temperature change from urban centre to rural area, but this hides the thermal detail to be seen en route.

The position of the peak temperature of a heat island is not static, but is likely on average to be at the urban core. However, on individual days it will shift downwind if the wind is blowing. Moreover, certain cities, e.g. Montreal, have a *reduction* in heat island intensity at the geographical centre rather than a peak, because of some temperature lowering feature, e.g. a lake (Oke 1987). In some cases there may be more than one recognizable peak.

At wind speeds above about 5m/s, temperatures across urban environments become more homogeneous and heat islands may not be discernible.

### **2.2.6 Intensity – characterizing heat islands**

To describe the strength of a temperature anomaly, two descriptors are commonly used:

- the heat island intensity
- the temperature gradient

The heat island intensity is the difference between background rural and highest urban temperatures (Oke 1973). It is usually calculated from the maximum urban temperature to be found in the urban area, and a rural one taken to be representative of what the urban site's temperature would have been, had the environment not been urbanized. Heat island intensity takes no account of the lateral separation of the two chosen sites, or the area of the temperature anomaly, and therefore the term is something of a misnomer. Some of the problems or uncertainties in determining heat island intensity are discussed later.

Temperature gradients, measured (in °C/km) over a relatively short distance, provide an indication of the strength of local heat island effects which can be compared more satisfactorily with data from other heat island experiments. Particularly steep gradients, up to 4°C/km (Oke 1987), are common at the outer edge of heat islands.

In studies of heat islands three values of heat island intensity are often quoted:

- maximum temperatures
- minimum temperatures
- mean temperatures

The first two indicators are of particular interest and correspond to the daytime and nocturnal heat island intensities respectively.

### **2.2.7 Examples of heat island intensities**

There have been numerous field studies of the urban heat island effect with data collected over a few days to a few years. The most common way of summarizing such studies is to quote the maximum heat island intensity measured. This is an important indicator of urban:rural differences, but requires qualifying in order to assess the heat island's significance in relation to energy use for cooling or heating. Time of day and year are particularly important, and ideally either a frequency

distribution of the heat island intensity or an intensity time integral for selected time-bands. Few studies provide this level of detail, at least in published form.

Rosenfeld makes the general statement: “On a clear summer afternoon, the air temperature in a typical city is about 2.5°C hotter than the surrounding area.” (Rosenfeld 1995)

Givoni (Givoni 1998) states that: “In large cities it is common to observe nocturnal air temperatures 3-5°C higher than the surrounding areas, and, in extreme cases, higher by up to 8°C. During the daytime hours, however, this difference in air temperature between the city and its surrounding area is smaller – only about 1-2 degrees – and often the daytime temperatures in a densely built-up area are lower than in the open country.”

Whether the daytime urban temperature is higher or lower than the more rural one, and how this difference compares with the nocturnal difference depends on many factors. The wide variation is illustrated by the following examples.

In Athens, using hourly data, daytime air temperatures have been reported to be between 4 and 15°C warmer in the summer than outside the city (Santamouris 1998). The highest urban:rural temperature differences were measured in the central areas at the bottom of street gorges subject to high volumes of traffic.

In Barcelona, using monthly means of daily maxima, compared with its airport on the outskirts the city was found to be cooler in the daytime in every month of the year, by up to 0.6°C, apart from in January and December when it was 0.2°C warmer. Average monthly differences for the minima indicated a nocturnal heat island of between 2.5-3.3°C. On 10% of days the urban minima were at least 5°C warmer than at the airport, with an absolute maximum difference of about 7-8°C (Moreno-Garcia 1994).

In Mexico City, using hourly data, daytime (11.00-15.00) temperatures were found to be between 3-5°C warmer on average than a rural site during the summer, and up to 6.5°C warmer on occasion (Jauregui 1997).

In Dallas, using transect data taken in the summer, the central core of the city (with very tall buildings) was found to be cooler at the time of maximum temperature, by about 1°C, than the area just outside it (Ludwig 1968).

It is clear that the extent to which urban temperatures differ from those of their surroundings varies considerably. In the daytime, urban areas may be warmer or cooler than further out. The examples above show urban areas to be from about 1°C cooler to 15°C warmer. It is difficult to generalize about summertime urban:rural differences as so much depends on the particular attributes (climate, topography, etc.) of a particular location.

### **2.2.8 Significance of urban:rural temperature differences**

The energy used for cooling buildings has not always been considered relevant to studies of the overall effects of heat islands (Brundl 1984). However, in the context of global warming there is increasing interest. This is particularly so in relation to climates with hot summers, or where air-conditioning is used extensively. It is also the case that air-conditioning use is increasing, with changing affluence or expectation.

Exceptionally hot periods can lead to a dramatic rise in the demand for air conditioning. After a series of heat waves over three years in Greece, it has been reported that annual purchases of air conditioning units increased eight times in the following years (Santamouris 1990).

Air-conditioning provision is increasing in cars. This probably increases fuel consumption, although it may be offset by a reduction in drag in the absence of a sunroof.

Although heat islands increase the use of energy for cooling in the summer, they reduce the energy required for heating buildings in winter. Landsberg compared heating and cooling degree days for several American cities and at airports outside them (Landsberg 1981). An amended table, incorporating errata, was published more

recently by Taha (Taha 1997). See Table 2.1. Note that the heating and cooling degree days are both calculated to a base of 18.3°C.

Table 2.1: Comparison of the reduction in heating days and increase in cooling degree days for urban areas compared to airport sites. Differences are shown as a percentage of the airport site. From Taha (Taha 1997) modified after Landsberg (Landsberg 1981).

Location	Heating degree-days			Cooling degree-days		
	Urban	Airport	% Diff.	Urban	Airport	% Diff.
Los Angeles	384	562	-32	368	191	+92
Washington DC	1300	1370	-6	440	361	+21
St.Louis	1384	1466	-6	510	459	+11
New York	1496	1600	-7	333	268	+24
Baltimore	1266	1459	-14	464	344	+35
Seattle	2493	2881	-13	111	72	+54
Detroit	3460	3556	-3	416	366	+14
Chicago	3371	3609	-7	463	372	+24
Denver	3058	3342	-8	416	350	+19

Energy requirements for air-conditioning are higher than for heating (Landsberg 1981), and both Landsberg and Taha concluded that the elevation of urban temperatures imposes a net energy penalty for urban areas because of increased cooling requirements.

## **2.3 The impact of urban development factors affecting the use of cooling energy**

Many factors affect the use of energy for cooling, but here only those essentially external to a building are considered. Thus, parameters such as the thermal characteristics of the building envelope, internal gains and the scheduling of the use of a building are not considered.

### **2.3.1 The impact of vegetation**

The presence of plants can reduce temperatures inside buildings in a number of ways and their effects can be felt *locally* or *at a distance* (the effects of planting around or on a building, or of local parks, etc.). Meir (Meier 1991) reviewed the literature on the local effects of landscaping on air-conditioning energy use. Four main ways in which vegetation can reduce the heat gain to buildings were identified:

- through shading of windows from solar gain
- through providing additional thermal resistance
- by reducing infiltration, and
- through latent heat transfer.

The relative importance of these methods “depends on the vegetation being used, the climate, the building structure and orientation. Direct gain is typically considered the factor most influenced by landscaping, and has therefore received the most attention. In humid locations, however, infiltrating air can be responsible for as much as 50% of the peak cooling load” (Meier 1991).

Barry et al (Barry and Chorley 1968) described the conditions inside a sea-level temperate forest. The mean annual temperature is 0.6°C lower than the surrounding open country, mean monthly differences may reach 2.2°C in summer, and on hot summer days the difference may exceed 2.8°C.

Hildebrandt et al (Hildebrandt 1998) described an initiative to plant 500,000 shade trees adjacent to dwellings in Sacramento to reduce cooling energy demand. An uncertainty identified was determining the net effect of trees in winter months. The bare deciduous trees chosen for the planting programme still block 30% of the sunlight that would otherwise reach building surfaces. However, they also act as

wind breaks, reducing infiltration and conductive losses. The net effect was assumed to be neutral.

It is important to appreciate that providing increased vegetation can bring unwanted effects. Taha et al (Taha 1997) notes that trees emit volatile organic compounds which can increase ozone production. Low emitting species are recommended, although the lowering of temperature associated with the introduction of trees may lower the production of VOCs by existing vegetation.

### *Experimental work*

Many studies have measured, in various ways, the effect of green areas on temperature, and humidity, but usually without explicitly relating this to the use of air-conditioning. Wilmers (Wilmers 1990/91) reports that only “large” green areas have measurable effects on the surroundings, and that the extent of the effect is limited to 100-500m distance because of convection. Temperature differences up to 2°C are normally measured.

Landsberg reported that “Large, coherent park areas have quite a measurable influence. In warm summer nights the parks are cool, even in the densely built-up area” (Landsberg 1981).

Meier’s review (Meier 1991) reported data on cooling effects almost exclusively from hot, including arid, climates, and they may not be applicable to temperate ones. The one study conducted in a temperate climate measured the change in the use of electricity for air-conditioning in mobile homes moved from a forested site to an open one. There was an 80% reduction in electricity use when the homes were located in the forested area.

Saito et al (Saito 1990/91) measured temperatures in Kumamoto City in the summer and found that the temperature difference at 15.00 between a park (150x150m) and the surrounding area was about 2.5°C. The cooling effect outside the park was reported to extend for only 20m.



Taha et al (Taha 1991) measured the air temperature along a transect through a 307m x 150m wooded area in California. The tree canopy was 5m high and covered 25% of the ground area. The wood stood in a rural area, surrounded mostly by dry fields, but was itself well-watered. Measurements were taken in October during a warm period. On average, the canopy was 2°C cooler during the day than the bare and open surrounding fields. At times this temperature depression reached 6°C.

The transect revealed that temperature reduced very quickly inside the canopy, achieving two thirds of the total depression in just the first 5m. This suggested that small belts of trees upwind of a building cluster may be effective in reducing cooling energy, and that extensive planting is not necessary. Reduced wind speeds inside and downwind of the wood were also recorded, suggesting that trees could be positioned advantageously to reduce infiltration of warmer external air into buildings.

The cooling effects of wooded areas were also examined in Israel (Shashua-Bar 2000) at 11 different urban sites, on calm summer days. The bulk of the cooling effect was attributed to shading. At noon, this averaged about 2.5°C with an additional 0.5°C of cooling attributed to other effects. Cooler air was noticeable up to about 100m from the sites.

Jauregui measured the effects of a large park (500 ha) in Mexico City (Jauregui 1991). The park contains fountains, artificial lakes, trees, as well as museums and playgrounds. In an early morning transect, at the time of largest temperature contrast, the park was found to be 2-3°C cooler than adjacent areas and the cooling effect extended about 2km (about the width of the park) beyond the park's boundary.

Satellite pictures taken in the infra-red spectrum can reveal the effect of vegetation on surface temperature, and, with less certainty, air temperature. For example, Kawashima (Kawashima 1990/91) looked at the Tokyo metropolis. However, the technique requires a knowledge of the variation of surface emissivity across the terrain being viewed and this information is often not available. The surface temperature of vegetated areas may also be of limited value as passing air is cooled beneath the (porous) canopy of vegetation as well as at its upper surface.

Nevertheless, Kawashima et al (Kawashima 2000), using representative values of emissivity based on standard surface category, first found a good correlation (coefficient of determination varying from 0.76-0.85, n=68) between surface and air temperature. Then the residual scatter about the regression line was investigated and found to be partly related to the density of vegetation at each station's site. Higher levels of vegetation were always associated with lower temperatures. This study looked at a wide area in Japan (200x200km) comparing satellite-derived surface temperatures with air temperatures from 68 automatic stations. The data related to winter nights.

The effects of shading by trees were investigated by Rosenfeld et al (Rosenfeld, Akbari et al. 1995); also reported in Akbari et al (Akbari 1997). They measured a 30-35% drop in air-conditioning energy use in two houses in Sacramento when shading from trees was provided. Measurements were made as the houses were found, and with shade trees (from 2.4-6m high) placed in front of the south and south west facing walls, and in front of the air-conditioners' condensing units. The absolute saving was about 4-5 kWh/day over the summer season for each house. Peak power for air-conditioning use was reduced by 0.6-0.8kW, representing savings of 27% and 42% (for the two houses).

Relatively cool air over parkland may be advected to adjacent areas and help to cool buildings. This has been investigated in West Tokyo (Vu 1998). Observations on a continuously sunny August day showed that the air temperature in a 0.6km<sup>2</sup> park at midday, measured at 1.2m height, was more than 2°C lower than that measured in the surrounding commercial and parking areas at the same height. It was also determined that the park could reduce the noon air temperature in an adjacent commercial area by up to 1.5°C over an area of about 0.5km<sup>2</sup>. A modelling exercise suggested that this temperature reduction would reduce electricity for air-conditioning by almost 15% over a one hour period (1pm-2pm), a saving of about 4000kWh.

Upmanis and Chen (Upmanis 1999) looked at the temperature differences between a park and the surrounding urban area in Göteborg, Sweden. A maximum difference of

5.9°C was observed over a distance of about 1.5 km. This was comparable to the maximum mean value (over 14km) of the urban heat island intensity for the city. 86% of the spatial variation in air temperature was accounted for by the distance from the park border.

Cooler air in a park may instigate a local circulation of air with movement out of the park in all directions at low level and into the surrounding urban area, with an area of calm in the middle of the park. This air-flow has been observed by Eliasson and Upmanis (Eliasson 2000), particularly in a park in Copenhagen, at night in calm conditions. The cooler air moved up to 200m from the borders of the park. This local flow could be helpful in cooling buildings overnight. However, the flow could also be in opposition to a general urban heat island circulation within a city, and act to reduce advection.

#### *Modelling work*

Honjo et al (Honjo 1990/91) used numerical modelling to estimate the effect of air flowing across a green area and on to an urban area again, in summer conditions in Japan. The green area was 100-400m long and set at 4°C cooler than the upstream and downstream urban areas. The study suggested that air temperature, at a height of 2m, could be reduced by about half the difference in the urban:green surface temperatures, i.e. 2°C. Moreover, the results suggested that a succession of relatively small green areas is more effective in cooling air than a single large one.

Modelling exercises on the cooling effects of air flowing over and through vegetation (Sánchez 1996; Tévar 1996; Sánchez 1998) gave air temperature reductions around 0.5-2.5°C for a ground to air difference of 20°C, and wind speeds from 1-4m/s. The cooling effect reduced with height above the vegetation, declining to zero at about 5m above. A lack of published data on the internal temperature profiles of forests was reported (a uniform value was used instead).

Rosenfeld et al (Rosenfeld 1998) have assessed the effect of planting shade trees (and increasing albedo by replacing roof and paving with lighter materials) in the Los Angeles basin. Modelling results indicated that the cooling effect on ambient air

temperature of planting 11 million trees would be 1.5°C at 2pm. This was calculated to lead to a reduction in peak power demand of 0.8 GW.

Raeissi and Taheri (Raeissi 1999) modelled the effect of shading alone from trees on a house in the climate of Shiraz, Iran. Because of the high angle of the summer sun at this latitude trees were considered inappropriate for south facing façades, and little direct radiation falls on north facing ones. For east and west facing façades the predicted reduction in daily cooling load was around 5% for each face, 10% in total. This ignores the temperature reduction associated with trees. The authors state that it is very difficult to predict the cooling effect of trees in a particular location, but that measurements in a heavy tree-populated area of Shiraz showed the air to be 2-5°C cooler than an area where very few trees were found. Using a reduction of 3°C, it was estimated that cooling load would be reduced by 40% for combined shade and cooling from trees planted on east and west sides of a house.

Evaporative cooling can also take place at artificial surfaces. Asaeda and Ca (Asaeda 2000) modelled and measured the surface temperature of paving material. It was found that the highest temperatures were associated with both impermeable, or highly porous materials, the latter drying out very quickly. Paving with a small pore size absorbs and holds rainwater (and also through capillary attraction draws water from below) and the evaporation of this results in a lower surface temperature. In measurements, a special small pore size ceramic pavement was about 10°C lower, at 43°C, than highly porous paving on a hot summer day at noon, when the air temperature was 35°C, wind speed 4m/s and relative humidity 43%.

### 2.3.2 The impact of albedo

Albedo is the proportion of total solar radiation reflected by a surface compared to the total incident upon it. It includes the reflection of infra-red and ultra-violet radiation and is thus different, generally less, than a surface's reflectance of light. Areas with lower albedo surfaces will absorb more solar energy and introduce more energy into their local environment.

Urban surfaces are composed of very different materials from rural ones and the albedo can be quite different. Most urban surfaces lie between 0.10 and 0.30 with most observational values lying around 0.15 (Atkinson 1985). Particularly high albedo (0.30-0.45) in urbanized areas can be found in North Africa (Taha 1997).

Although in general, the albedo of urban areas is considered to be lower than rural areas, it can be seen from Table 2.2 that it depends on the particular composition of the surface mosaic, e.g. coniferous forests have a lower albedo than brick. Table 2.2 lists the albedo of a variety of common surfaces.

Table 2.2: Albedo of common surfaces. [From: Taha (Taha 1988), Oke (Oke 1987) and Chandler & Gregory (Chandler and Gregory 1976) quoting various sources]

Surface	Albedo 0=100% absorption 1=100% reflection
Water (large altitude)	0.09
Desert	0.34-0.52
Wet sand	0.16
Black earth, dry	0.14
Black earth, moist	0.08
Grey earth, dry	0.25-30
Grey earth, moist	0.10-12
Bare, dry soil	0.30
Dry grass wizened by sun	0.19
Green grass	0.26
Wet grass	0.33-0.37
Heather wasteland	0.10
Deciduous forest	0.10-0.20
Coniferous forest	0.05-0.15
Crops	0.15-0.25
Concrete	0.10-0.35
Brick	0.20-0.35
Streets	0.14
Asphalt pavement	0.10

### *Experimental work*

The geometry of a surface has been shown to affect albedo. Using hardware models, Aida (Aida 1982) showed that the form of streets and buildings reduced the albedo by 20% when compared to that observed over a flat surface of the same material. Street gorges provide multiple opportunities for solar absorption and the concrete models showed that the greater the building height to street width ratio, i.e. as street gorges become street canyons, the lower the effective albedo.

If the albedo of a building surface (a roof or wall) is lowered, the increased heat gain directly increases the cooling energy use and peak demand of the building (Rosenfeld et al. 1995). Rosenfeld measured the impact of raising albedo on summertime air-conditioning energy use in three dwellings in Sacramento. Changing the albedo of a house roof from 0.18 (as found) to 0.73 reduced the seasonal cooling energy by 80% (264kWh/year) (Akbari et al. 1997). Tests on two bungalows showed that a white-roofed one (albedo of 0.68) used 51% of the cooling energy used by a bungalow with a metal roof and yellow south east wall.

Asaeda et al (Asaeda 1996) compared the surface temperature, heat storage and emission of infra-red radiation of different paving material in Japan in the summer. Asphalt surfaces became hotter than concrete or bare soil and, in peak conditions, emitted an extra  $150\text{W}/\text{m}^2$  of infra-red radiation and 200W sensible transport compared to a bare soil surface. The upward infra-red radiation was rapidly absorbed in the first 200m of the lower atmosphere, thereby warming it. It was concluded that paving of low albedo and low thermal conductivity may encourage hotter daytime temperatures, and paving with low albedo and high conductivity may (because more heat is stored beneath the surface) promote warmer nights. Water permeable paving material was recommended to encourage latent heat cooling.

Simpson et al (Simpson 1997) tested the effect of different roof coatings on surface temperature and air-conditioning energy. Quarter scale models placed in rock landscapes were monitored in the summer of 1990. White roofs (of albedo 0.75) were up to 20°C cooler than grey (of albedo 0.30), or silver ones (of albedo 0.50), and up to 30°C cooler than brown roofs (of albedo 0.10). The temperature of the silver and grey roofs was similar, despite quite different albedos, and this appears to

be because the silver roof had a lower emissivity. Reductions in total and peak air-conditioning load of about 28% and 18% respectively were measured for uninsulated brown-roofed models compared to white ones.

Parker et al (Parker 1997) measured the saving in air-conditioning energy from albedo changes in nine residential homes in Florida between 1991 and 1994. Roofs were whitened at midsummer. Comparing the energy consumption for similar weather periods before and after modification, the mean saving was 19% (ranging from 2-43%). Peak load savings (coincident with utility peak loads at 5-6pm) averaged 22%. The cooling energy reductions were reported to be influenced by other factors, such as roof insulation, air-conditioner sizing and air duct system location.

#### *Modelling work*

Taha et al (Taha, Akbari et al. 1988) simulated the effect of increasing the albedo of a single storey house in Sacramento. The house was modelled with increased albedo of the roof and walls. The results for a four day period in early July showed that the peak cooling power and cooling energy reduced linearly with increasing albedo, in the proportion of 1.6kW (and 23kWh) for every unit increase in albedo. The effect was more pronounced for uninsulated houses.

Rosenfeld et al (Rosenfeld, Akbari et al. 1995) simulated the effects of raising albedos in the Los Angeles Basin. Urban areas were identified and average albedo increased from 0.13 to 0.26. The results showed that central Los Angeles became 2-4°C cooler at midday in the summertime. This would have a significant impact on air-conditioning energy use. Peak power consumption for Los Angeles would be reduced by 0.6-1.2GW.

Akbari et al (Akbari 1999) extended the investigation to predict the energy saving from more reflective roofs to the whole of the United States. Existing roof albedo was assessed from digitized aerial photographs in three US states, and ranged from 0.19 to 0.25, although there was some uncertainty as to whether these were rather high. (New, white, asphalt roof shingles had been measured and found to have an albedo of 0.25. Other colours were lower.) The building energy simulation

programme DOE-2 was used to predict the change in energy consumption (heating and cooling) when the roof albedo was increased from 0.25 to 0.55 (residential buildings) and to 0.70 (flat-roof commercial buildings). The annual electricity savings for cooling were 6-17% (residential) and 3-9% (offices and stores).



### **2.3.3 The impact of urban layout**

“Cities consist of intersecting lines of high heat capacity mineral blocks, of various heights, rising into the air from a bed of tarmacadam dotted with grass. The blocks “roughen” the surface and increase turbulence, and the street gorges between channel the air (Barry and Chorley 1968).”

The effect of the urban environment is generally to lower wind speeds in the city compared to surrounding rural areas. However, there is a diurnal pattern. Daytime urban wind speeds are considerably lower than rural ones, but at night-time the greater turbulence over the city allows horizontal momentum from faster moving air at high level to be transferred to city level, making urban wind speeds greater than in rural areas. This urban:rural difference increases with wind speed and it is therefore less noticeable in summer, when wind speeds are generally less in temperate latitudes (Barry and Chorley 1968; Oke 1987).

Wide streets and other open spaces encourage the flow of air and improve the opportunity for ventilation in the inner parts of a city. Conversely, the more closely spaced, and the taller buildings are, the lower the ground velocity of the air compared to the wind speed in the open (Givoni 1971). A grid system of street layout encourages the penetration of air deep into the city (Golany 1996).

Slower air speeds in urban areas reduce the dispersion of heat generated in the city, and the effects of inadequate ventilation can be critical [particularly for pollutant dispersal] during calm periods with high radiation (Barlag 1991). One mechanism for air movement into a city is through country winds, i.e. air moving into a city to replace city air rising because of buoyancy.

The proportion of the sky that a building can “see” determines, to a large degree, its radiation balance. The lower surfaces of tall buildings alongside narrow streets, i.e. in street gorges, see the least sky. These buildings receive more long-wave radiation from buildings opposite, and cool at a slower rate, than buildings in the open.

Both theory and measurements indicate (Givoni 1998) that it may be possible to plan cities so that daytime air temperatures near the ground are lower than rural ones, particularly in hot-dry regions. A densely built area, with high albedo, would reflect more radiation back to the sky than a rural one.

Although there is a peak temperature effect at the centre of a city, this is to a large extent the result of numerous small pockets of temperature anomaly. However, building density and energy use intensity do often increase at the centre of a city. Böhm (Böhm 1998) analysed temperature data for Vienna (a city of falling population) and found that the urban heat island and its trend cannot be taken as constant for the whole city and concluded that the urban effect is more strongly influenced by the local surroundings of a particular site than by the city as a whole.

Givoni (Givoni 1998) states that exhaust heat from air-conditioning systems of high-rise buildings may sometimes be rejected at ground level exacerbating the discomfort of pedestrians in summer. High level condensers, or heat rejection, have a minimum impact on ground-level air temperature.

#### *Experimental work*

Barlag et al (Barlag and Kuttler 1991) encircled the city of Bochum with anemometers and determined from 18 months' data that more than 10% of urban ventilation was due to air flowing into the town from the country because of the urban:rural temperature difference. These country breezes coincided with the presence of high-intensity urban heat islands. It was suggested that country breezes would have been more prevalent had the urban geometry been more appropriate. The authors recommended that urban layouts should include straight, smooth, little-polluted, open aisles to the city centre with air passing over cooling surfaces en route.

Country breezes induced by city heat islands can be enhanced, in hot regions according to Givoni (Givoni 1998), by leaving open stretches, avenues, parks, etc., leading air from areas of low density towards the centres of high density. Such winds have been observed in Mexico City, and in London (Chandler and Gregory 1976).

Eliasson (Eliasson 1994) measured temperatures in and outside Göteborg in Sweden for three years to determine the effect of urban geometry on temperature. Using 1.5 year's averaged data: in the summer, five hours before sunset, both the urban gorge and open urban area temperature were about 1.8°C warmer than the rural temperatures. As sunset approached, both urban-rural differences increased, but with the gorge reaching a maximum difference (5.5°C) 1.5 hours after sunset and the open urban space (5°C) 1.5 hours before sunset. Moreover, the gorge temperature declined only slightly during the night (to 5°C) at 04.00 hours, whilst the open urban site dropped to about 3.5°C.

Haeger-Eugensson and Holmer (Haeger-Eugensson 1999), also in Göteborg, looked at the way air advects into a city at night because of the temperature difference. This urban heat island circulation, once set in motion, acts as a regulator of the heat island intensity. A higher city temperature would increase the flow of cooler air into the city from outside and moderate the heat island. The authors found the circulation was not constant, but pulsed, as Chandler also observed for the margins of London (Chandler 1965).

Measurements (Santamouris 1997) in street gorges in Athens found that air temperature is not very dependent on their orientation, and is mainly controlled by air movement. However, the surface or film temperature of the sides of the gorge is strongly influenced by orientation.

Street width affects city air temperatures (Givoni 1998). Measurements in Seville in the summer (over one day), revealed that although the lowest air temperature (at one metre) was found in a wide street at the beginning of the day, by 3pm, the "coolest" place (30°C) was in a narrow alley (height to width ratio of 1:10) and was some 4-6°C cooler than the wide street.

The population size of a town or city has been used as a surrogate for urban mass and is quite well related to the maximum heat island intensity there. However, urban form varies and different regression lines are found for European cities compared with North American ones. Recently, work by Torok et al (Torok 2001) suggested

that Australian towns are likely to have smaller maximum heat island intensities than either the US or Europe, for the same population size. This is probably because of the predominantly single storey buildings and wide streets in Australian towns.

### *Modelling work*

A numerical simulation by Sakakibara (Sakakibara 1996) compared the thermal environment of an infinitely large, flat, open surface (a car park) with a set of “street canyons”. Both areas had asphalt top layers of the same thickness. The results showed that the urban canyon absorbed more heat in the daytime and released more at night than the car park. The larger the ratio of wall height to street width the greater the heat storage effect. The results were presented as evidence that urban geometry results in heat islands.

Mills (Mills 1997) considered the efficiency of building configurations in relation to heating and cooling requirements over the whole year. Solar exposure and sky view factor were compared for different building spacings and for different latitudes. Simulation modelling suggested that tall structures at close spacings were most efficient at equatorial latitudes in limiting solar receipt and increasing longwave emission. At latitude 60°, maximizing heat gain and minimizing heat loss during winter were said to be the dominant concern, with more open spacing of buildings recommended.

In hot climates (e.g. Rome, Athens), thermal comfort outdoors in summer is improved if shade is provided. Experimental and modelling work (Santamouris and Littlefair 1997) looking at street gorges, found that self-shading of street surfaces from the sun was maximized if their orientation was North-South. Over the six summer months, sunlight penetrated to the ground for less than half the time it did in an East-West orientated street. The obvious need for East-West communication leads to a recommended compromise using an urban layout with a grid of streets orientated at 45° off the NSEW compass points. Such a street layout is to be found in Santa Cruz, Seville (Coronel 1997).

The impact of estate form on total sensible heat flux from urban surfaces (building walls and roof, and ground) was simulated by Hoyano et al (Hoyano 1999). In a large

housing estate in Japan different configurations of residential blocks (staggered layouts, square, diagonal, etc.) were identified and modelled. Total sensible heat flux on a clear summer's day at noon varied from around  $130 \text{ W/m}^2$  for parallel, diagonal and interspersed blocks, to  $300 \text{ W/m}^2$  for square layouts (i.e. 17-40% of incoming solar radiation). This was attributed to both the materials used (albedo) and the spatial form of the blocks.

In Hong Kong, Lam (Lam 2000) considered that ignoring the over-shadowing of office buildings would over-estimate the annual cooling load. This was confirmed using site surveys of average over-shadowing of façades at different times of the year and subsequent modelling using the building simulation model DOE-2.1E. However, the over-estimation was just 2%. This is probably due to the high angle of the sun in the main cooling season at this latitude, reaching  $88^\circ$  at noon in July, when even unshaded south-facing façades receive very little solar radiation.

### 2.3.4 The impact of anthropogenic heat

Heat is released into the urban environment from a variety of combustion processes (transport, space and water heating, and cooling, etc.) and the use of electricity for lighting and other uses. In winter this anthropogenic heat flux can match or exceed the solar flux, but this is not usually so in summer, except perhaps in city centres.

McGoldrick and Harrison (Harrison 1984) determined the heat fluxes from the transport, service, industry and the domestic sectors for each kilometre square of Greater London. The results showed a wide range of heat release from less than  $1\text{W/m}^2$  to more than  $300\text{W/m}^2$ . This latter high flux led to the conclusion that in the core of London (an area 5 km across), the artificial heat flux exceeds the natural flux for every month of the year.

Ichinose et al (Ichinose 1999) made a similar appraisal of anthropogenic heat release for Tokyo. This city has many tall buildings and these can lead to very high anthropogenic heat release densities when considering plan area. The highest energy release density,  $1.590\text{ kW/m}^2$ , was found for a 1 km square in winter containing an office and hotel each approximately 50 stories high. Hot water supply contributes half of this and it is not clear whether the loss to sewers and away from the urban area is included or not. In the summertime, energy consumption was estimated to reach  $120\text{ W/m}^2$  in central Tokyo. The influence of this was reported to be relatively small.

Table 2.3 compares summertime anthropogenic heat release from all sources within three cities with the net radiation (short and longwave) received from the sky.

Table 2.3: Average summertime anthropogenic heat release compared to net radiation input. Source: Oke (Oke 1987) quoting various sources

Urban area	Year	Anthropogenic heat, $\text{W/m}^2$	Net solar heat, $\text{W/m}^2$
Montréal (45°N)	1961	57	92
Budapest (47°N)	1970	32	100
Vancouver (49°N)	1970	15	107

These data refer to total energy use, and do not shed light on the effect of the way in which the heat is released into the environment. Clearly, heat discharged into streets from, for example, traffic and air-conditioning plant will have an immediate and direct effect on urban temperature. Heat discharged from tall chimneys may have a much smaller effect (Oke 1988).

Anthropogenic heat release is more significant when both the per capita energy use and the population density are high. It can be seen from Table 2.3 that anthropogenic heat can be of a similar magnitude to solar radiation and it is therefore to be expected that there should be a measurable temperature rise in urban areas that is attributable to it.

#### *Experimental work*

Measurements in Athens (Santamouris, 1998) found higher air temperatures (by 2°C) in a street with a large amount of traffic than in a parallel pedestrianized one with the same form. However, the warmer street also had a lower albedo and therefore the temperature difference was attributed to a combination of this with anthropogenic heat.

#### *Modelling work*

Taha (Taha 1997) reports that meteorological simulations showed that anthropogenic heat emissions in a large city core can create a heat island of 2-3°C during the day and night. The modelling also showed that the effect on temperatures from suburban anthropogenic heat release was negligible.

Stanhill and Kalma (Stanhill 1995) looked at Hong Kong and the opposing effects of increasing anthropogenic heat release with the one-third reduction in solar radiation due to pollution there over a 35 year period. They concluded that the effects balanced each other and that mean air temperature difference had not changed. The large reduction in solar radiation was partly attributed to the increased optical depth of clouds due to anthropogenic aerosol.

Residential air conditioning is often provided by mounting units on the façades of buildings. In narrow streets, the heat rejected can cause an appreciable rise in air

temperature. Papadopoulos (Papadopoulos 2001) used CFD and Suncode (a building simulation model) iteratively to determine this temperature rise for a narrow street gorge in Athens. For the air near to where the air-conditioning units were operating the temperature rose by about 6°C because of the heat rejection from the units. This was a local phenomenon but would be significant because it would affect the efficiency of the cooling.

This compares with the results of a study in Hong Kong (Chow 2000) looking at the possible adverse effects of positioning air-conditioning units within a re-entrant part of the façade of a high-rise (82m) residential block. Using CFD and an energy model, it was found that the mean performance of a hundred units arranged up the side of a high rise block was lower than in an open position. The mean COP was reduced by about 10-15% in windy conditions (4m/s at 10m height), and 15-25% under no-wind conditions. The effects of solar radiation on the wall surfaces where the units were mounted was considered negligible.



## 2.4 The effect of external (or weather) conditions on the efficiency of air conditioning plant

Section 2.2 has described the basic characteristics of urban heat islands, while section 2.3 has reviewed the current knowledge of the more important parameters that contribute to their existence and effect on the use of cooling energy for buildings. This section considers briefly how the external conditions affect the efficiency of cooling plant which may lead to a further change in the use of cooling energy, while the next section investigates the energy demand in non-domestic buildings in the UK.

A common indicator of the efficiency of refrigeration plant is the coefficient of performance (COP). This is defined as the ratio of the energy extracted by chilling plant to the energy input to drive the plant (Jones 1967).

For an idealized system operating under a Carnot cycle, the COP may be written as a function of the absolute temperature of the evaporator (where chilling takes place) and the condenser (where heat is rejected). Thus:

$$COP = \frac{T_{evaporator}}{(T_{condenser} - T_{evaporator})}$$

Real plant do not operate at a COP as high as given by this simplified formula for a variety of reasons. However, this relationship underlies chilling plant performance and it shows that as the temperature at which heat has to be rejected increases the performance decreases (in the limit, asymptotically to zero).

Milbank (Milbank 1989) estimated that a temperature rise of 4.5°C would more than double the average full-load usage of a typical air-conditioning system, while reducing refrigeration efficiency by about 10%.

The actual sensitivity of any particular building and its plant to changes in external temperature is complex. For example, if air-conditioning plant has been over-specified, it may normally operate at part-load for much of the time, and at poor efficiency. An increase in external temperature may improve the plant usage and offset the underlying decrease in efficiency of the refrigeration cycle.

In some buildings, the relative humidity is controlled as well as temperature by using humidification/dehumidification plant. Relative humidity is often lower in cities than outside them, but this is because of the often higher urban temperatures (Lee 1991). However, there are absolute differences, and in a comparison of a central London weather station and Gatwick airport (40km to the south), Lee found that central London air is, on average, less humid than rural air during the day in summer. The difference was about 1mb of vapour pressure, or of the order of 10% drier.

## **2.5 Energy demand for cooling in non-domestic buildings in the UK**

### *Energy data*

Domestic buildings are not considered in this study as residential air-conditioning in the UK is not significant. If air temperatures rise or the incidence of exceptionally hot summers increases this might change in the future, but currently the climate is not extreme enough, given the internal gains in domestic buildings, to encourage cooling plant in dwellings. Non-domestic use of air-conditioning is well-established, although the majority of UK non-domestic stock is not air-conditioned.

In considering the significance of the use of energy for cooling, it is important to appreciate four things:

- current cooling energy use as a proportion of total energy use
- current degree of saturation of the market for air-conditioning
- the reasons for the current demand for air-conditioning
- the prospects for the future demand for air-conditioning

### *Current energy use*

Looking at the whole of the service sector, 48PJ of electricity were used in 1994 for cooling (Pout, Moss et al. 1998). This is 17% of the sector's total electricity use, or 6% of its total delivered energy use. Use of electricity for cooling by sub-sector is shown in Table 2.4.

Table 2.4: Use of electricity for cooling in the service sector (Pout, Moss et al. 1998)

(Individual values are rounded for clarity)

Sub-sector	Electricity used for cooling, PJ delivered
Warehouses	22
<b>Commercial offices</b>	<b>11</b>
Retail	4
Communications & Transport	3
Sports & Entertainment	3
Health	3
Hotels & Catering	2
Other	1
Government	0.3
Education	0.1
<b>Total</b>	<b>48</b>

Apart from warehouses, which tend to be sited outside the central heat island areas, commercial offices use the most significant amount of energy on air conditioning, viz. 11 PJ/year. This level of energy use was regarded as a “small, but significant and growing end use in buildings” in 1988 (Herring 1988).

#### *Current degree of saturation*

Averaged over the UK, approximately a quarter of non-domestic floor space has full or partial air-conditioning (Haselden 1997). Of this area, about 80% has full air-conditioning and 20% partial air-conditioning (Pout, Moss et al. 1998).

The occurrence of air-conditioning is not uniform, and “the larger and more modern a property, the greater the likelihood that it will have full air-conditioning.” (Pout, Moss et al. 1998)

#### *Reasons for the current demand*

Willis et al (Willis 1995) argue that the main reasons for the growth in air-conditioning are institutional, i.e. financiers demand it, and based on unrealistically high internal gain assumptions. They stated:

“The major reason behind the huge growth in air-conditioned office space in the last 10-15 years [1980-1995] is that the rental premium for this space is greater than the extra cost involved in construction. This has been compounded by corporate

standards and the fear of overheating from equipment gains, which were vastly overestimated in the 1980s.”

and later:

“Institutional lenders tend to work to a formula when deciding upon funding for a building. This typically includes air-conditioning with control to  $21\pm 1^{\circ}\text{C}$ , lighting to 500-600 lux, and floor power loadings of  $25\text{W}/\text{m}^2$  to  $100\text{W}/\text{m}^2$ . These criteria are fairly inflexible. The allowance for floor loading encourages the use of air-conditioning when the probable actual small power loads would not merit it.”

Parry et al (Parry 1991) report that “office users now attach a premium to air-conditioned buildings, with the result that air-conditioning is now virtually standard in new constructions in urban areas, especially in London and the South East”.

Other reasons are: a desire to maximize the use of urban land (the use of deep plan buildings), and to be able to control indoor air quality better in a polluted environment.

#### *Prospects for the future*

“In 1992 over half of all air conditioning plant sales were for new buildings, and less than 20% was for the replacement market. If this situation continues, the amount of air conditioned floor area in the stock will increase substantially in the future.” (Pout, Moss et al. 1998) Financial incentives appear to promote the incorporation of air-conditioning into new office space, and are likely to continue to do so unless opposing disincentives appear.

There are also climatic forces that may encourage greater use of air-conditioning. The mean annual temperature at Heathrow airport has increased by  $1.3^{\circ}\text{C}$  from 1960 to 1995 (Levermore 1997). To reflect this rise in temperatures, and a predicted continuing increase at  $0.2^{\circ}\text{C}/\text{decade}$ , the CIBSE have prepared a revised weather data file for use by buildings services’ engineers (Levermore and Keeble 1997). The publication of this guide in 2002 (CIBSE 2002) perhaps gives extra emphasis to the reality of general warming and the need to plan ahead for its impact on energy use.

The frequency of occurrence of particularly warm seasons and years is also expected to increase.

“During the decade 2050-60, a hot summer (such as that in 1995) will change from being a one-in-90 year event to a one-in-three year event. Similarly, a very mild winter (such as in 1988-89) will change from being a one-in-30 year event to become a one-in-five year event.” (Levermore and Keeble 1997)

Periods of exceptionally hot weather can have profound effects on people’s attitude to the need or desire for air-conditioning, perhaps particularly in the (currently insignificant) domestic market in the UK. In Athens, an eight-fold increase in annual sales of air-conditioning units followed a succession of heat waves in 1987-89 (Tsinonis 1993).

In the year 2010 the rising temperatures are predicted to lead to a decrease in annual total heating degree days by 14%, and an increase in cooling degree hours by 124%, at Heathrow (Levermore and Keeble 1997).

## **2.6 London’s heat island**

Sections 2.3 and 2.3 have referred to heat island observations in cities around the world. This section reports in more detail on data available for London.

Since Howard first identified the heat island, the urban climate of London has been extensively studied, and was described in detail in *The Climate of London* (Chandler 1965). Meteorological Office temperature data for London (1931-60), reported by Chandler, show the annual mean temperature of central London to have been 1.4°C warmer than the surrounding country. Daytime maximum temperatures (represented by the annual mean of the daily maxima) were 0.9°C warmer. Monthly mean differences showed central London to be warmer by about 1.6°C in the summertime and 1.2°C in the winter. Maxima (mean of values) were lower, about 1°C warmer in the summertime and 0.7°C in the winter.

An indication of the distribution of the temperature anomalies is also described by Chandler, for the period 1951-60 (Chandler 1965). Central London (at Kensington)

in the daytime in the summer was warmer than Wisley (rural) by between 0.6 and 2.2°C for about 60% of the time and cooler by between 1.7 to 0.0°C for about 40% of the time. Only for about 1% of the time did the urban temperature exceed that of the rural site by between 2.8 and 4.4°C in the daytime.

The heat island effect in London varies from year to year. For example, the years 1933-34 were milder and calmer than the preceding years and drier than those which followed. These years were notable for having particularly strong heat islands (Chandler 1964). Of perhaps longer term importance is the trend identified by Lee (Lee 1992), looking at the temperature difference between St.James's Park and Wisley for the period 1962-89. He found that daytime heat islands have decreased over time, from about 0.5°C down to 0.25°C in the summer, and night-time heat islands have increased by about 0.5°C. (These are mean values.)

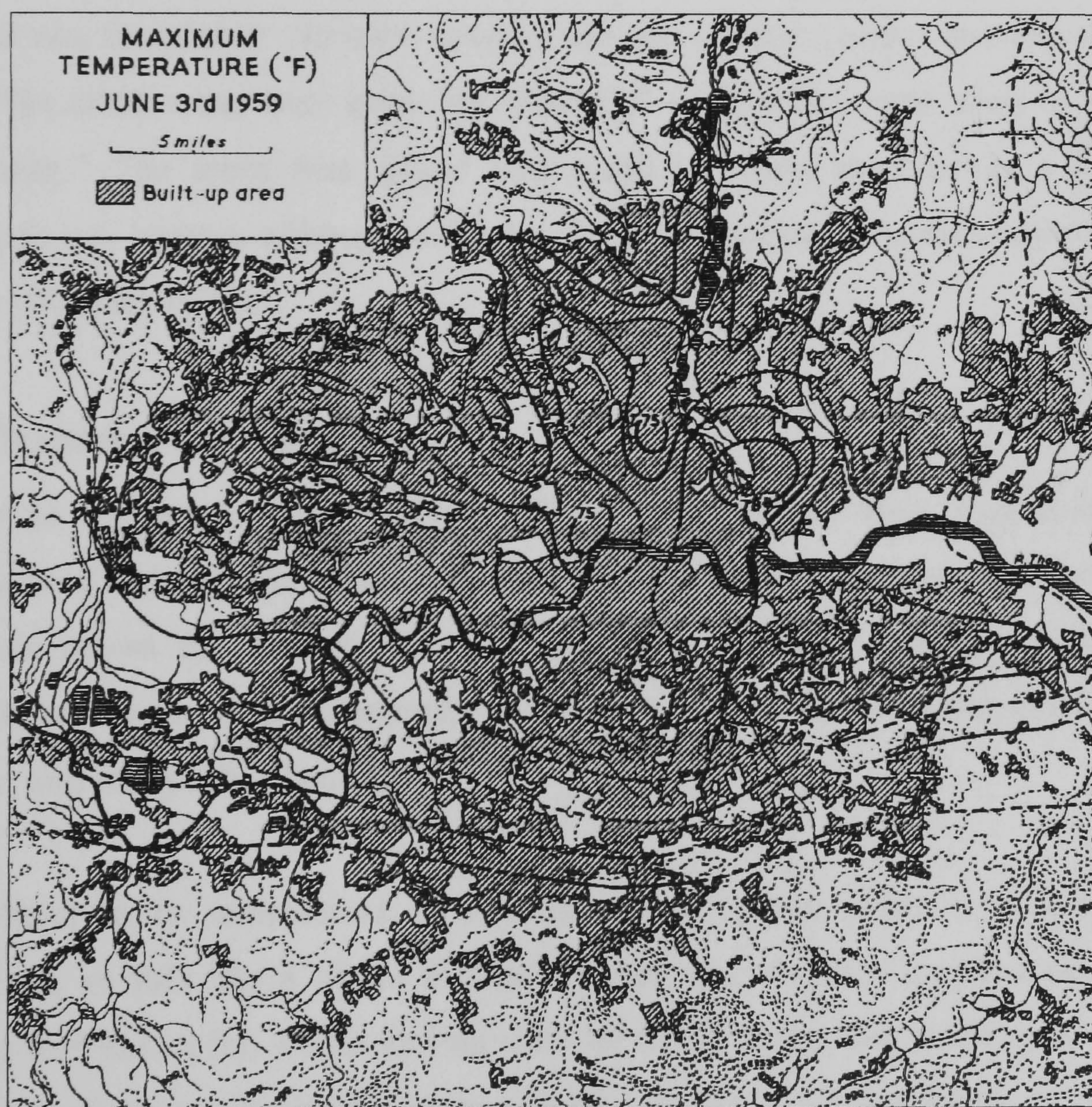


Figure 2.3: Contours of the temperatures on a sunny summer day in London from *London's Urban Climate* (Chandler 1962)

Figure 2.3 shows the maximum temperatures reached in and around London on a sunny summer day in 1959. The wind speed, measured at Heathrow airport, was about 4.5m/s, temperatures are shown in Fahrenheit, and estimated isotherms are dotted (Chandler 1962). The main heat island was not in the centre, but to the east of the city near West Ham and Bromley. This is due to the direction of the wind, which after early morning was from the south west. It can be seen that in Regent's Park the maximum temperature reached was significantly cooler, about 1.5°C less, than the temperature of 25.5°C (78°F) at the heat island's maximum intensity.

An analysis of the London heat island in the exceptionally hot and dry summer of 1976 concluded that the magnitude of the daytime heat island was no greater that year than normal (Lyall 1977). Weather data from several sites in and around London were used, and isotherms drawn. On the hottest day of the year, 26 June 1976, it was found that: "In most country districts outside London maxima were 34-35°C. The urban areas were generally about 2°C warmer than rural areas to the north and south." The main heat island was displaced west, possibly as a result of afternoon sea breezes although evidence for such breezes has been reported to be scarce (Wheeler 1997).

## **2.7 Chapter 2 Conclusions**

The urban environment modifies microclimate in numerous ways. In general, urban climates are warmer and less windy than in rural areas. However, a review of the literature shows that the modification to urban climates is highly variable, and depends on the particular topography, regional wind speeds, urban morphology, time of year, and many other factors.

The alteration to temperature – the urban heat island effect – is particularly important, as this has a direct impact on fuel use: warmer temperatures reduce heating fuel use in the winter and increase air conditioning use in the summer. The literature reveals a considerable body of work describing the conditions in cities and how they differ from their more rural surroundings. Measurement work around

buildings, scale models, and simulation work have all been used to try and identify the processes that govern the microclimatic changes.

The bulk of the literature describes studies directed at understanding urban climatology, rather than the impact the urban heat island effect has on energy consumption in buildings. Nevertheless, from the many studies that do consider the energy implications, a number of key findings emerge.

The urban heat island intensity (difference between urban and rural temperatures) varies from a few degrees to over ten degrees centigrade. This intensity varies through the day (usually greatest at night), through the year, and from season to season. It also varies from place to place within an urban area, and can be negative. Maximum heat island intensities are associated with clear skies, and low wind speeds (less than 5m/s).

The most important reasons for urban areas being warmer are the increased effective albedo (solar energy absorption) of the urban fabric, and the greater ability of the latter to store absorbed heat. In rural areas, heat absorbed by vegetation is used to evaporate water and dispersed. In urban areas, the scope for this conversion to latent heat is much reduced.

Anthropogenic heat (from traffic, buildings, etc.) is a significant but not generally dominant reason for urban areas being warmer. However, in certain high density areas, anthropogenic heat release matches or exceeds the solar input for much, if not the whole of the year.

The key ways of mitigating the impact of the urban heat island effect on the use of cooling energy are to:

- Increase the albedo of the urban fabric
- Increase the amount of vegetation, particularly trees



Modelling studies have indicated that if the average albedo of the urban areas in the Los Angeles Basin were increased from 0.13 to 0.26, central Los Angeles would become 2-4°C cooler at midday in the summer. Peak power consumption would reduce by 0.6-1.2 GW.

A combined measurement and modelling study (in Tokyo) has shown that cool air advected from a park to a commercial area had a potential of reducing air-conditioning by almost 15% between 1pm-2pm.

The effects and impacts of the different factors involved in forming the urban heat island are summarized in Tables 2.5 and 2.6, together with some of the main evidence.

Table 2.5: Summary of features and evidence of their effects from literature review

FEATURE	IMPACT M=measured S=modelled or simulated
<p><b>Vegetation</b></p> <ul style="list-style-type: none"> <li>• Shades buildings, windows and people from direct solar radiation.</li> <li>• Evapotranspiration cools air</li> <li>• Reduces air speed and thus: reduces infiltration and increases thermal resistance</li> <li>• Emits VOCs</li> </ul>	<p>Large green areas are cooler by up to 2-3°C. (M)</p> <p>The temperature inside a sea-level temperate forest was cooler by 0.6°C over a year, and up to 2.8°C on hot summer days. (M)</p> <p>Cooling in a park extended outside by between 20m (small park, Kumamoto City) and 2000m (very large park, Mexico City). (M)</p> <p>Mobile homes moved from an open site to a forested one showed an 80% reduction in electricity use for air-conditioning. (M)</p> <p>Shading of houses and their air-conditioners by trees reduced air-conditioning electricity use by 30-35%, or 4-5kWh/day/house over the summer. Peak power was reduced by 0.6-0.8kW (27-42%). (M)</p> <p>Cool air advected from a park to a commercial area had a potential of reducing air-conditioning by almost 15% between 1pm-2pm, a saving of 4000kWh. (M &amp; S)</p>
<p><b>Albedo</b></p> <ul style="list-style-type: none"> <li>• Affects the absorption of solar radiation</li> </ul>	<p>Lightening a surface (raising the albedo) reduces heat gain and air-conditioning energy used.</p> <p>Changing the albedo of a house roof in Sacramento from 0.18 (as found) to 0.73 reduced the seasonal cooling energy by 80% (264 kWh/year). (M)</p> <p>In the summer, white roofs (albedo 0.75) were up to 20°C cooler than grey ones (albedo 0.30), and up to 30°C cooler than brown ones (albedo 0.10). (M, using models)</p> <p>Air-conditioning energy for 9 houses in Florida reduced by 19% (2-43%) after the roofs were whitened. Peak load savings averaged 22%. (M)</p> <p>If the average albedo of the urban areas in the Los Angeles Basin were increased from 0.13 to 0.26, central Los Angeles would become 2-4°C cooler at midday in the summer. Peak power consumption would reduce by 0.6-1.2 GW. (S)</p>
<p><b>Urban layout</b></p> <ul style="list-style-type: none"> <li>• Reduces wind speeds and dispersion of pollution</li> <li>• Reduces radiative cooling of building surfaces</li> <li>• Affects albedo</li> </ul>	<p>In Göteborg, summertime temperatures 5 hours before sunset were 1.8°C warmer (in an urban gorge, and an open urban area) than in a rural area. (M)</p> <p>In Seville, in the summer, the lowest temperature was found in a wide street at the beginning of the day, but by 3pm, the “coolest” place was in a narrow alley, and was some 4-6°C cooler than in the wide street. (M)</p> <p>The form of streets and buildings reduced albedo by 20% compared to that observed over a flat surface. As street gorges deepen, effective albedo reduces. (M, using models)</p>
<p><b>Anthropogenic heat</b></p> <ul style="list-style-type: none"> <li>• Increases temperature, and thus rate of chemical reactions of pollutants</li> <li>• Releases water vapour</li> </ul>	<p>The artificial heat flux in the core of London (5km across) exceeds the natural flux for every month of the year.</p> <p>In the US, the anthropogenic heat emissions in a large city core can create a heat island of 2-3°C during the day or night. Suburban energy use has a negligible impact on air temperature. (S)</p>

Table 2.6: Quantitative summary of the effects of the urban environment

Parameter	Effect of urban environment			
	General	Notes	London	Notes
Mean annual temperature	0 to +2°C	Northern hemisphere urban areas	+1.4°C	Central London wrt Rural (1931-60)
Mean summer temperature	-		+1.6°C	Central London wrt Rural (1931-60)
Mean winter temperature	-		+1.2°C	Central London wrt Rural (1931-60)
Maximum daytime temperatures	-1 to +15°C	For a range of cities	-2 to +4.4°C	Kensington wrt Wisley (1951-60)
Heating degree days	-3 to -32%	For a range of US cities [base 18.3]	-10%	(1951-60) [base 15.6]
Cooling degree days	+11 to +92%	For a range of US cities [base 18.3]	-	
House heating fuel cost	-		-20%	House at uniform 18.3°C, October to April
Wind speed	-20 to -100% *	at 10m [* heat islands can induce winds faster than regional ones]	-5%	Kingsway wrt SE England (mean, annual difference)
Humidity, absolute	-		-10 to +10%	drier by day, moister by night

Most work on the impact of the UHI effect on cooling loads has been carried out in areas which already have hot summers, e.g. Mexico, Tokyo, California, places where air conditioning is considered almost essential. In London, detailed investigations of the urban climate were carried out in the 1960s. It was found then that London was usually warmer than its rural surroundings on summer days (by up to 4°C), but for one third of the time it was cooler. No recent detailed studies of the intensity of the London UHI have been found, nor of the spatial variation, or impact on air conditioning. With increasing use of air-conditioning, and predictions of rising air temperatures and the frequency of hot summers, there is a need to establish the current impact of the urban environment on cooling energy use. The next chapter introduces the measurement of London's heat island.

## **CHAPTER 3**

### **Measuring the London heat island**

## **CHAPTER 3 – Measuring the London heat island**

### **3.1 Measuring the heat island**

The urban heat island in London has been recognized for many years and the literature on detailed measurements of the London heat island is dominated by that of Chandler. In studies in the 1960's, Chandler (Chandler 1965), using mainly maximum:minimum thermometers, showed a temperature elevation of some 4°C above the rural surroundings on summer days. There have been subsequent measurements by others, but none has been found that would provide appropriate data for determining the effects of the urban environment on cooling energy use. Investigations of UK heat islands have been focussed predominantly on urban climatology per se, rather than on the impacts on building services and energy.

Since Chandler's last detailed survey, there have been three important changes to the city that might affect temperature:

- changes to the building stock (taller buildings),
- changes to the anthropogenic heat release (higher traffic levels, greater use of air-conditioning)
- and changes to air pollution (reduced black smoke).

Given these changes, and the availability now of micro data-loggers, it was considered appropriate to reassess the temperature field, and in greater spatial and temporal detail than has been possible before. The findings of the monitoring provide evidence of the magnitude of the urban heat island currently experienced in London, and measured data for determining the impact on energy use. This research is the first study to carry out a long-term, wide-spread and simultaneous measurement of hourly temperatures in London.

### **3.2 Uncertainties**

#### **3.2.1 Urban temperature measurement**

It is well known that it is difficult to choose a site that is representative of an urban area's temperature as a whole (Chandler 1962; Chandler 1965; Lee 1991). Temperature varies from one side of the street to the other, in proximity to

anthropogenic sources of heat, and walls warmed by the sun, and wind direction, etc. The problem can be partially overcome by sampling at several points in an area and averaging.

To measure air temperature, sensors must be shielded from solar radiation. The traditional double-louvred Stevenson screen is often too obtrusive for urban monitoring and some other arrangement may have to be used. However, even the use of Stevenson screens may introduce an error as they are painted white, i.e. absorb about 20% of solar radiation, and are usually unaspirated in urban monitoring, allowing a build-up of heat inside the box. Lower urban wind speeds, found especially in urban gorges, will reduce the air exchange within the screen and increase the measured temperature. The same box used at a rural site is likely to be better ventilated. For the U.K. climate, it has been suggested that a Stevenson screen can introduce a measurement error of up to 2.5°C in ideal conditions (bright sunshine and low wind speed) (Met.Office 1981).

### 3.2.2 Reference temperature measurement

A reference temperature is required to represent the temperature that an urban area would be at, if it had not been urbanized. This ideally requires the site to be close enough to the urban site to experience the same weather, and yet far enough away not to be influenced by the urban area. The ease with which these two criteria are satisfied depends on the terrain and topography. Some of the factors that can confound the rural reference site's appropriateness are given in Table 3.1.

Table 3.1: Factors affecting the appropriateness of reference temperature measurement

Factor	Effect
Presence of water	Temperature buffering
Katabatic flows	Atypically cool temperatures at night and early morning
Elevation differences	Inversions may introduce a large error (Landsberg 1981). Lapse rate used for height correction may be different
Airport effect	Local heat island may exist, e.g. Dorval airport has been shown to possess its own heat island, (Oke 1973) and Heathrow airport has been described as having the largest positive temperature anomaly in the country compared to other stations [...attributed to urbanization] (Deacon 1990).

### **3.2.3 Heat island intensity measurement**

No formal definition of heat island intensity has been found and it is thus open to interpretation. In particular, the need or otherwise for simultaneity of measurement of the urban and rural temperatures is unclear. However there is a presumption of simultaneity in heat island measurement reported in a study by Runnalls and Oke of the Vancouver area (Runnalls 2000). Nevertheless, standard daily minimum and maximum temperature readings are often used, as these are widely available, but differing diurnal patterns at the two sites can lead to minima (and maxima) occurring at different times (Unwin 1980). A simultaneous definition of heat island intensity has been used for this study.

Either of the urban and rural sites may be subject to local weather effects, e.g. a sudden cooling because of a thunderstorm, which can lead to the largest, but transient, temperature differences being observed in a measurement programme (Jauregui 1997). If the maximum heat island intensity is recorded as the difference of a single measurement pair, the recorded intensity may be of limited utility in characterizing the location.

### **3.3 Field measurement methodology**

As it is not possible to monitor air temperature everywhere at once, a sample of locations must be chosen. There are two main approaches that can be adopted:

- Identify different kinds of environment that are suspected of being warmer or cooler and locate stations at these sites
- Adopt a fixed grid system and overlay this on the environment, positioning stations at the grid nodes, and investigate temperature anomalies

The first, targeted, approach can provide greater detail of the chosen types of sites, but an advantage of the second approach is that the monitoring proceeds without such pre-conceptions, and to an extent, a greater range of environments is likely to be included.

It is the second grid-based system that was adopted in this study, and its design had to take into account several factors:

- Given the size of the London urban area (a diameter of about 30 miles) and the logistics of establishing and maintaining measurement stations, coverage could not be as comprehensive as would be desired.
- It is desirable to know the physical extent of the heat island, and this meant measuring from the core of London through the developed area and out to beyond the urban fringe.
- There can be a great logistical advantage in monitoring stations being in a straight line.
- Given the importance of the centre of London (as an area where many buildings are air-conditioned and the heat island already known to be more intense) it is desirable to monitor in more detail in this area.

A solution that satisfies these criteria is a multi-transect radial grid. Arbitrarily, the eight compass points were chosen for the direction of eight transects, or radial arms. These come to a *focus* at one site in London, and as they do so they naturally provide greater detail for the central area. Stations are spaced at a fixed distance away from each other but this spacing is halved for the innermost area.

The choice of focus site was based mainly on selecting a convenient location that was near Oxford Street that seemed likely to be close to the centre of the heat island. The British Museum provides a useful landmark and this was chosen as the centre of the monitoring array. In fact there is not one focus site but four stations in the roads surrounding the Museum, a few hundred metres apart. Permission to monitor in this area had also been obtained early on. Further details of the monitoring array are given in the next section.



### 3.4 Site selection

#### 3.4.1 Site surveying

As mentioned, the monitoring sites have been selected to lie along continuous transects across the urban conurbation of Greater London. The focus of all transects is the British Museum, just north of Oxford Street. The transects are illustrated in Figure 3.1.

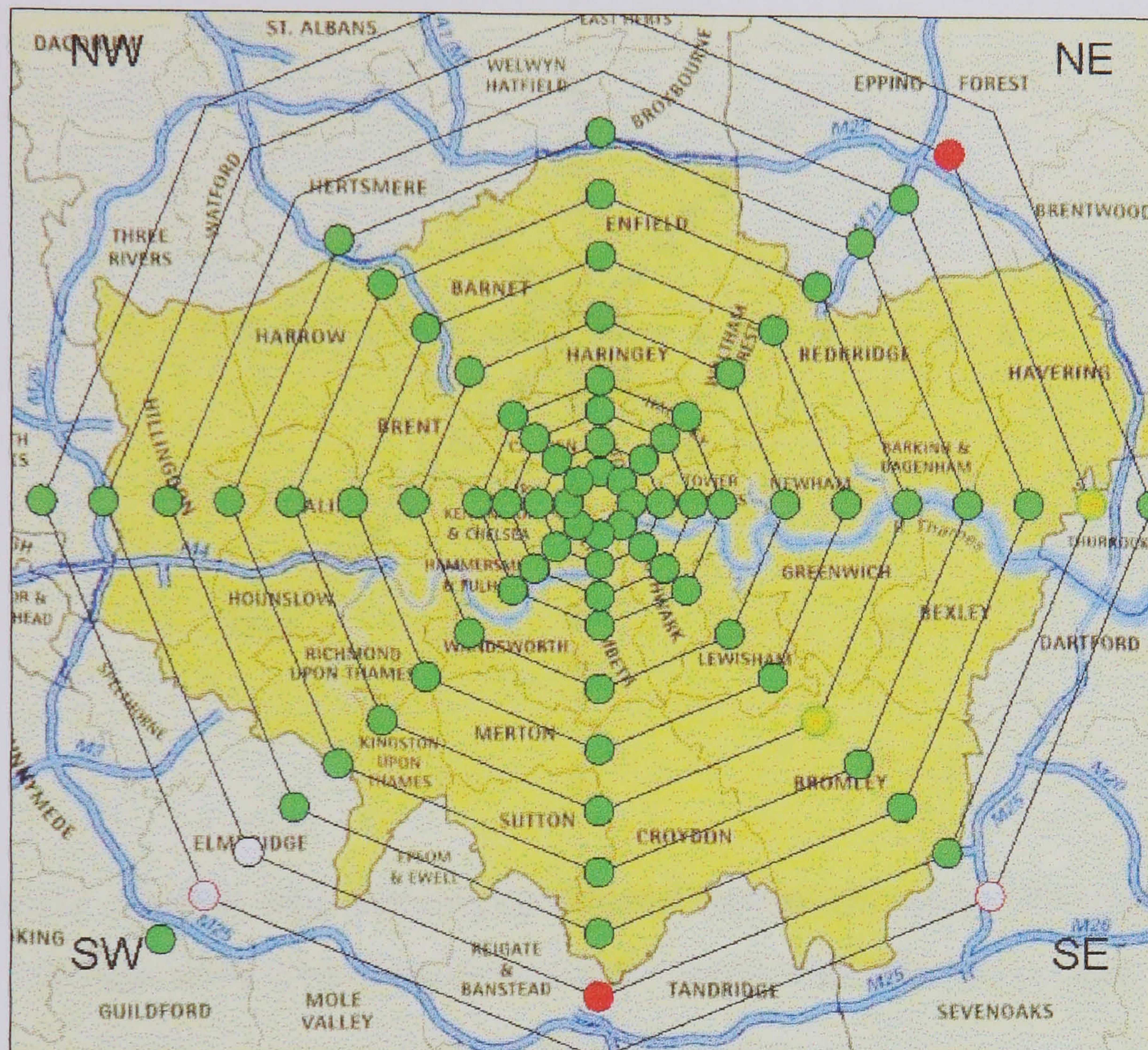


Figure 3.1: Illustration of the transects across London

Points along the eight transects (N, NE, E, SE, S, SW, W, NW, involving 8 to 12 measurement points/transect) are spaced, starting at the focus, as follows:

0, 1 mile, 2 miles, 3 miles, 4 miles, 6 miles, 8 miles....and every two miles until a rural area is reached.

These points were located on a map and then each position visited, surveyed and digitally photographed to find a suitable position for a measurement station. Approximately one hundred sites were surveyed over an area of about 700 square miles, from which 80 stations were ultimately established. Because of the land use pattern of Greater London, the number of sites in each transect varied, as, for example, the NW transect reaches a rural environment sooner than the W transect; 8

and 11 sites are needed respectively. Figure 3.2 shows more clearly the disposition of the measurement sites and their status. (See key below.) The diagram is a schematic – actual positions were up to 0.25 mile from these points, particularly at the rural sites. A Global Positioning System was used to record the actual positions.

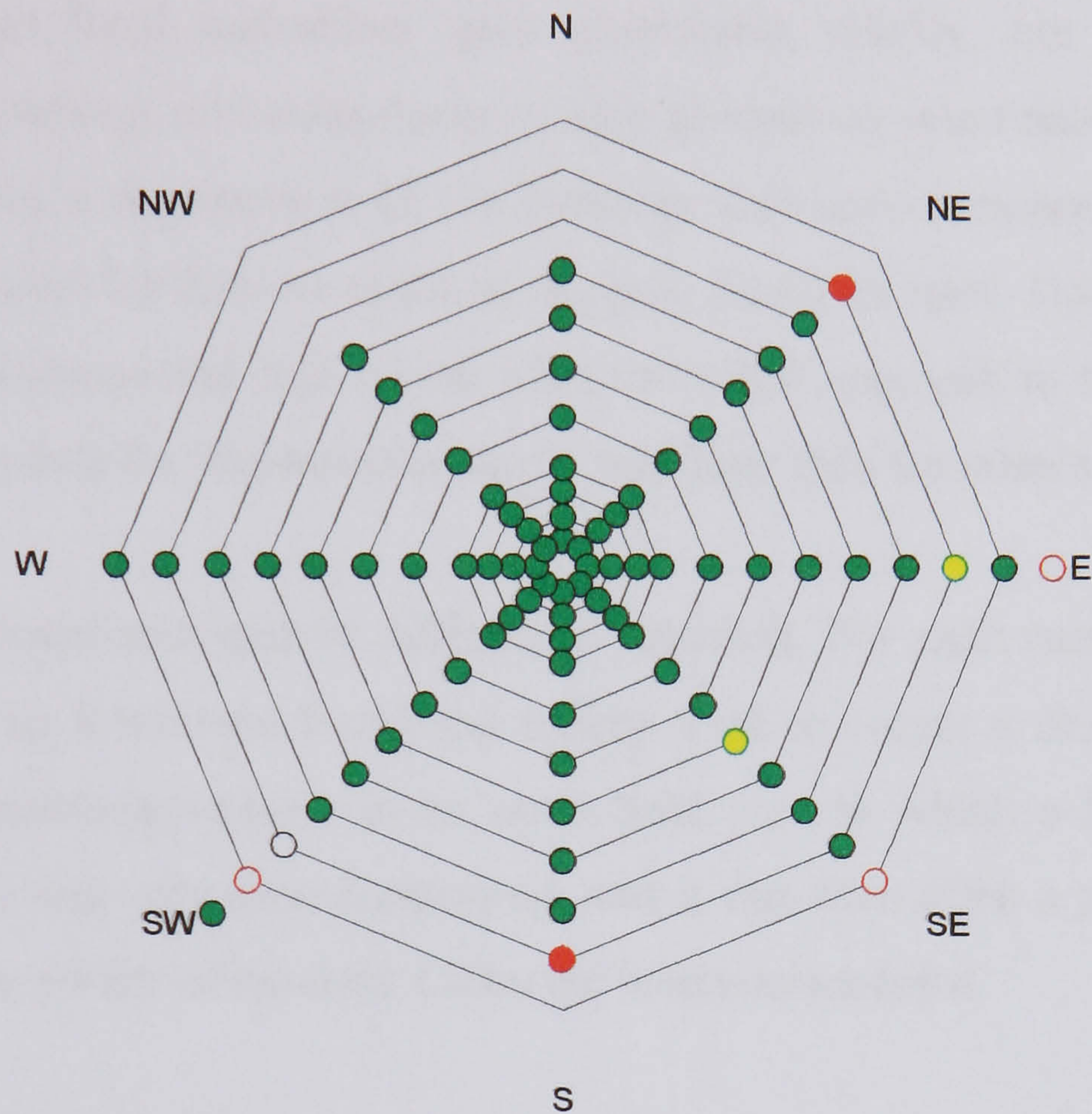
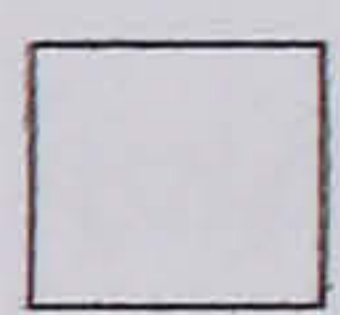






Figure 3.2: Transect map showing operational stations (in green). The concentric octagons are spaced every two miles (every mile near the centre)

**KEY to Figure 3.2:**

-  Open circle = area surveyed & suitable site found and permission sought
-  Red open circle = no suitable site found
-  Red circle = area surveyed & suitable site found and permission refused or no response
-  Yellow circle = area surveyed & suitable site found and permission granted
-  Green circle = measurement station operational

No. of suitable sites found = 81

No. of sites operational = 79

N.B. The map above does not show the four operational stations at the focus, or the double station at the western rural site.

### **3.4.2 Local Authority authorization**

Each measurement station consists of a bracket mounted on a lamppost or tree. Each local authority (33 in London and 15 surrounding London), and each landowner for the non-street sites, had to be contacted in order to request permission to attach the brackets. Most local authorities gave permission readily, but a few required considerable coaxing, and reassurance, before permission was finally granted. In one instance, it was a requirement of the authority that only lampposts that had been structurally tested for their mechanical integrity could be used. Unfortunately, these tests were not completed until a year after the initial approach to the authority, and for this reason data for Westminster start a year later than for other sites.

Rural sites proved particularly difficult to establish. For each rural site (including sites such as in Richmond Park) the survey tried to locate a dead tree (to avoid effects of evapotranspiration) in an open field area to which a bracket could be attached. This was very time consuming, and it was then often a problem to locate and contact the owner of the land. Often the land was tenanted.

### **3.4.3 Choice of reference site**

To quantify the urban heat island a rural temperature is required for comparison. This subtraction of a reference temperature from urban temperatures is based on the premise that the reference temperature represents what the urban temperatures would have been, had the area not become urban. A reference site is ideally close to the urban site, so that regional weather movements are common to both sites, but far enough away not to be influenced by the urban environment.

With very large conurbations, a reference site must of necessity be remote, and probably more remote than desired. In London, eight rural sites were planned, at the ends of the transects, but because of the difficulties described above only three sites could be established. Of these, two were in fact planned as penultimate sites on their transects.

In deciding how to proceed, the temperature data for the three rural sites were analysed in detail to see what the differences were and what factors these were associated with. The conclusion was that two out of the three sites were being

influenced by local development and were not “rural enough”. Hence, all elevations of urban temperature have been quoted with reference to one site, a site in a country park 18 miles west of London: Langley Country Park.

### **3.5 Logging equipment**

#### **3.5.1 Bracket, pole and logger can; design and manufacture**

##### *3.5.1.1 Data loggers*

Air temperatures were measured hourly using *Tinytalk* data loggers. These were tested for individual differences. (See section 3.5.2.) *Tinytalk* loggers are small, being supplied inside a small plastic capsule, similar to a 35mm photographic film capsule, and are programmable. The loggers take discrete readings at the chosen interval (one hour was used). However, because of their heat capacity and the covering of the can this represents an average reading. Hourly data were required for later input to a simulation model and because the timing of temperatures is important in assessing the demand for cooling.

##### *3.5.1.2 Logger cans*

*Tinytalk* loggers come in plastic capsules with press-on lids. As these might be pulled off when retrieving a logger, aluminium cans with screw tops were located and tested. These have the added advantage of having a lower absorptivity to radiation. The *Tinytalks* fit inside the can, with tape over the battery and a cork to raise the *Tinytalk* up inside so that the interface socket can be reached easily at data transcription time.

A steel washer was bonded to the bottom inside of the can to provide magnetic attraction. A self-sticky plastic cup-hook stuck on top of the can retains it over a horizontal wire in the radiation shield. See Figures 3.3 and 3.4.



Figure 3.3: *Tinytalk* logger

Figure 3.4: Replacement logger cans

### 3.5.1.3 Radiation shielding

Conventional Stevenson screens can lead to erroneously high temperatures (up to 2.5°C) (Met.Office 1981) in still, sunny conditions, because of the relatively high absorptivity of white paint, especially if dirty. For this study, it was particularly desirable that the effects of solar radiation on the measurement of air temperature were minimized as the data were to be used for investigating the impact on air-conditioning energy use, rather than, for example, pedestrian comfort levels. To achieve this, the temperature sensor and data logger were housed in an aluminium can, which was then suspended between two concentric cylinders of polished stainless steel – giving triple-shielding. An upper stainless steel cover was also provided with a free passage of air to all parts. A diagram of the measuring device, which was manufactured specially, is shown in Figure 3.5. The radiation shield in turn was welded to a spacing arm and plate for attachment to a lamppost column. The offset from the lighting column was approximately 300mm. Two types of spacing arm were made: one (pictured) was bendable for adjusting the shield to the vertical after attachment to a tree; another had an arched design to be more aesthetically pleasing on lighting columns, particularly in more visually sensitive areas of the city.

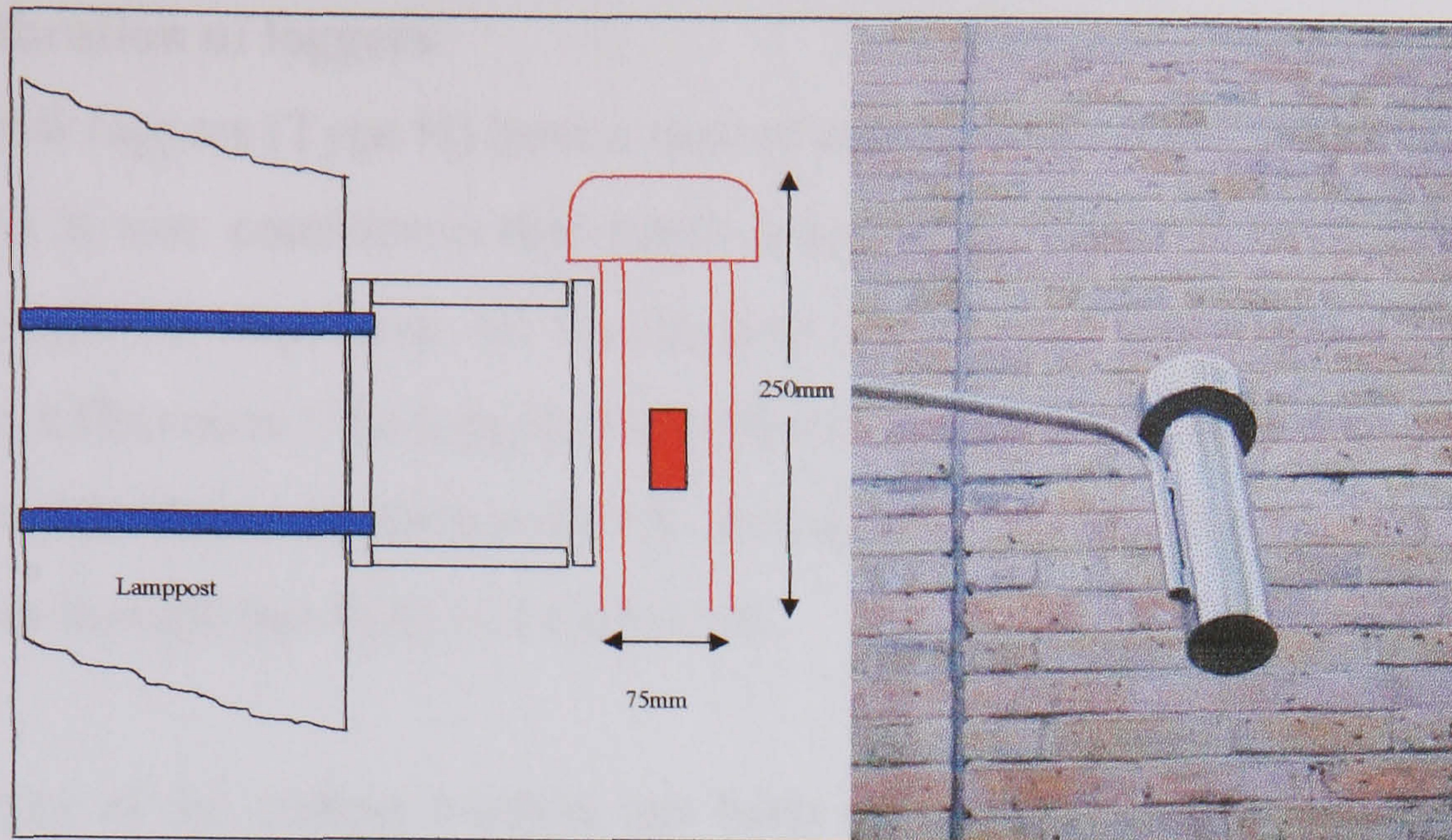


Figure 3.5: Schematic of prototype & picture of a final design of the air temperature measuring device

#### 3.5.1.4 Impact of mounting type on temperature

To address the possibility that a hot black lamppost might significantly heat the air near a datalogger (and give an unrepresentative reading), an outdoor test was set up.

Six radiation shields were made up using concentric plastic tubing covered in aluminium foil with foil covered funnels on top. These were rigidly suspended from a one metre horizontal bracket above at varying distances from the end of the bracket. The bracket was secured to a lamppost in a (somewhat) sheltered area with a *Tinytalk* inside each shield.

The data showed no impact of the lamppost on the temperature measured over the three week period of the test - even on sunny still days. It was therefore decided that the radiation shields would be mounted approximately 300mm from the lamppost.

#### 3.5.1.5 Pole for data collection

To download the data from the *Tinytalk* loggers they must be removed from the radiation shield. As this is 6 metres above pavement level a suitable tool had to be devised. A telescopic pole was obtained 0.98m long extending to 5.2m. A height of 6.4 metres can be reached by a typical adult. A fitting for the end of the pole was constructed; essentially a plastic funnelling tube containing a powerful magnet.

### **3.5.2 Calibration of loggers**

The *Tinytalk* loggers (Type H) have a quoted accuracy of  $\pm 0.2^{\circ}\text{C}$  with a resolution of  $0.25^{\circ}\text{C}$ . As it was considered that small temperature differences (less than half a degree) might be important, all the loggers were tested together to identify their individual differences. The loggers were placed in a closed filing cabinet and left for three days. The data were then analysed, excluding the initial period when individual differences through handling were apparent.

The validity of the testing method has been checked by comparing samples from different areas of the filing cabinet to ensure that there were no systematic differences. All checks showed that the testing was valid and that the deviations of the *Tinytalk*'s readings followed a normal distribution. However, the data showed that the mean values of the individual *Tinytalks* were within about 0.30 to 0.38 of the grand mean of all *Tinytalks*. This was rather higher than the quoted accuracy of  $\pm 0.2^{\circ}\text{C}$ , but unimportant as the data from all the *Tinytalks* were individually corrected according to the test results. (Errors due to the 8-bit resolution of the loggers ( $0.25^{\circ}\text{C}$ ) cannot be eliminated for individual readings.)

See Appendix 1 for a fuller description of the calibration check, and subsequent post-monitoring calibration check.

### **3.6 Installation**

A contractor with an hydraulic platform was used for all installations at lighting columns – a requirement of most local authorities. Installations at tree sites were self-installed using a portable ladder, with the bracket screwed directly to the tree trunk using stainless steel screws to allow easier removal. Brackets were positioned at 6m height.

An initial batch of 18 measurement stations was set up in May 1999, and became operational from 1 June 1999. These covered the western and north western transects, and the four sites at the focus of the transects (the British Museum area). Sites in Westminster were not covered at this stage, as described earlier.

Subsequently, additional sites were set up as permission was obtained from the local authority or landowner. This proceeded until late summer '99, when approximately 65 measurement stations had been installed. In April 2000, permission was granted by Westminster Council to proceed with installation and 6 sites were added in central London, together with some additional rural sites. A parallel rural reference site in the west was also added, creating a London-wide monitoring array of almost 80 stations recording hourly data.

### 3.7 Data collection

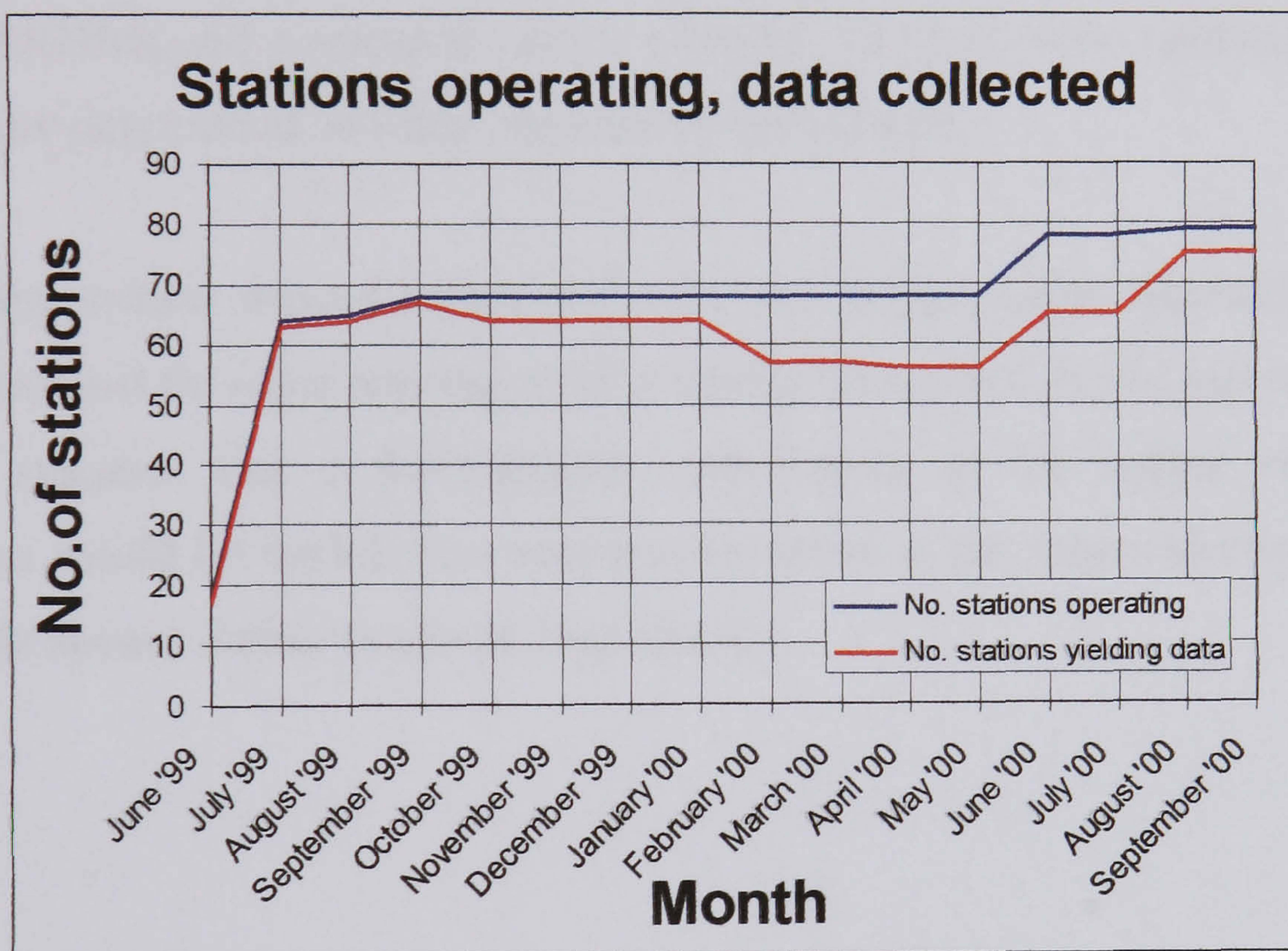


Figure 3.6: Number of stations operating, and data collected

Figure 3.6 shows the number of stations installed and the number from which data were collected month by month. The difference represents loggers that were lost and had to be replaced. The main reason for the loss of loggers is not known, although mis-registration of the hook on the wire when refitting a logger is one cause. Theft was probably very minor. Loss rates increased in March '00 but dropped again in August, again for unknown reasons. Only one logger actually failed, internally.



Data were collected from all sites every two months with the data transferred to a portable Psion computer. A 2 Mbyte flash memory card (data are maintained without power) was used in the Psion as a precaution against data loss should there be computer problems – and this proved valuable.

### **3.8 Chapter 3 Conclusions**

The London area was surveyed and permission obtained to set up monitoring stations at 80 locations positioned along radial transects. Obtaining authorization from local authorities and landowners was a time-consuming task but permission was usually readily given. Data loggers were mounted on lighting columns at 6m height with suitable shielding and a retrieval system devised. The individual calibrations of all loggers were determined and data normalized accordingly.

The logging system proved robust and only one logger failed internally. Several loggers were lost for other reasons, most probably because of in situ mis-registration, and this suggests that a self-aligning modification to the logger containment mechanism would be useful. The next chapter looks at the data collected and what this reveals about London's current heat island.

## **CHAPTER 4**

### **The London heat island: measured results for the summers of 1999 and 2000**

# **CHAPTER 4 – The London heat island: measured results for the summers of 1999 and 2000**

## **4.1 Introduction**

This section describes the heat island dataset, which covers two summers, 1999 and 2000. The heat island is not constant, for example it varies with wind speed, and some of the factors that affect it are explored in this chapter. An analysis of variance is presented in chapter 5.

Two important types of information are presented: an indication of the maximum temperature difference that was found in London at different times (the heat island intensity); and the way temperatures varied in different parts of the study area (the spatial variation).

The analysis presented is based on the data gathered in the summer of 1999 (August and September) and the summer of 2000 (July to September). Respective figures and results for the two summers are labelled “a” and “b”.

## **4.2 Intensity**

### **4.2.1 Mean daily profile**

Figures 4.1a and 4.1b show the temperature difference between central London (focus) and the reference station 18 miles west in a country park (Langley). The average of two stations around the British Museum has been used to represent the city temperature. There is continuous data for these two stations in both years. All hourly data are plotted, with the mean value for each hour and the standard deviation ( $\sigma$ ) about this. The graph shows:

- The heat island can be negative
- There is wide variation in the hourly heat island intensity in a range from -4 to +8°C.
- The mean heat island is more pronounced at night reaching around 3-3.2°C.
- Mean minima occur around 10am and in the afternoon at 3pm (about 0.8°C) with a slight rise in between to 1.3°C.

- The two summers have very similar mean profiles, with mean 24 hour heat island intensities of 2.1 and 1.9°C respectively.

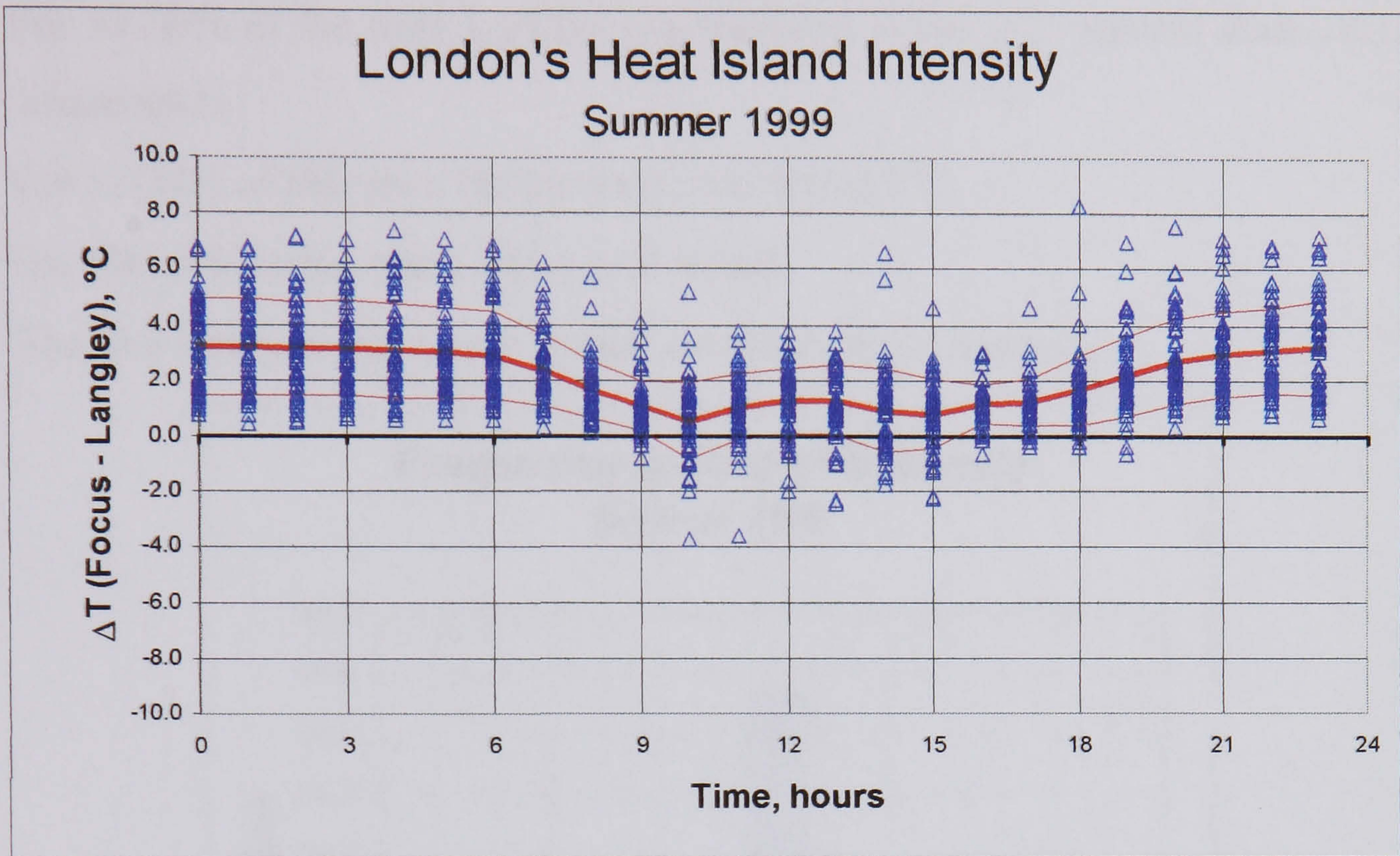


Figure 4.1a: London's heat island intensity (all data, mean &  $\pm$  standard deviation)

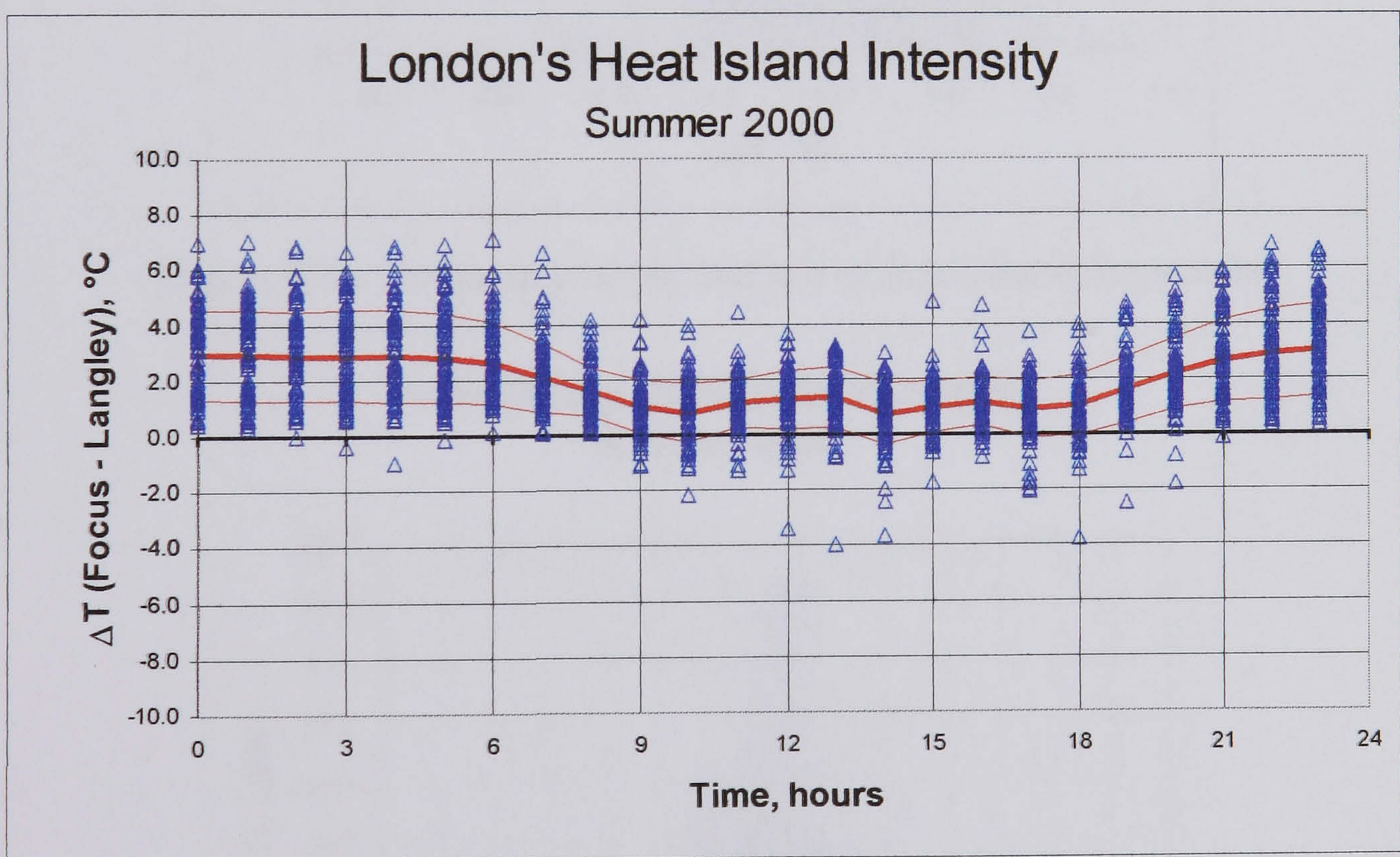


Figure 4.1b: London's heat island intensity (all data, mean &  $\pm$  standard deviation)

## 4.2.2 Frequency distribution

Figures 4.2a and 4.2b use the same data as before, but show how frequent different heat island intensities were. The distribution shows that:

- For 33-36% of the time London was between 1 and 2°C warmer than the rural temperature.
- For 12-14% of the time, the intensity was above 4°C.
- For 6% of the time, there was a cool island.
- The two summers have very similar distributions of intensity.

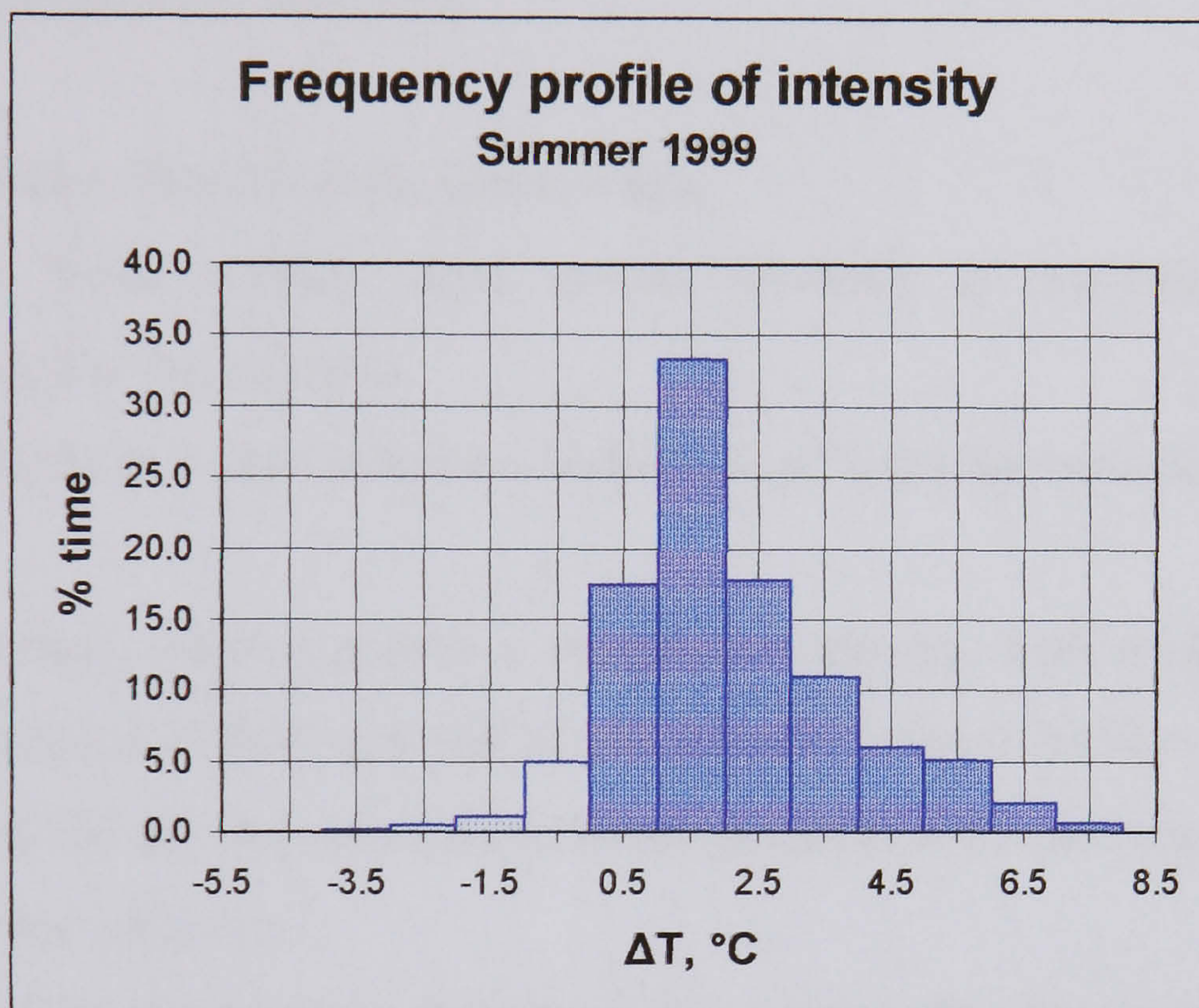


Figure 4.2a: Frequency of occurrence of heat island intensities

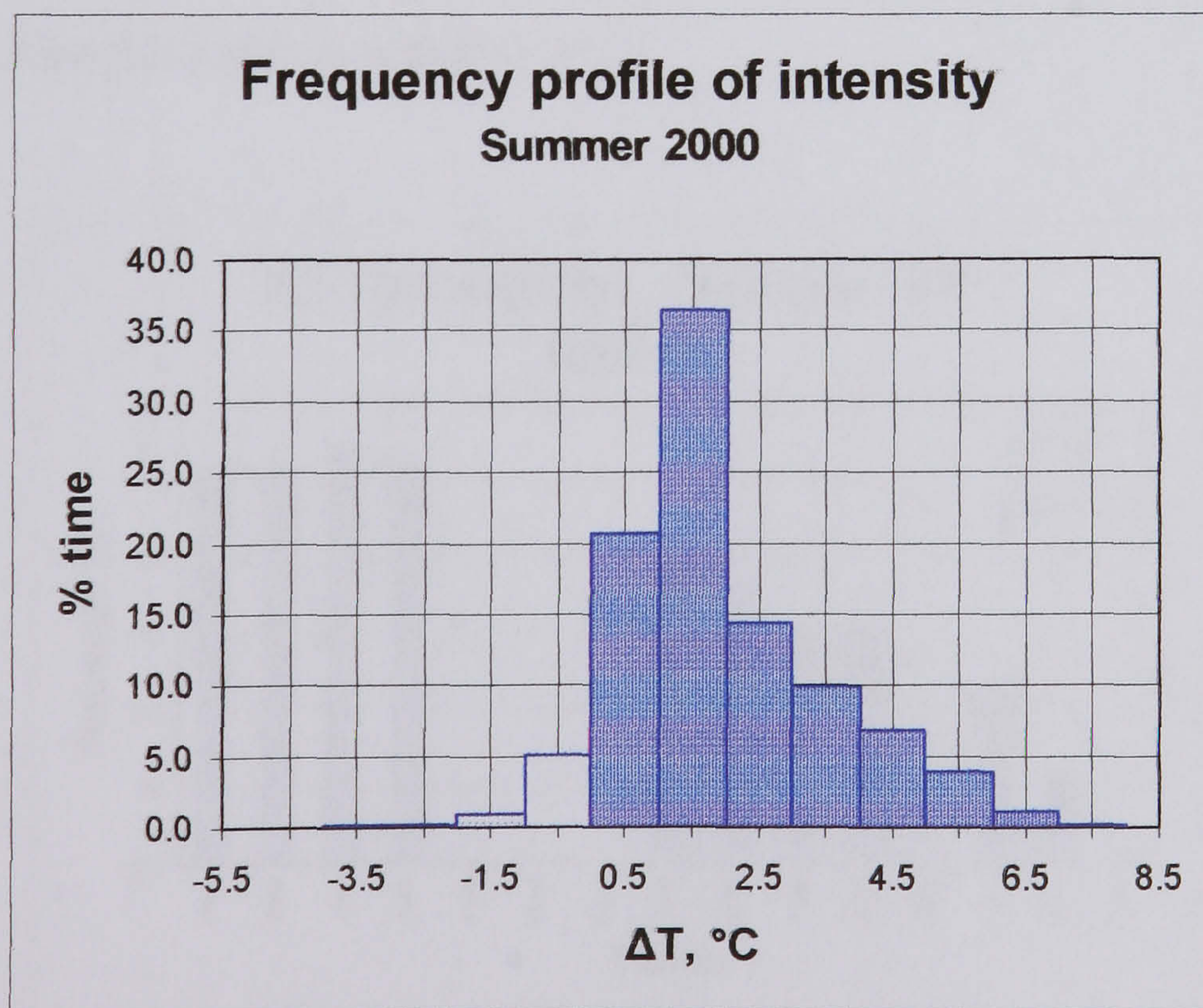


Figure 4.2b: Frequency of occurrence of heat island intensities

### 4.2.3 Percentiles, night and day

Figures 4.3a, b and 4.4a, b show examples of 50th and 90th percentiles of heat island intensity. Each graph shows the results from the four focus stations around the British Museum and the other stations on the west transect, as far as the rural reference station labelled WW11, 18 miles away. In 1999, there were no monitoring stations in Westminster (WW01 to WW03). Other gaps occurred because of partial data loss. The data were divided into approximately daytime (08:00-19:00 BST) and night-time data (20:00-07:00 BST).

These figures show that for these summer data:

- The four focus stations were almost identical at night-time, but more differentiated in the daytime.
- At night, there is a clear reduction in heat island intensity with distance from the centre
- In the daytime, there is almost a temperature plateau, with evidence of a cliff between stations WW09 and WW10 (14-16 miles west of the focus).
- For 10% of the day the central London temperature was more than 2.7°C warmer than the rural reference.
- For 10% of the night it was more than 5.1°C warmer than the rural reference.
- The general pattern of intensity distribution is very similar for both summers, and the intensities the same to within 0.5°C.

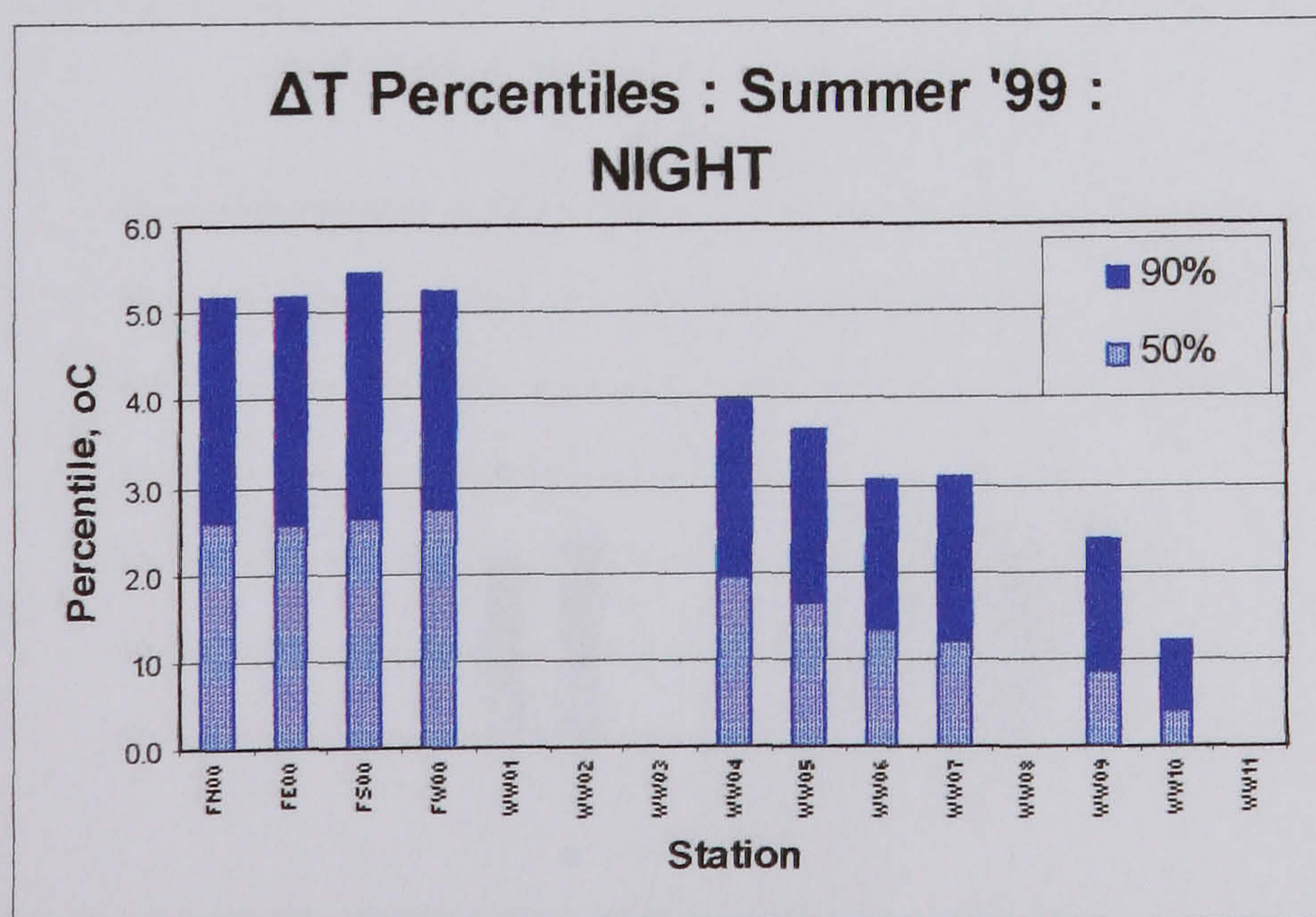


Figure 4.3a: 50 and 90<sup>th</sup> percentiles for the night-time heat island intensity

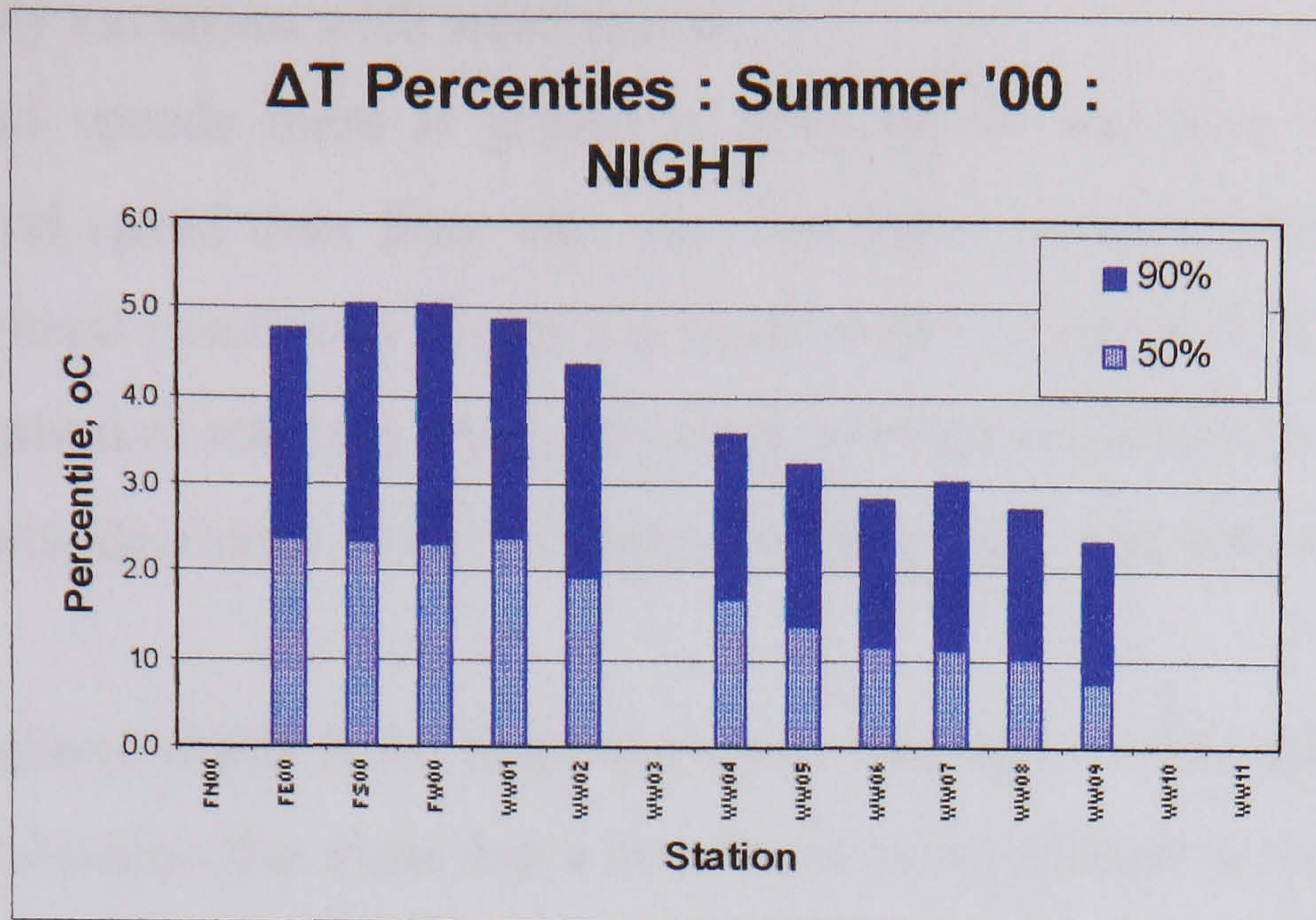


Figure 4.3b: 50 and 90<sup>th</sup> percentiles for the night-time heat island intensity

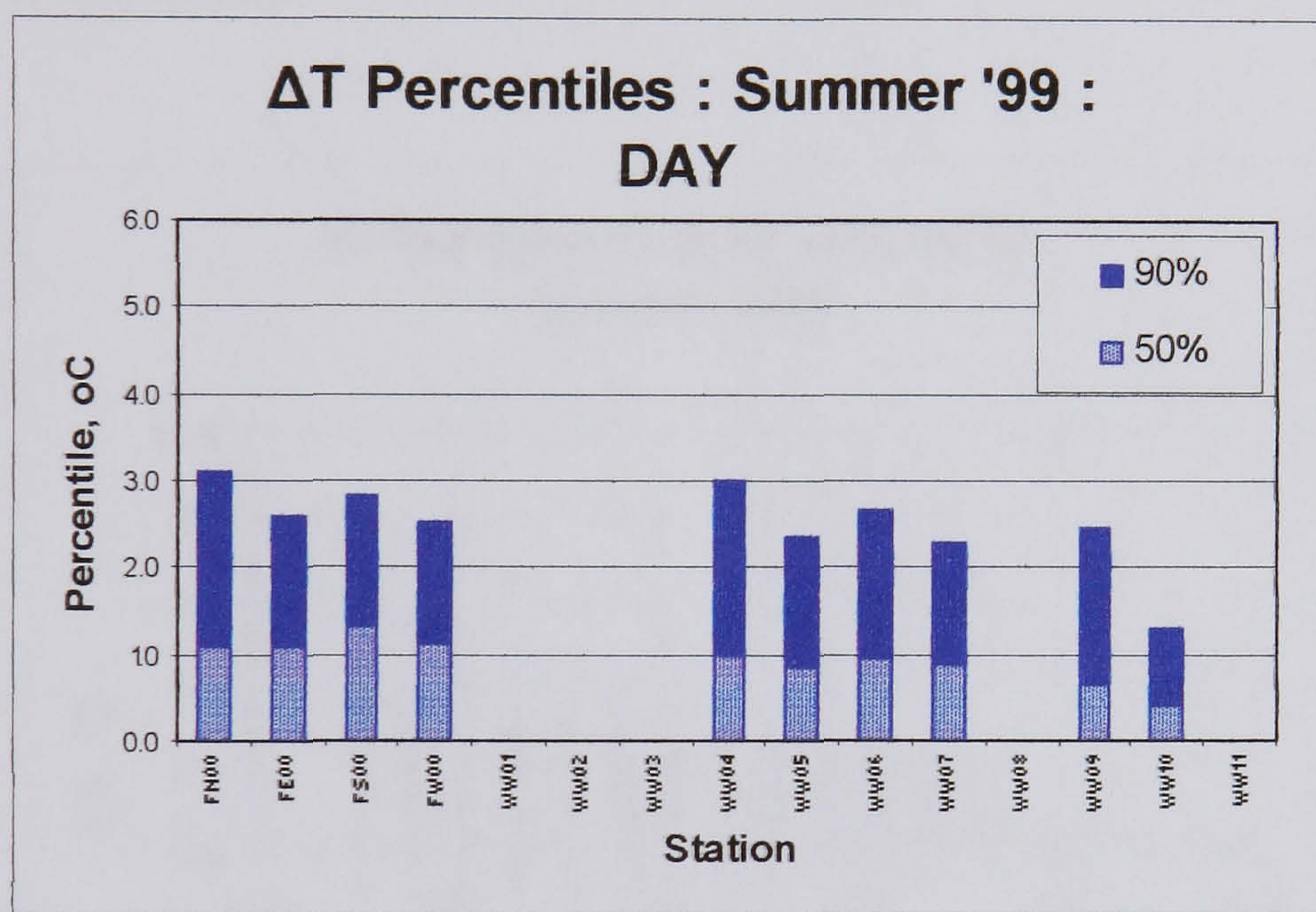


Figure 4.4a: 50 and 90<sup>th</sup> percentiles for the daytime heat island intensity

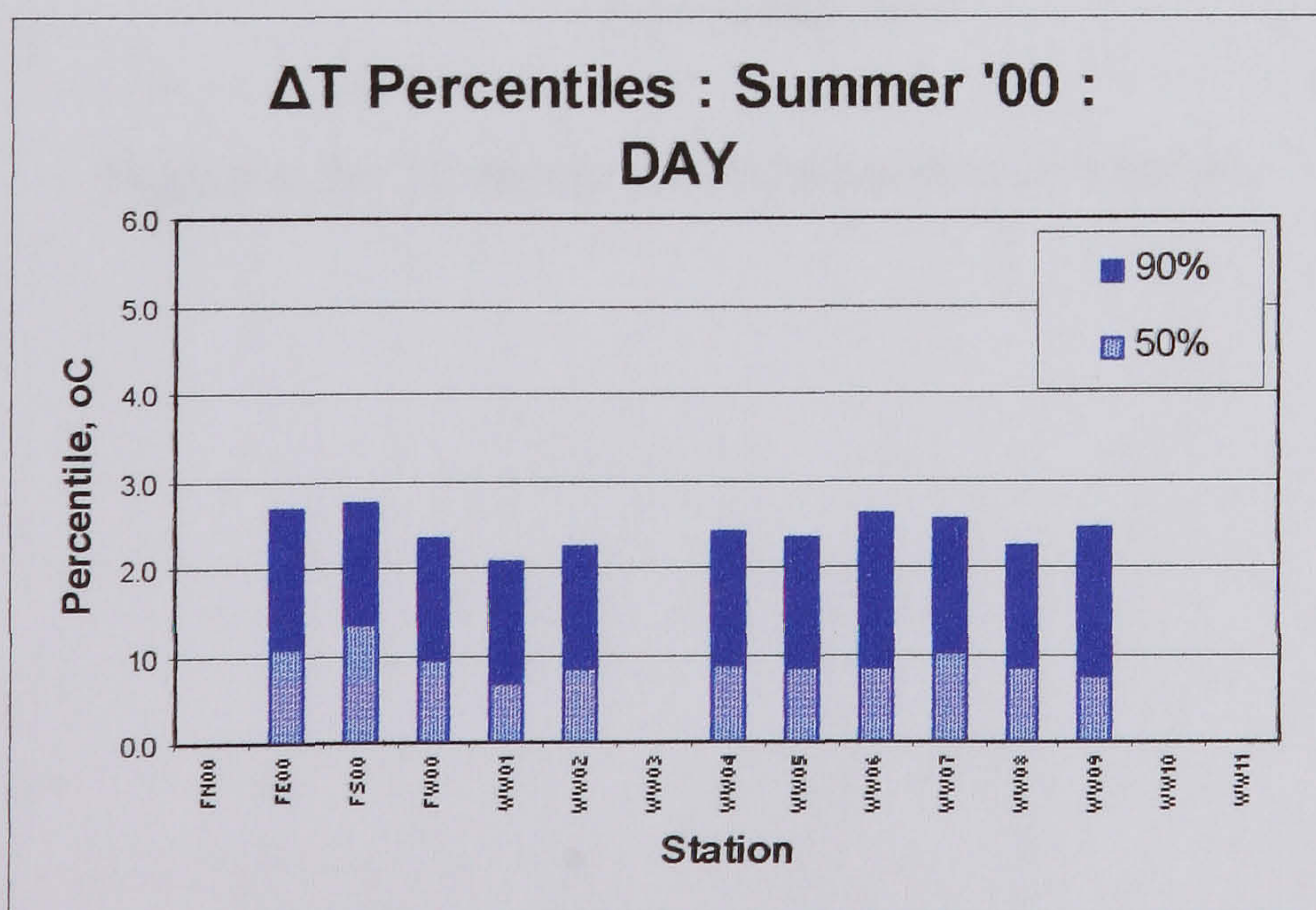


Figure 4.4b: 50 and 90<sup>th</sup> percentiles for the daytime heat island intensity

#### 4.2.4 Intensity variation with wind speed

At higher wind speeds there is greater mixing of air and heat islands may be dissipated. Wind speed data from one site, Heathrow Airport, have been used to indicate the general conditions across the study region. Figures 4.5a and 4.5b show the hourly variation of intensity with increasing wind speed. It can be seen that:

- The intensity decreases with increasing wind speed, and this is true for both summers.
- At speeds above about 6m/s, there are fewer data and the variability in intensity makes the situation less clear, but a downward trend appears to be maintained.

Wind speeds tend to be lower at night and this is one of the reasons for higher night-time heat island intensities.

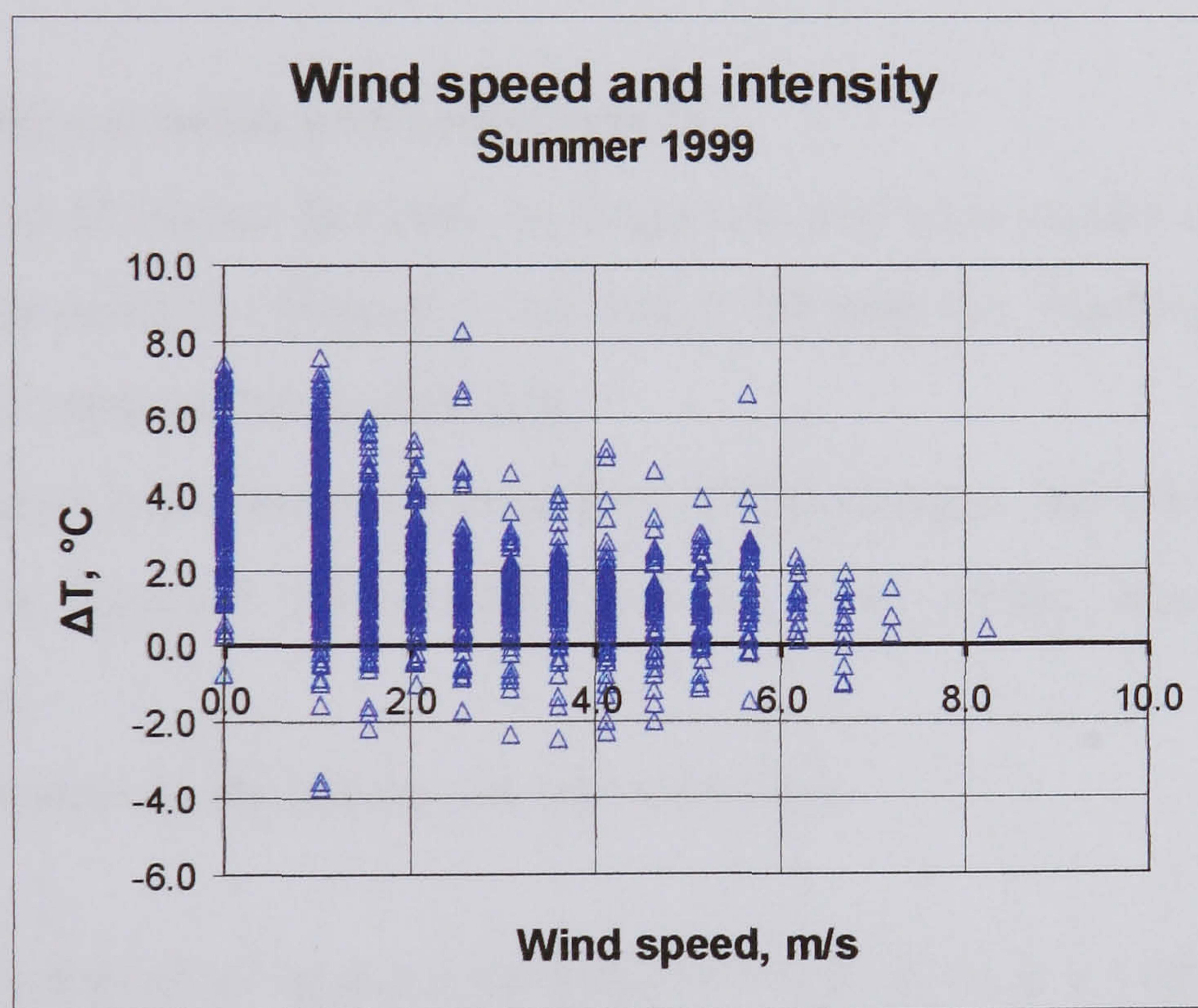


Figure 4.5a: Wind speed and heat island intensity



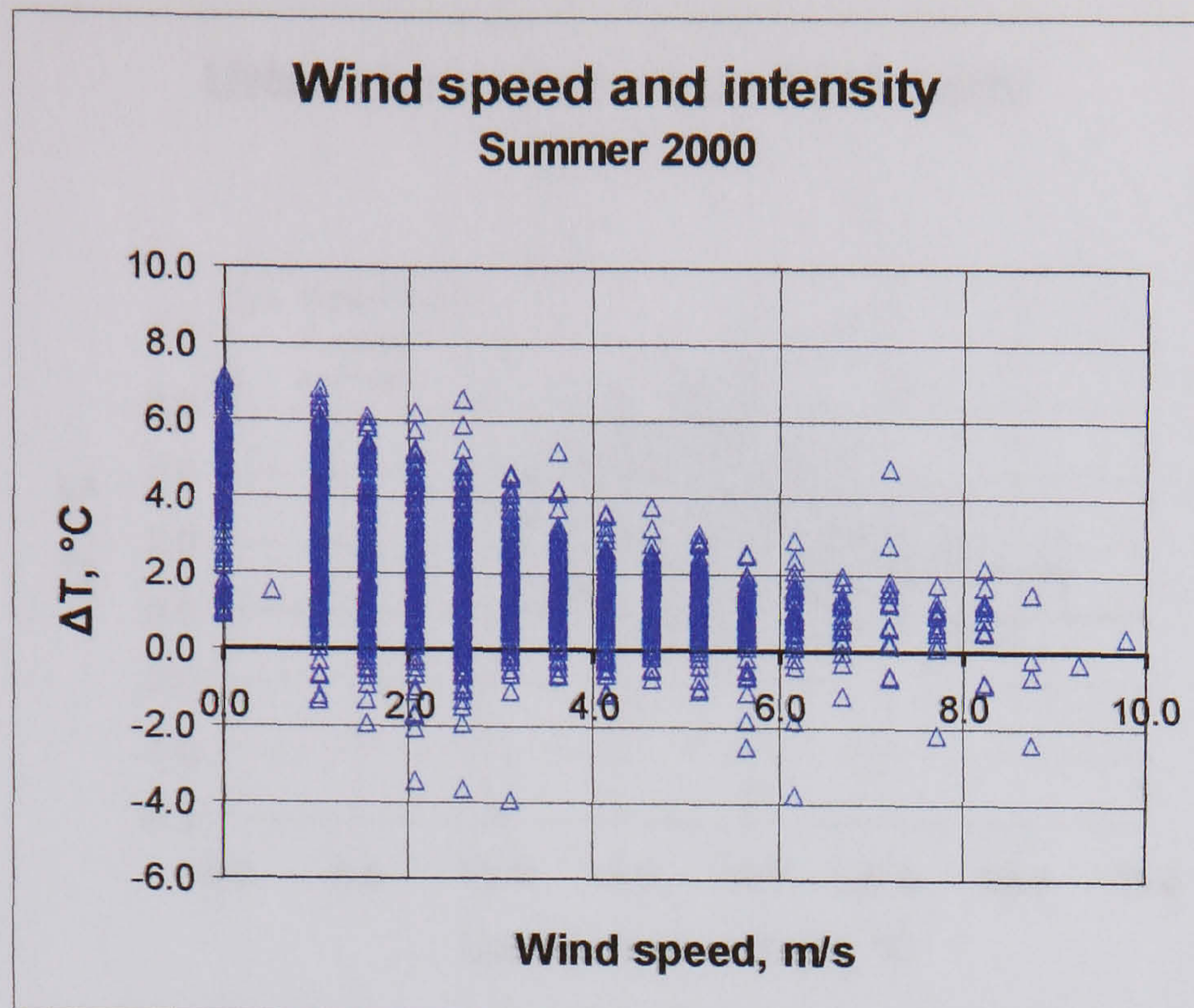


Figure 4.5b: Wind speed and heat island intensity

#### 4.2.5 Intensity variation with temperature

The temperature difference between an urban site and rural station can be related to the absolute temperature. Figures 4.6ab and 4.7ab plot the hourly intensity against urban and rural temperature respectively.

- There is a poor relationship between heat island intensity and urban temperature.
- There is a stronger relationship between heat island intensity and rural temperature.
- These relationships are similar for both summers.

The intensity is related to rural temperature ( $r^2 = 0.25-0.32$ ,  $n > 1400$ ), with the heat island reducing with increasing rural temperature. In contrast only 2-5% ( $n > 1400$ ) of the variation in intensity is explained by the changing urban temperature.

The main reason for this is that although the reason for the existence of the heat island is the urban environment, the greater driving force for its variation is the rural temperature. Urban temperatures are buffered, or restrained in part. In the limit, the urban temperature might vary very little and only slowly, whereas the rural temperature would still swing diurnally. It is therefore to be expected that, in London conditions, the temperature difference is more strongly related to rural temperature than urban temperature.

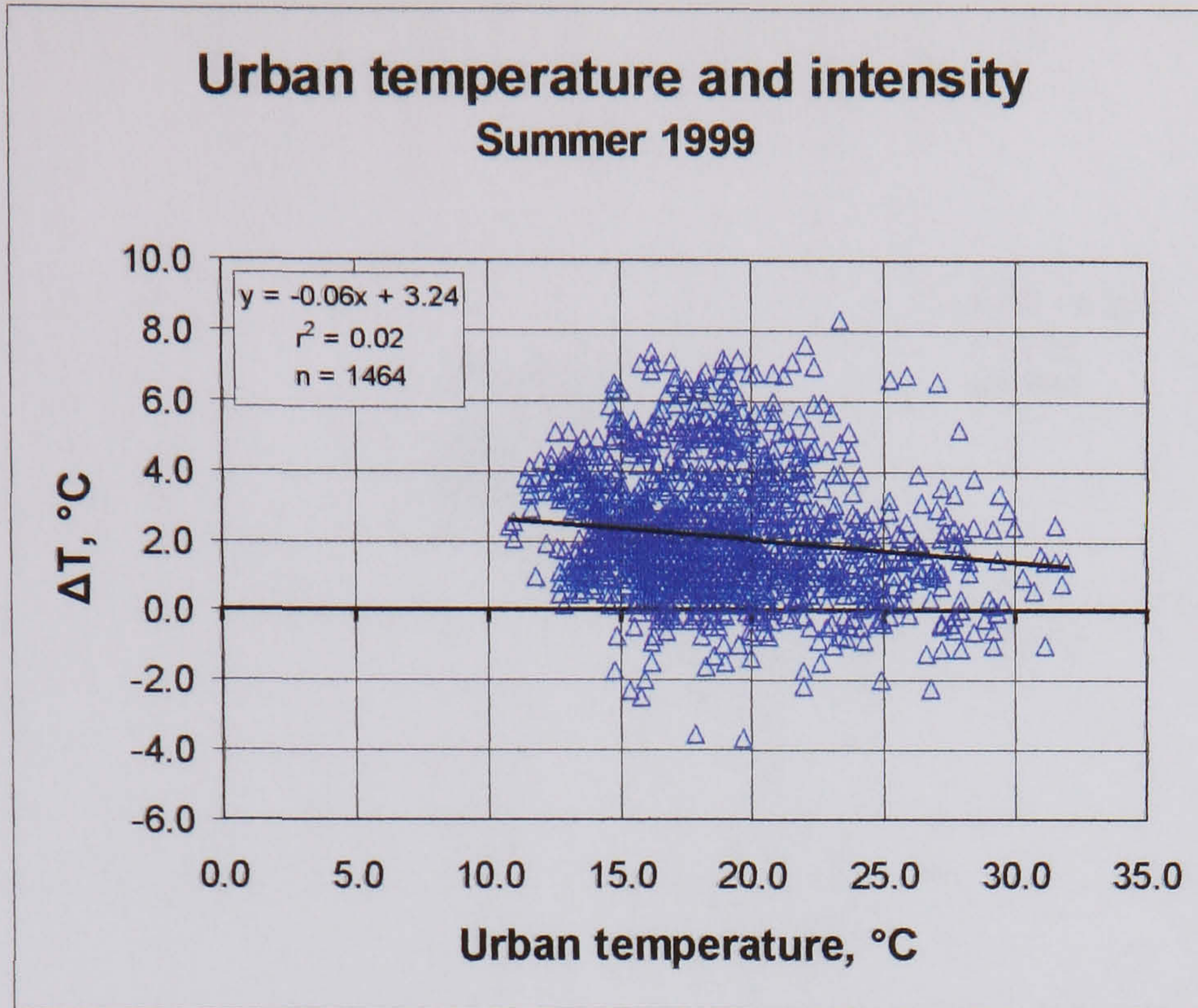


Figure 4.6a: Urban temperature and heat island intensity

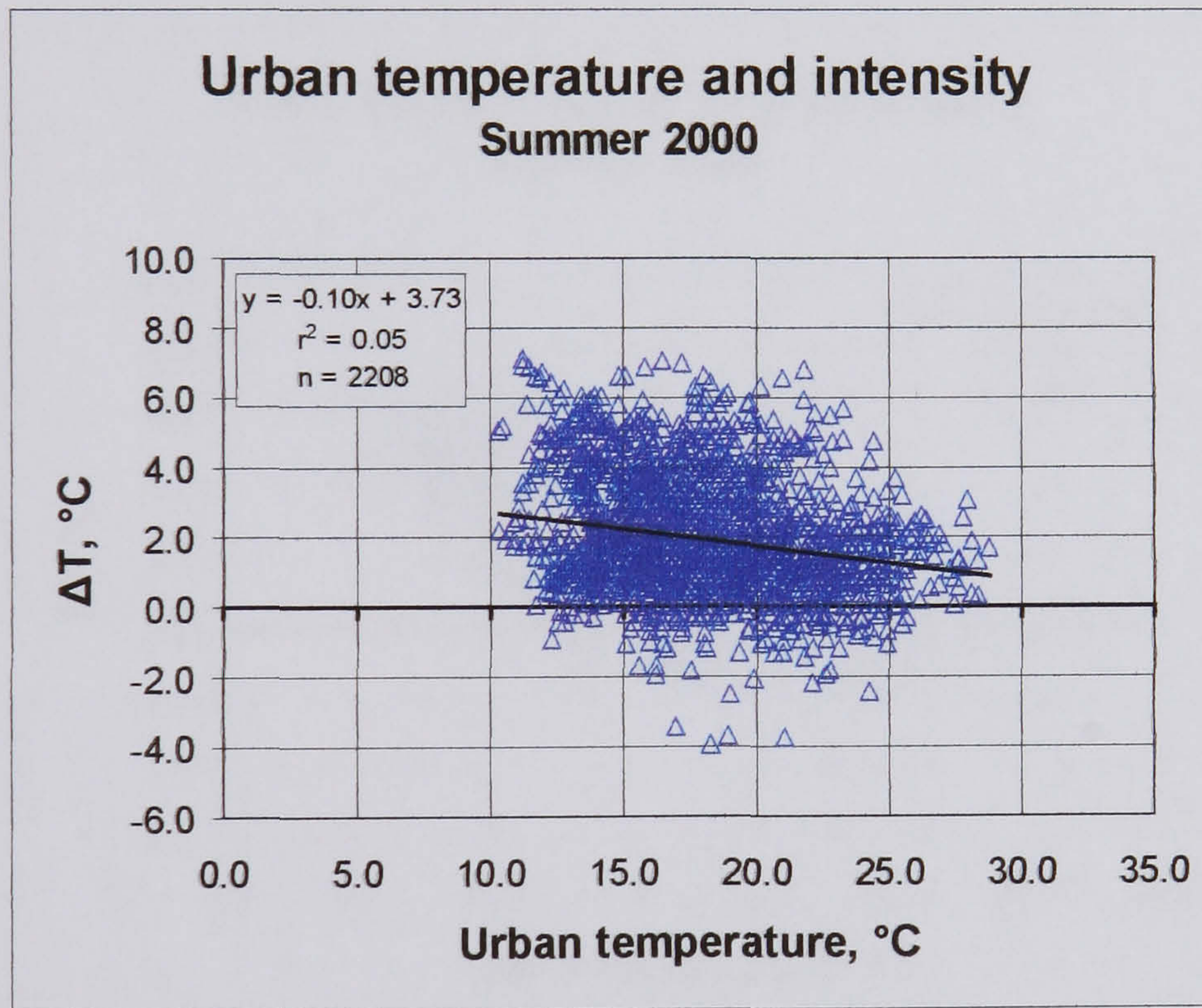


Figure 4.6b: Urban temperature and heat island intensity

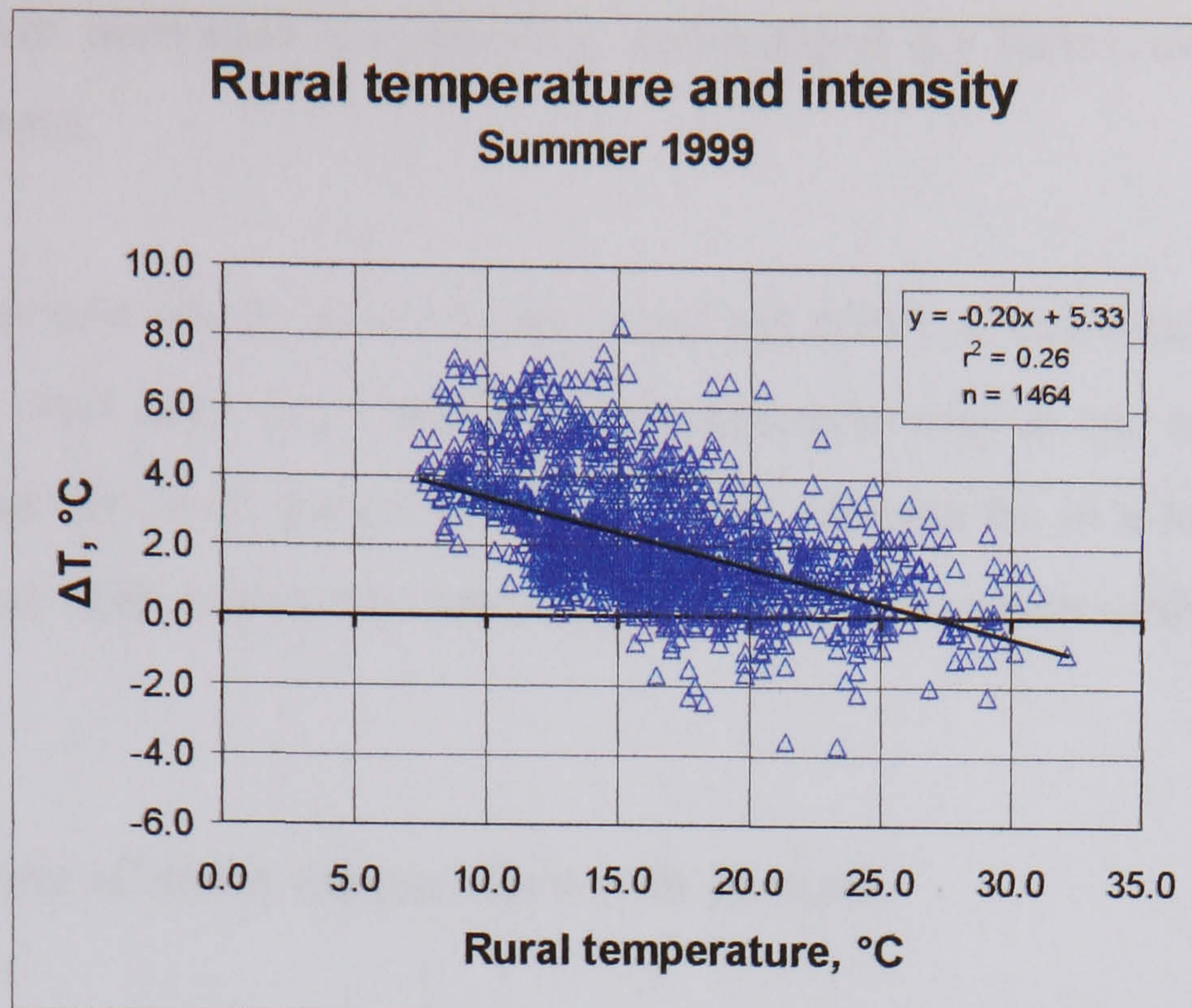


Figure 4.7a: Rural temperature and heat island intensity

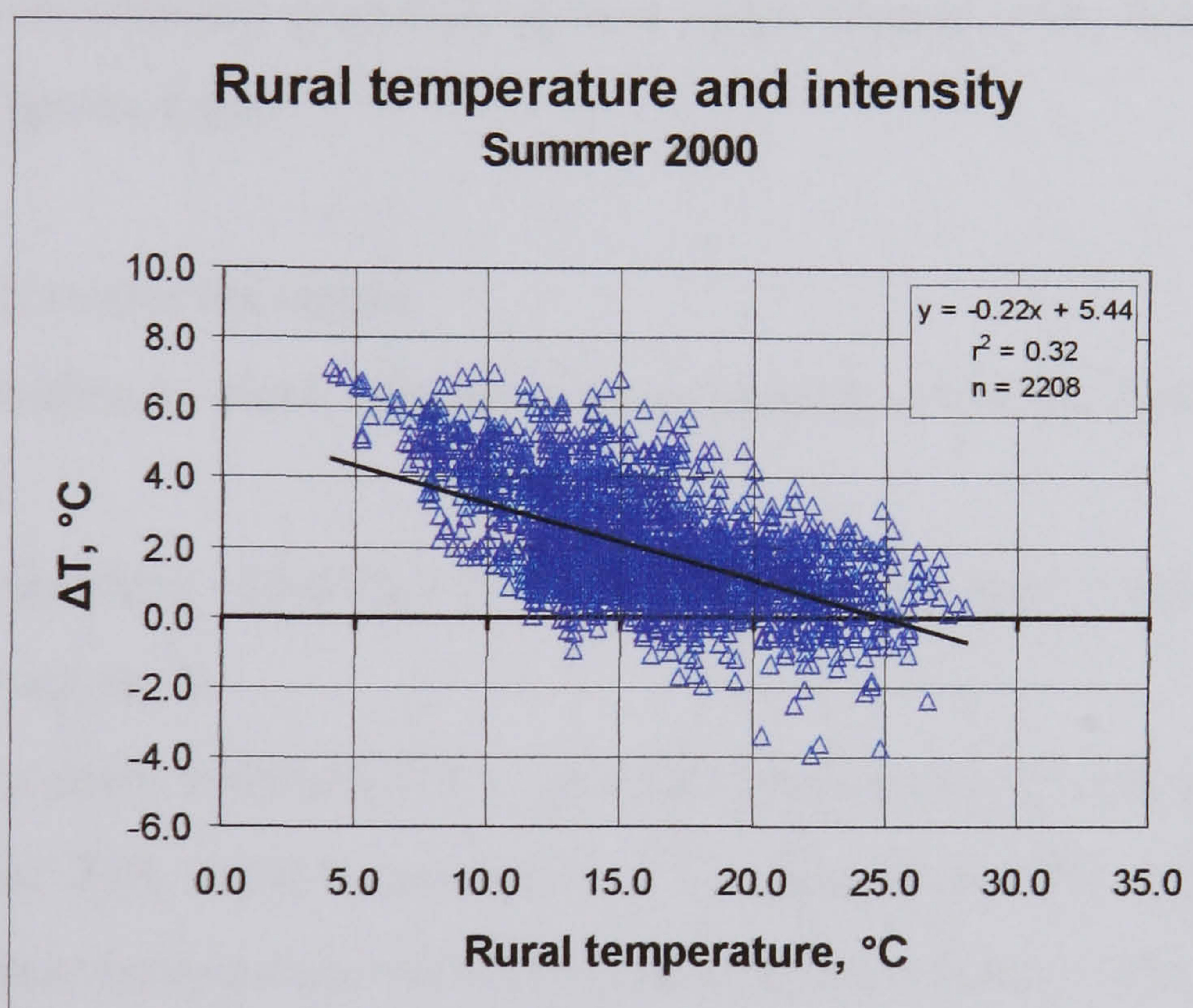


Figure 4.7b: Rural temperature and heat island intensity

### 4.3 Spatial variation

The foregoing considered the heat island intensity as revealed by a central London temperature and a rural reference station. This section considers the variation of temperature with location in greater detail. The more central urban micro-environments are, in general, different from the more rural ones. However, each particular micro-environment varies by how much it exhibits characteristics of

urbanization, viz. increased heat capacity, and reduced sky factor, albedo, vegetation and air movement.

The term urban heat island refers to the broad net effect of city micro-environments differing from rural ones. An urban micro-environment may at one extreme be at the bottom of a narrow street gorge and at the other extreme be in a large urban park. The temperature from micro-environment to micro-environment within a city will be different.

### **4.3.1 Variation of mean temperature with distance**

#### *4.3.1.1 All data*

It is reasonable to assume that the mean temperature of measurement stations will tend to reduce with increasing distance from London. The mean temperature for all data (from 50-60 stations) is plotted against radial distance,  $X_r$ , from London (from the focus) in Figures 4.8ab.

- It is warmer nearer the centre.
- The relationship is clear, despite average data for different weather conditions being used.
- A large proportion (58-67%) of the variance of 24 hour mean temperature is related to varying  $X_r$ .
- Residual variation is around 0.5°C generally, and occurs at varying  $X_r$ .
- The summer 2000 period was about 0.5°C cooler than 1999, but the gradient of reducing mean temperature with  $X_r$  is essentially the same (< 4% difference).

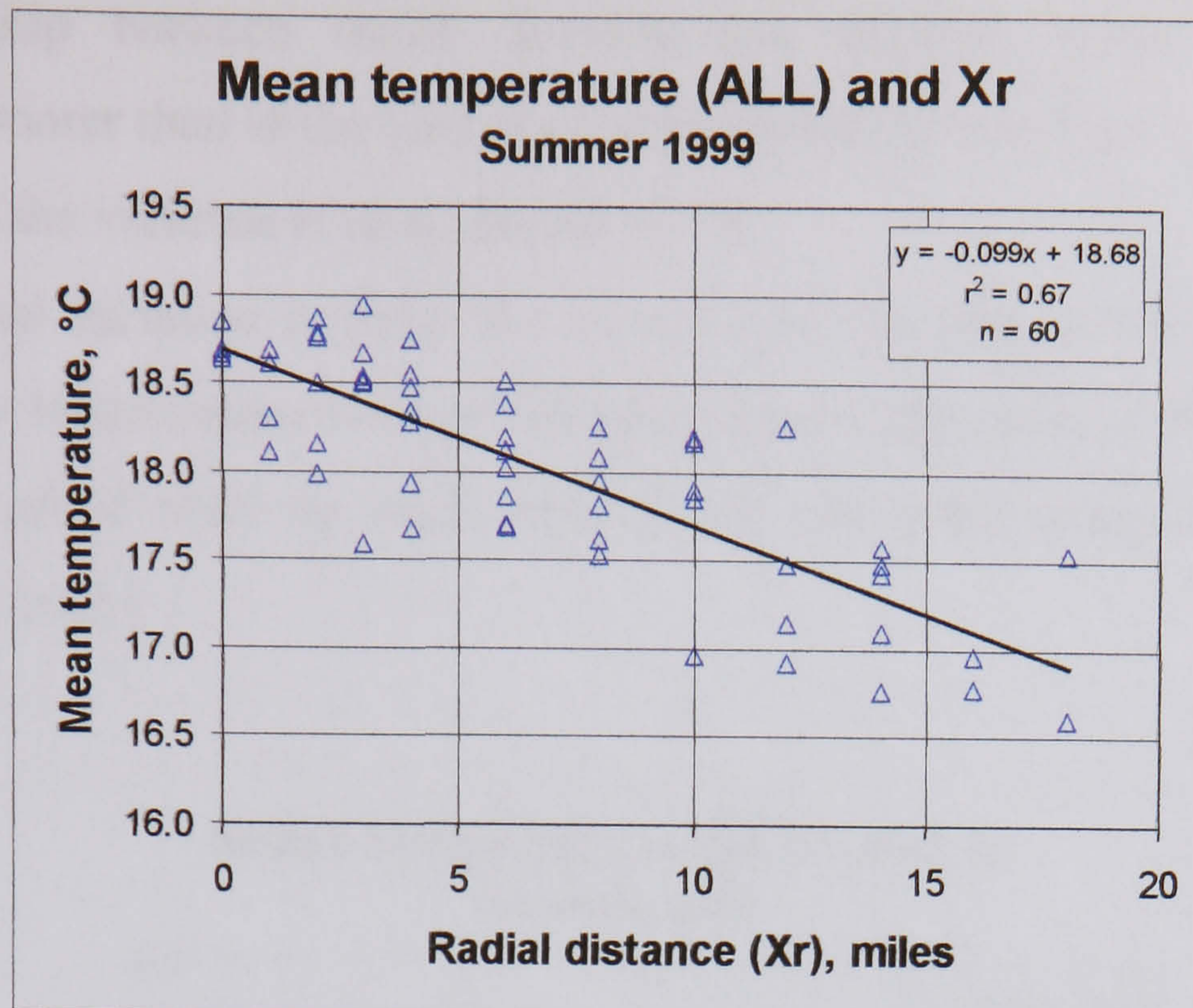


Figure 4.8a: The change in mean temperature with distance from London

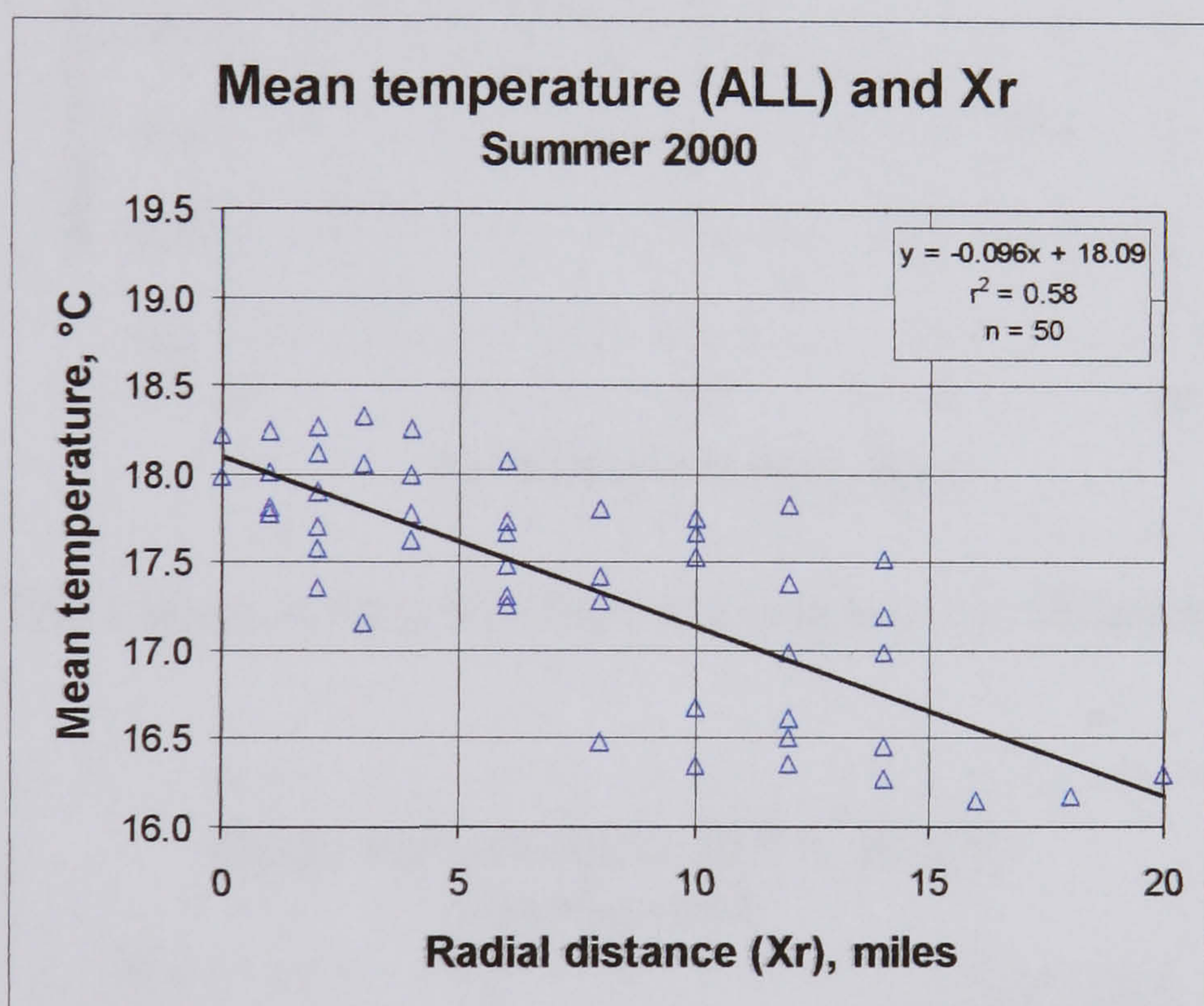


Figure 4.8b: The change in mean temperature with distance from London

#### 4.3.1.2 Daytime data

Less variation is expected in daytime temperatures (as depicted in Figures 4.1a and 4.1b) and this is shown in Figures 4.9a and 4.9b. Daytime data are defined as the 12 hours' readings from 07.00 to 18.00 GMT inclusive, as these cover the working hours in buildings.

The relationship between radial distance and daytime mean temperature is considerably poorer than in the case of all data considered together:

- 62-75% of the variance is unexplained by  $X_r$ .
- The residual variation is about the same as for all data, but there is much less variation in mean temperature, so the proportion explained is much less.
- The gradients of reducing mean temperature with radial distance are similar for the two summers.

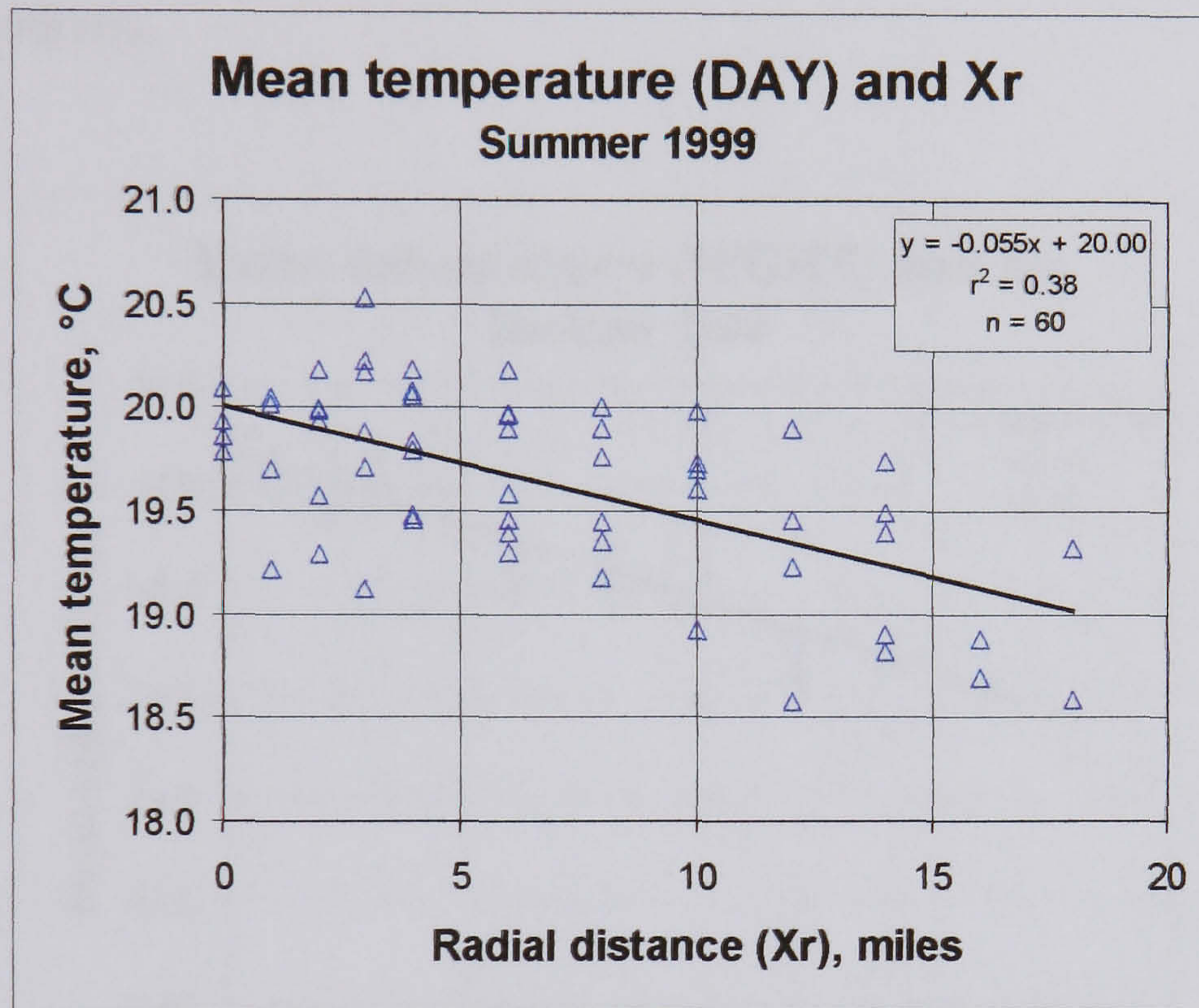


Figure 4.9a: The change in daytime mean temperature with distance from London

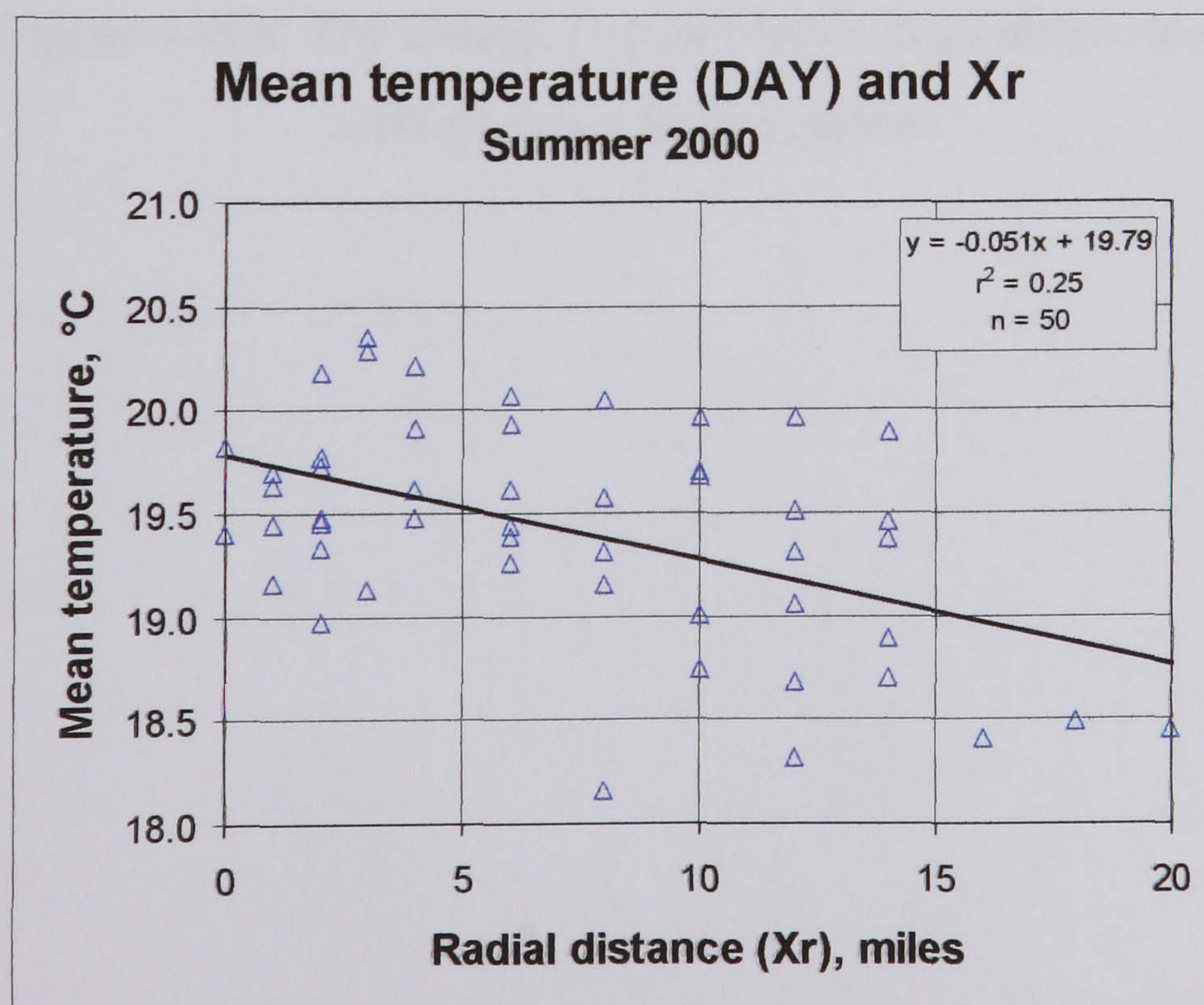


Figure 4.9b: The change in daytime mean temperature with distance from London

### 4.3.1.3 Night-time data

Figures 4.10ab show the change in mean night-time temperature (19.00 to 06.00 GMT inclusive) with radial distance.

It can be seen that the relationship at night is much stronger than in the daytime:

- 69-75% of the variance of night-time mean temperature is explained by radial distance from London.
- The gradients of reducing mean temperature with radial distance are similar for the two summers.

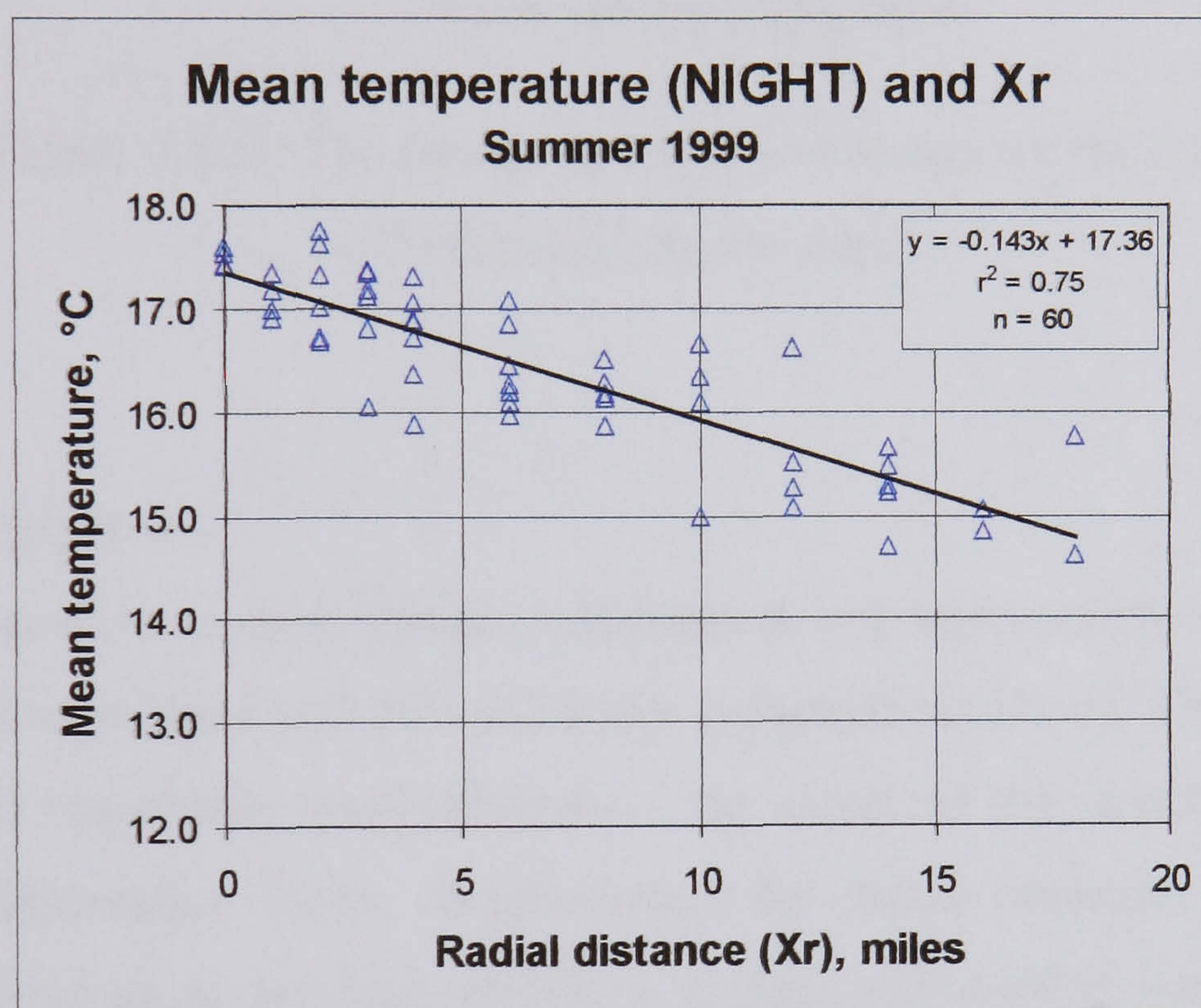


Figure 4.10a: The change in night-time mean temperature with distance from London

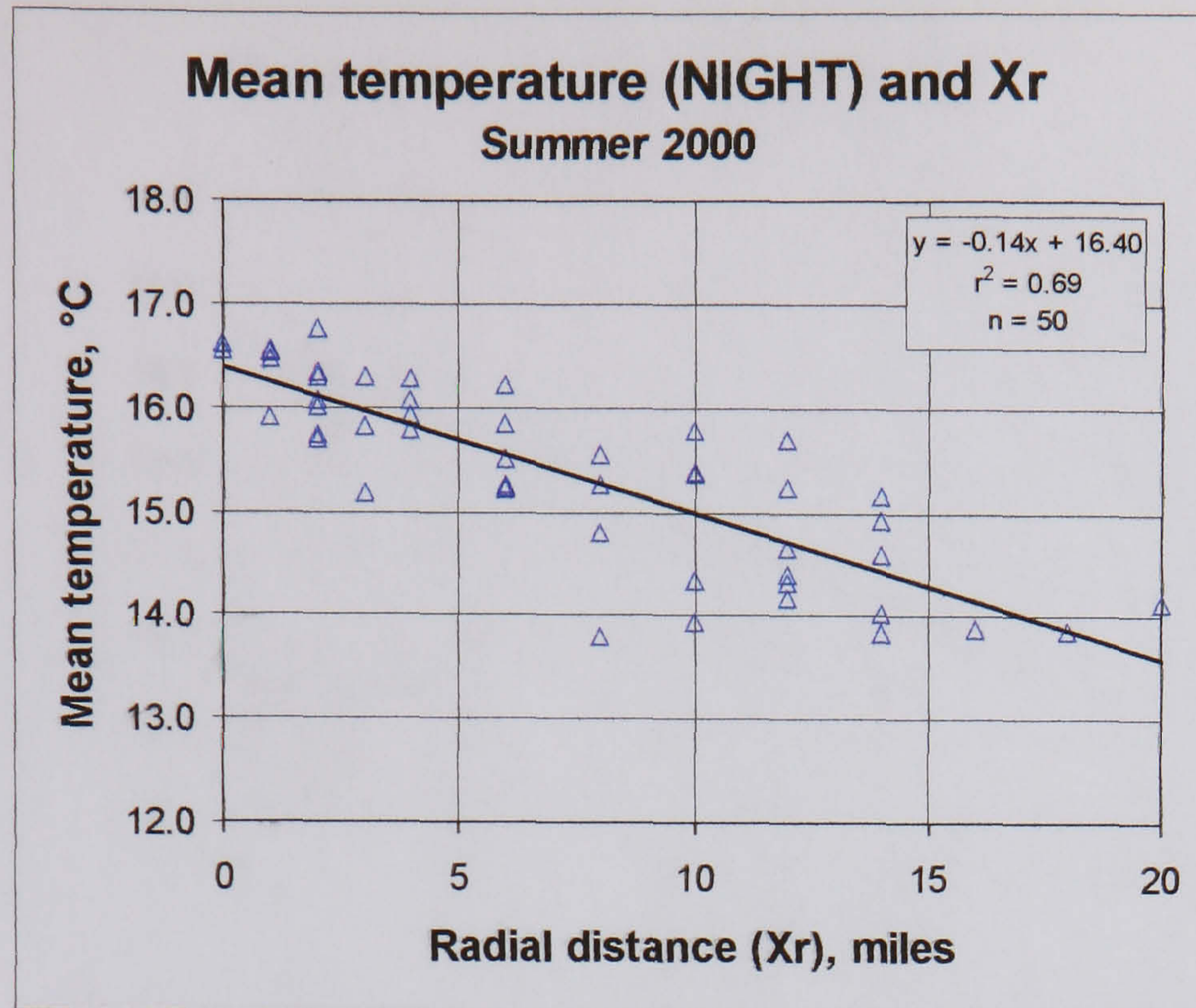


Figure 4.10b: The change in night-time mean temperature with distance from London

#### 4.3.1.4 Adjusted focus

There is no reason to assume that the relationship between temperature and distance should be well-correlated with this particular geographical centre. The focus that has been chosen is essentially quasi-arbitrary – the centre of the monitoring array. By choosing an alternative focus, re-calculating the radial distances from this new centre, and repeating the previous graphs, a stronger relationship was found between distance and mean temperature. See Figures 4.11ab to 4.13ab. The revised foci were located using the optimization tool in MS Excel which uses an iterative technique, here to maximize the coefficient of determination.

The optimization of the origins for maximizing the coefficients of determination,  $r^2$ , shows:

- In each case (all day, daytime, night-time) a stronger relationship is found when the focus is adjusted.
- The directions of the optimized displacements are always East and South, i.e. in the SE sector wrt the monitoring array's focus.



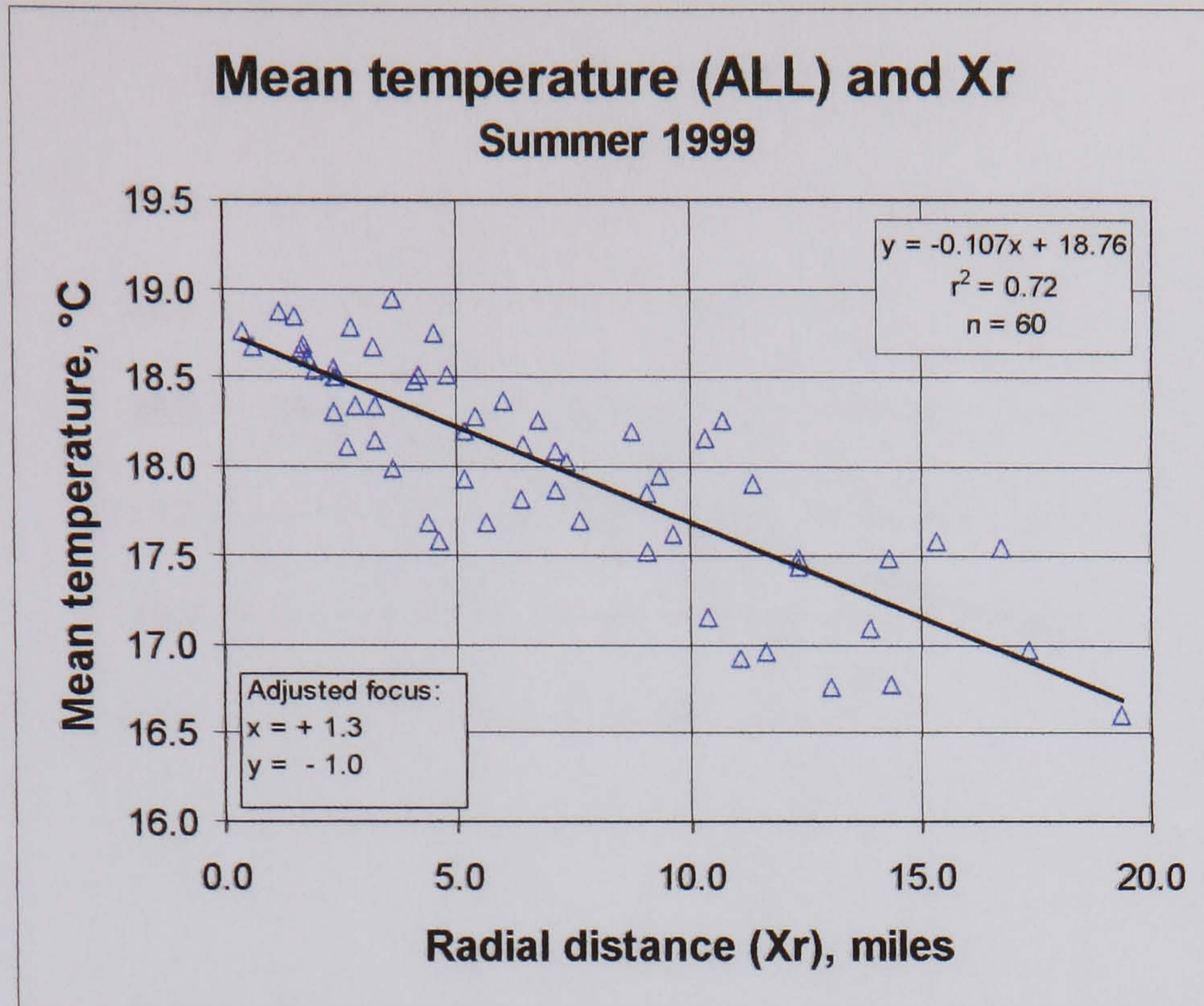


Figure 4.11a: The change in mean temperature with distance from London (adjusted focus)

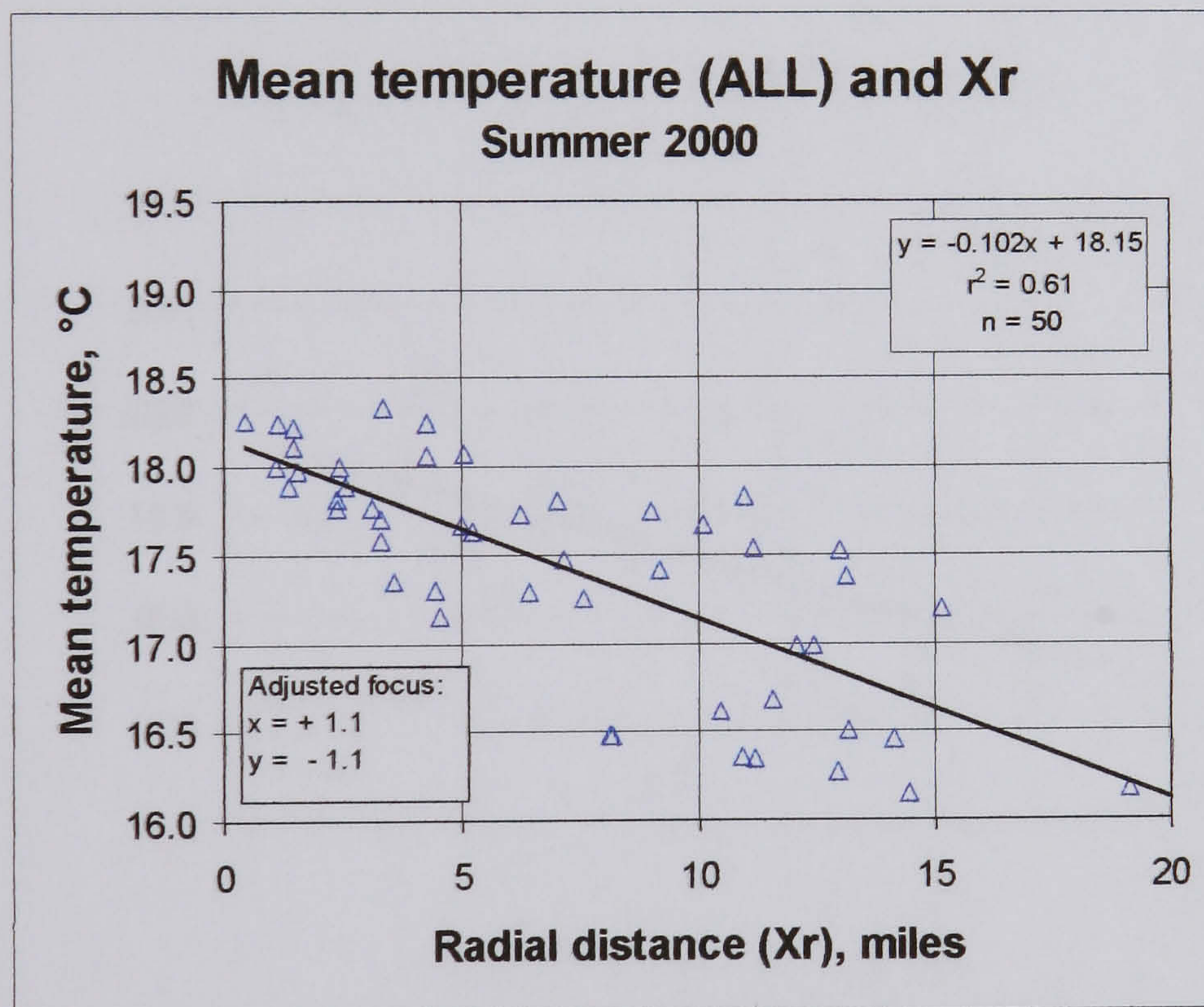


Figure 4.11b: The change in mean temperature with distance from London (adjusted focus)

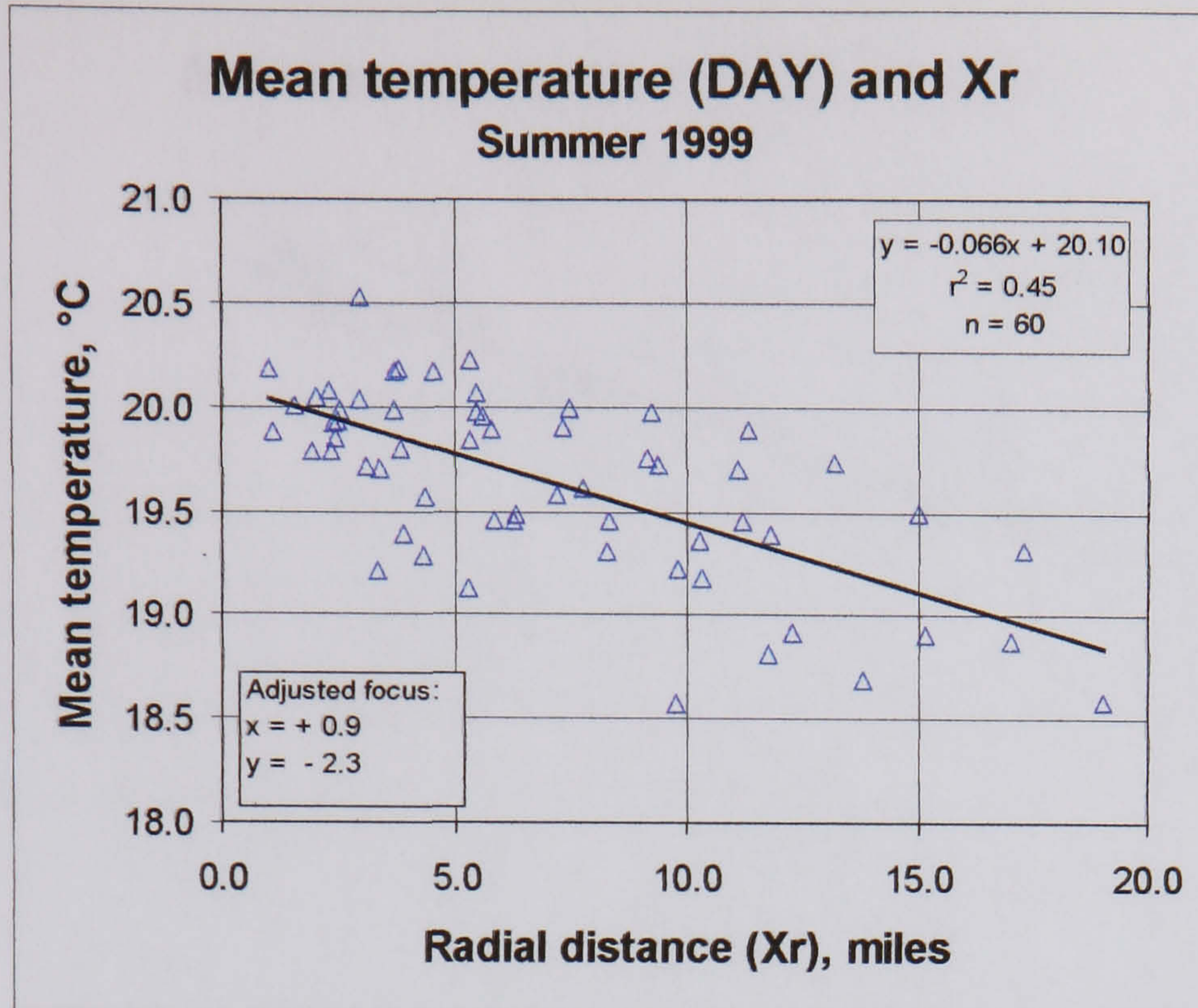


Figure 4.12a: The change in daytime mean temperature with distance from London (adjusted focus)

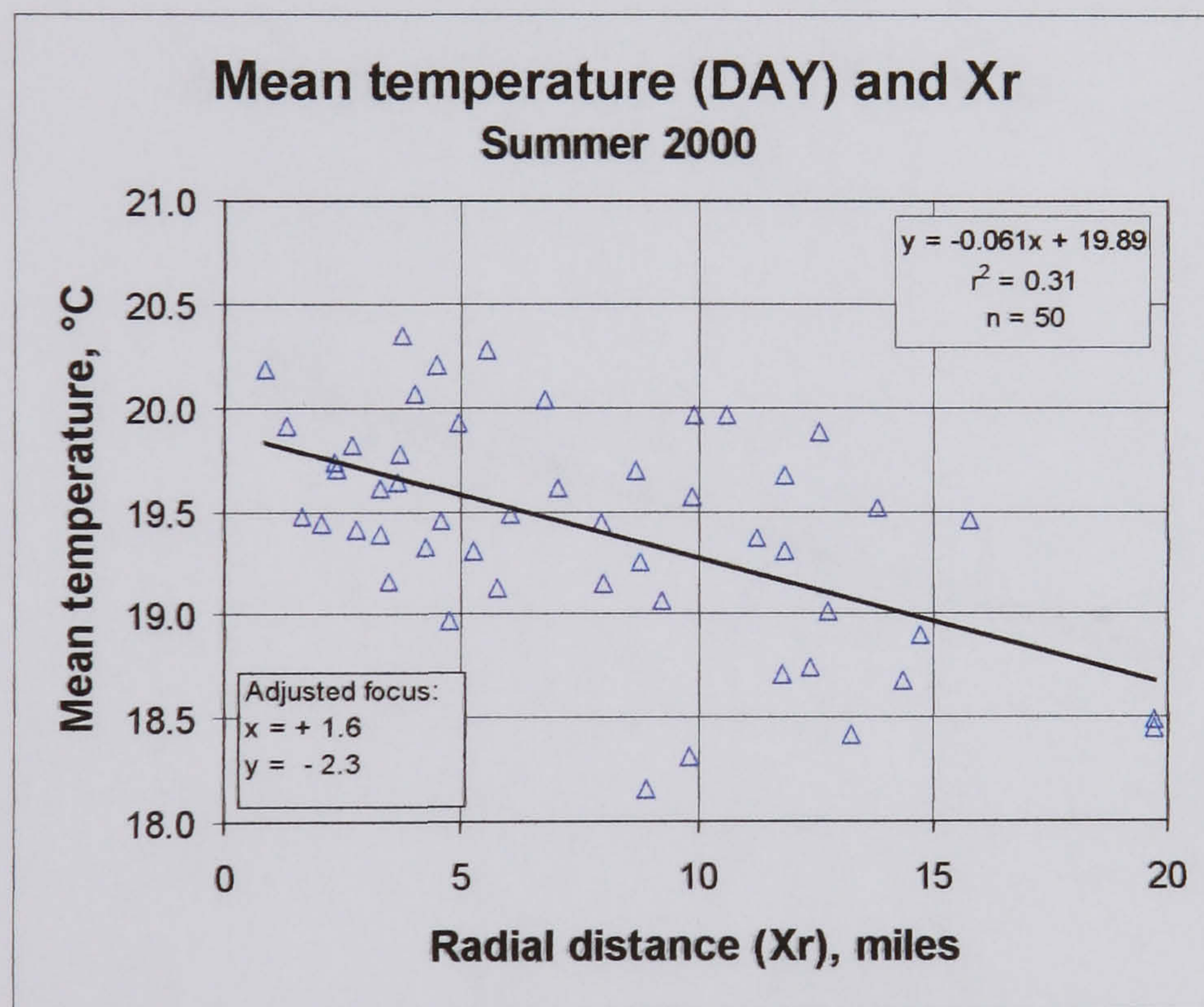


Figure 4.12b: The change in daytime mean temperature with distance from London (adjusted focus)

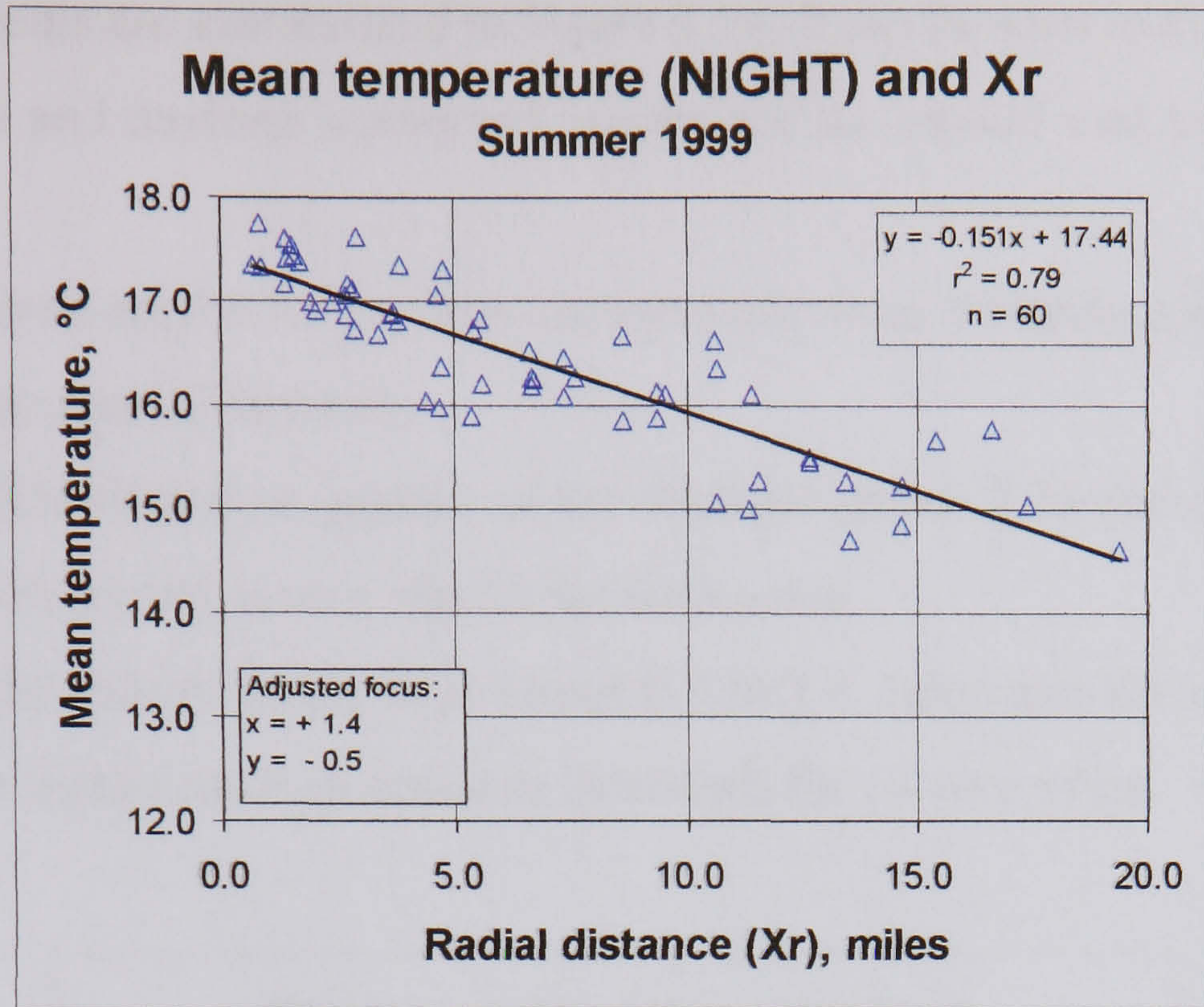


Figure 4.13a: The change in night-time mean temperature with distance from London (adjusted focus)

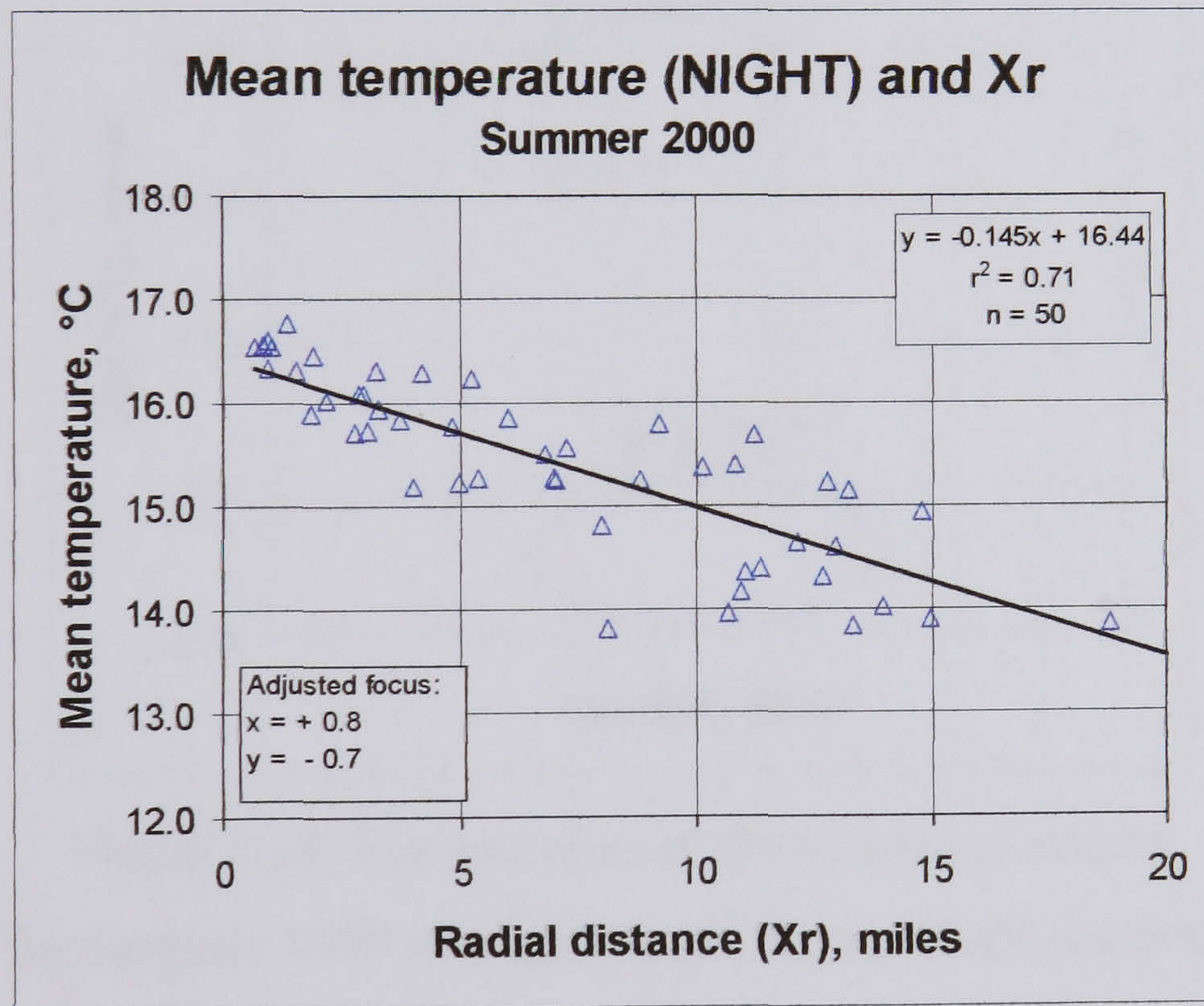


Figure 4.13b: The change in night-time mean temperature with distance from London (adjusted focus)

The displacements are summarized in Figure 4.14. It can be seen in this graph that:

- Night-time and daytime optimized origins are all located east and south of the focus.
- The optimized origins for the two summers are close: 0.6 mile apart (Night-time) and 0.7 mile apart (Daytime)
- The shift Southwards is greater in the daytime (about 2.25 miles) than at night (about 0.6 mile) and is very similar for both years.
- The shift Eastwards varies from about 0.7 to 1.6 miles and the movement from daytime to night-time is in opposite directions for the two years.

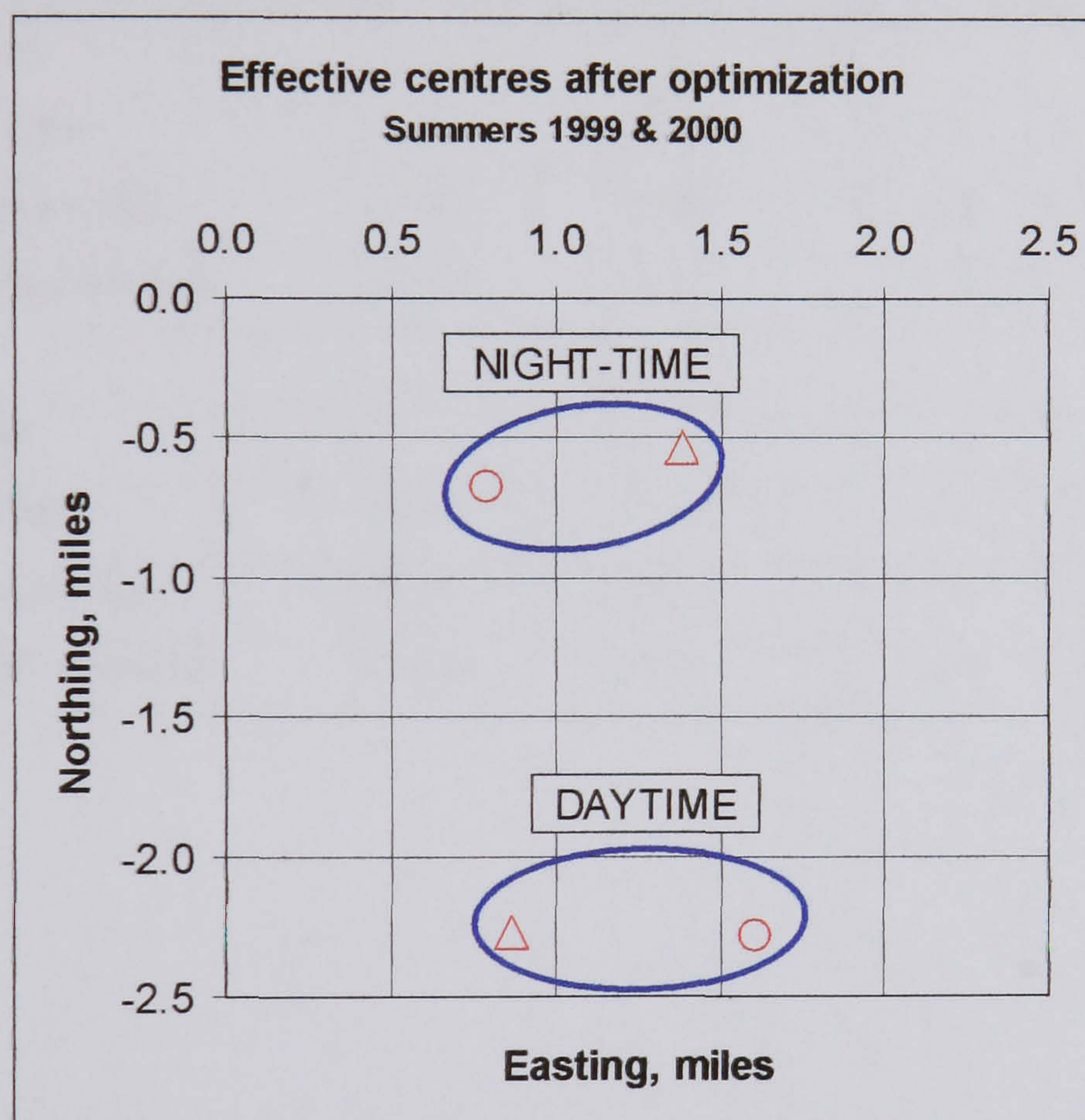


Figure 4.14: The positions of the optimized origins for Summer 1999 (triangles) and Summer 2000 (circles).

Summary of variation of mean temperature with distance:

- The majority of the spatial variation in mean DAYTIME temperature is NOT explained by considering the distance of a point from the centre of London.
- The opposite is the case for mean NIGHT-TIME data (and all data together).
- In each case, a better fit is obtained if the effective thermal centre is taken to be in the SE sector of the city, relative to the monitoring focus.
- The effective thermal centre shifts southwards during the daytime.

The adjustment to the focus, optimizing the regression, significantly improves the amount of variance explained. However, a good relationship exists for night-time data without any adjustment. Table 4.1 summarizes these results.

Table 4.1: Summary of variance in mean temperature explained by distance of each measurement station from London

Summer mean data	Variance explained by distance from focus, %		Adjustment, miles	
	original focus	adjusted focus	x	y
<b>1999</b>				
All data	0.67	0.72	+ 1.3	- 1.0
Daytime data	0.38	0.45	+ 0.9	- 2.3
Night-time data	0.75	0.79	+ 1.4	- 0.5
<b>2000</b>				
All data	0.58	0.61	+ 1.1	- 1.1
Daytime data	0.25	0.31	+ 1.6	- 2.3
Night-time data	0.69	0.71	+ 0.8	- 0.7

### 4.3.2 Mean thermal centres compared with contours

The positions of the mean thermal centres obtained in 4.2.1 by optimized regression (circled) can be visually compared with the mean isotherms for the same periods, plotted as contours in Figures 4.15ab-17ab. The contours have been produced by first interpolating between the 50-60 stations' data to produce temperatures for each cell of a fixed rectilinear grid (100x66) across London. (See Appendix 2 for details of the visualization tool used) The cross-hair on each plot shows the location of the focus of the monitoring array, at the British Museum. All contours are spaced at 0.2°C intervals, but the colour scale varies from plot to plot to maximize visual clarity.

As would be expected, there is close agreement between the centre of temperature as revealed by the pattern of isotherms, and the centre located from optimizing the regression of mean temperature with distance from an adjusted datum. It can be seen that:

- At night-time, there is a single warm centre (Figures 4.17ab).
- In the daytime, there are multiple centres of warmth, so the regression centre does not itself reside in the warmest area, but lies between warmer areas (Figures 4.16ab).
- For night-time data, there is considerable consistency in the pattern and location of the contours between the two summers (Figures 4.17ab).
- For daytime data, there are areas of consistency between the two years, e.g. the warm (residential) area 3 miles SW of the monitoring focus; the depression 2-3 miles NW of the focus associated with Regents Park and Primrose Hill Park (Figures 4.16ab).
- The depression 8 miles SW of the focus in summer 2000 data is caused by the addition of a measurement station in Richmond Park. This identifies a cooler area associated with a park, but also shows the sensitivity of the contour plots to individual stations. At increasing distances from London the inter-station spacing increases and contours are interpolated from fewer data.

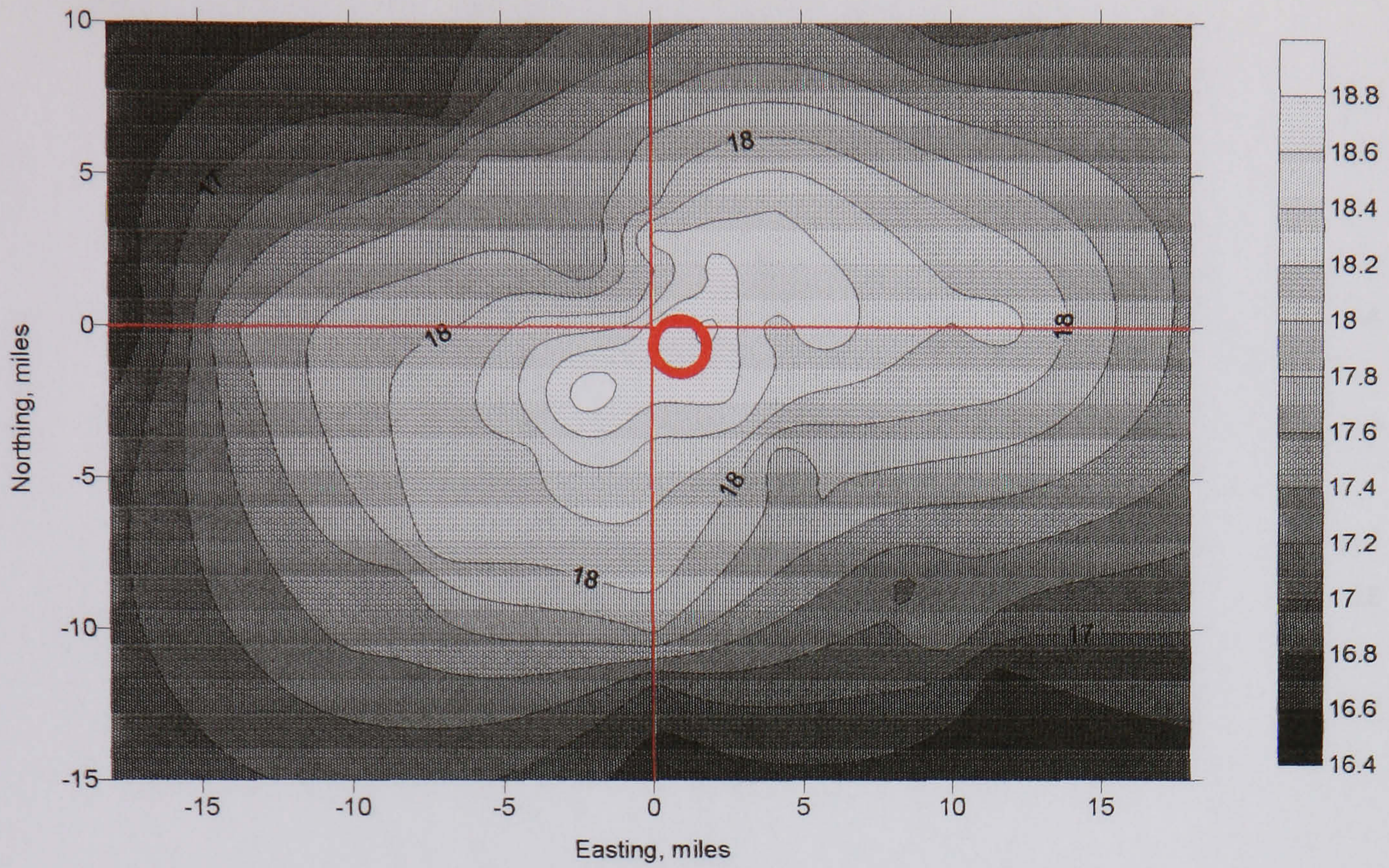


Figure 4.15a: Mean temperature Summer 1999 (ALL)  
and effective thermal centre

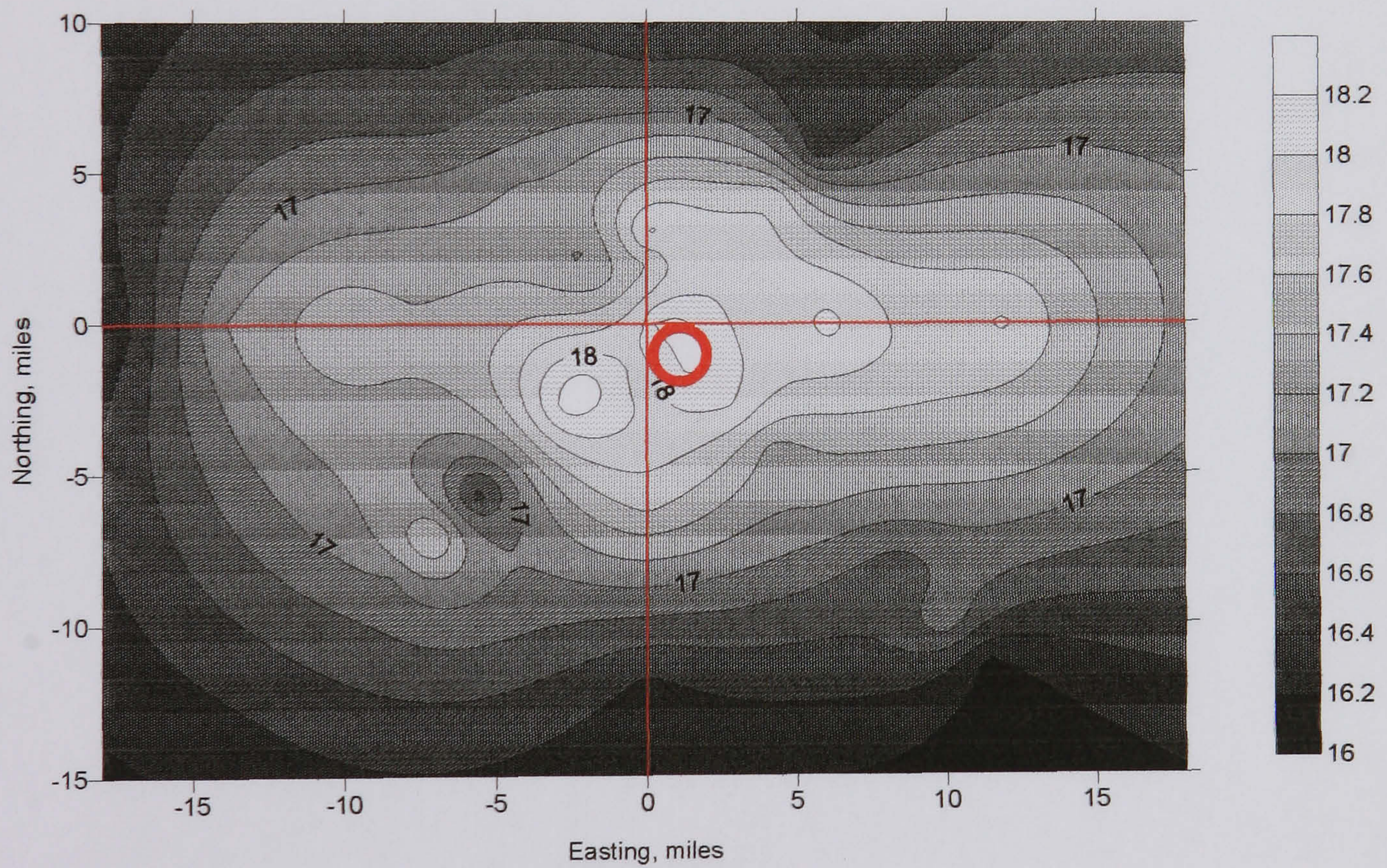


Figure 4.15b: Mean temperature Summer 2000 (ALL)  
and effective thermal centre

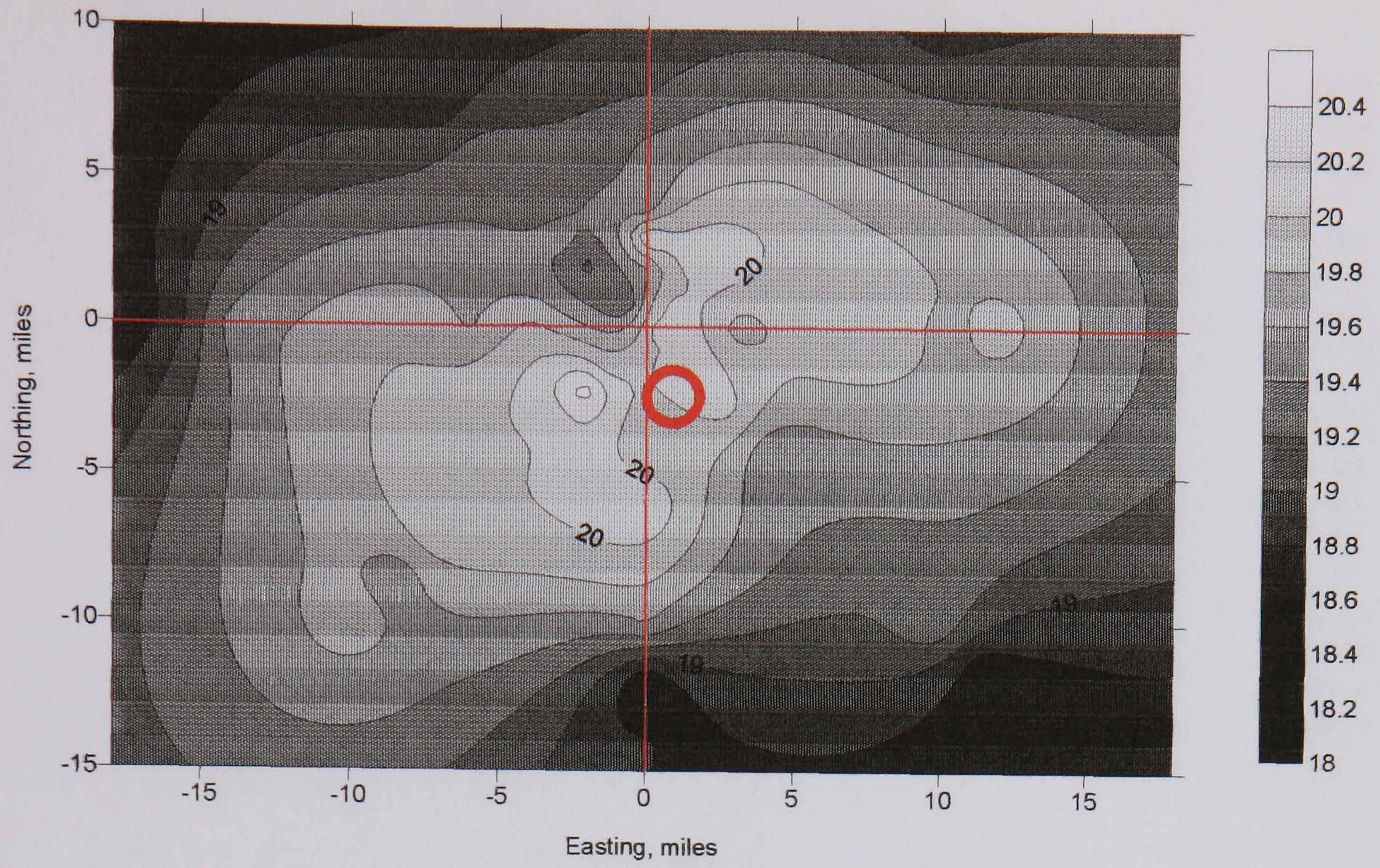


Figure 4.16: Mean temperature Summer 1999 (DAYTIME)  
and effective thermal centre

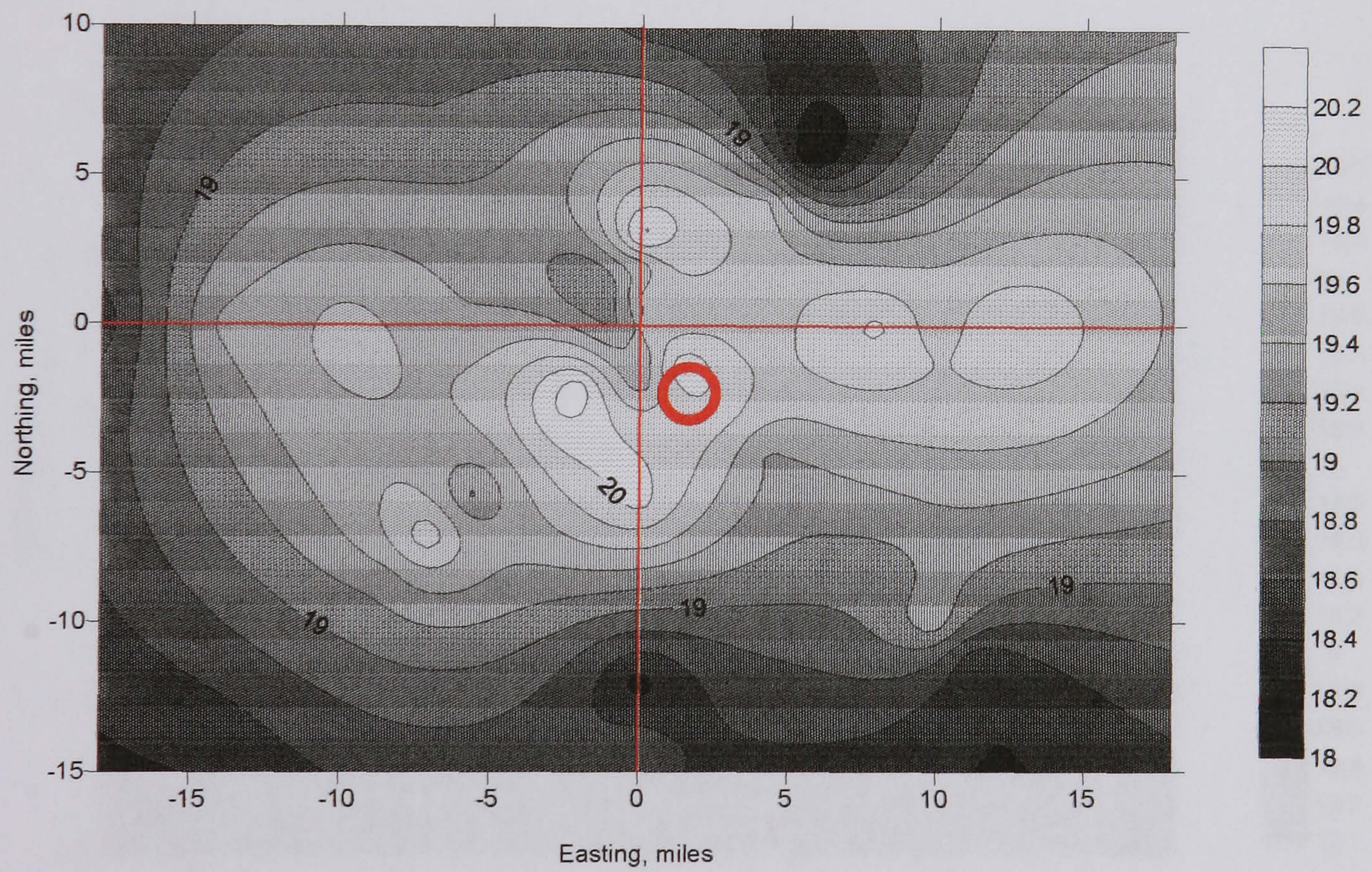


Figure 4.16b: Mean temperature Summer 2000 (DAYTIME)  
and effective thermal centre



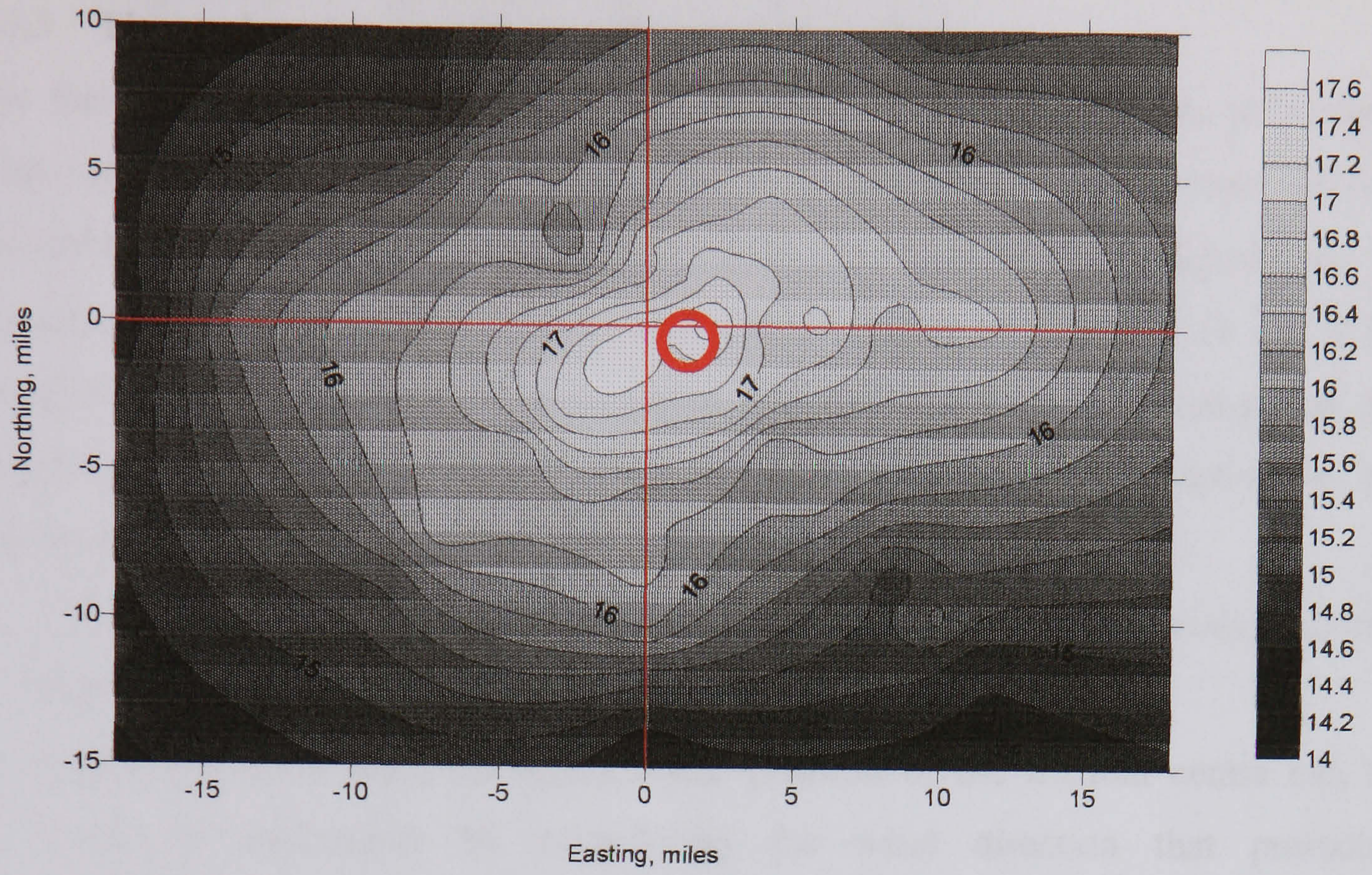


Figure 4.17a: Mean temperature Summer 1999 (NIGHT-TIME)  
and effective thermal centre

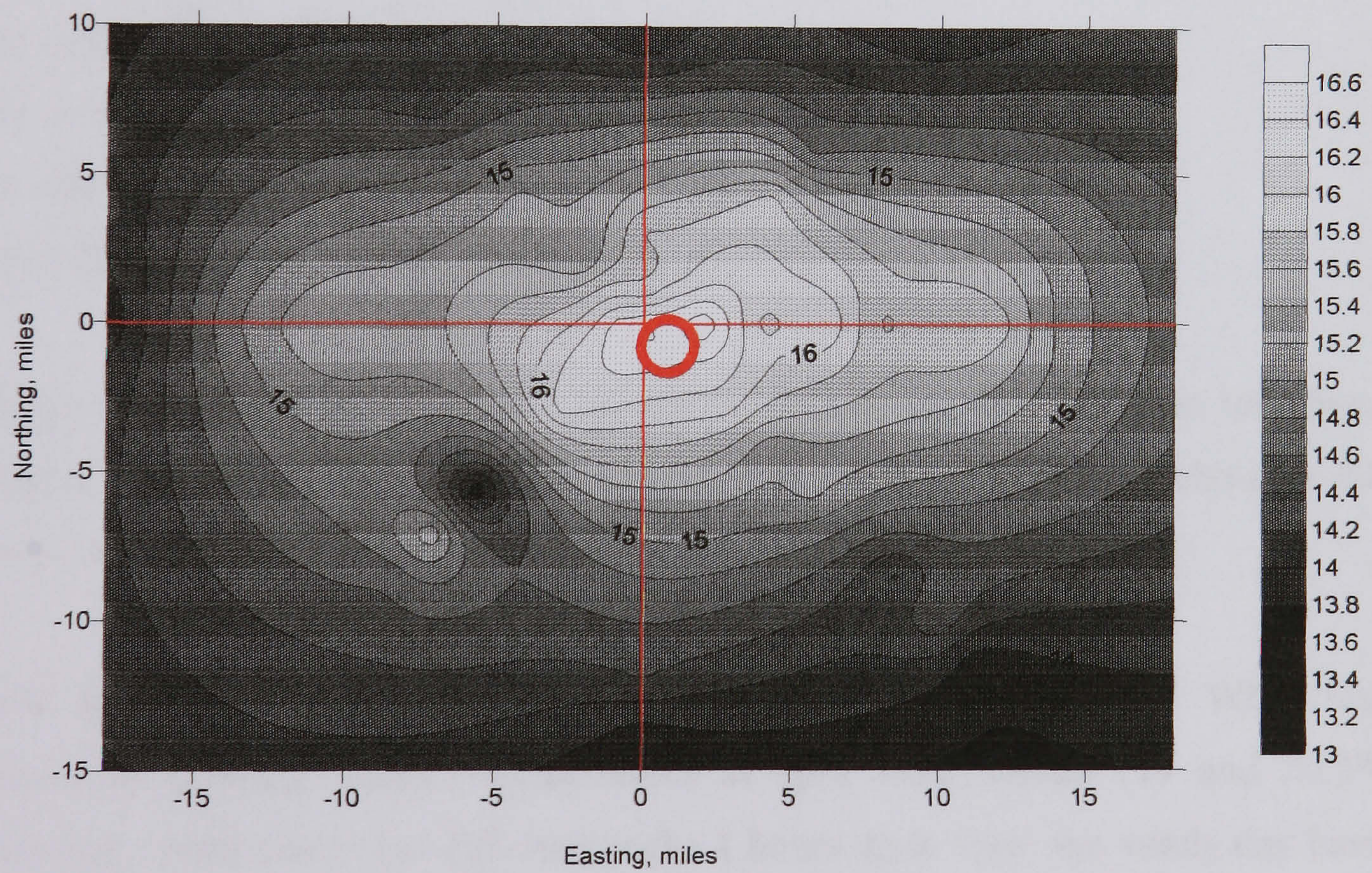


Figure 4.17b: Mean temperature Summer 2000 (NIGHT-TIME)  
and effective thermal centre

### **4.3.3 Thermal centre movement with wind direction**

The thermal centre shifts in response to a change in wind direction. The indications from visually tracking the movement of the isothermal centre hour by hour are that this centre can move several miles. To illustrate this, the temperature distribution on consecutive nights at the same time (midnight) is shown in Figures 4.18 and 4.19. Wind direction and speed are also shown. Neither day had been sunny and the temperature was similar. However, it was breezy, but the wind direction on the second night was opposite to that on the first one. It has been found that:

- The thermal centre appears to move 3-4 miles in line with the wind direction change.
- Examining other days, the approximate position of the thermal centre can be predicted consistently by considering the wind direction that prevailed beforehand, particularly in the previous two hours.

### **4.3.4 Intensity distribution by wind speed**

The temperature distribution across the study area will depend on wind speed because air flow will tend:

- to reduce or dissipate temperature differences
- to shift centres of warmer or cooler areas downwind.

This affects the shape of the contours.

Figures 4.20 and 4.21 show the intensity distribution at 9pm (BST) on two days in August '99 (13 and 31 August). The first day was windy, the second relatively calm. Mean wind speeds for the days were 2.8m/s and 0.7m/s.

Both days had similar total solar energy inputs (3418 and 3678 Wh/m<sup>2</sup>/day). Maximum (contour centre) temperatures at 9pm were similar (19 and 20.5°C). However, cloud cover was different in the 4 hours up to 9pm: the windy day having almost 8/8 cover, and the calmer day 6/8 cover.

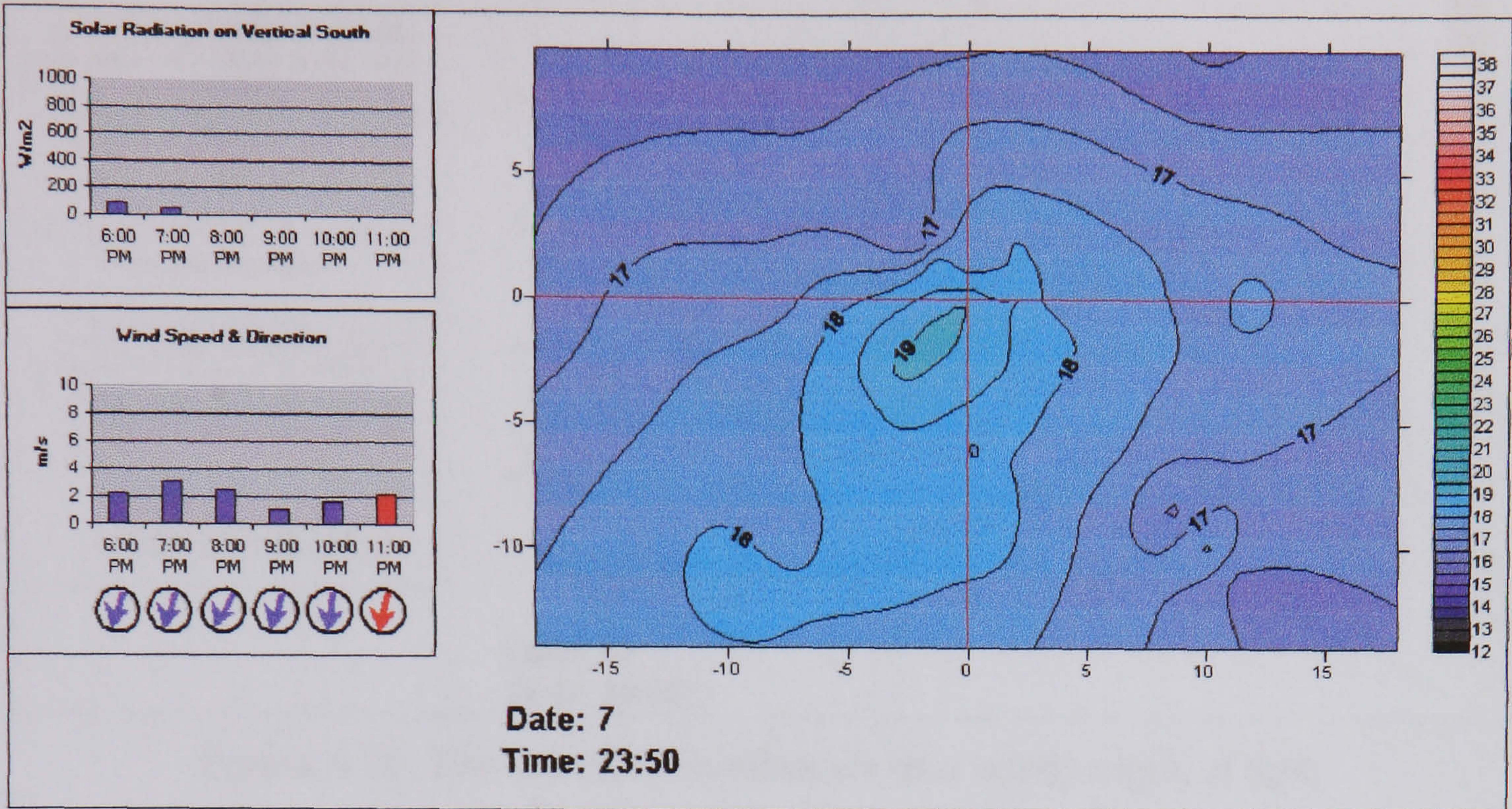


Figure 4.18: The temperature distribution at 23.50 on 7 August 1999.

The thermal centre is SW of the focus

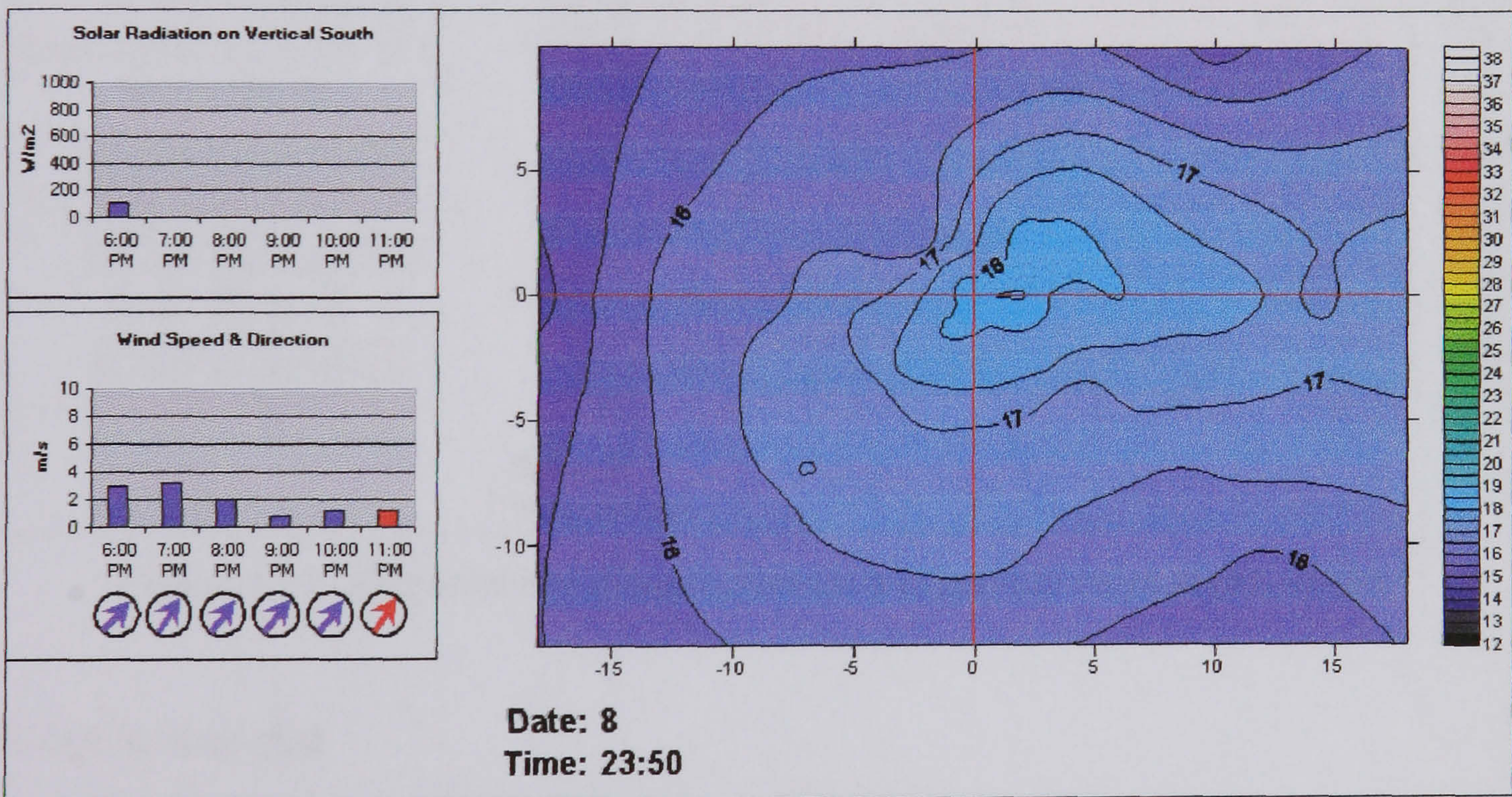


Figure 4.19: The temperature distribution at 23.50 on 8 August 1999.

The thermal centre is E to NE of the focus

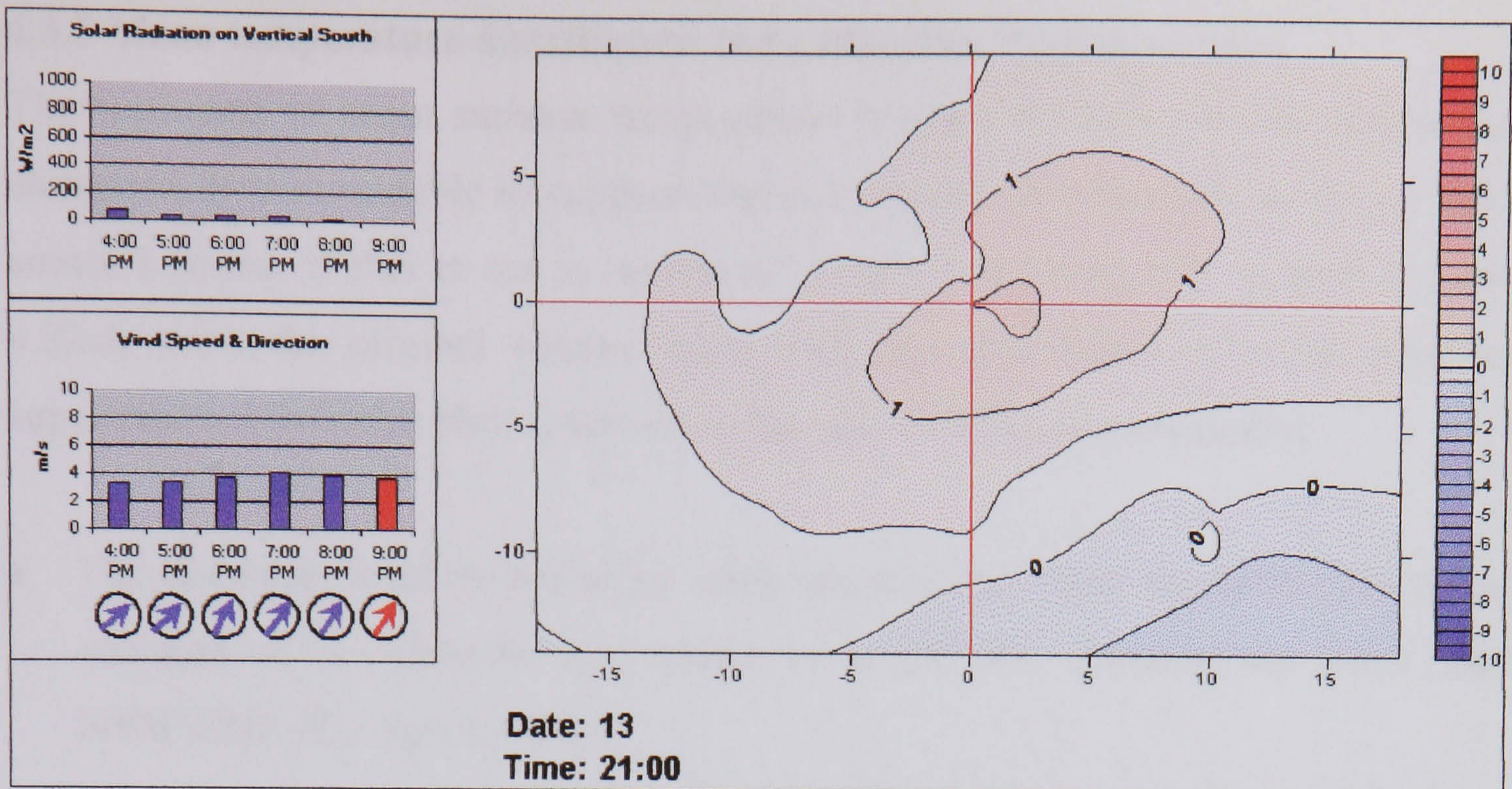


Figure 4.20: The intensity distribution on a windy night, at 9pm

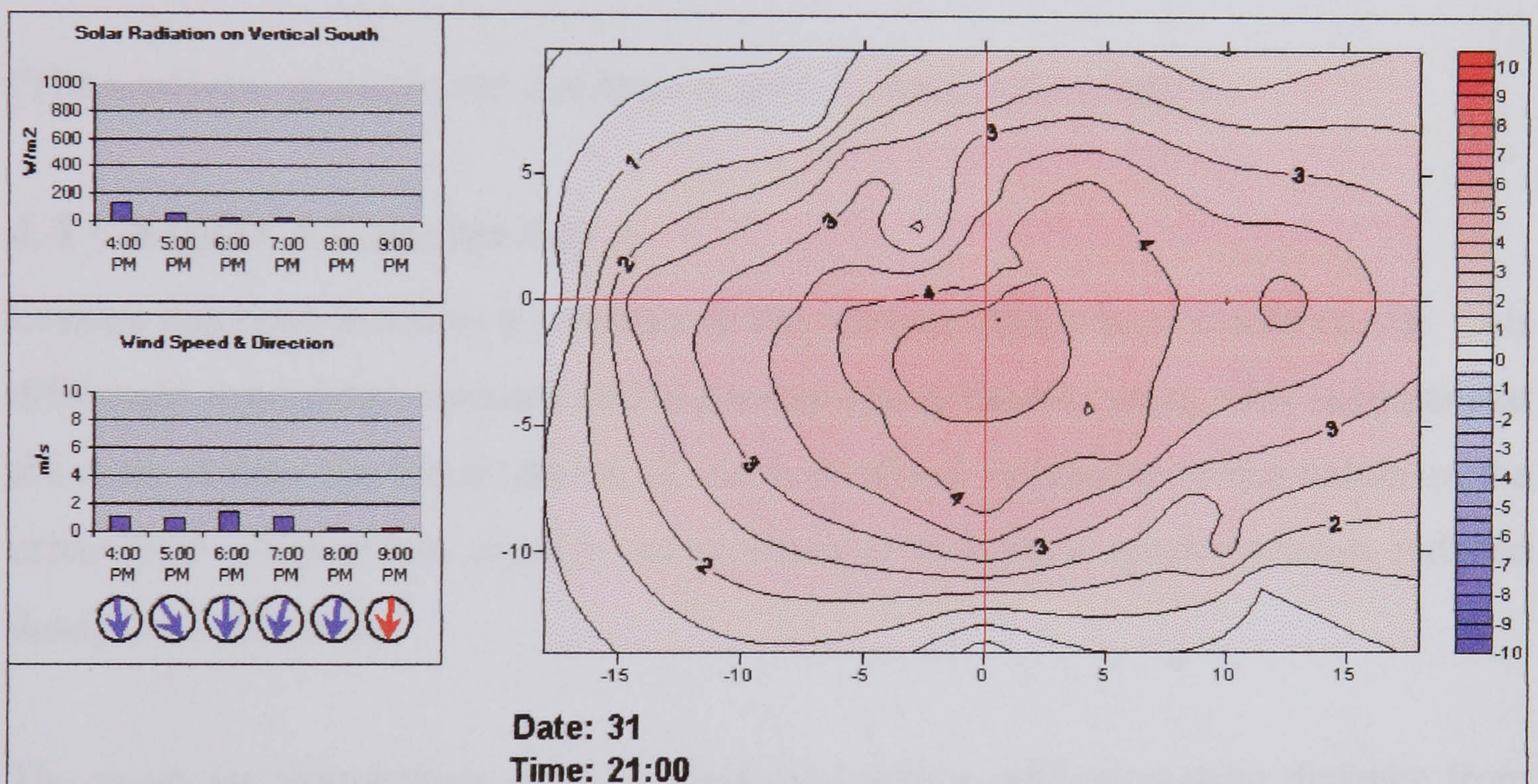


Figure 4.21: The intensity distribution on a relatively calm night, at 9pm

It can be seen that:

- The distribution on the windy day is less pronounced (smaller gradients), and stretched out in line with the wind direction.
- The shift in thermal centre with wind direction can also be seen.

It should be noted that the difference in cloud cover would be responsible for some of the contrast between the two distributions.

### **4.3.5 Mean temperature distribution and prevailing wind directions.**

The isotherms of mean summer temperatures (Figures 4.15ab) are not circular but elongated. It is reasonable to suppose that one reason for this might be the air flow across London, if this is not symmetrical in direction through the period. Figures 4.22ab show the original contour plots with the distribution of wind direction superimposed (as polar plots), centred on the optimized regression centres.

- The dominant wind direction for each summer was from the SSW. The mean contours of temperature are spread in a SW:NE direction for 1999, and WSW:ENE direction for 2000.
- There is *some* correspondence apparent between prevailing wind direction and contour shape, but other factors are clearly important.

(The northerly spikes in the distribution are a measurement artefact.)

## **4.4 Chapter 4 Conclusions**

London has been found to be warmer in the summer than a rural reference site. This difference is greatest overnight and at a minimum in the afternoon. This suggests that the main reason for the existence of the heat island in London is the nature of the urban form – higher heat capacity, more effective absorption of solar energy, reduced dissipation efficiency.

The mean air temperature at a site tended to reduce with increasing distance from London, in or near parkland, or at higher wind speeds. A change in wind direction was accompanied by a shift in the location of the centre of the heat island.

The next chapter uses analysis of variance to establish more formally some of the factors that affect the London heat island.

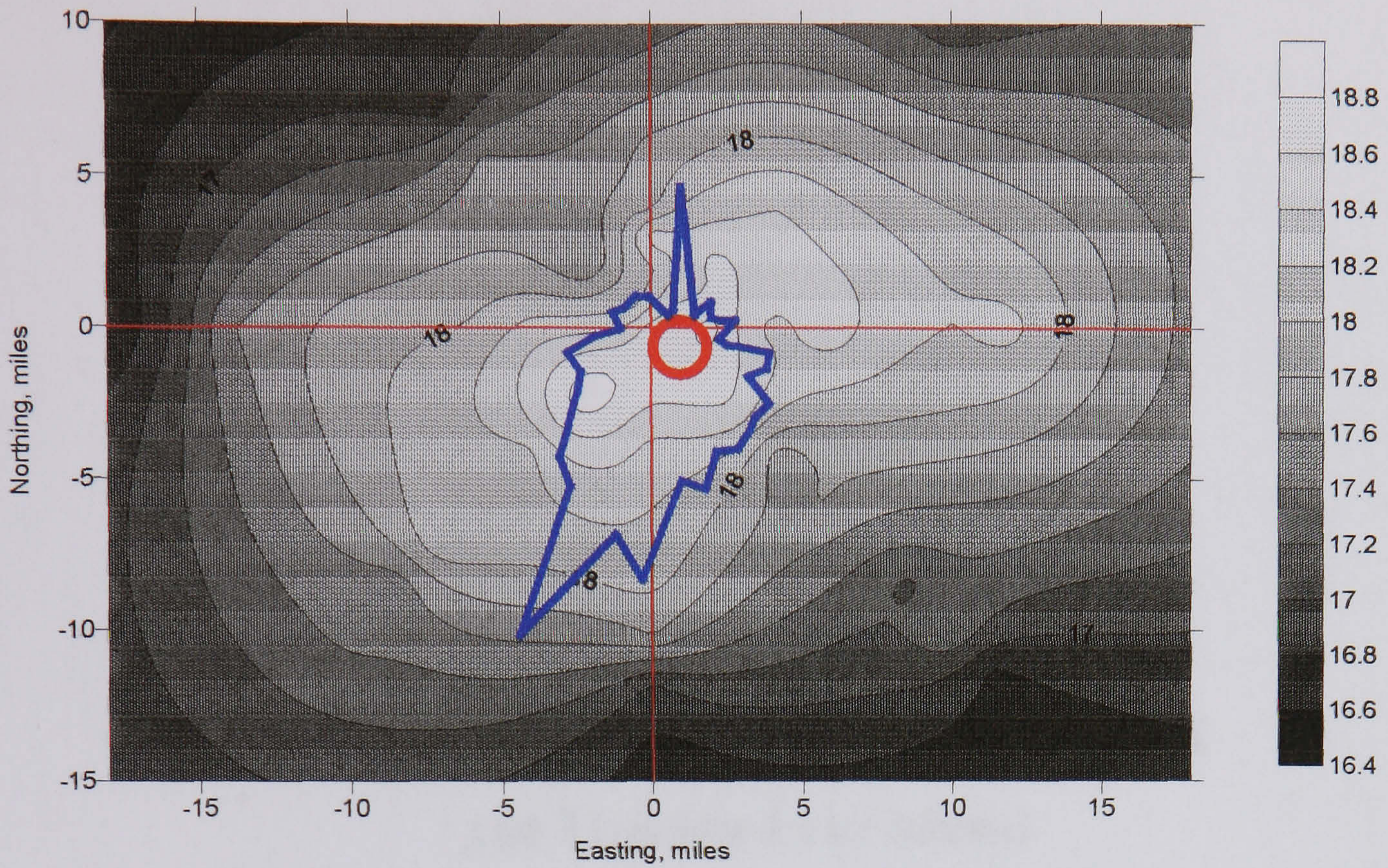


Figure 4.22a: Mean temperature Summer 1999 (ALL)  
and wind direction distribution

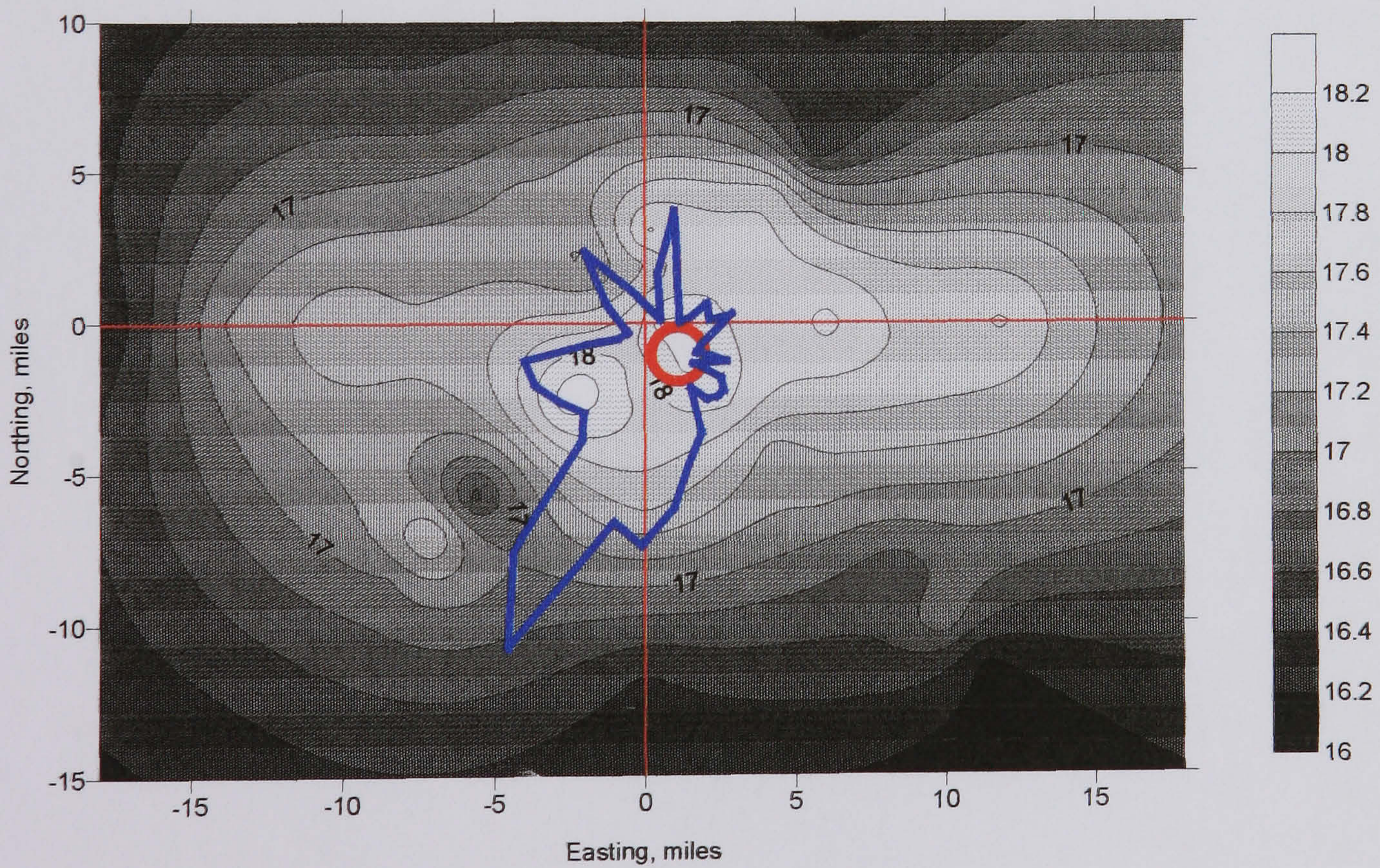


Figure 4.22b: Mean temperature Summer 2000 (ALL)  
and wind direction distribution

## **CHAPTER 5**

### **Statistical analysis of factors affecting the London heat island**

# CHAPTER 5 – Statistical analysis of factors affecting the London heat island

## 5.1 Introduction

This chapter attempts to identify local or site-related factors, as well as confirming the weather related ones, that are associated with differences in temperature or heat island intensity. By controlling for weather factors and looking for associations with site characteristics, an attempt can be made to identify the impact on air temperature of urban factors. These may be useful in either predicting the effects of the heat island on energy consumption, or in trying to mitigate the effects of it.

The data used for the analysis presented in this chapter are daily, and cover the summertime of August and September 1999, and July, August and September 2000, i.e. 153 days over two years. Daytime and night-time data are considered separately. Daytime data consist of the mean temperature differences from 08:00 to 17:00 GMT inclusive. Night-time data cover 22:00 to 04:00 inclusive. The day and night hours have been restricted for this analysis in order to emphasize the daytime and night-time differences.

Figures 5.1 and 5.2 show the distribution of the daytime and night-time data to be close to normal, a prerequisite for parametric statistical analysis.

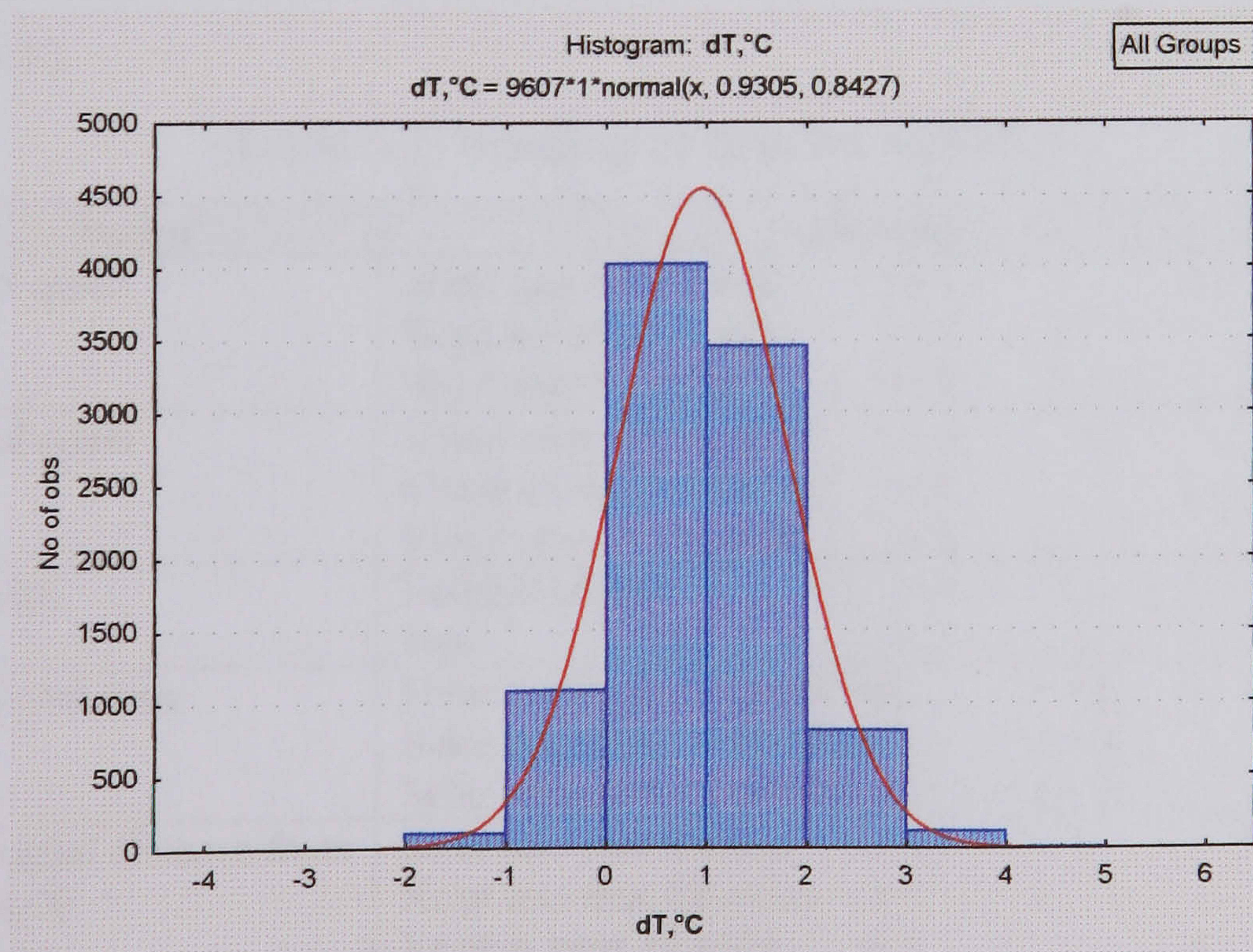


Figure 5.1: The distribution of mean daytime local heat island intensity (dT) for the summertime data



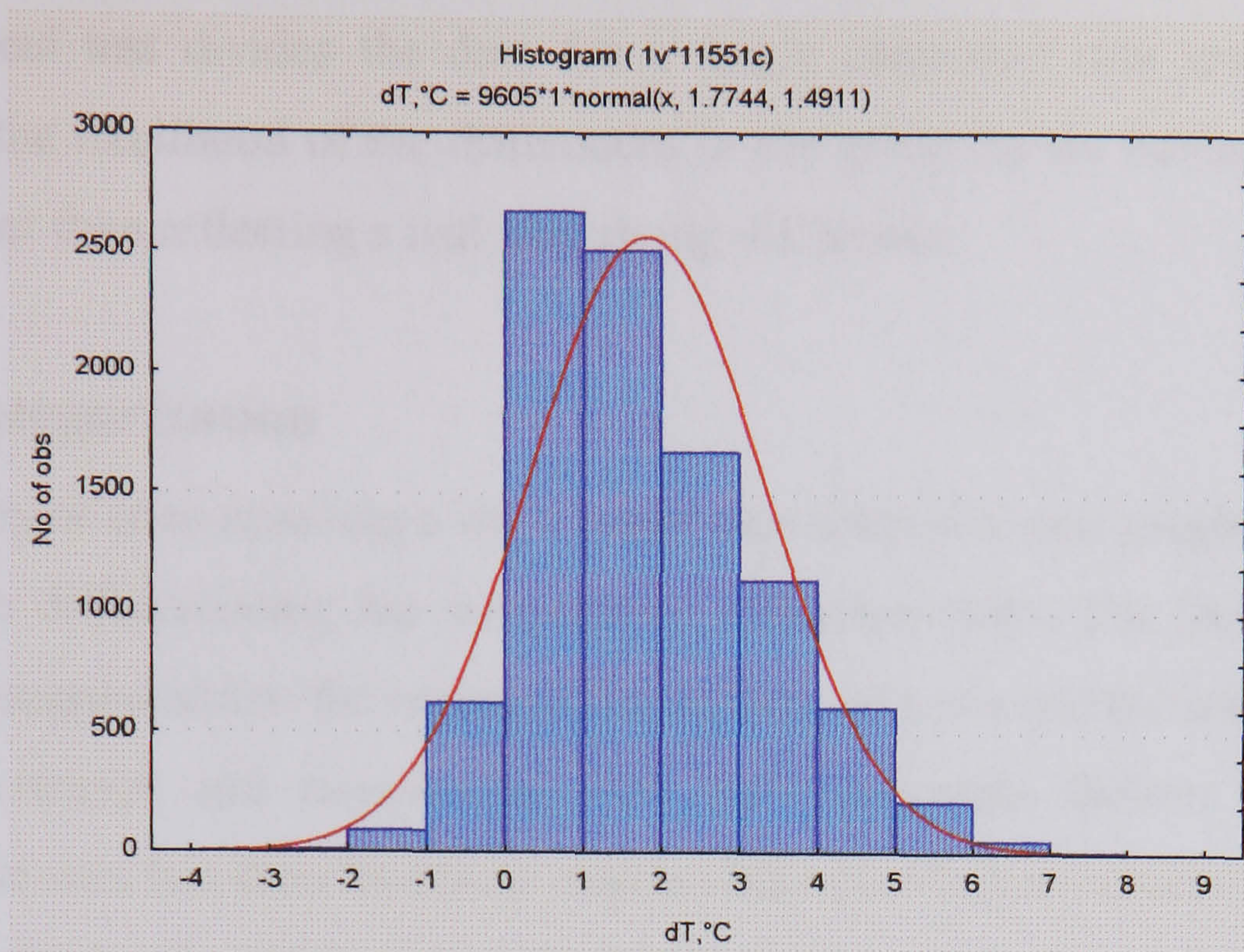


Figure 5.2: The distribution of mean night-time local heat island intensity (dT) for the summertime data

An explanation for the variation in local dT shown in these two figures is sought in this chapter.

## 5.2 Banding the data

By choosing likely explanatory factors (wind speed, etc.) and banding their values, it is possible to test for significant differences in the mean dT for each factor. A series of one-way analysis of variance tests (ANOVAs) was run on the following factors (see Table 5.1).

Table 5.1: Banding of data for ANOVA

Factor	Banding
Wind speed	Wind speed $\leq 3$ m/s ::= 1
	Wind speed $\leq 5$ m/s ::= 2
	Wind speed $> 5$ m/s ::= 3
Cloud cover	Cloud cover $\leq 4$ oktas ::= 1
	Cloud cover $\leq 6$ oktas ::= 2
	Cloud cover $> 6$ oktas ::= 3
Rainfall	Rainfall of zero ::= 0
	else ::= 1
Solar radiation	Solar radiation $\leq 200$ W/m <sup>2</sup> ::= 1
	Solar radiation $\leq 400$ W/m <sup>2</sup> ::= 2
	Solar radiation $> 400$ W/m <sup>2</sup> ::= 3
Site radial distance from focus, Xr	Xr of less than 4 miles ::= 1
	Xr of less than 10 miles ::= 2
	Xr of at least 10 miles ::= 3
Site greenness, Inner	Greenness of less than 30% ::= 1 (see section 5.4)
	Greenness of 30% or more ::= 2
Site greenness, Outer	as Inner
Site category	1..8 (see section 5.3)

This statistical test divides the data for a single parameter into groups and then determines the likelihood of the differences in the group means having occurred by chance, rather than reflecting a real underlying difference.

### 5.3 Site categorization

A simple way of encompassing a site's major characteristics was sought which might be useful in differentiating the temperature difference data. The literature review (Chapter 2) suggested that the nature of the surfaces at a site and the access to the sky for energy receipt and re-emission were both important factors. Each of the measurement sites has therefore been categorized according to criteria based on type of surface (which affects heat capacity) and sky view. Eight categories were defined and are shown below in Table 5.2. A list of all the categorized sites appears in Appendix 3.

The categories are aimed at representing increasing urbanization, i.e. increasing local heat capacity, and decreasing vegetation and sky view. It does not allow a good description of every site, but it does allow most of the sites to be categorized reasonably consistently.

Table 5.2: The categorization of the measurement station sites

Category No.	Height/Width ratio of street, $x$	Surface	Example site
1	$x=0$	Grass, etc.	Rural fields, or large park, or trees
2	$x=0$	Hard and grass	Housing near park or field
3	$x=0$	Hard	Urban derelict or unbuilt area or car park
4	$0 \leq x < 0.3$	Hard, very wide gorge	Low density residential area
5	$0.3 \leq x < 0.5$	Hard, wide gorge	Medium density urban area
6	$0.5 \leq x < 1$	Hard, wide gorge	High density urban area; around focus
7	$1 \leq x < 2$	Hard, medium gorge	Liverpool Street station site
8	$x \geq 2$	Hard, narrow gorge	Grafton Street*

\*Category 8 is defined, but there are limited data, for one site only.

### 5.4 Site greenness

Although implicit in the site categorization of 5.4.2, vegetation has been assessed independently and in more detail. A sample of 24 sites was chosen (the same sites as used in the simulation work, Chapters 7 and 8) and an inner and outer circle defined

centred on each measurement station. An inner 125m radius area was assessed for percentage greenness, and the annulus to 500m radius assessed separately. These percentages are referred to here as Inner and Outer site greenness. A fuller description of the determination of site greenness from aerial photographs is given in Appendix 4.

## 5.5 One-way ANOVA results

Figures 5.3 to 5.18 show the mean values of dT when grouped by the various weather and site factors. Solar radiation for the night-time data refers to the solar radiation during the earlier part of the day. The 95% confidence interval for each group mean is shown by the vertical bars. Daytime and night-time graphs have separate scales. The important aspects of each graph are whether there is a discernible trend in the group means and whether they are clearly separated from each other, i.e. the bars of the confidence interval do not overlap.

All eight factors are found to be statistically significant ( $p=0.003$  or less) in dividing the daytime and night-time data into groups with different mean values. Table 5.3 summarizes the directions of the effects on dT.

Table 5.3: Summary of the effects of various factors on the daytime and night-time temperature differences measured in London

<b>Factors associated with increasing dT</b>	<b>Factors associated with decreasing dT</b>
Solar radiation Site category	Wind speed Cloud cover Rainfall Site radial distance Site greenness, Inner & Outer

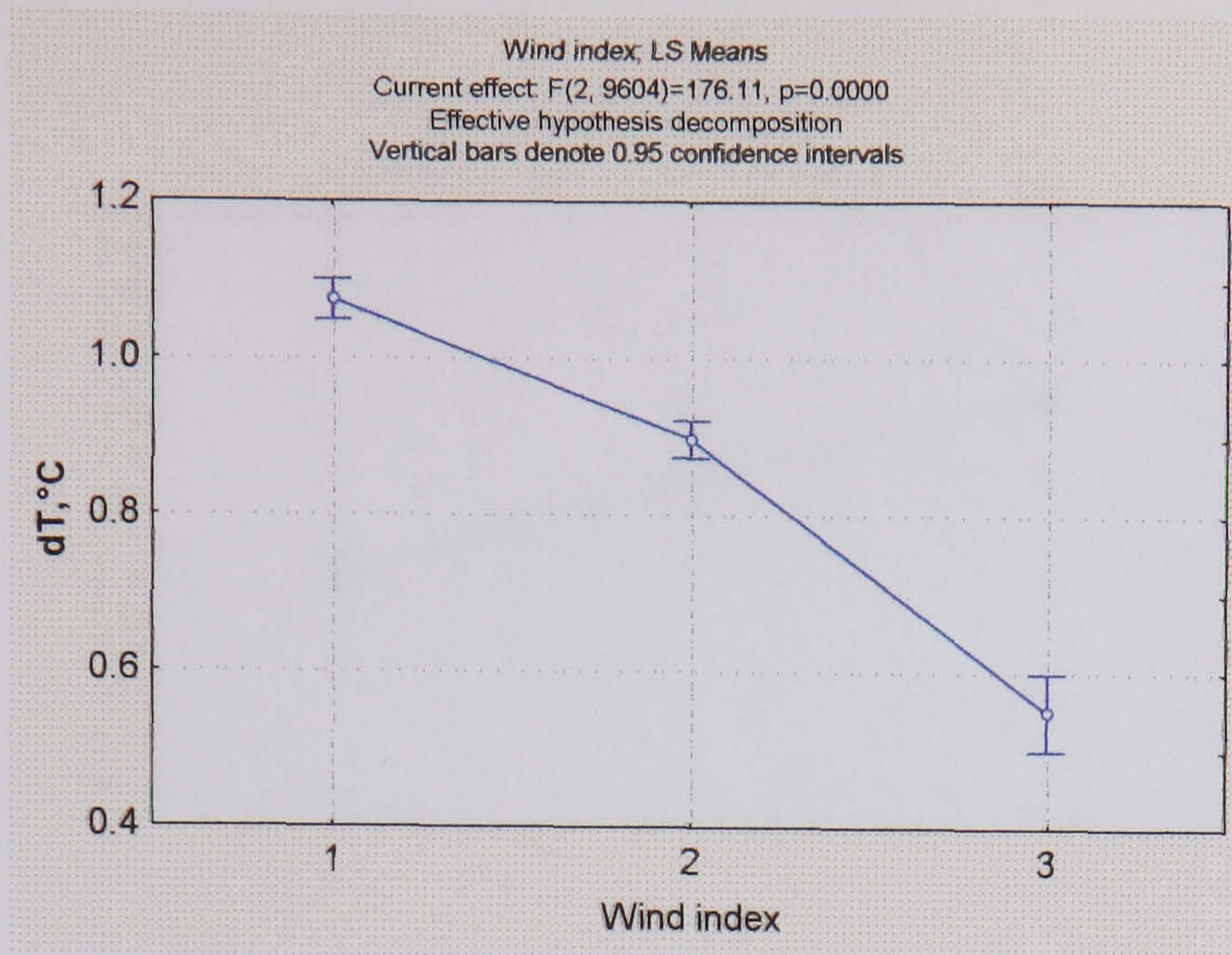


Figure 5.3: Mean dT grouped by wind speed (DAYTIME)

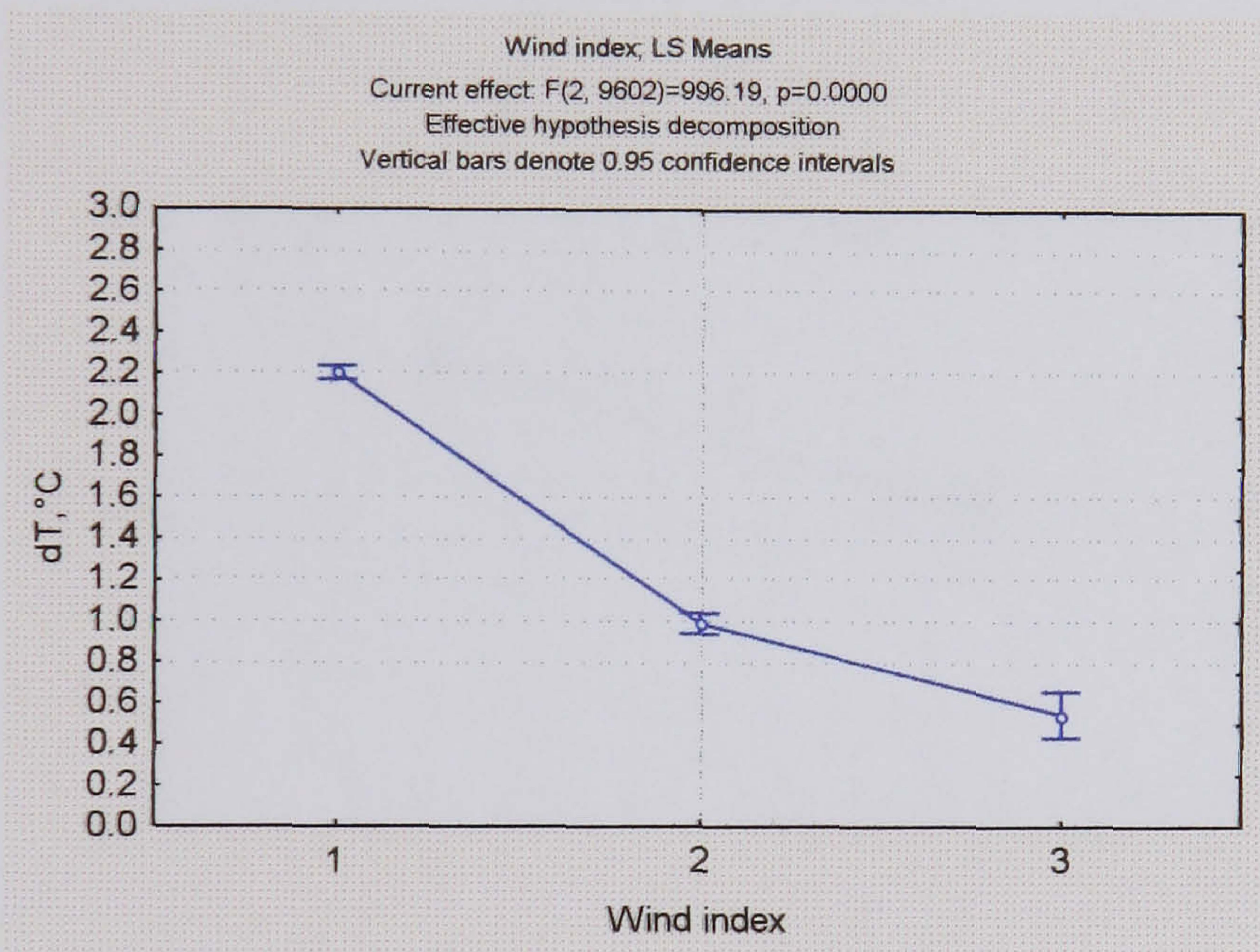


Figure 5.4: Mean dT grouped by wind speed (NIGHT-TIME)

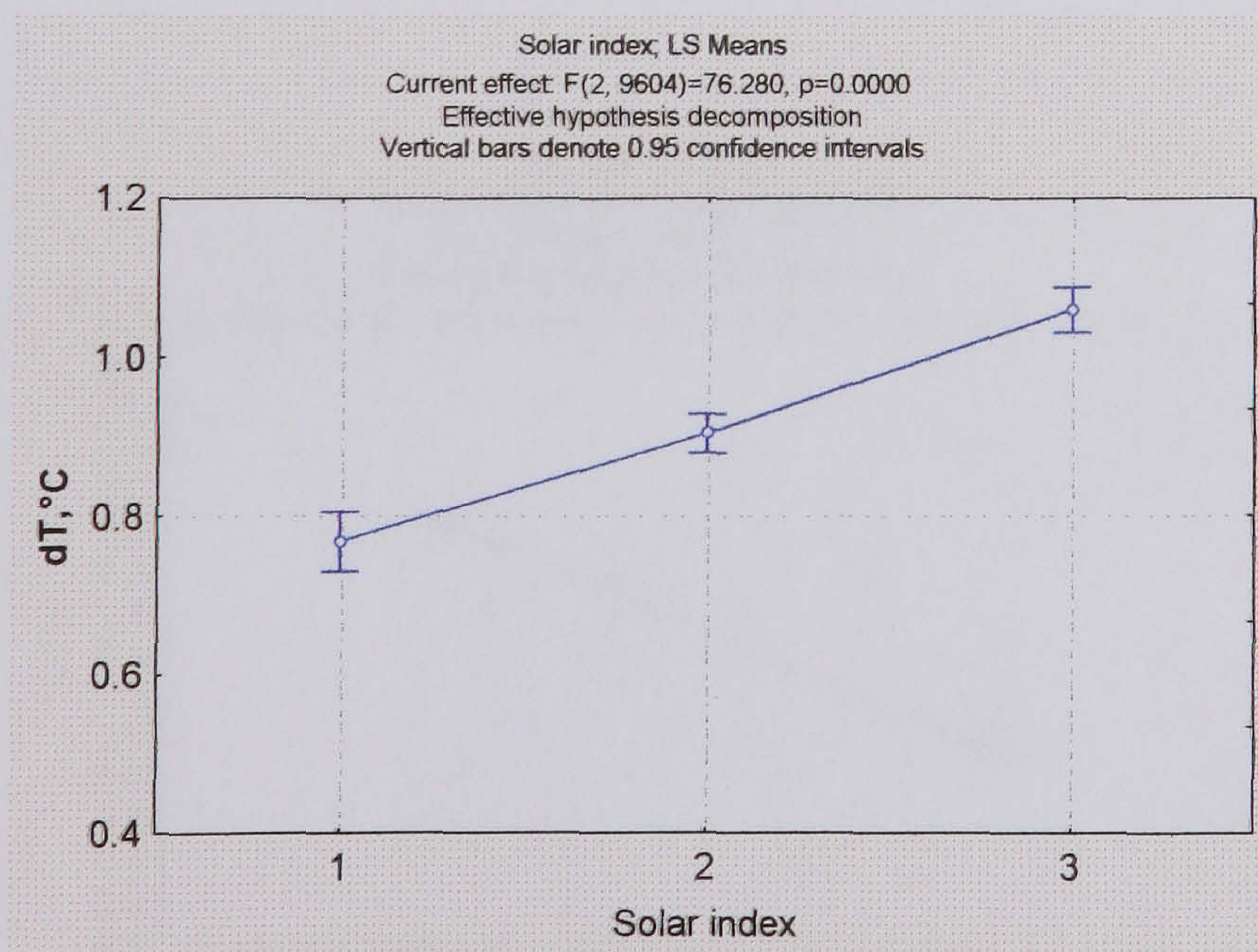


Figure 5.5: Mean dT grouped by solar radiation (DAYTIME)

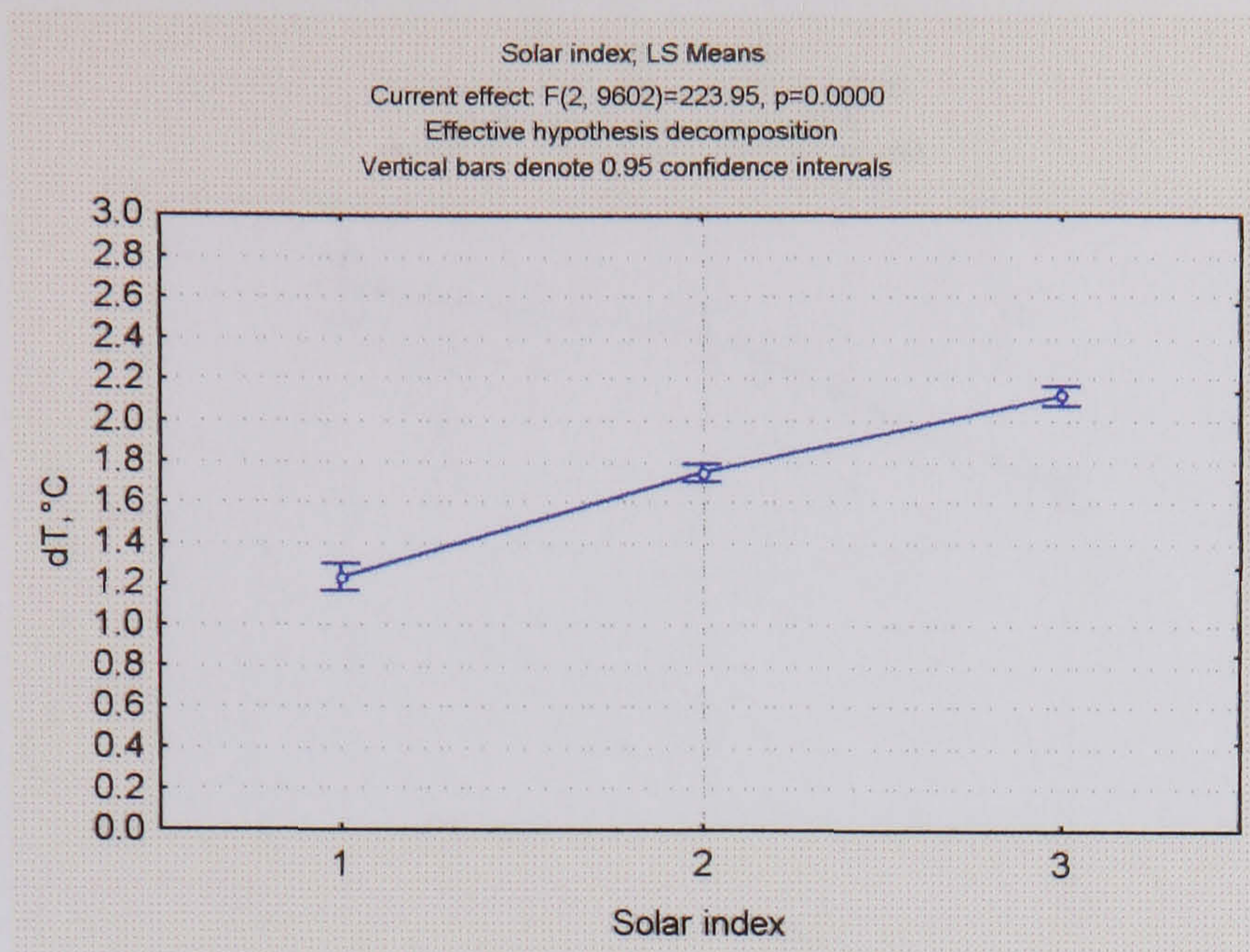


Figure 5.6: Mean dT grouped by solar radiation (NIGHT-TIME)

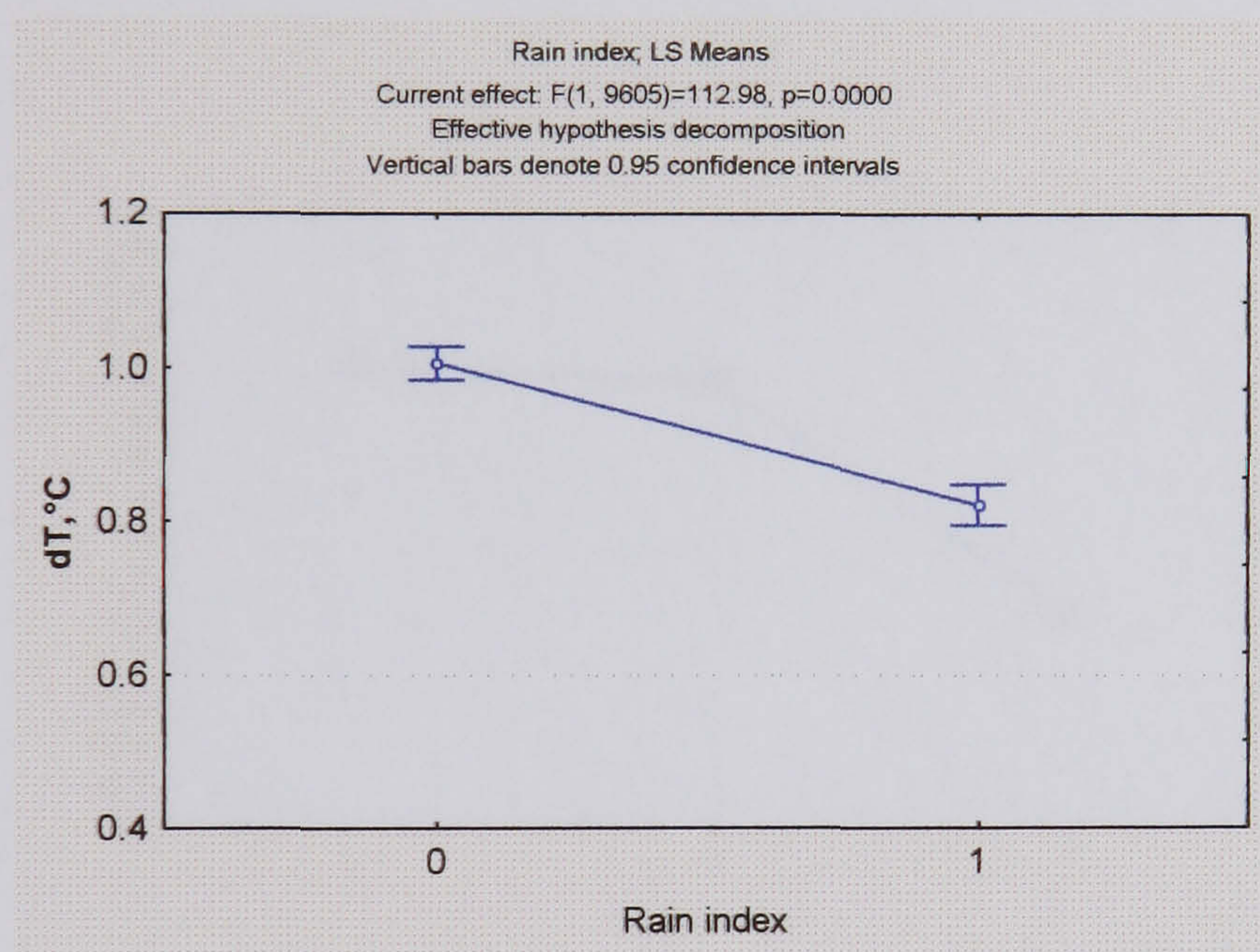


Figure 5.7: Mean dT grouped by rainfall (DAYTIME)

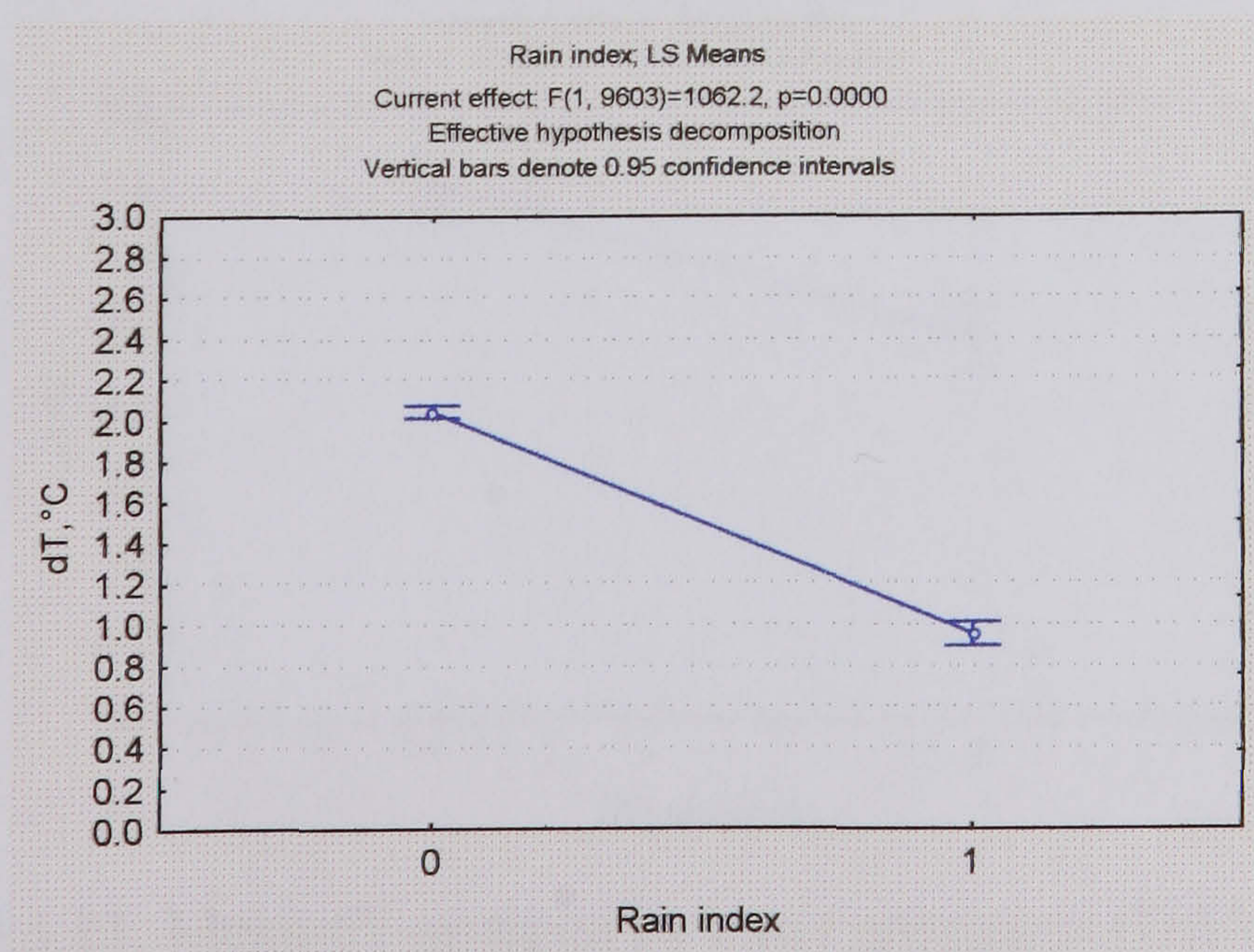


Figure 5.8: Mean dT grouped by rainfall (NIGHT-TIME)

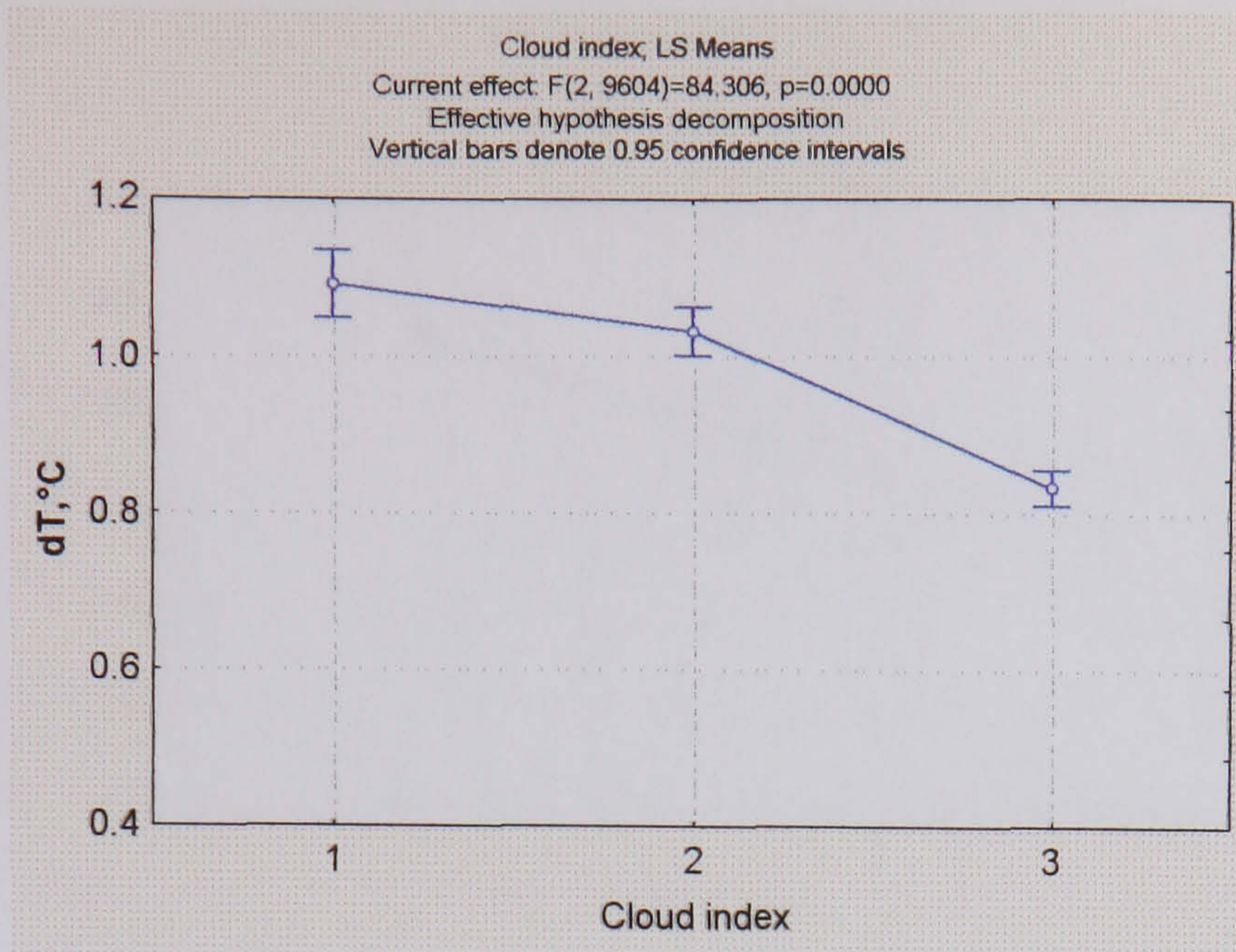


Figure 5.9: Mean dT grouped by cloud cover (DAYTIME)

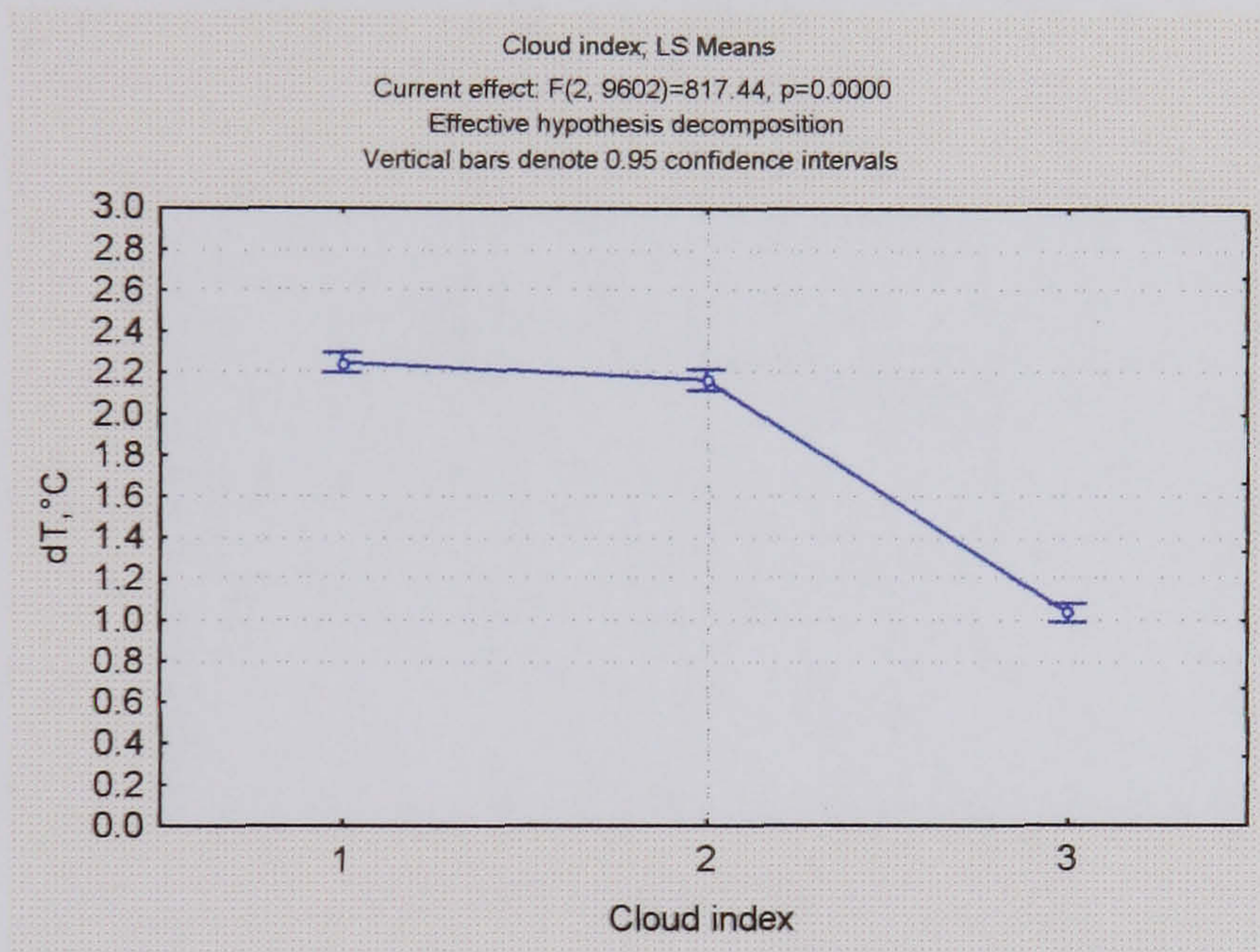


Figure 5.10: Mean dT grouped by cloud cover (NIGHT-TIME)

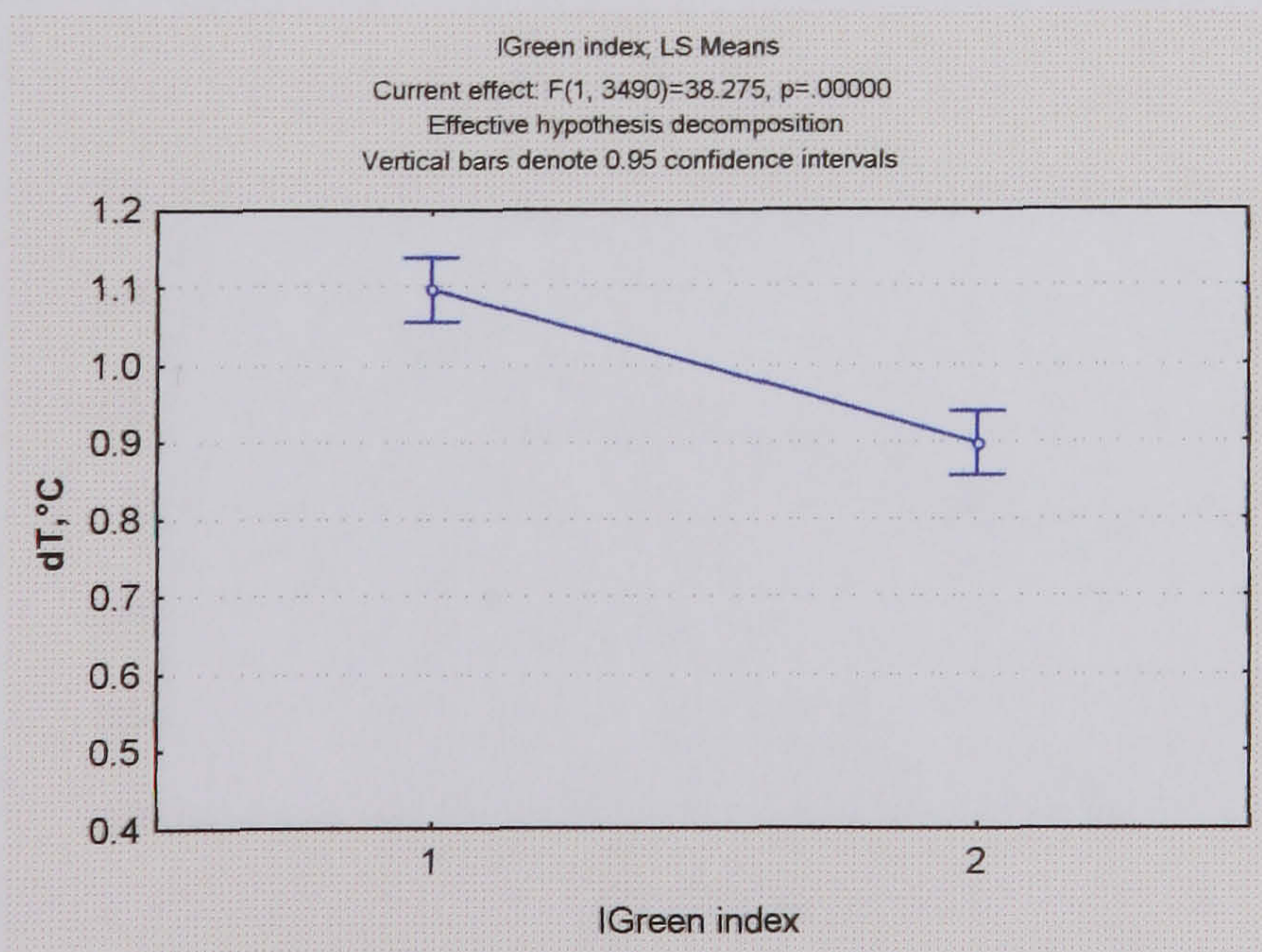


Figure 5.11: Mean dT grouped by inner greenness (DAYTIME)

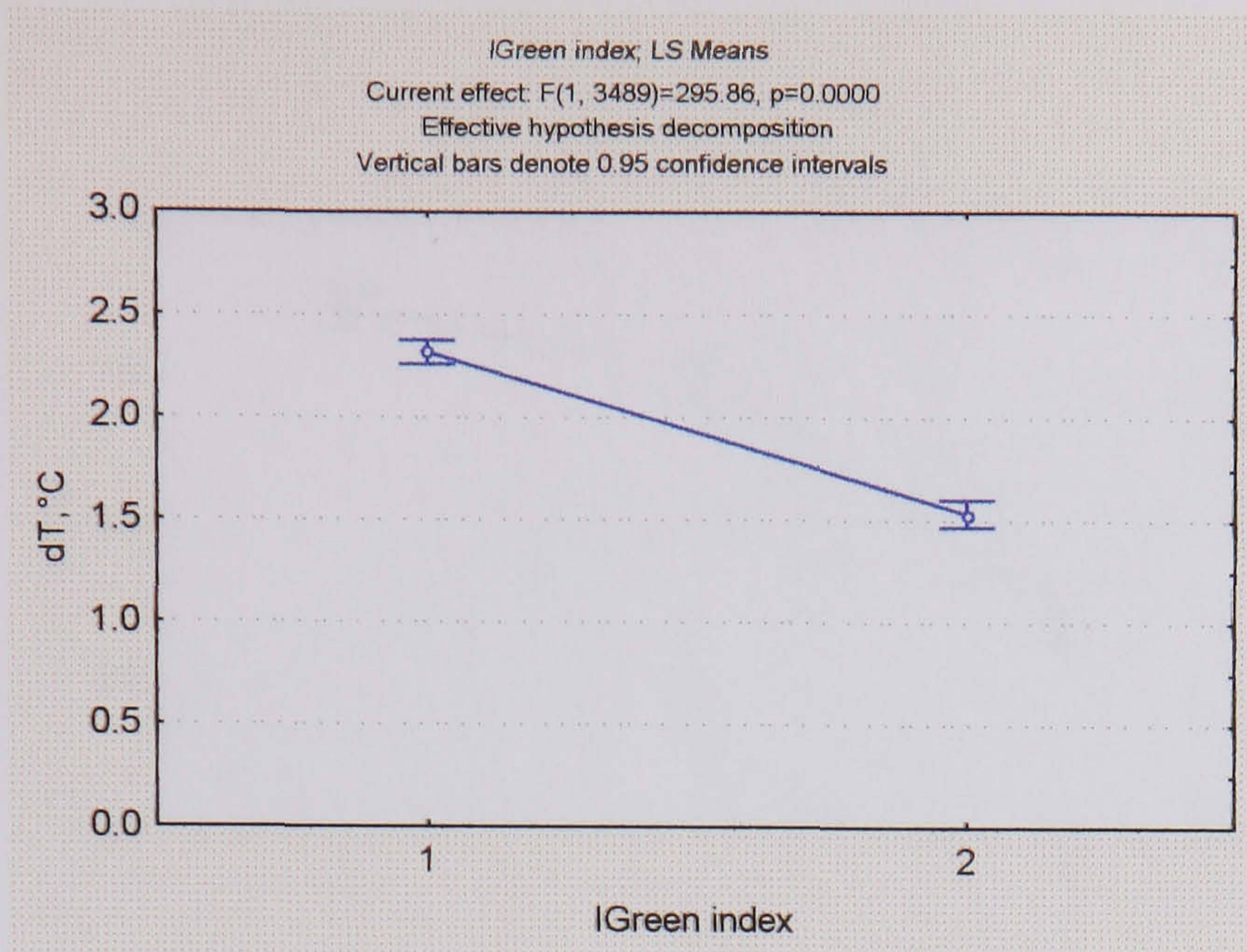


Figure 5.12: Mean dT grouped by inner greenness (NIGHT-TIME)

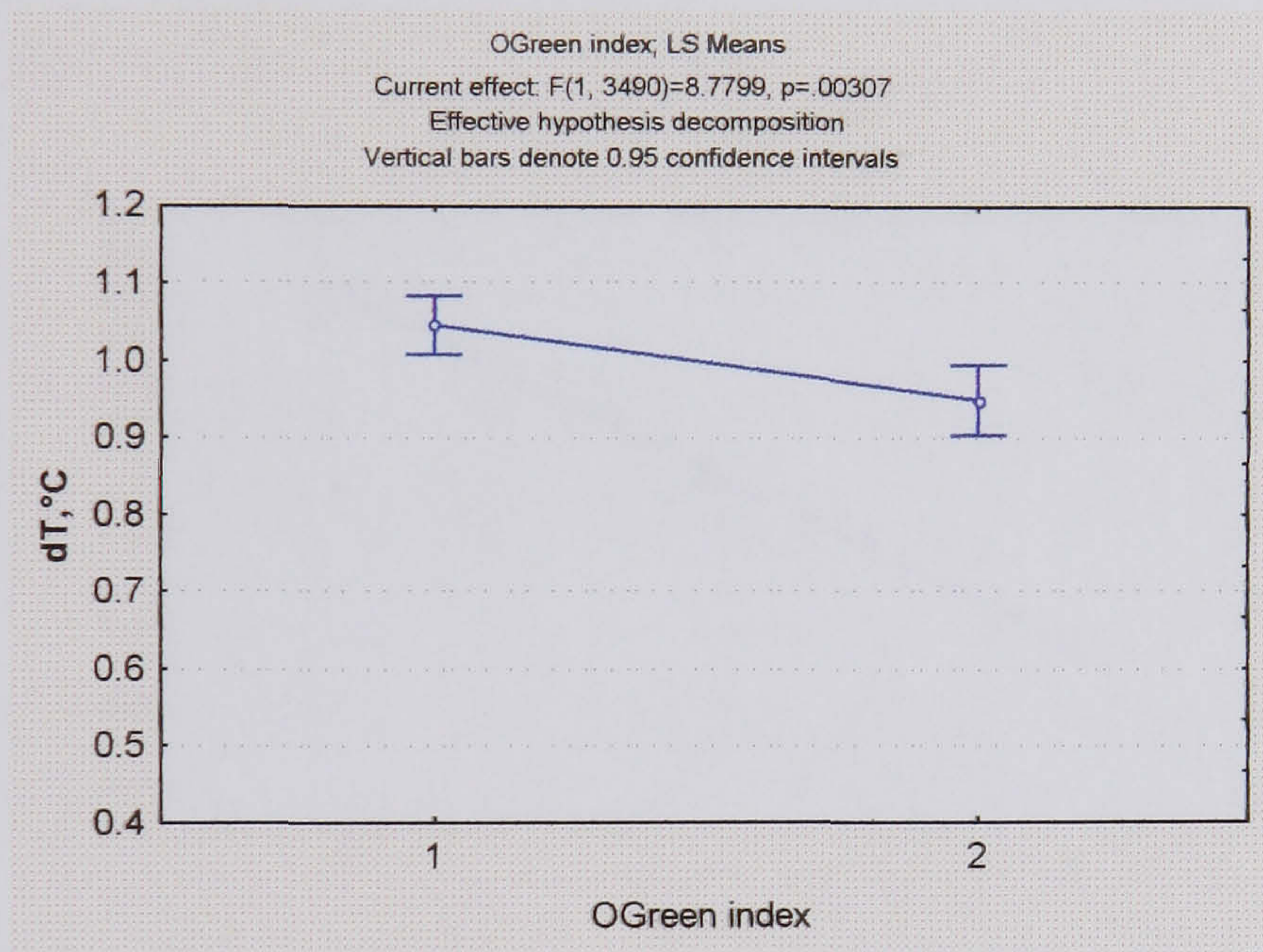


Figure 5.13: Mean dT grouped by outer greenness (DAYTIME)

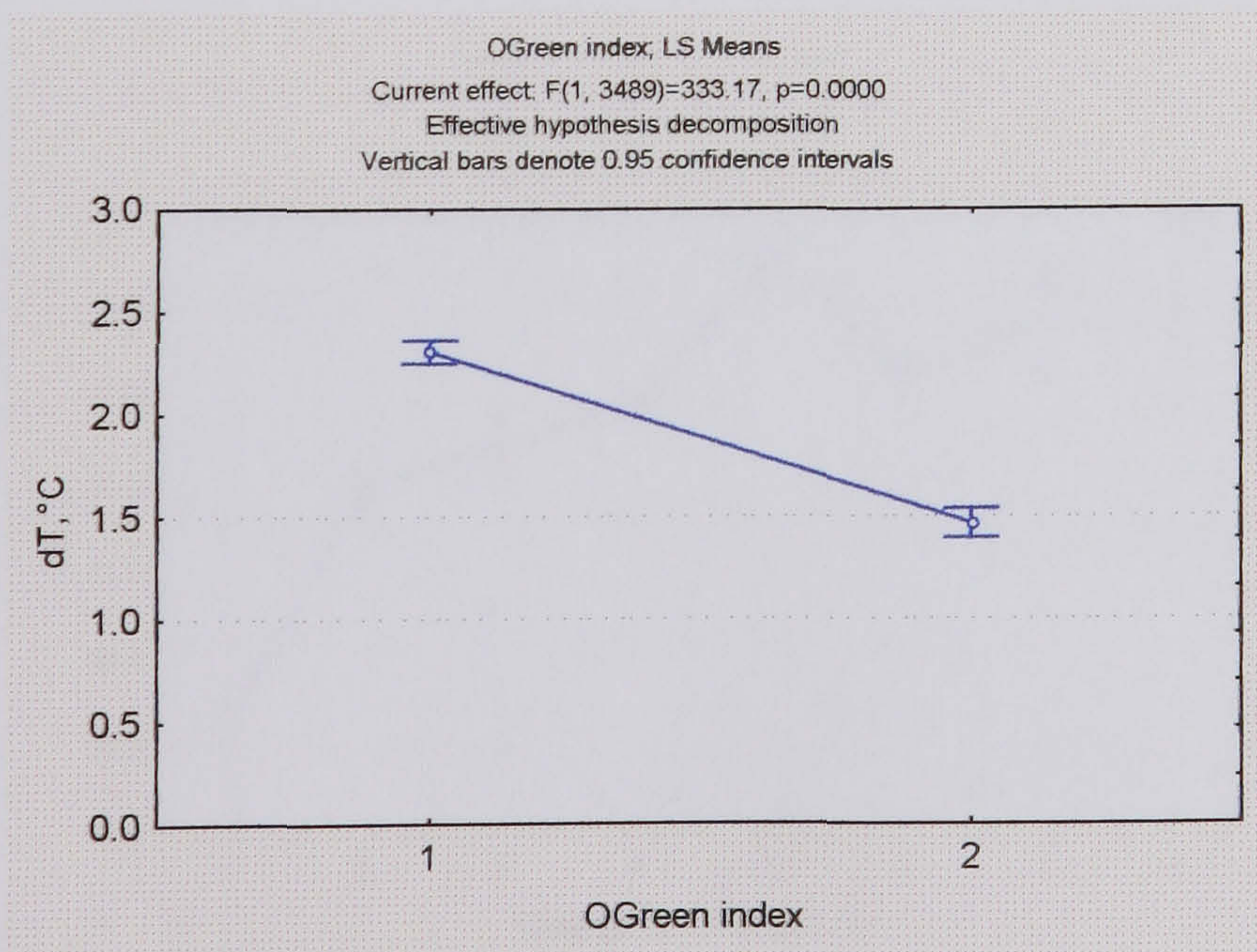


Figure 5.14: Mean dT grouped by outer greenness (NIGHT-TIME)

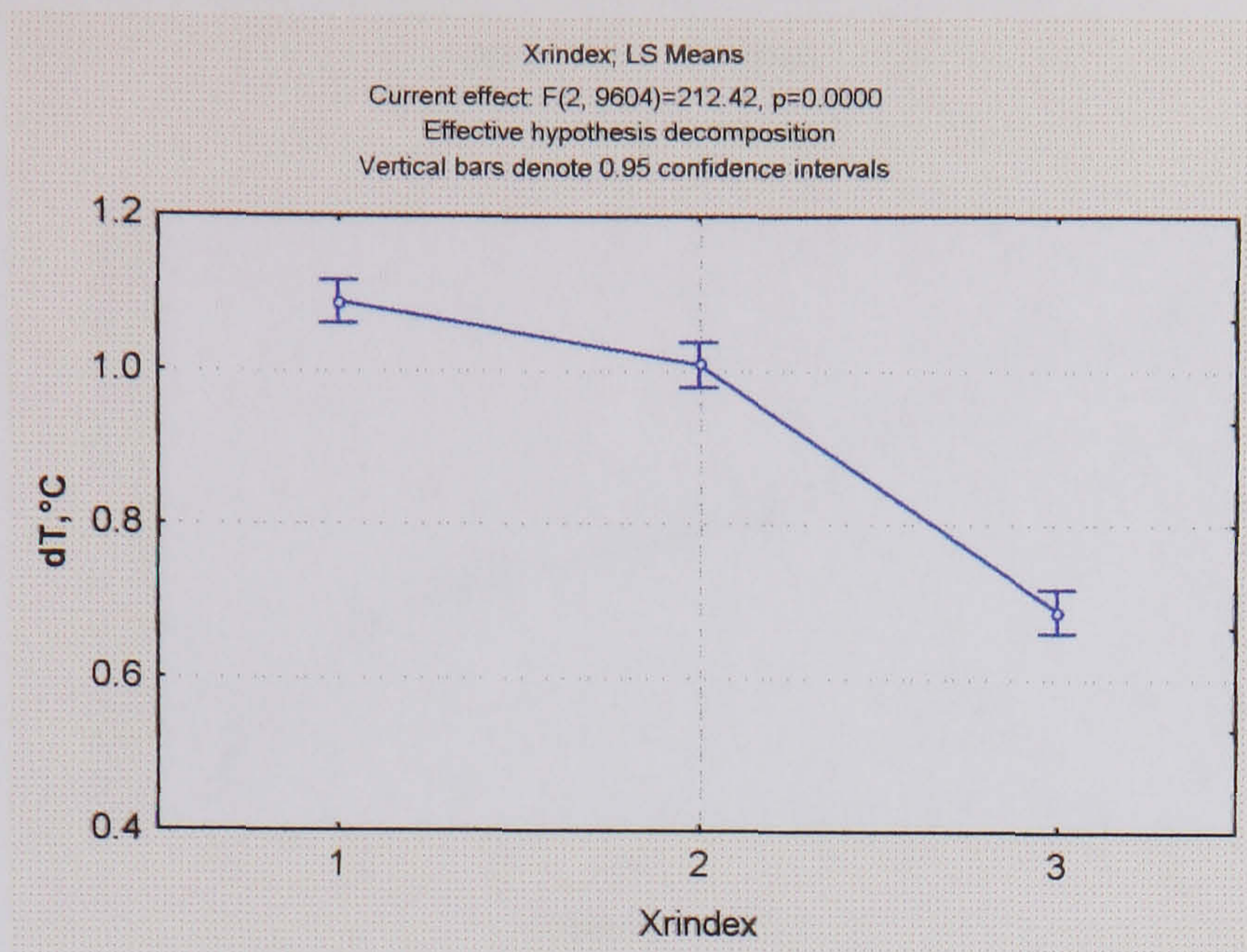


Figure 5.15: Mean dT grouped by radial distance (DAYTIME)

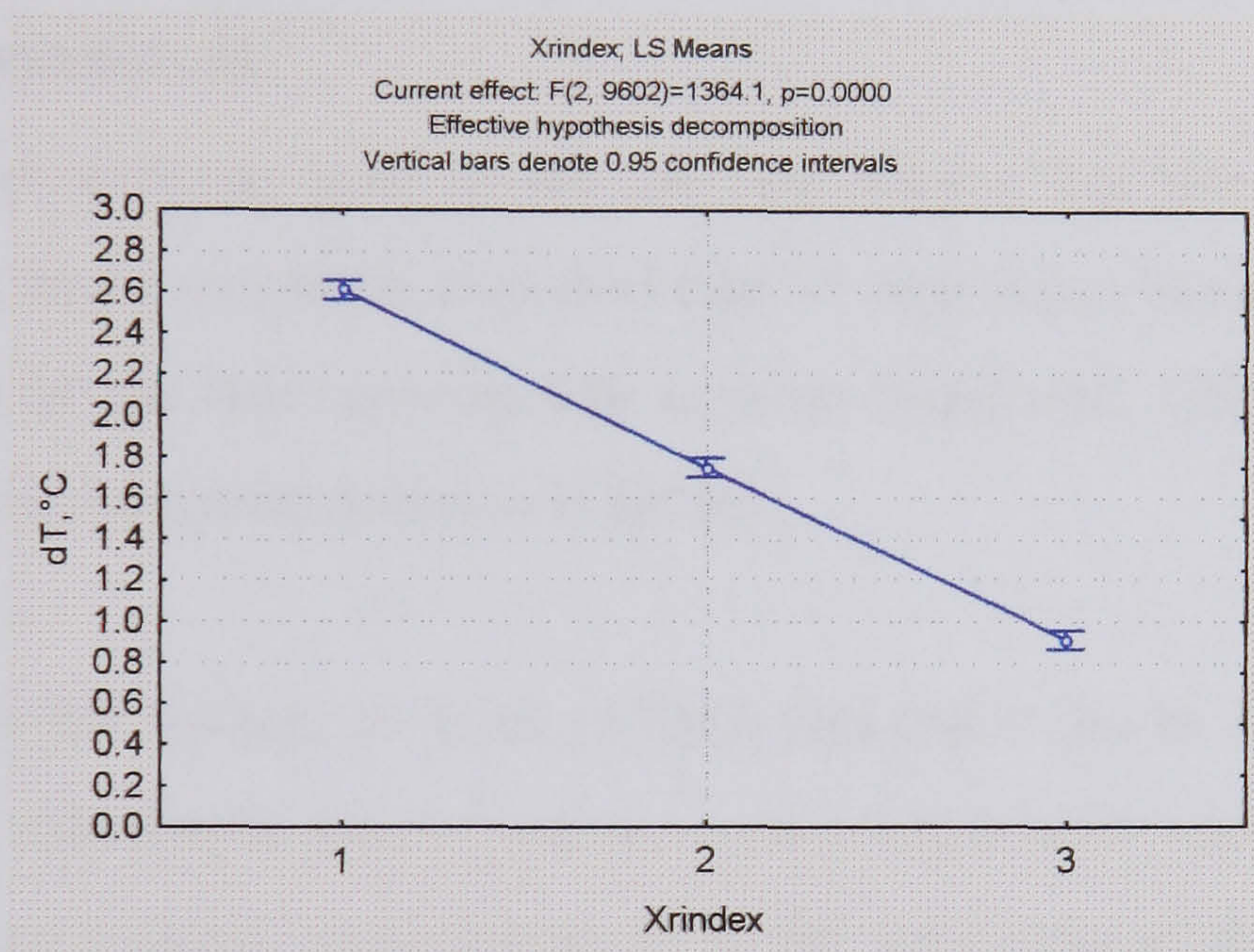


Figure 5.16: Mean dT grouped by radial distance (NIGHT-TIME)

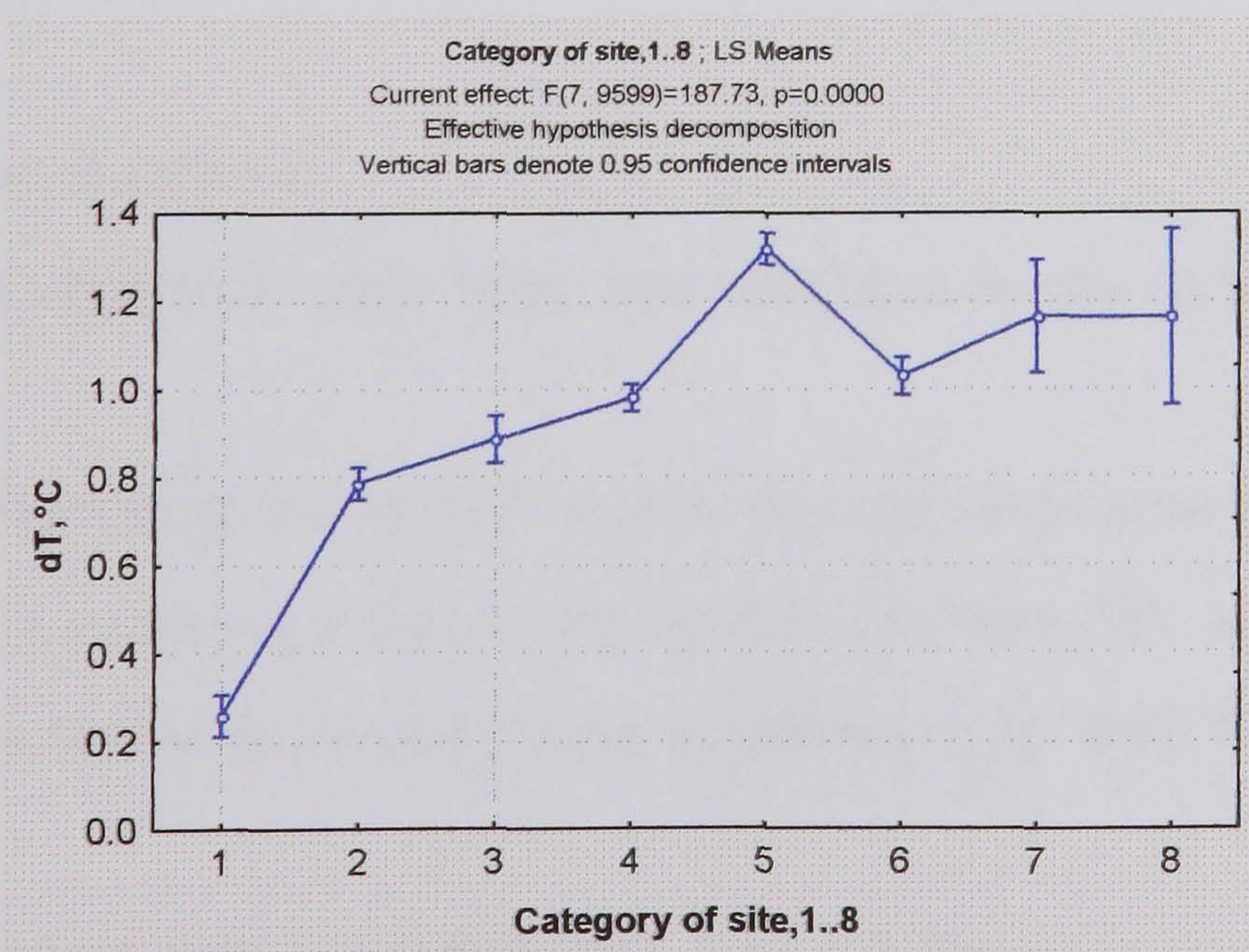


Figure 5.17: Mean dT grouped by site category (DAYTIME)



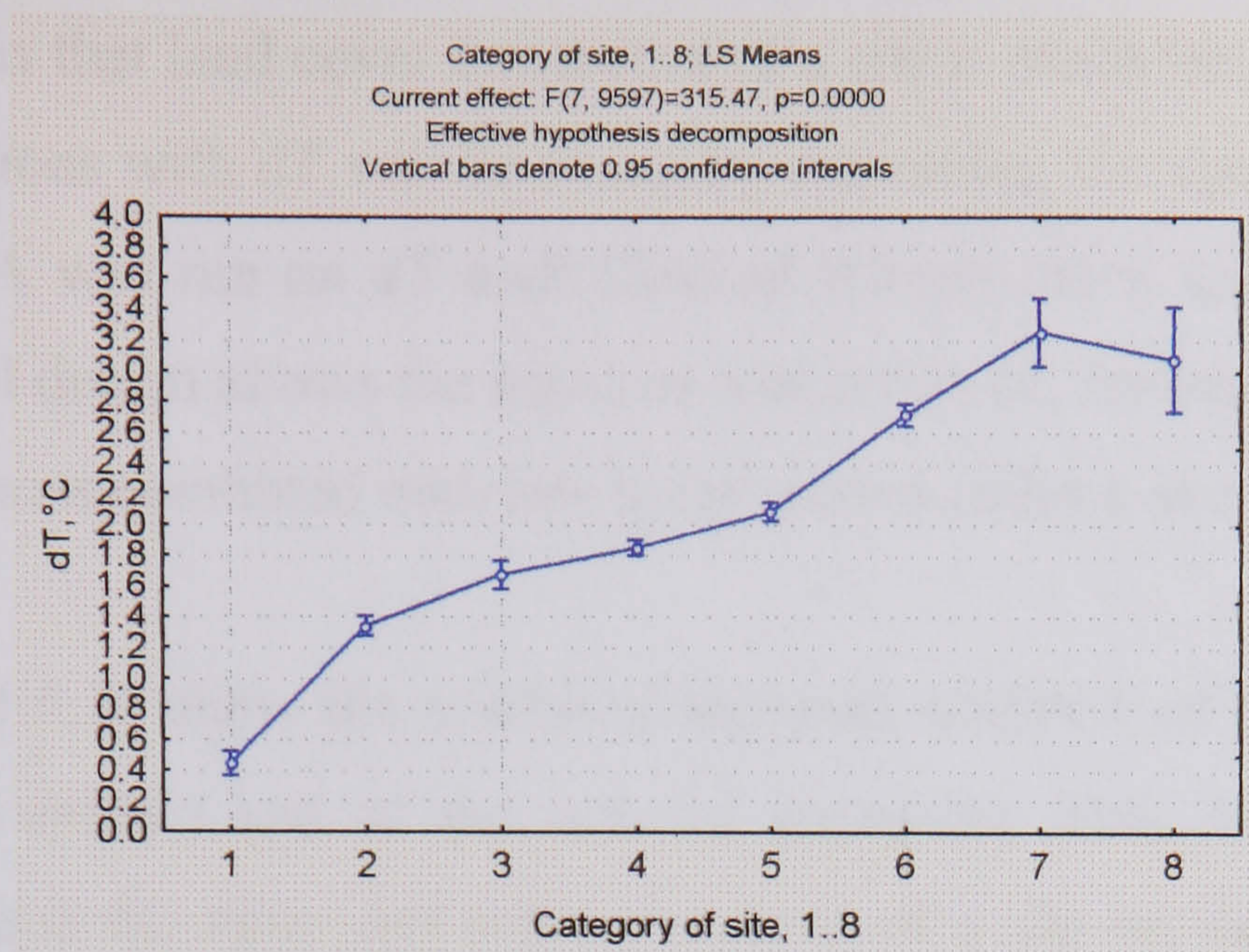


Figure 5.18: Mean dT grouped by site category (NIGHT-TIME)

## 5.6 Upwind greenness

The greenness percentages used above are site means, but the land cover varies around each site, and it might be expected that, if vegetation has a cooling effect on air, it is the state of the land upwind that is more important. This is tested here for daytime data when evapotranspiration is active.

The greenness by 45° sector, at inner (150m) and outer (up to 500m) distances as before, had been calculated: 8x2=16 values were available for each site. The upwind versions of the two indexes were produced in the same way as described in section 5.4 (using the same 30% banding threshold), but are based on the upwind versions of the variables.

They were derived as follows:

- The wind direction each hour was rounded to the nearest 45° compass direction.
- The greennesses of the two 45° sectors adjacent to this were averaged.
- This gave a mean greenness of the upwind quadrant (90° sector) for one hour.
- The values for the daytime hours in a particular day were then averaged.

The upwind greenness was computed each hour for the 153 days of the dataset for the 24 sites whose greenness had been assessed from digital photographs (Appendix 4).

The assumption is that land cover downwind of a site is much less relevant, and that stronger associations with dT will be found by examining the upwind land cover. A factorial ANOVA was run on dT and: Upwind IGreen index and Upwind OGreen index. A factorial design allows the separate evaluation of, for example, the effect of high outer greenness combined with low inner greenness for a site.

Figures 5.19 and 5.20 show the results of factorial ANOVA of both the site mean greenness (used earlier) and of the upwind greenness. This ANOVA shows the interaction between the inner and outer greenness of a site on the mean dT for the grouping.

The main points from looking at site and upwind greenness are:

- **Any** high greenness (inner or outer for the whole site, or inner or outer upwind) is associated with a group of sites that have a lower temperature.
- Sites with high **upwind** inner and outer greenness are cooler by 0.42°C than sites with low upwind inner and outer greenness.
- Sites with high **site** inner and outer greenness are cooler by 0.29°C than sites with low site inner and outer greenness.
- When there is low **inner** greenness (site or upwind), the effect of outer greenness is greater where this is upwind (0.38°C reduction compared to 0.27°C).

The results show that greenness is associated with a lower air temperature. When two areas of green land are in line with the wind direction towards the measurement station there is a maximum reduction of mean temperature (0.42°C) between this group and the group with areas of low green land in line with the wind direction.

When a site has low inner greenness, the effect of outer green land on reducing the temperature is more pronounced when this is in line with the wind direction. This and the other results seem intuitively correct, but the confidence bands shown on the ANOVA figures, which are based on a sample of 24 sites, mean that the distinction between site and upwind, or dynamic percentage greenness is indicative of a likely effect rather than good evidence for it.

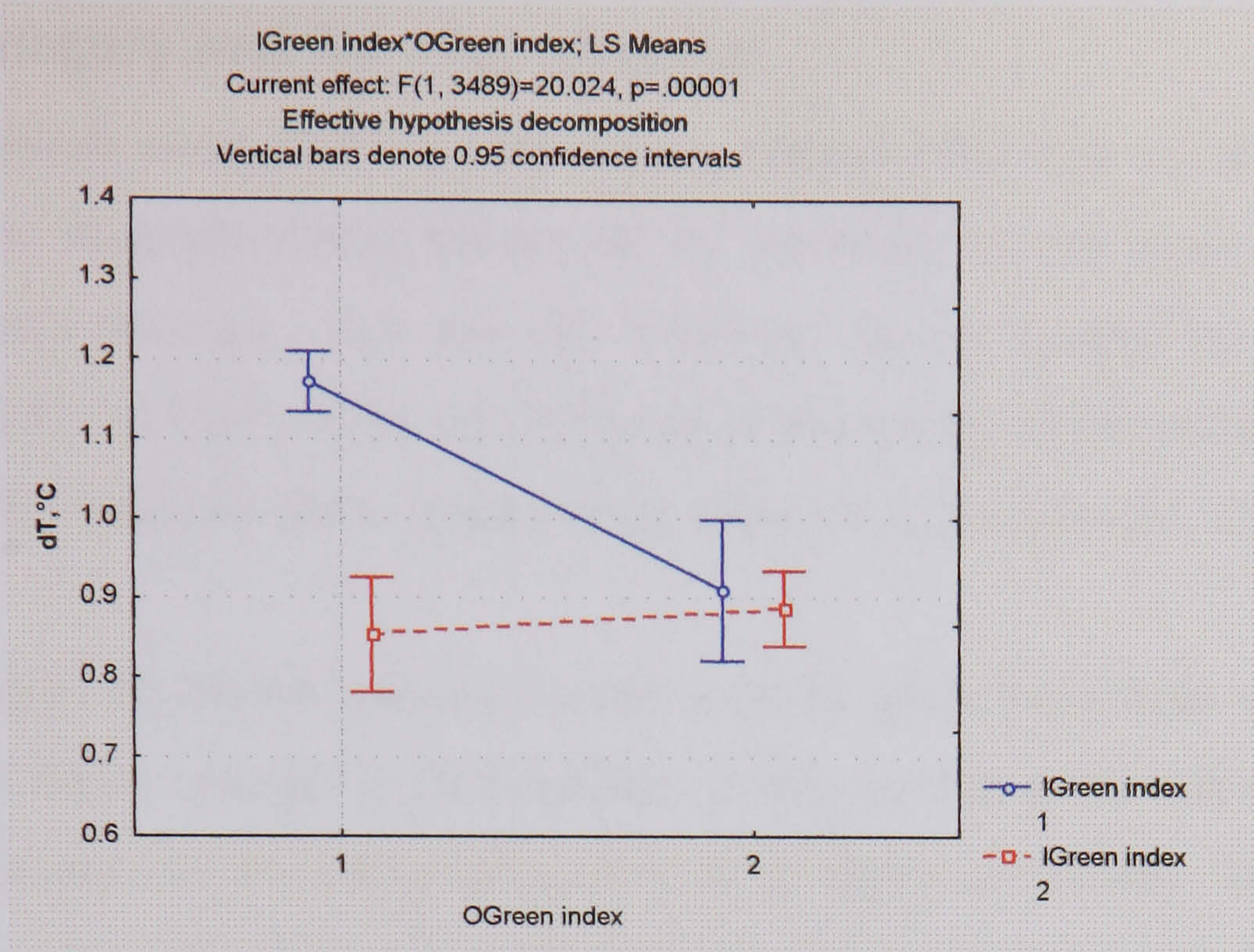


Figure 5.19: Mean dT grouped by inner and outer site greenness (DAYTIME)

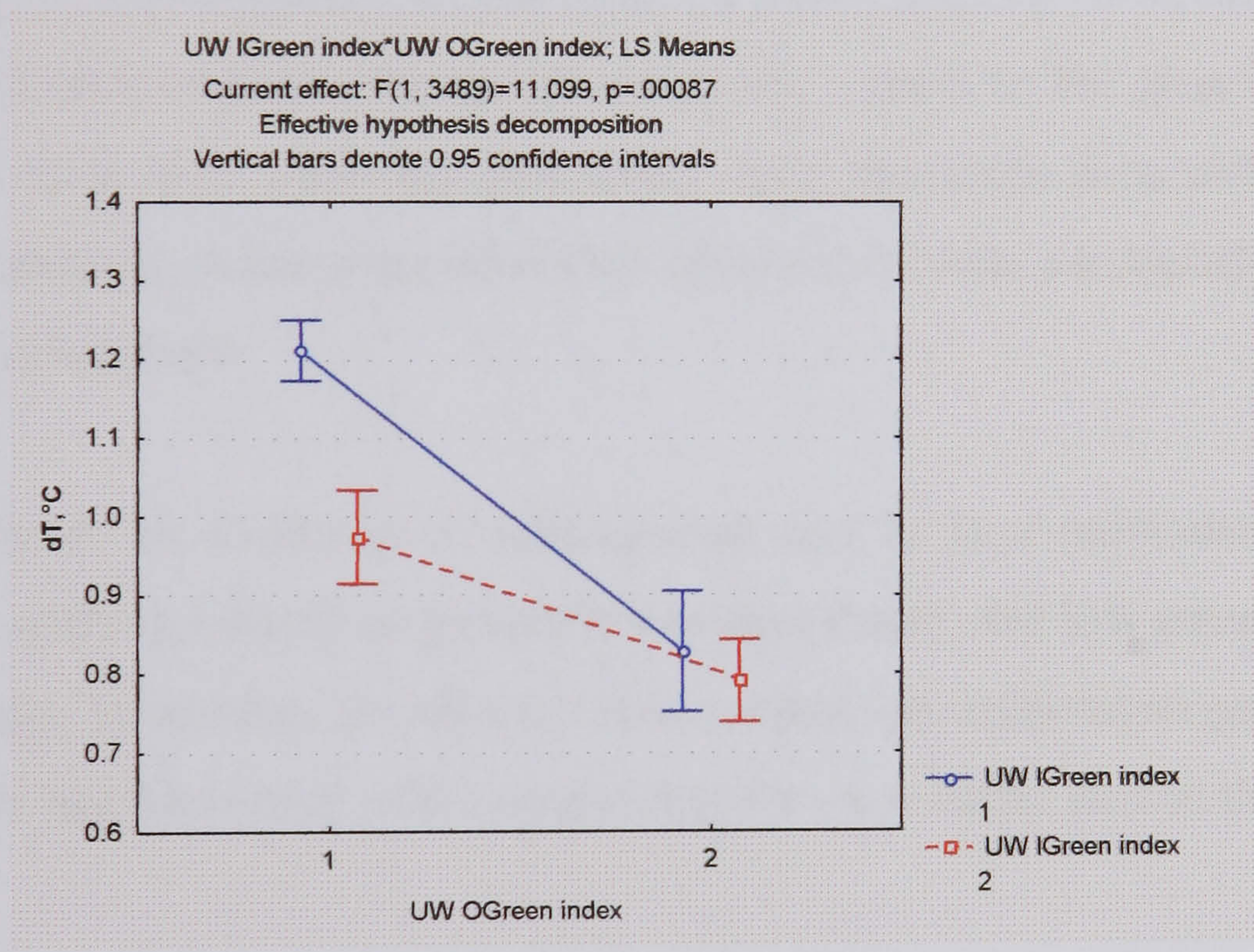


Figure 5.20: Mean dT grouped by inner and outer upwind greenness (DAYTIME)

## 5.7 Site category and $X_r$ – introduction

It has been shown using ANOVA that the temperature difference at a site depends on many factors. Weather-related factors are not particular to the urban environment, but site-related ones are. This and the following section control for some of the weather factors in order to look more closely at the impact of the nature of a site on its temperature and how this is related to the effect of radial distance,  $X_r$ .

Radial distance,  $X_r$ , shows how deep a site is in the urban field. This will always be an important factor because the temperature at any point in a city will depend partly on the temperature in the surrounding area, from which air advects. To what extent air mixes vertically depends on wind speed, atmospheric stability, and local topology (tall buildings encourage mixing).

Site category is superimposed on the effect of radial distance. It would be expected that it would raise or lower the temperature with respect to the general urban field temperature in an area. There are potentially open sites even deep within the urban field, and greenness (often associated with open sites) exists particularly deep within the London urban field.

Site category is an indicator of urbanization and is thus correlated with radial distance, as urban development generally becomes denser and less green the closer to a city one gets. To identify the effect of site category on temperature separately from  $X_r$ , ANOVA has been used while controlling for each radial step in the monitoring stations.

It helps in revealing the effect of a factor if conditions are chosen that encourage or allow it to be emphasized. As mentioned before, choosing windy days will reduce the heat island intensity (in the limit, to zero) and it would be difficult to establish relationships with such data. For this reason, this analysis uses periods that are relatively calm, dry, and sunny. Specifically the conditions for the data used are:

("Solar index">1) and ("Rain index"=0) and ("Wind index"<3)

i.e. at least medium solar radiation, dry, and not very windy. (If more extreme criteria, e.g. “very sunny”, are imposed the number of compliant cases becomes too small.)

Additionally, to increase confidence, only cases in a 57 contiguous day sample are used and in the summer of 2000. All the stations in this sample are available all the time (no missing hourly data) for the whole of the period. To produce this complete and parallel set of station data, the following 16 stations below have been excluded:

FN00, NN04, NN05, NN06, NE04, NE07, NE08, EE02, EE03, SS03,  
WW03, WW10, NW01, NW04, NW06, NW08

This leaves 61 stations for the analysis.

The results of the ANOVA are reported in the next section.

### **5.8 Site category and $X_r$ – ANOVA results (DAYTIME)**

The ANOVA of  $dT$  with site category has been performed for radial distances of 1, 2, 3, 4, 6, 8, 10, 12 and 14 miles from the focus. If site category operates independently at all distances, it would be expected that the sites with lower temperatures would be the ones with lower categories (associated with more open and sometimes greener sites). This is a relative effect. For example, category-4 sites might tend to be the warmest at an intermediate radial distance but the coolest sites further in towards the centre of the heat island where higher category sites are to be found. Figures 5.21-5.29 show the results for daytime data. The y-axis of each graph has a variable range, but a fixed scale step of  $0.2^{\circ}\text{C}$ , to emphasize the trends.

It can be seen that the results are quite consistent. Between 1 and 8 miles from the focus, at each of the six radial steps the site-category means are ordered with lower categories being cooler, and higher categories, up to and including category-5, being warmer. At 10 miles, the pattern is almost identical but there is a slight but insignificant drop in temperature for category-5. At 12 miles and beyond, the pattern starts to break down.

At the inner distances ( $X_r=1$  to 3 miles), there are higher categories sites: category-6 and a single category-8 site. The single category-7 site was not available for this dataset. Above category-5 the temperature is consistently lower, although this is significant only for  $X_r=1$  and 2 miles. These sites are not associated with large green areas and it is possible that the temperature is lower because of the increased overshadowing of the street gorges where the measurements were taken.

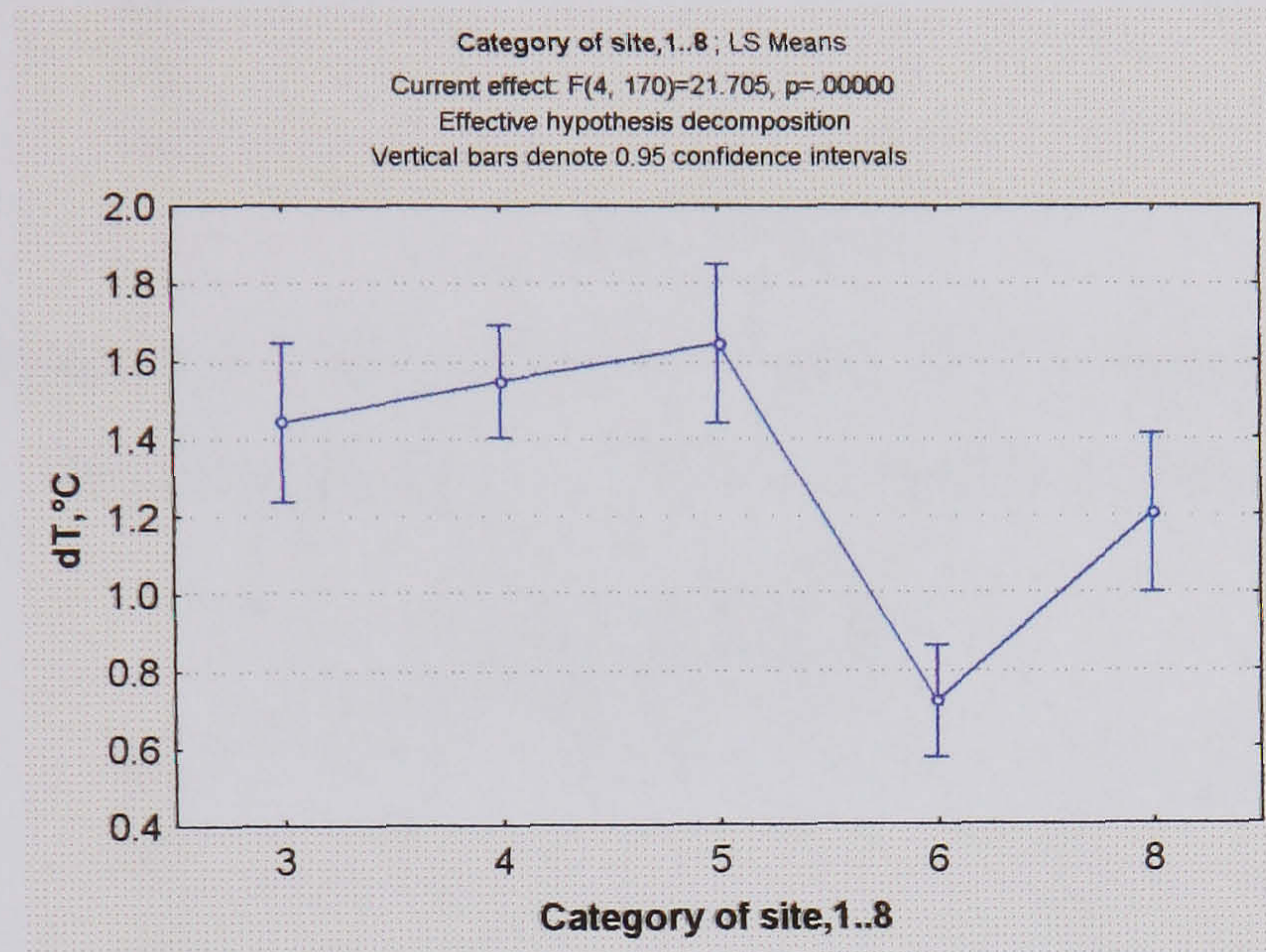


Figure 5.21: The variation of mean dT when grouped by site category, for  $X_r=1$  mile (DAYTIME)

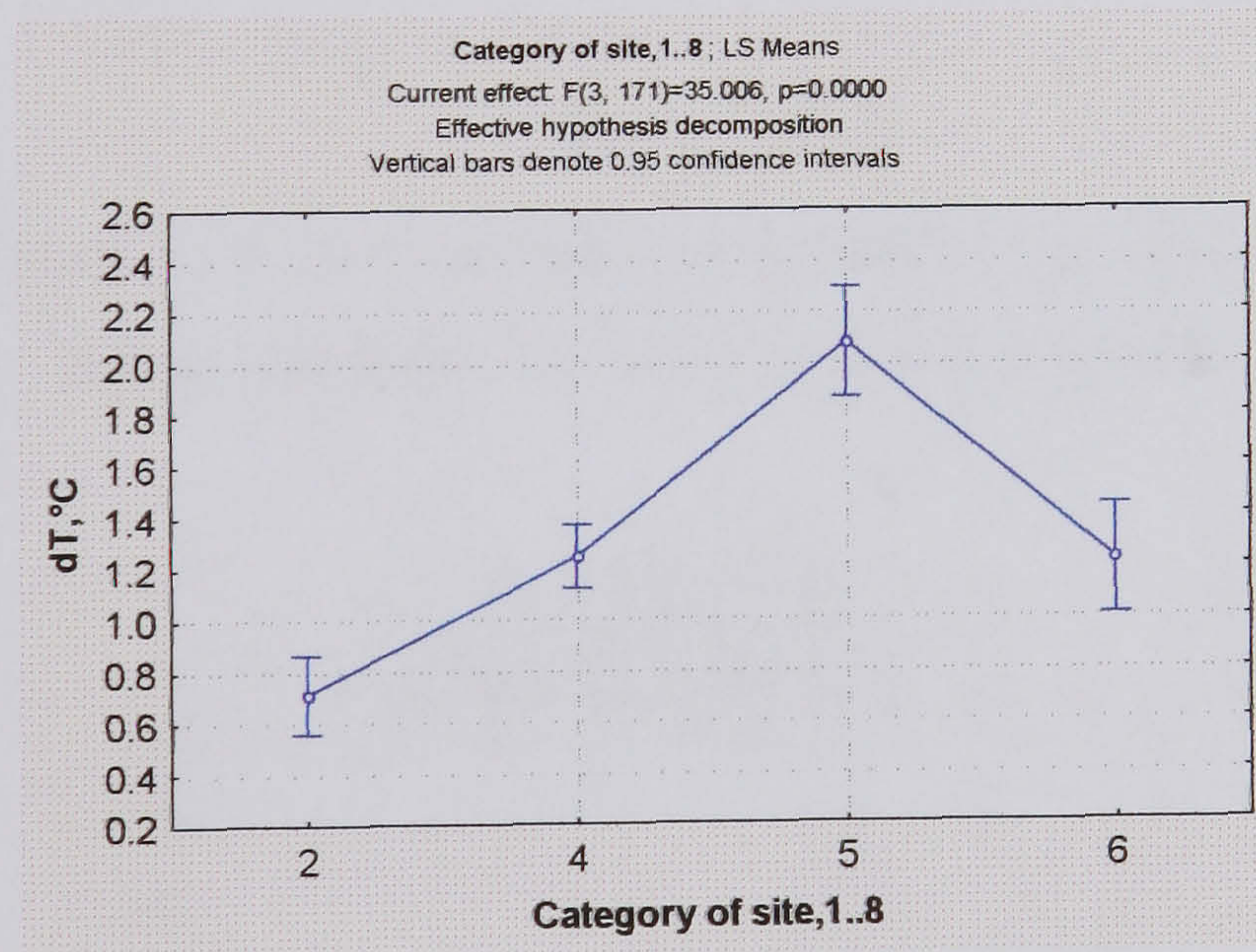


Figure 5.22: The variation of mean dT when grouped by site category, for  $X_r=2$  miles (DAYTIME)

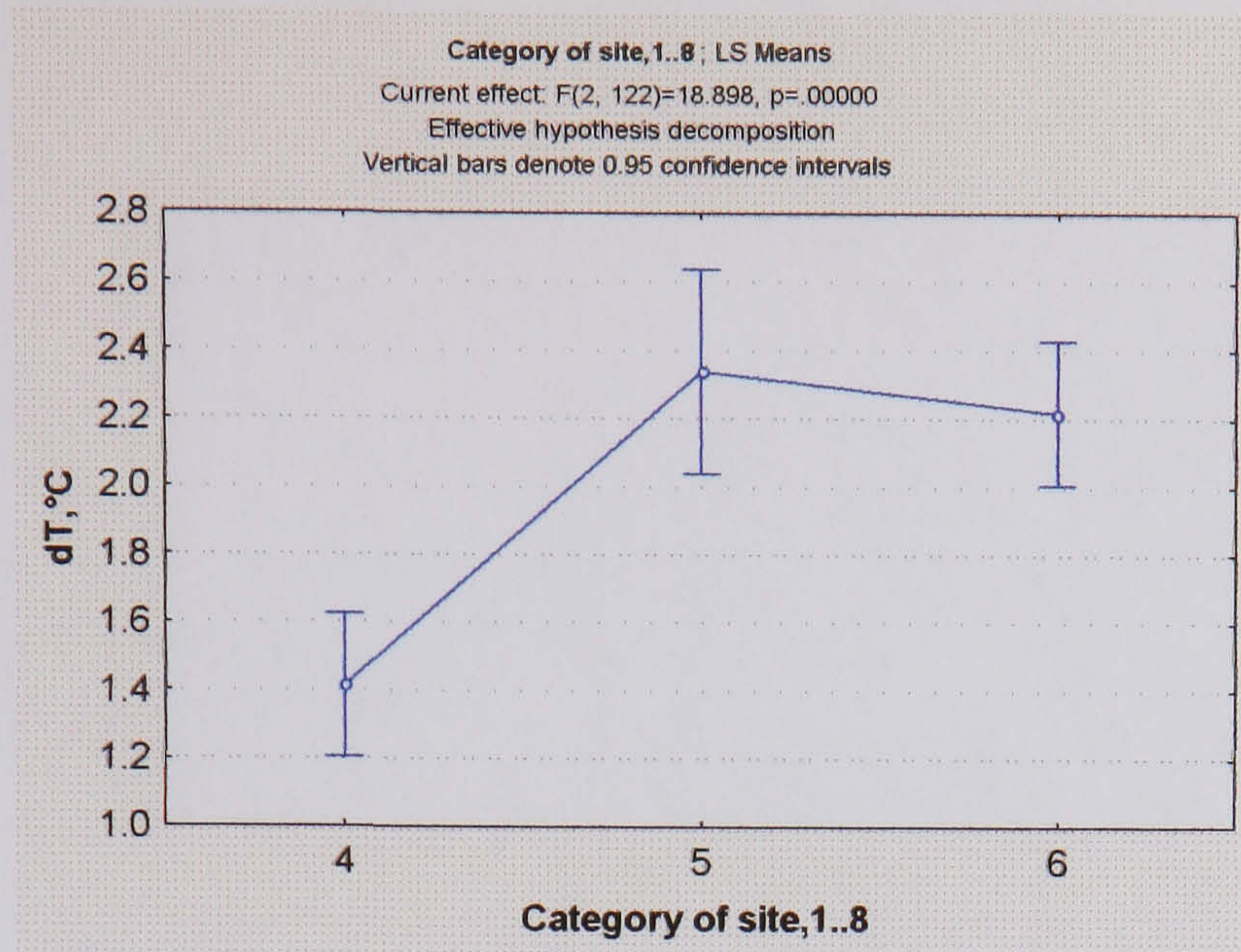


Figure 5.23: The variation of mean dT when grouped by site category, for Xr=3 miles (DAYTIME)

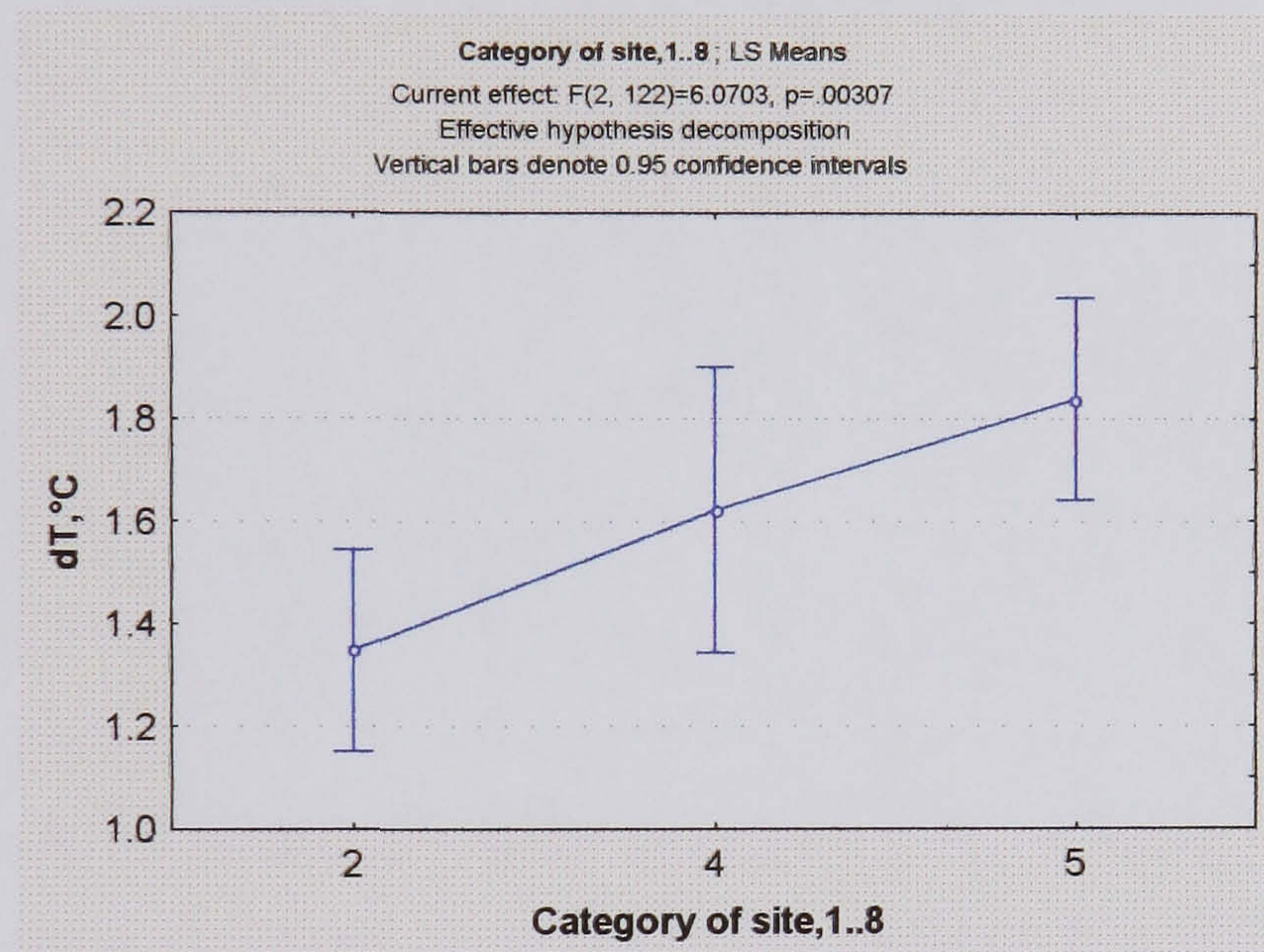


Figure 5.24: The variation of mean dT when grouped by site category, for Xr=4 miles (DAYTIME)

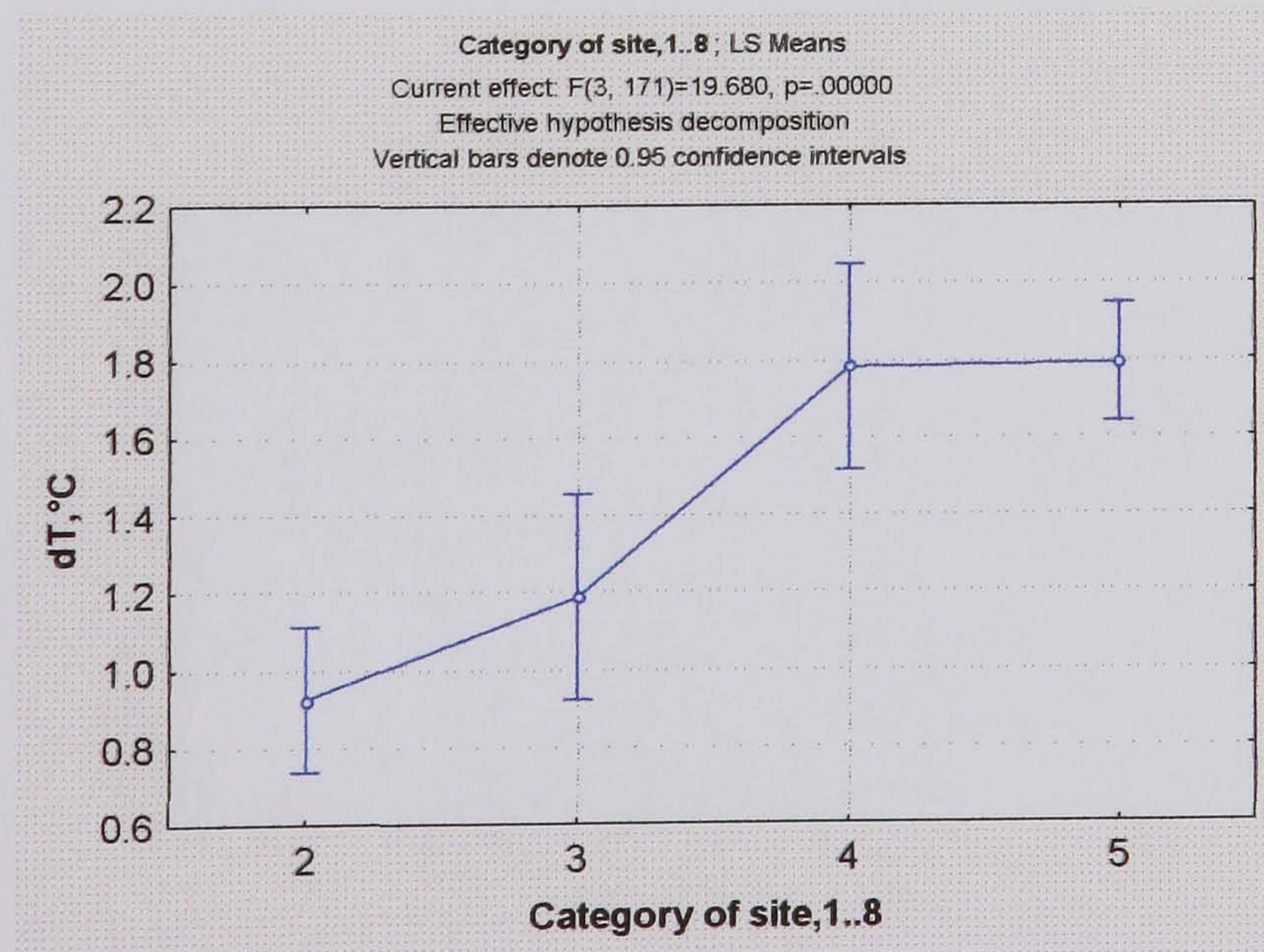


Figure 5.25: The variation of mean dT when grouped by site category, for Xr=6 miles (DAYTIME)

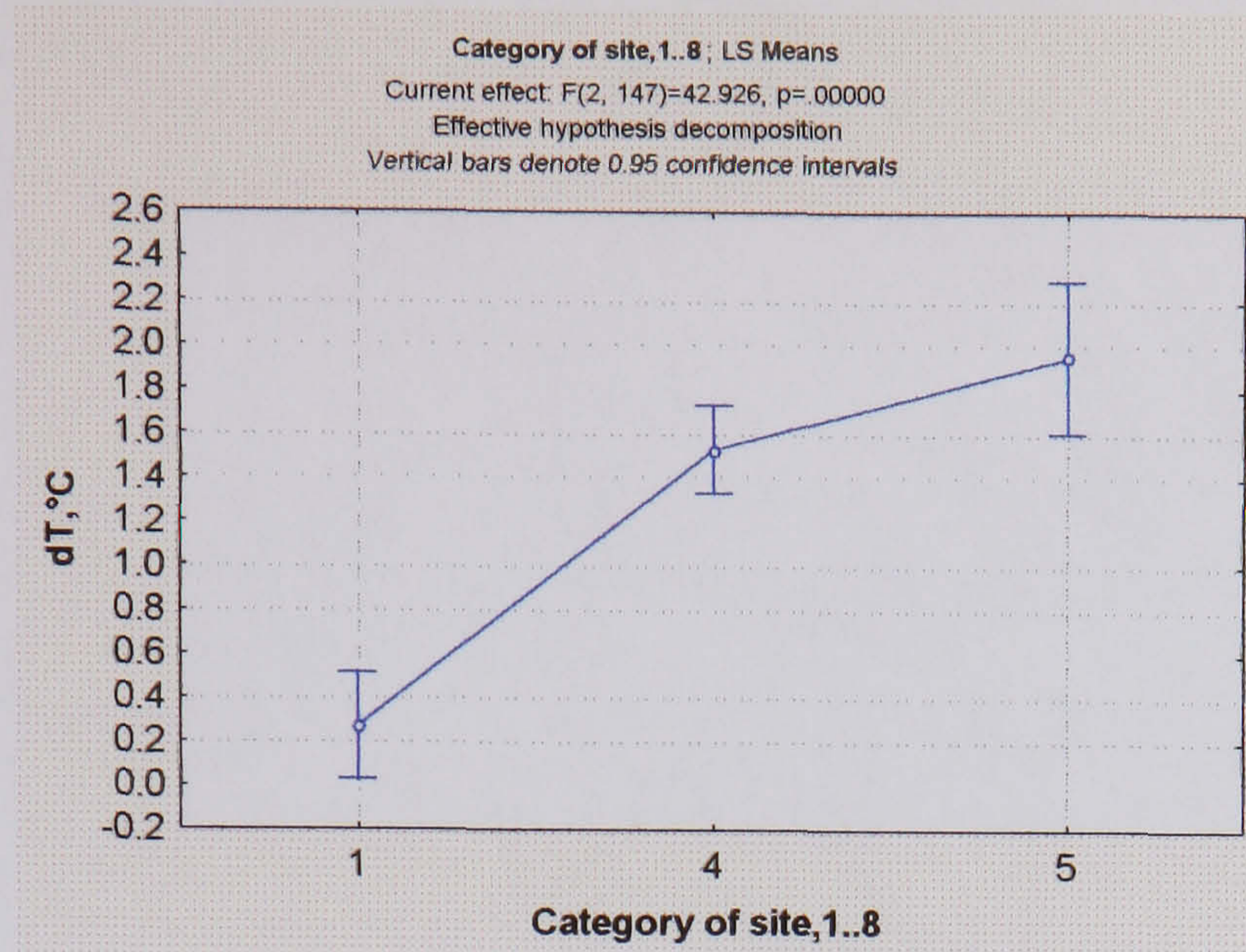


Figure 5.26: The variation of mean dT when grouped by site category, for  $X_r=8$  miles (DAYTIME)

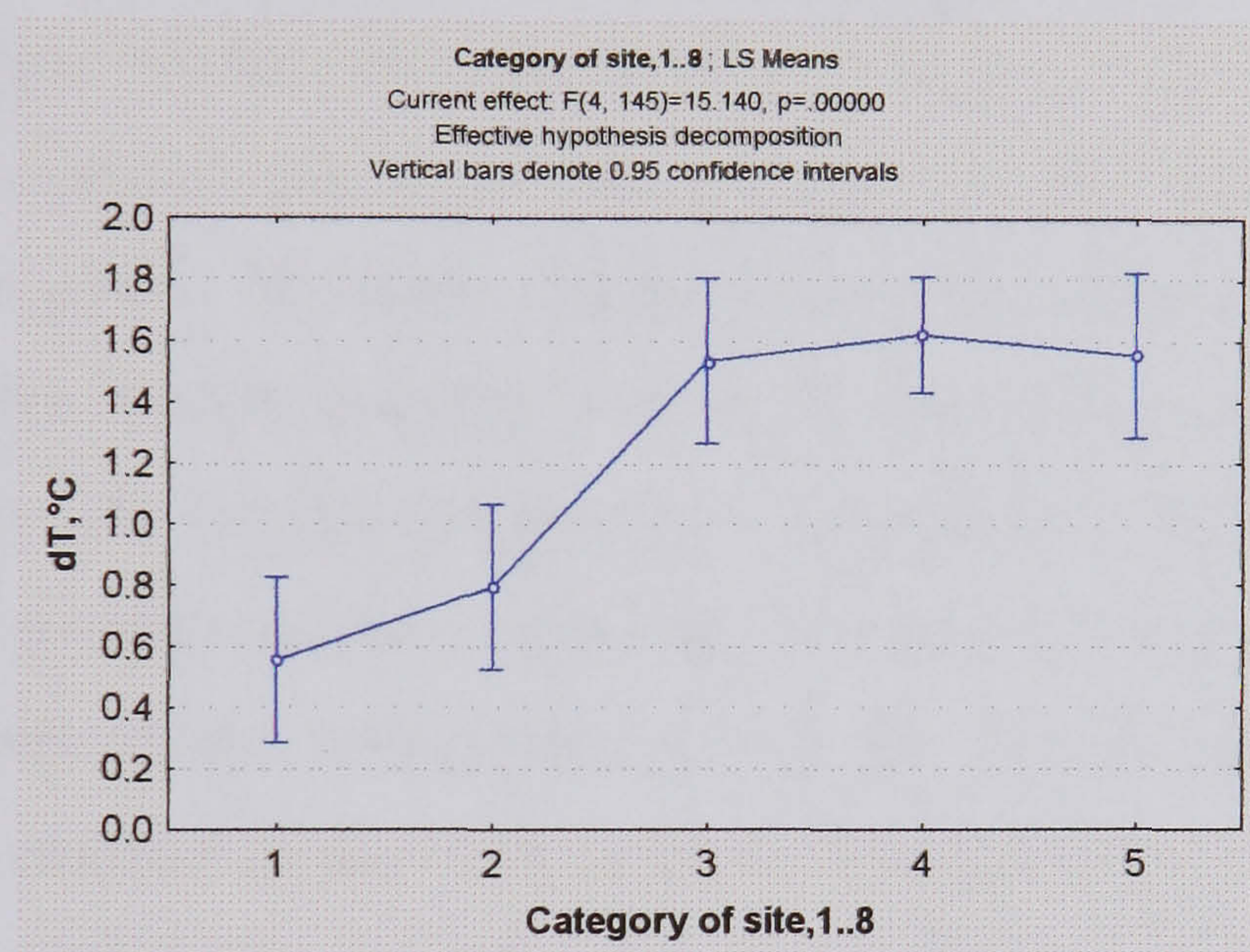


Figure 5.27: The variation of mean dT when grouped by site category, for  $X_r=10$  miles (DAYTIME)

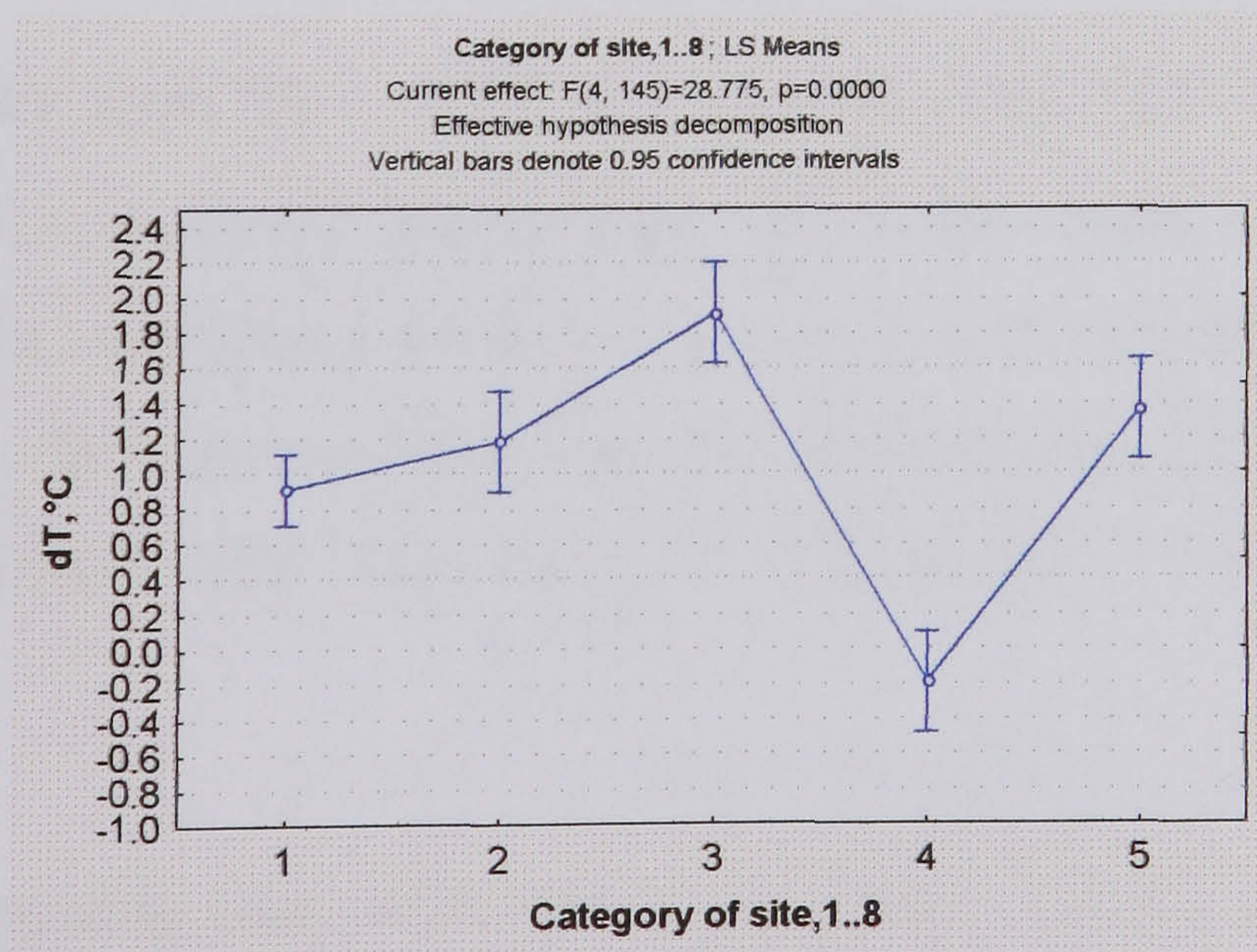


Figure 5.28: The variation of mean dT when grouped by site category, for  $X_r=12$  miles (DAYTIME)



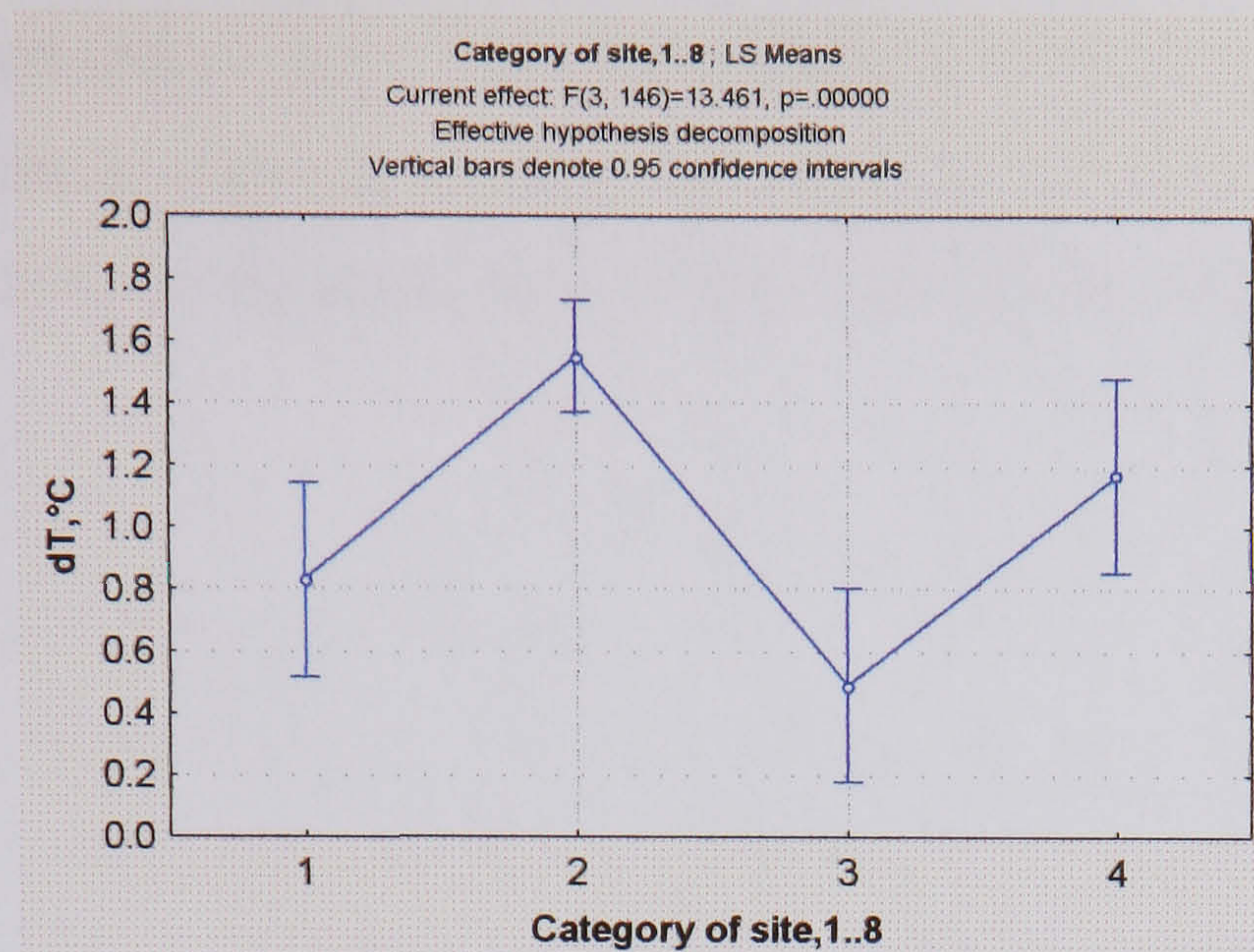


Figure 5.29: The variation of mean dT when grouped by site category, for  $X_r=14$  miles (DAYTIME)

These results suggest that this site categorization is useful in determining the relative daytime mean heat island intensity for sites at a given radial distance, at least up to 8-10 miles from the centre. At further distances from the centre it might be expected that the relationships would change because of the unevenness of urban development as the city spreads out. London did not grow radially in a homogeneous way, and consists now of numerous satellite towns that have grown into a semi-merged whole. Moreover, the shape of the metropolitan area is not circular and this leads to less dense areas being reached sooner in some directions than others. That is, the position or relative depth within the general urban heat island, on which site-category is superimposed, is not always consistently indicated by radial distance,  $X_r$ , alone.  $X_r$  would be expected to be more reliable in the inner areas than further out.

### 5.9 Site category and $X_r$ – ANOVA results (NIGHT-TIME)

The previous section analysed daytime data. When this analysis is repeated for the night-time, with the same data selection criteria, the mean temperature differences of the site-categories for a given radial distance often tend to be ordered in a similar way to the daytime data but there is significantly increased scatter. See Figures 5.30-38.

It is perhaps surprising that night-time heat islands (which are generally more uniform and mono-centred) would be associated with a poorer relationship with site category. This may imply that site characteristics, or at least those embodied in this site categorization, are less relevant in determining temperature at night than in the

daytime. It has been shown earlier that radial distance alone accounts for about 69% of the variance in mean night-time summer temperature between the stations, but this reduces to about 25% in the daytime. There is less residual variation to explain at night.

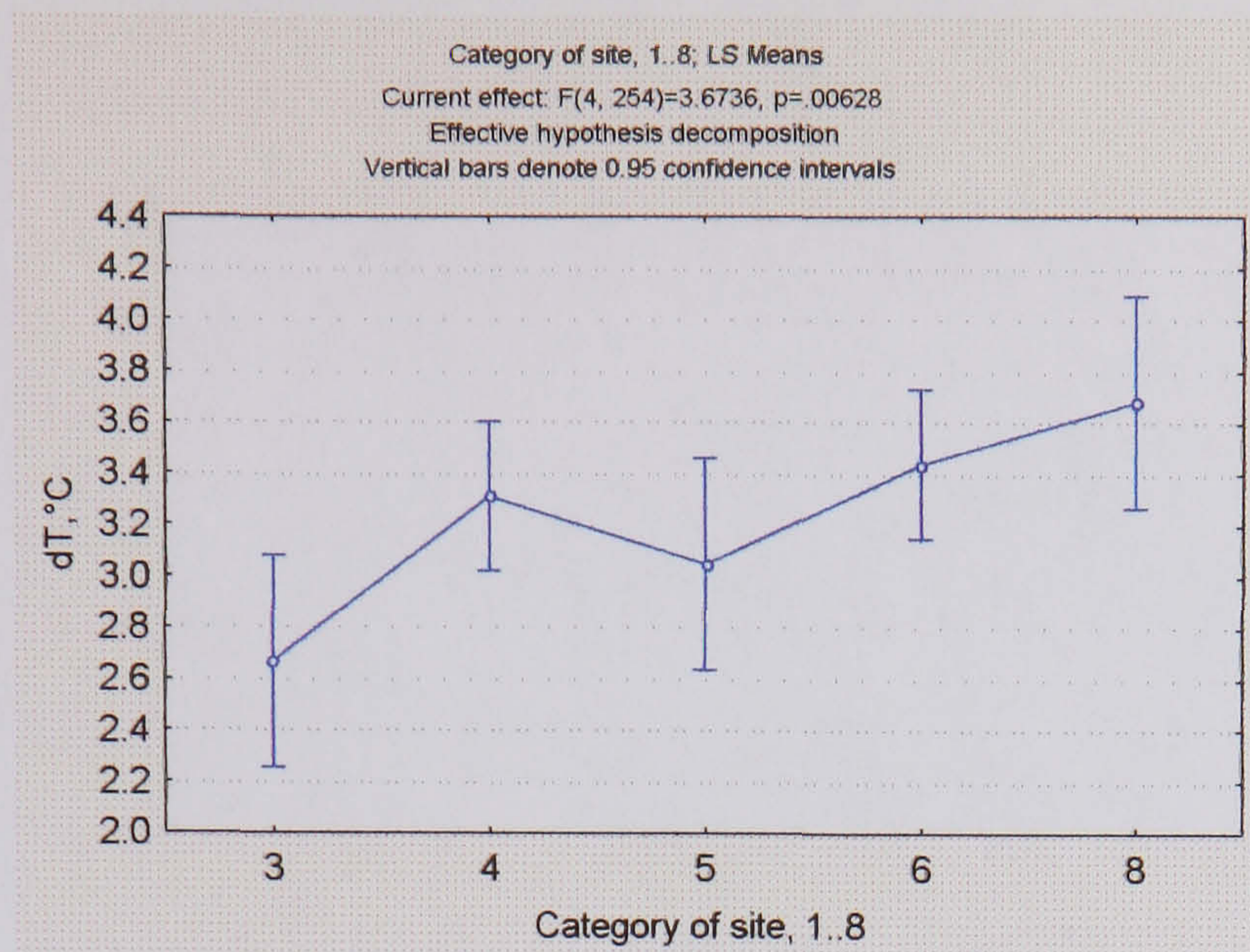


Figure 5.30: The variation of mean dT when grouped by site category, for  $X_r=1$  mile (NIGHT-TIME)

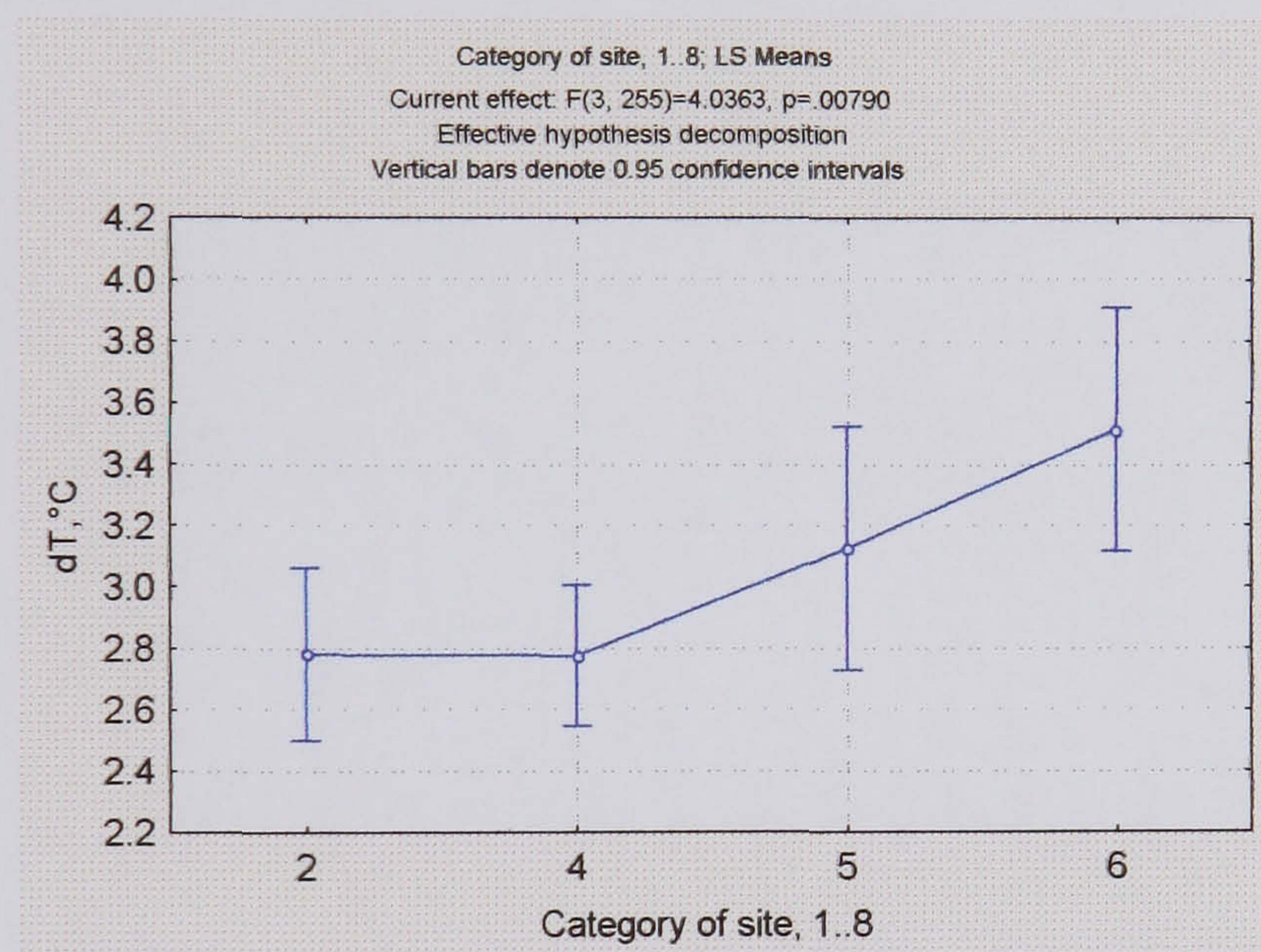


Figure 5.31: The variation of mean dT when grouped by site category, for  $X_r=2$  miles (NIGHT-TIME)

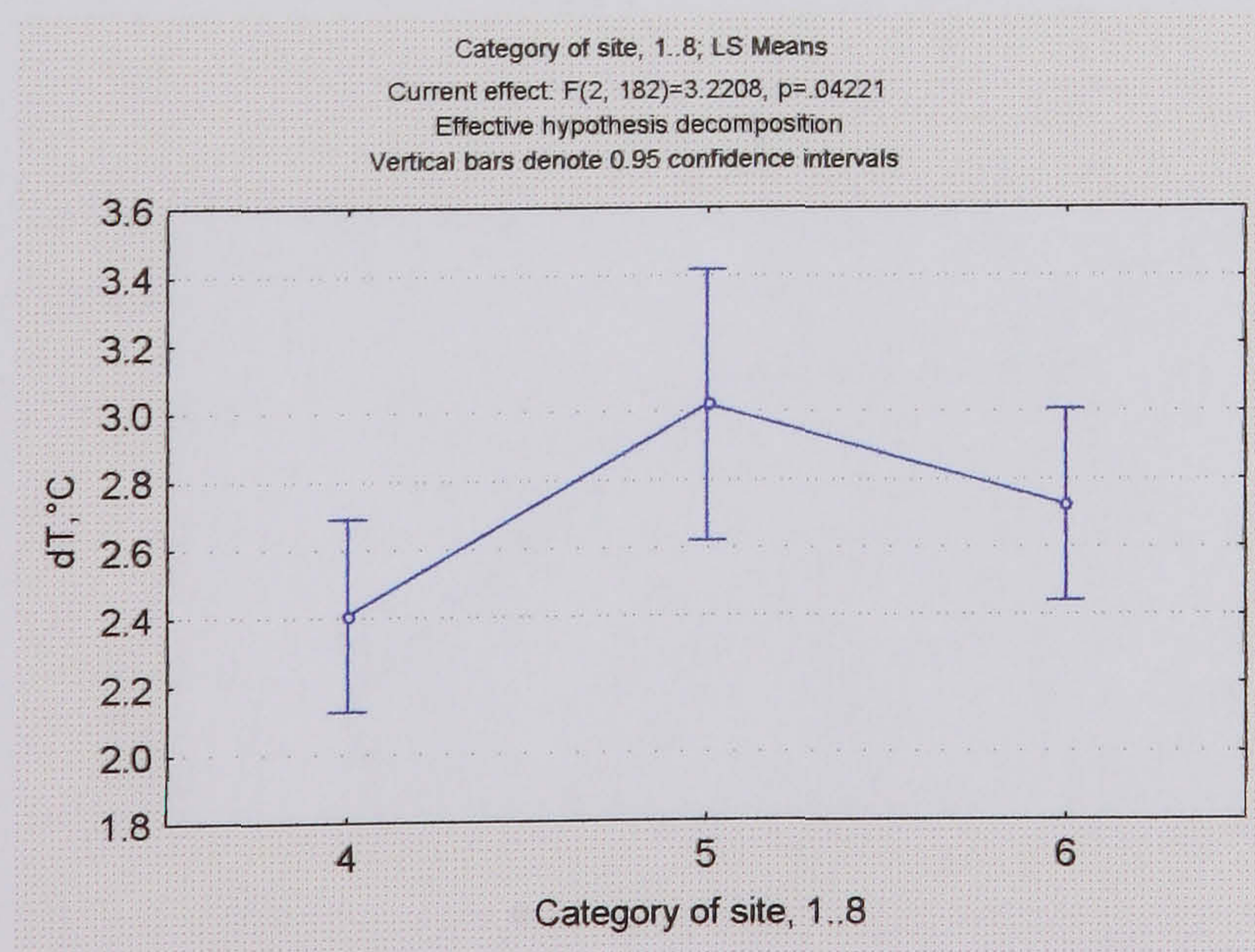


Figure 5.32: The variation of mean dT when grouped by site category, for  $X_r=3$  miles (NIGHT-TIME)

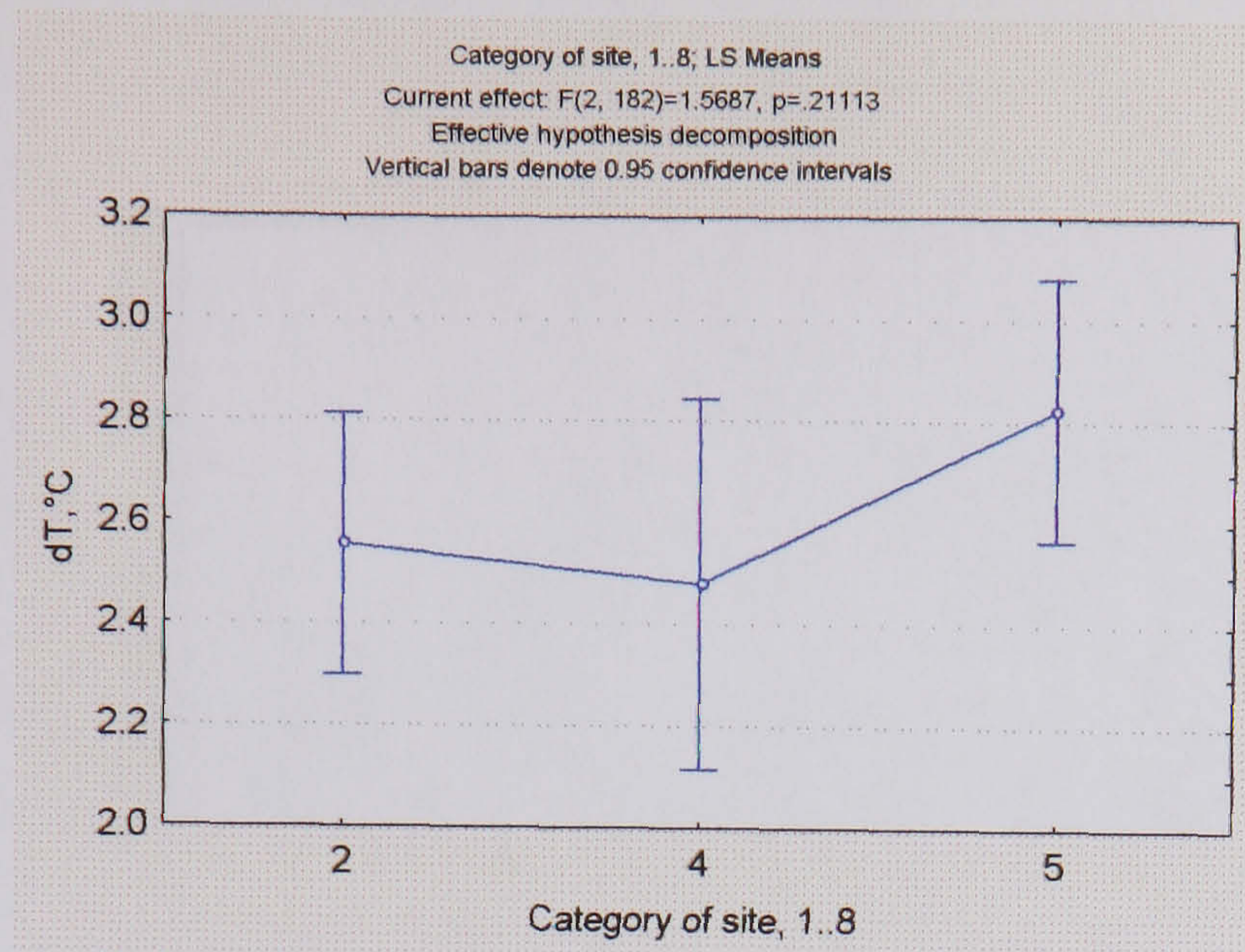


Figure 5.33: The variation of mean dT when grouped by site category, for Xr=4 miles (NIGHT-TIME)

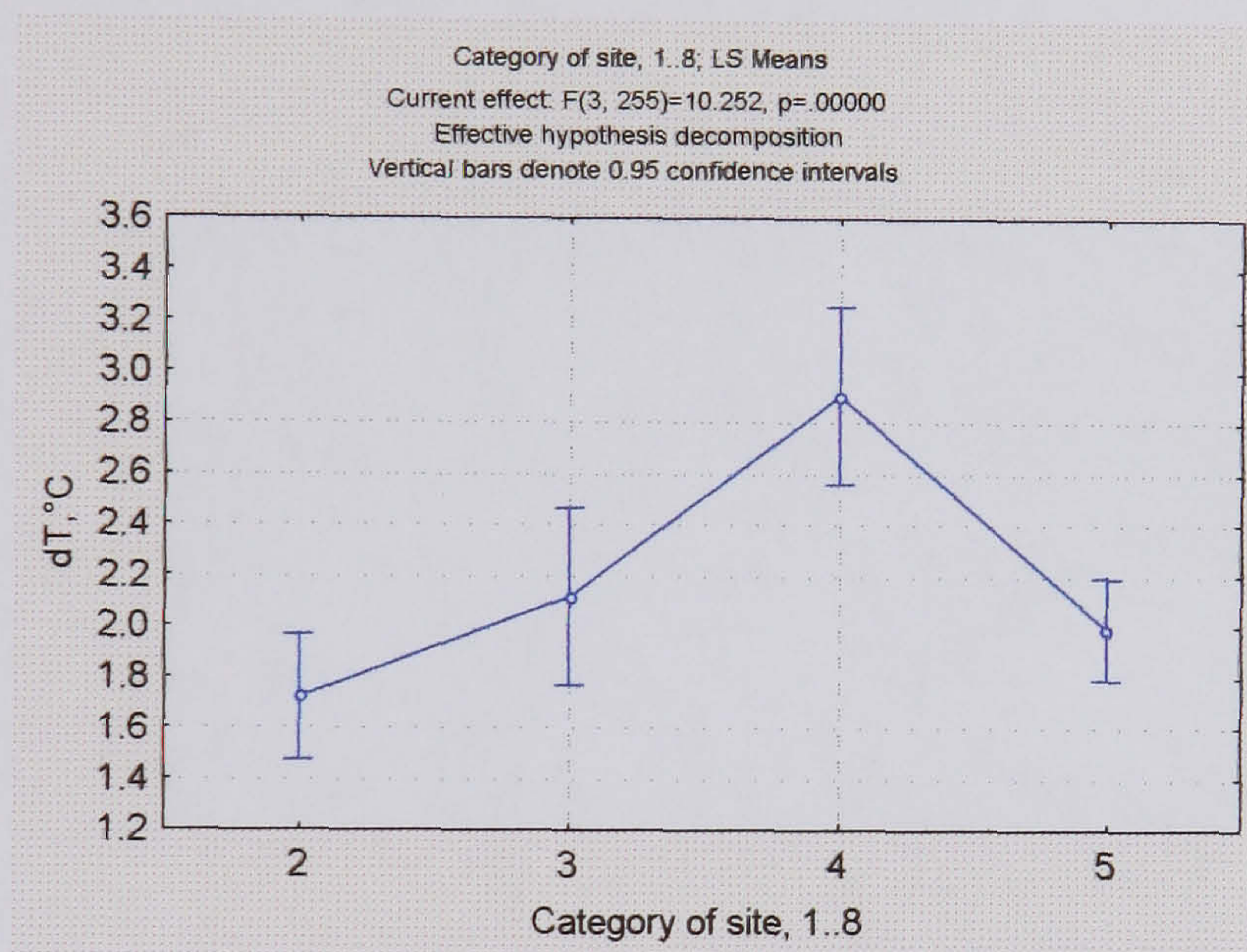


Figure 5.34: The variation of mean dT when grouped by site category, for Xr=6 miles (NIGHT-TIME)

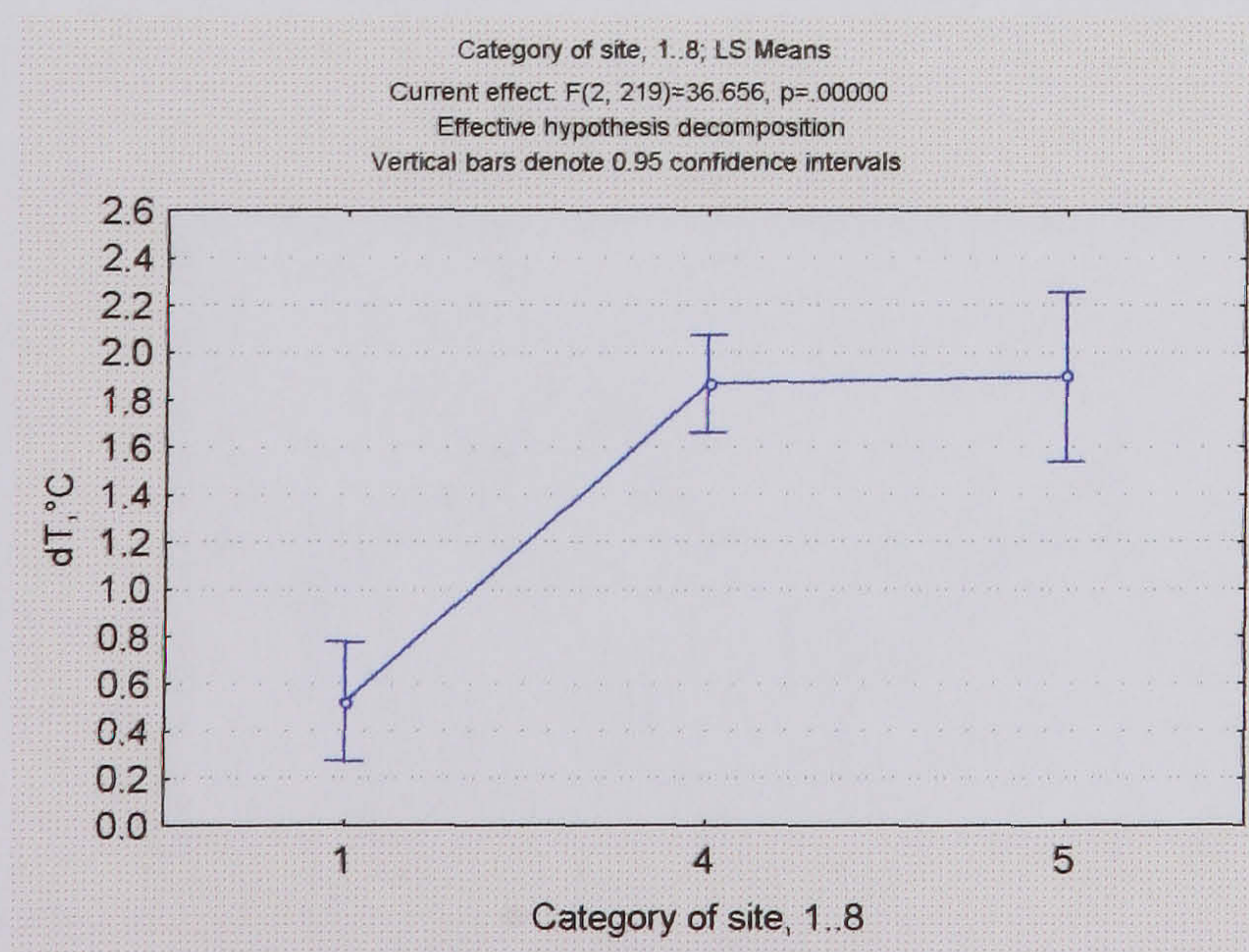


Figure 5.35: The variation of mean dT when grouped by site category, for Xr=8 miles (NIGHT-TIME)

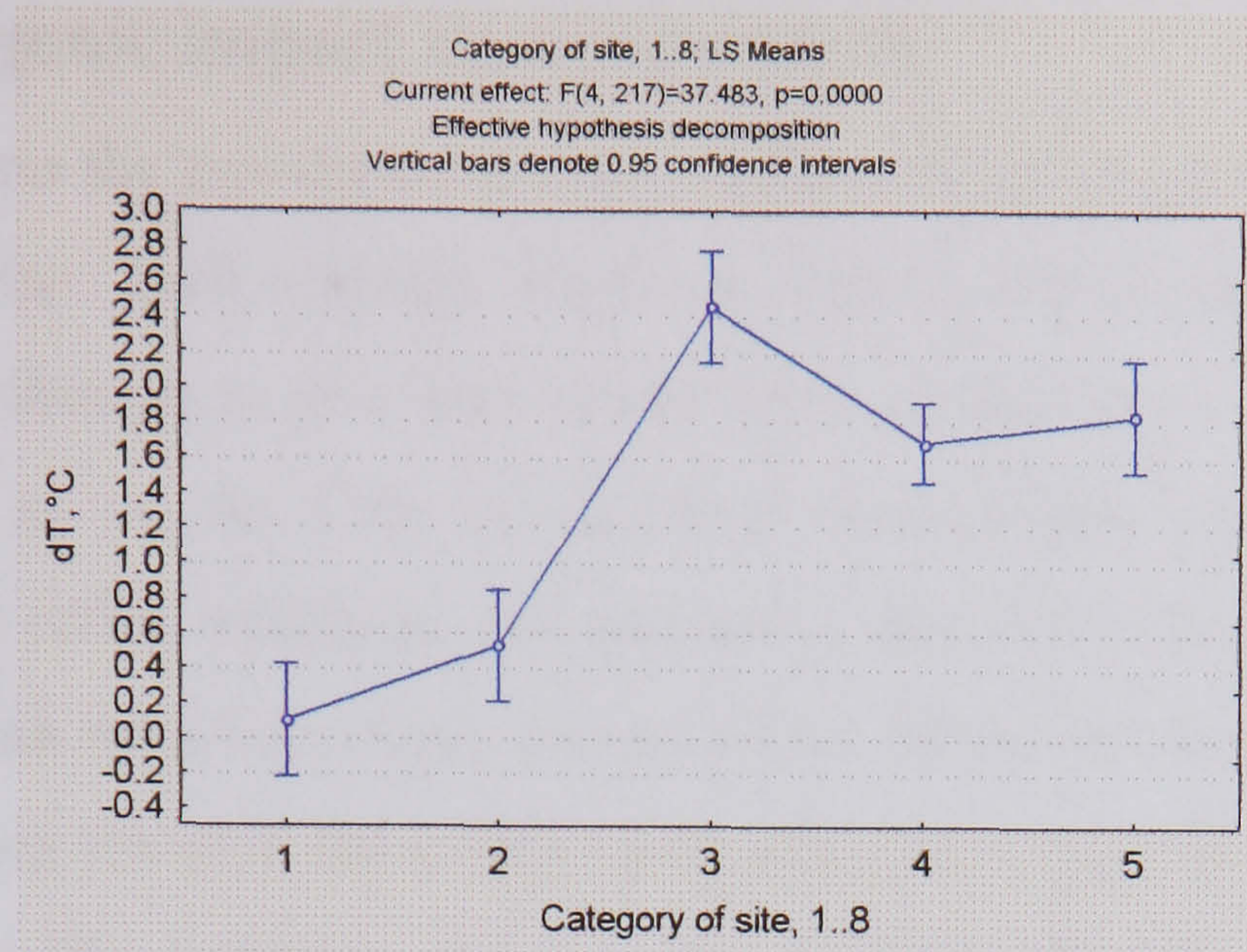


Figure 5.36: The variation of mean dT when grouped by site category, for Xr=10 miles (NIGHT-TIME)

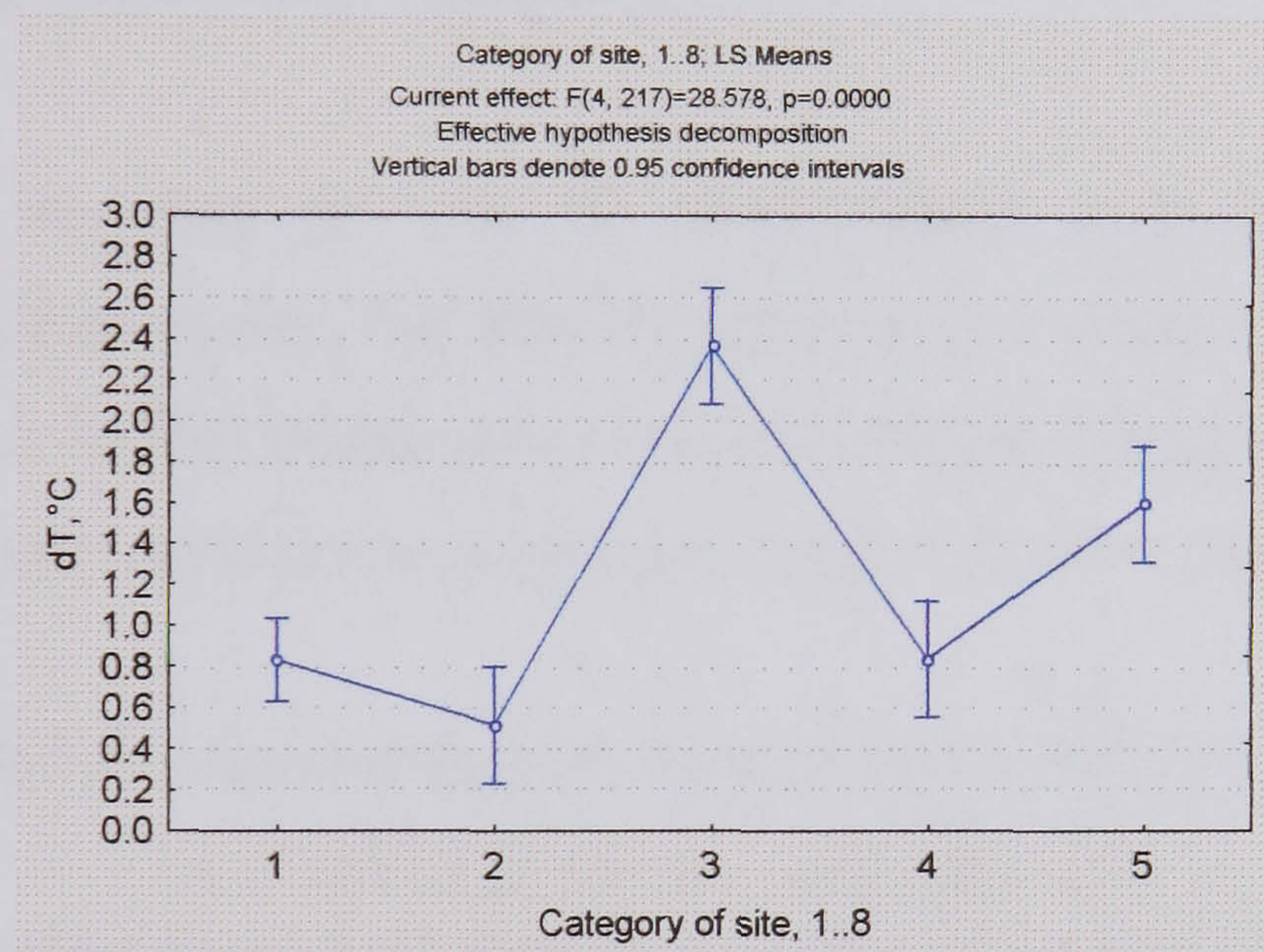


Figure 5.37: The variation of mean dT when grouped by site category, for Xr=12 miles (NIGHT-TIME)

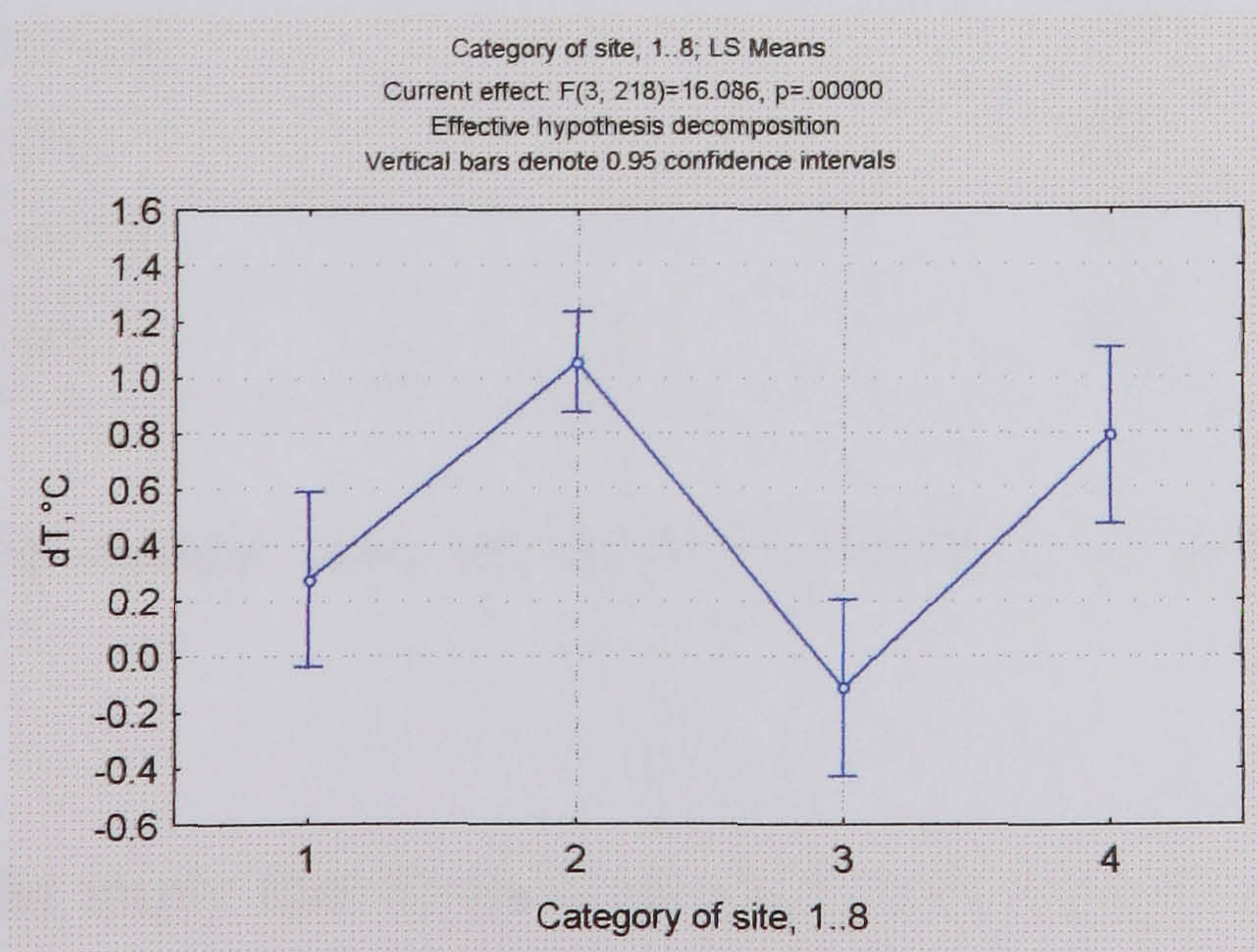


Figure 5.38: The variation of mean dT when grouped by site category, for Xr=14 miles (NIGHT-TIME)

## 5.10 Anthropogenic impact on temperature

Heat is released into the environment from traffic and buildings and this contributes to a temperature rise. Such releases are more densely distributed in the city and to identify this contribution to the heat island the temperature at two sites has been considered. One is in the City of London, Bishopsgate, along a busy road, surrounded by tall office buildings, and another is near the British Museum at Great Russell Street, again on a busy road, but with four storey buildings in the main. The average temperature for each day of the week was computed, for the period 07:00 to 12:00 inclusive in the morning. It was assumed that this time period would be associated with a relatively high emission of anthropogenic heat, from traffic and from buildings. Approximately 140 days of summertime data were used: August & September '99 and August to 20 September '00.

The assumption was that the rate of anthropogenic heat release would vary significantly from day to day, but that in particular it would be at a minimum on Sunday morning. A further assumption was that because a large amount of data was used, weather effects would not be important. Table 5.4 shows the results.

Table 5.4: Mean summertime temperatures (1999 & 2000)  
for 07.00-12.00 at two main road sites

Day	Bishopsgate	Gt. Russell St.
Monday	19.4	18.9
Tuesday	18.2	17.9
Wednesday	18.7	18.4
Thursday	19.5	19.0
Friday	19.1	18.9
Saturday	19.0	18.6
Sunday	18.9	18.5

For these data, the coolest days are in fact weekdays, at both sites, rather than Sundays.

These results might imply that there is no significant change to the anthropogenic heat release on Sunday mornings. However, it may be that the dataset (over 140 days) is not sufficiently large to remove the effects of differences in the weather on

Sundays compared to other days. To test this the same means have been computed for the rural reference station. Figure 5.39 compares the variation in mean temperature there with that at Bishopsgate.

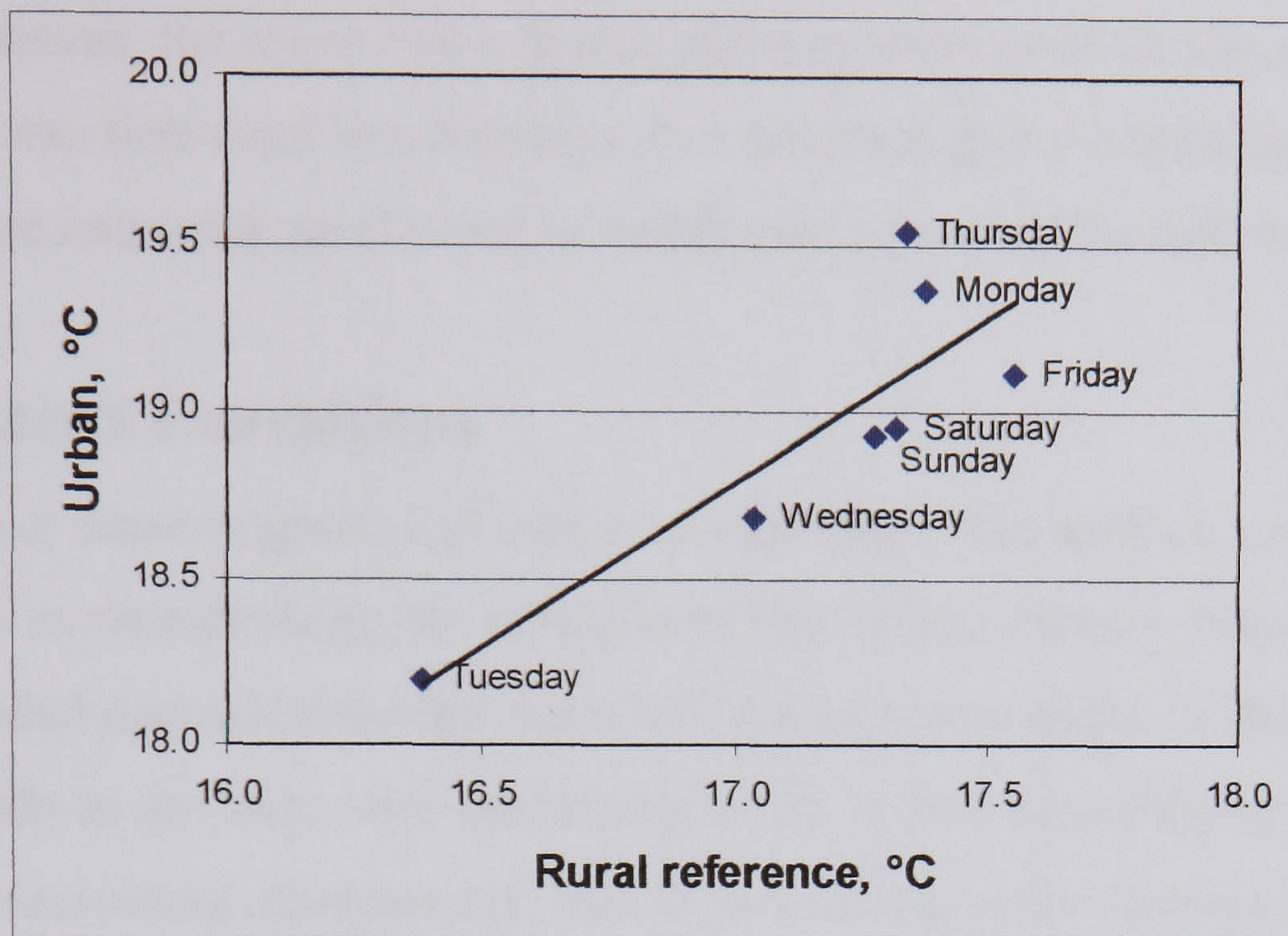


Figure 5.39: Comparison of the mean temperatures for different mornings at two sites

The graph clearly shows that the mean temperature at the urban site rises as that at the rural site 18 miles away does. The latter is not subject to anthropogenic heat and thus the variation at the urban site appears to be mainly as a result of different sets of weather applying to different days of the week.

If there is anthropogenic heat variation between Sunday mornings and other days the impact of the difference appears to be small, at least for average effects over months. The range of mean temperature variation for different mornings of the week in the summer is the same at the rural reference site as at the urban site, viz. 1.2-1.3°C.

One reason for the lack of evidence for an anthropogenic effect on temperature could be that anthropogenic heat input does not change very much from day to day. For example, air conditioned spaces in offices can be maintained at comfort conditions regardless of whether they are occupied on Saturday and Sunday. Hotels and other tourist and visitor facilities will be operating seven days a week in the city.

A further test was made with a subset of 32 days which were selected as 16 matched pairs (a Sunday and a non-Sunday with the same solar radiation and wind speed). Again it was expected that the temperature rise from 07.00-12.00 would be less on Sundays for the same weather conditions because of lower anthropogenic heat release. However, the reverse was found, and moreover *rural* Sundays had a higher temperature rise than rural non-Sundays. It is assumed that the matching of days for solar radiation and wind speed alone is insufficient to control for differences.

## 5.11 Chapter 5 Conclusions

An eight level site-categorization based on sky-views and surface nature has been found useful in characterizing the variation of heat island intensity between sites. For any given radial distance from the centre of London (up to about 10 miles), the mean intensity tends to decrease with decreasing levels of this site-category number (1 to 8), i.e. with decreasing urbanization. This is particularly so for daytime data.

Evidence for the role of anthropogenic heat release in raising temperatures was not found. An examination of a time of presumed low anthropogenic heat release (Sunday mornings) found no evidence of a reduction of temperature then compared to the same time on other days of the week. This result may be contrasted with that for another city that has been studied in some detail. It is reported that anthropogenic heat (from traffic, air-conditioning) in Athens makes a major contribution to the heat island there (Littlefair 2000). In that city, higher intensities are associated with higher urban temperatures, and the maximum intensity occurs in the daytime – the opposite to London.

Greenness at a site was associated with lower air temperatures than harder surfaced sites. Temperatures at hard sites (in the first 150m radius) were 0.27°C cooler if the surrounding area up to 500m radius was green rather than hard. For data where the 45° sector annulus (150-500m) *upwind* of a hard site was green, the mean temperatures were 0.38°C cooler. These results were indicative only of greenness producing a cooling effect at a distance as the uncertainty in the statistic was too high.



In section 2.3.1 of the literature review (Chapter 2) it was revealed that experiments had shown that vegetation was found to lower air temperature. Reductions varied but were generally between 2 and 3°C, which would be very significant for London as this is comparable to the heat island intensity. However, most results were for cities in different climates from London. The next chapter describes experiments made in central London to investigate greenness and other features to provide more detailed, specific evidence of the effect of site factors on local air temperature. The following chapter then introduces the use of the main measured data as input to a simulation model to predict the energy impacts of the temperature variation.

## **CHAPTER 6**

### **Field investigation of urban factors – short-term tests**

# **CHAPTER 6 – Field investigation of urban factors – short-term tests**

## **6.1 Introduction**

To supplement the long term air temperature data, short-term tests were carried out in London in the summer of 2000 aimed at identifying the effect of a park on air temperature, and the relationship between air and surface temperature within street gorges on sunny and cloudy days. The literature review had suggested that it would be worth investigating these areas in London as vegetation and surface colour are important potential ways in which an environment can be modified. This section reports these experiments. Pictures of the measurement sites are provided in Appendix 5.

Two situations were investigated:

- The environment close to a park
- The environment within street gorges

and the following hypotheses were tested:

- The air temperature is significantly different inside and downwind of a park compared to outside
- Local street air temperature is related to local street surface temperatures
- Surface temperature varies significantly with surface finish

## **6.2 Park test**

Parks usually contain vegetation which through evapotranspiration converts incoming solar radiation into latent rather than sensible heat, thereby reducing the surface temperature and in turn the air temperature. Elevated vegetation, for example tree canopies, intercepts solar energy before it reaches the ground, both providing shading and a better opportunity for the heat to be dispersed. Many observations have confirmed the cooling effect of parks although their influence beyond their boundaries is uncertain.

Landsberg reported that large parks situated in urban areas are cooler on warm summer nights (Landsberg 1981). Saito has investigated air and surface temperatures in Kumamoto City in Japan and found that the urban air temperature distribution is related to the distribution of green covering (Saito, Ishihara et al. 1990/91). Givoni reported a small park (300m x 300m) to be 1.5°C cooler at midday than the mean air temperature in adjacent streets 150m away (Givoni 1998). Observations by Vu on a continuously sunny August day showed that the air temperature in a 0.6km<sup>2</sup> park at midday was more than 2°C lower than that measured in surrounding commercial and parking areas (Vu, Asaeda et al. 1998). However, the majority of the existing work on the effects of vegetation has been carried out in warmer climatic zones

### **6.2.1 Method**

A park was chosen three kilometres to the north west of the city, at Primrose Hill, adjacent to one of the existing heat island monitoring stations. The park is approximately 1km long and 0.5km across. See Figure 6.1. The area is mostly residential with a main shopping street to the north east of the park.

A transect across the park was chosen which started and finished in residential streets either side of the park. At each of ten positions along the transect, air temperature and air speed were measured in turn. Some details of the sites are given below:

Sites 1, 9 and 10 are in residential streets. Sites 9 and 10 are tree-lined streets.

Sites 2 and 3 are in the main shopping street. The street has few trees.

Sites 4 to 8 are in the park. The park has a gentle slope rising from the SE to NW. At site 5, the land rises steeply to the summit at site 6. The park is open short grass, but with many trees bordering the paths.

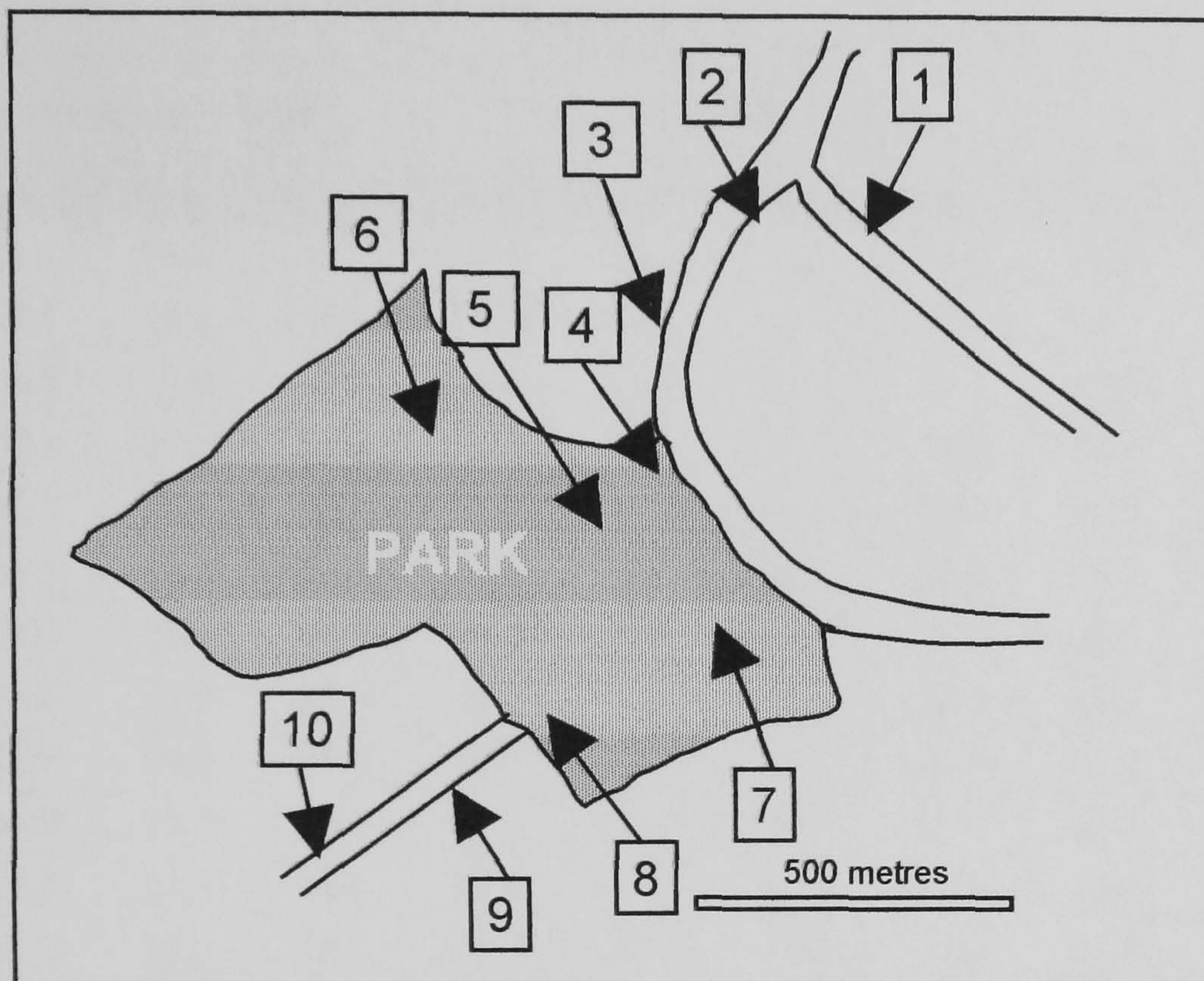


Figure 6.1: The positions of the measurement sites at Primrose Hill park

The test was carried out on a sunny day when it is assumed that the contrast in temperature between the air in the park and the air outside would be higher. Measurement started at 06.30 on 25 August 2000 and continued until 19.10. Air temperature was measured using a shaded fast response digital thermometer (accuracy  $\pm 0.3^{\circ}\text{C}$ ). At each measurement site time was allowed for the temperature reading to stabilize, approximately two minutes. Air speed was measured at 2m height using a hot wire anemometer (accuracy  $\pm 0.3 \text{ m/s}$ ) taking one second readings for a minute and averaging them. Fourteen single direction traverses of the transect (7 pairs) were made over a 13 hour period.

### 6.2.2 Results

As the data from different sites were gathered at different times, it was necessary to interpolate between the out and home pairs of readings to generate quasi-simultaneous values. It was assumed that the rate of change of air temperature was linear over the double traverse time period of 1-1.5 hours. Table 6.1 shows the complete set of aligned hourly air temperature data. Air speeds were around 6 m/s at

the highest point of Primrose Hill Park, 2 m/s lower down, and 1-1.5 m/s in the streets.

Table 6.1: Primrose Hill tests: hourly aligned air temperature data

Time	Air Temperature, °C									
	OUTSIDE PARK			INSIDE PARK					OUTSIDE PARK	
	Site-1	Site-2	Site-3	Site-4	Site-5	Site-6	Site-7	Site-8	Site-9	Site-10
7:00 am	17.1	16.8	16.7	16.3	16.5	16.1	16.3	16.0	16.4	16.7
8:00 am	18.7	18.2	18.3	18.2	18.2	18.1	18.3	17.7	18.2	18.5
9:00 am	20.6	19.9	20.4	20.1	19.8	20.0	20.3	19.3	19.6	19.9
10:00 am	22.5	21.6	21.8	21.5	21.5	21.4	22.0	21.0	20.7	21.5
11:00 am	23.7	22.3	22.9	22.5	22.1	21.8	22.5	21.7	22.0	23.1
12:00 pm	24.1	22.8	24.3	22.8	22.2	22.5	22.8	23.1	22.1	23.3
1:00 pm	24.5	23.3	25.7	23.4	22.8	23.1	23.3	23.5	22.9	23.6
2:00 pm	25.2	23.9	26.1	24.3	23.1	23.3	23.7	23.7	23.9	24.0
3:00 pm	25.8	24.4	25.8	24.5	23.4	23.1	23.9	23.2	23.4	24.0
4:00 pm	24.9	23.9	25.0	24.3	23.5	23.1	23.7	23.2	23.8	23.8
5:00 pm	24.2	23.3	24.4	23.6	22.7	22.5	23.8	22.9	23.8	23.6
6:00 pm	23.2	22.2	22.4	22.1	21.7	21.2	21.8	21.5	22.2	22.0
7:00 pm	21.8	20.7	21.4	20.4	20.5	20.0	20.4	20.4	20.6	20.9

### 6.2.2.1 Mean park and streets temperature through time

These data have then been grouped and averaged according to their location inside or outside the park and are shown in Figure 6.2.

It can be seen that:

- $\Delta T_{(\text{streets} - \text{park})}$  decreases initially from 0.5°C at 7am to a minimum at 10am, and then rises to a maximum of 1.1°C at 15:00 in the afternoon
- The peak  $\Delta T_{(\text{streets} - \text{park})}$  coincides with the time of highest temperatures
- $\Delta T_{(\text{streets} - \text{park})}$  is always positive, i.e. the mean of the park measurements is always cooler than the mean of the measurements in the streets outside

The reducing  $\Delta T$  in the morning until 10am is probably associated with the greater solar exposure in the park compared to the overshadowing in the streets at a time of low sun angle.

The mean temperatures over the 13 hours for the two groups of data are 22.1°C (streets) and 21.5°C (park) with a mean  $\Delta T$  of 0.6°C. Considering the two groups of data as matched pairs, the mean reduction in temperature in the park of 0.6°C is statistically significant at the 0.1% level (t-test).

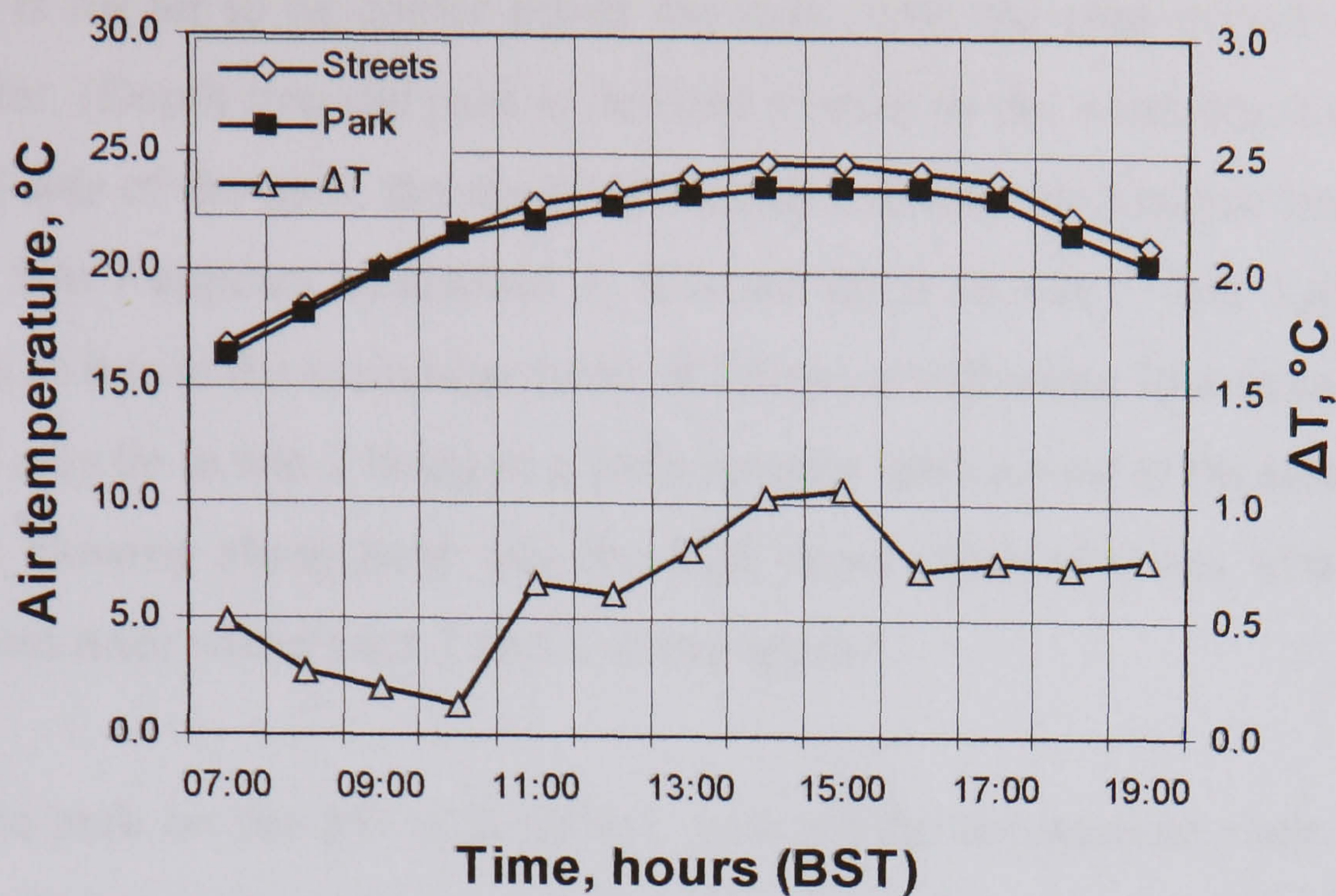


Figure 6.2: Hourly mean air temperature inside and outside the park

#### 6.2.2.2 Variation of temperature with position

The wind direction during the test was initially from the NE but veered to the E or SE later on. With this general wind direction the order of measurement of the different sites was roughly the same as the order of increasing urban or park fetch. For much of the time, air appeared to be arriving at the entrance to the park (site 4) from the adjacent high street (sites 2 and 3). If the park has a cooling effect, successive sites would be expected to be increasingly cooler. Figure 6.3 plots the mean temperatures of each site over the test period.

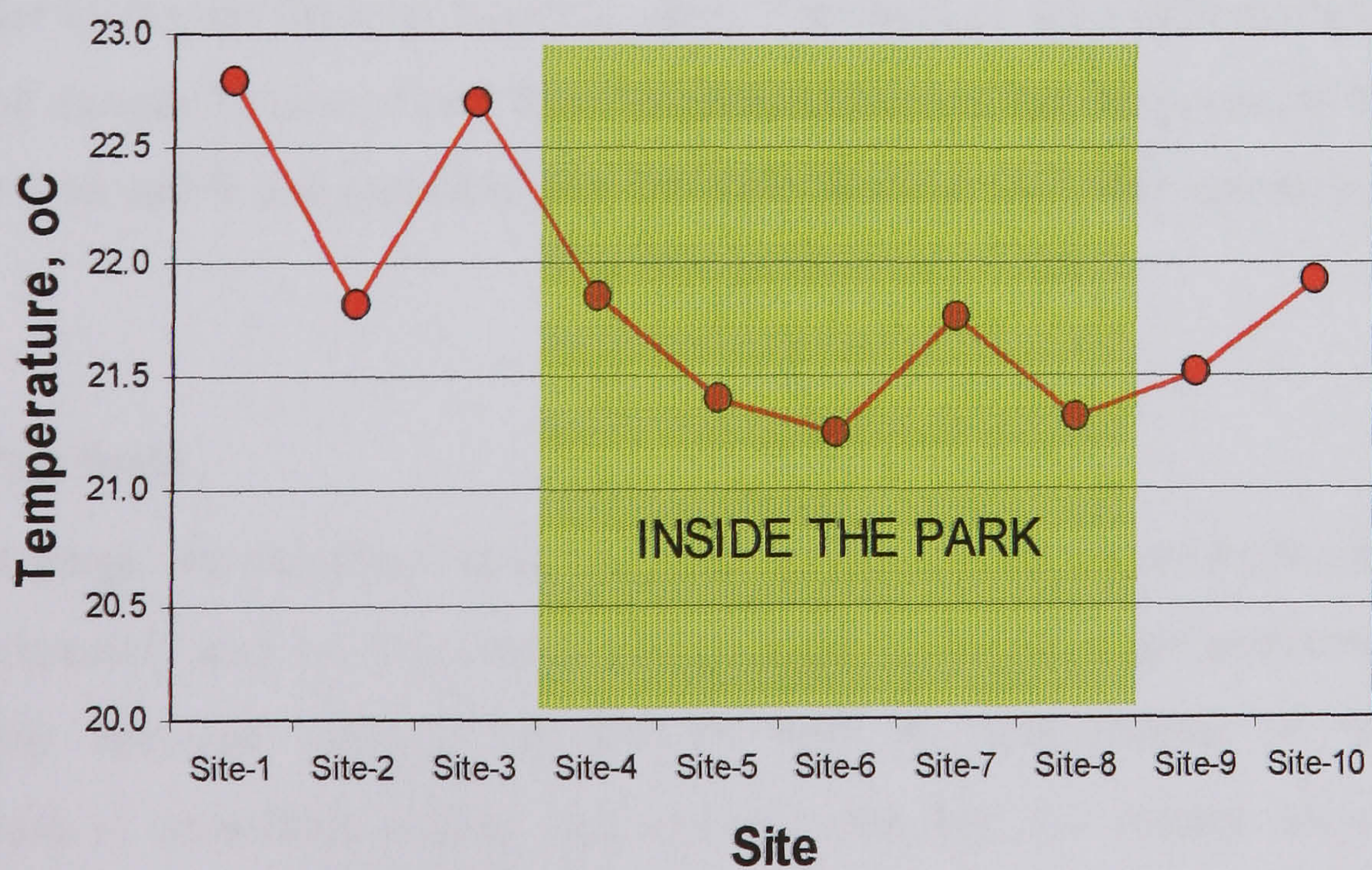


Figure 6.3: Mean temperature over 13 hours at each site

The trend is for air to be cooler inside the park, with the sites deeper in the park being cooler. (Depth into the park is defined relative to the wind direction.) On the downwind side of the park, the air is increasingly warmer as distance from the park increases. Site 7 appears anomalous as it is not far from site 5. Site 2 also appears anomalous as it is in the main high street of Primrose Hill some 50m from site 3. The difference may lie in site-2 being at a wide junction with a road to the south-east. Air was often blowing along here into the high street. This site was also mostly in shadow from trees whilst sites 1 and 3 were exposed.

Outside the park on the SW side (sites 9 and 10) the temperature rises again. The wind direction in this street was usually along and away from the park, although sometimes the air blew, weakly, towards the park.

#### *6.2.2.3 Cooling influence beyond the park*

In the south western end of the transect, air moved along the street from the park. The direction was variable, but mainly away from the park. As already noted, the three sites 8, 9 and 10 showed air temperature increasing with distance from the park (Figure 6.3).

This street was uniform in being shaded by trees along its length and with residential buildings (mostly flats) along it of similar height. The street was apparently being kept cooler by the air flowing from the park. The limit of the extent of the influence of the park cannot be determined from the data collected, but it appears to be at least from site 8 to site 9 and possibly site 10. This is some 200-400 metres beyond the park.

### **6.3 Gorge tests**

The street gorge is a defining feature of urban environments and its high surface area of hard materials and semi-enclosed nature modify the local air temperature. The relationship between surface temperature and air temperature in the urban environment is important. Aerial and satellite imaging can record surrogates for surface temperature over an entire city with relative ease compared to ground based measurement. If urban air temperature can be inferred from these surface values,



there is the potential for detailed mapping of the urban heat island. However, the vertical surfaces of street gorges can be more difficult to assess from high altitude.

Previous work has found that the relationship is not always clear. Barring found that the variation in street surface temperature along a street is much greater than the variation in air temperature along the same path (Barring 1985). Eliasson, considering nocturnal data, concluded that surface and air temperature patterns in cities are very different – and that deducing air temperature using IR thermographic data was to be avoided (Eliasson 1996). Clearly, air in a city is not usually static and it would be expected that its temperature would assume some more moderate value resulting from contact with a multitude of warmer and cooler surfaces. Micro-advection was thought to be a likely reason for a relatively uniform nocturnal air temperature in Göteborg (Eliasson 1996).

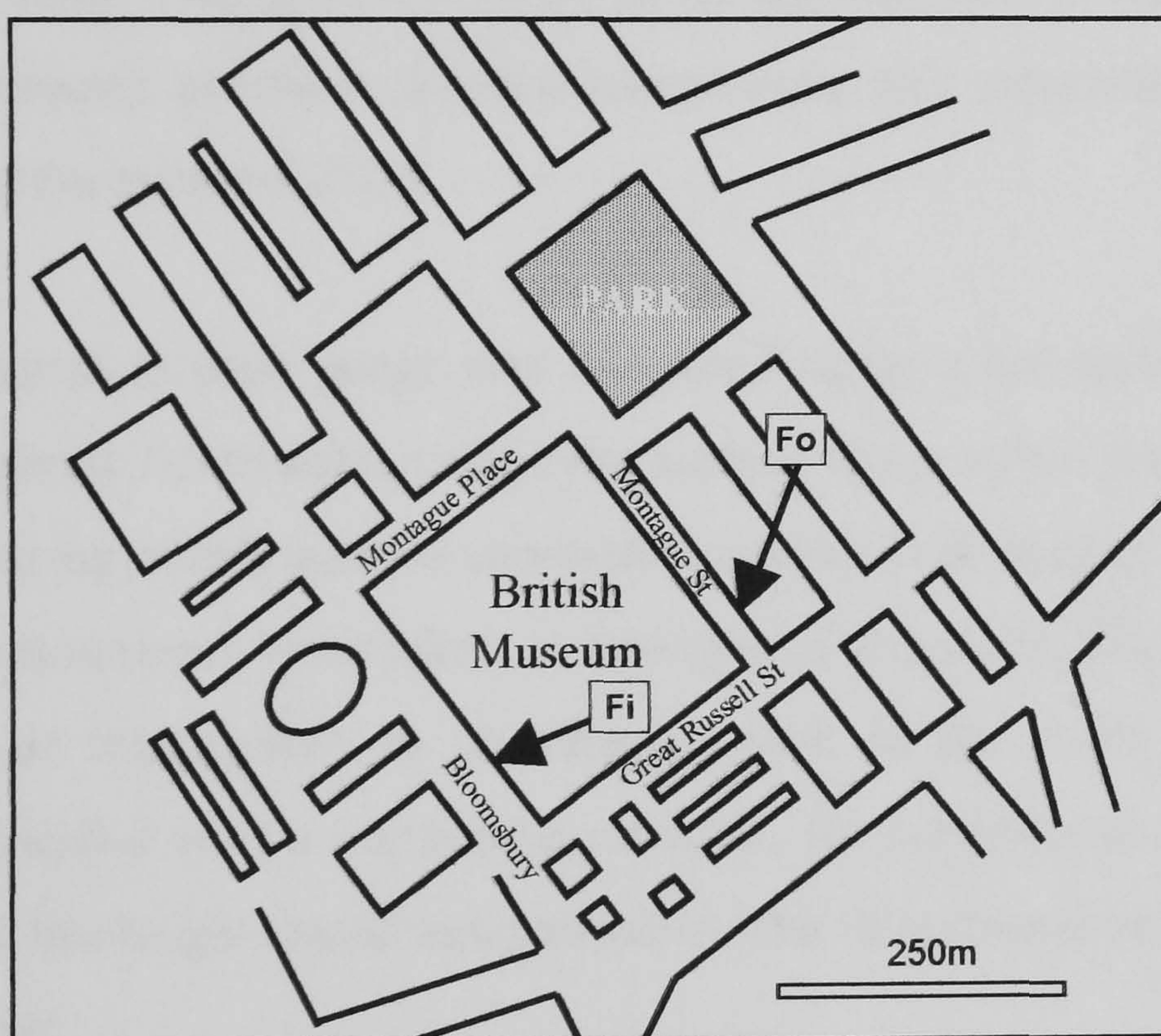


Figure 6.4: The positions of the measurement sites around the British Museum  
Fi and Fo are two particular façades chosen for comparison

### 6.3.1 Method

Four streets around the perimeter of the British Museum were chosen for the tests. These formed a square of roads with different façades, widths, vegetation and orientations (See Figure 6.4). The street gorges had a height to width ratio of between 0.5 and 0.8, were between 13-19 metres high and were 19m across (42m for

Montague Place). Bloomsbury and Great Russell Street were heavily trafficked. A typical small park (150 x 150m) lay near the junction of two of the roads. An advantage of choosing this location was that the air temperature at 6m height in all four streets was already being monitored hourly as part of the main array of 80 stations.

As in the park test, simultaneous measurements in the four streets were not possible. Instead, each street was visited in turn and, at each site, up to 16 surface temperature measurements were made together with the local air-speed. The whole façade was not measured; rather, a section near to the existing air temperature monitoring station was sampled as follows. A façade section, about 50m long, was divided into a 3x2 grid (left : centre : right) and (upper : lower). This was done for both sides of the road, together with ground surface sampling of the inner and outer footways and sections of the road. This gave 16 gorge sampling locations in each street and 64 surface measurements per hour. Surface temperature was measured using an infra-red thermometer (accuracy  $\pm 2^{\circ}\text{C}$ ).

The local air speed in each gorge was measured using a hot-wire anemometer by sampling over about 3-5 minutes (while the surface temperature measurements were being taken), during which some 6 sub-measurements each lasting 20 seconds were taken. The measurements were taken at a height of about 2m. Measurements were also made of air temperature in an adjacent park in the shade, using a digital thermometer shielded with a concentric reflector, for comparison with the four air temperatures, at 6m height, made automatically. The instruments used were the same as in the park test.

A test was made on a sunny day (11 September 2000, from 6:35 am to 7.10 pm) and on a cloudy day (21 September 2000, from 6.15 am to 3:10 pm) to see the effect of this change in the ratio of direct:diffuse solar energy, and reduced insolation. Rain cut short the test on the cloudy day; surface characteristics would have changed and air speed could not be measured.

On a separate day, the reflectivity (to daylight only) was measured on a number of surfaces to both characterize the variation found and to see how this related to the

temperature differences found. Reflectivity was measured using grey card of reflectance 18% and a luminance meter. Measurements were taken of the road, footway, and several walls. Walls at higher levels (4m plus) were tested by fitting the grey card to a telescopic pole.

### 6.3.2 Results

All data were time aligned by linear interpolation. For some missing data, occasional substitution was used if this was valid, e.g. there was generally a trend in the temperature measured across a road from: inner footway : inner road : outer road : outer footway. Some measurements were accidentally missed, shown with a dash. Table 6.2 shows an example of part of the sunny day data, for Montague Place (footway temperatures, and left and right façade temperatures omitted). Different parts of the street gorges are labelled with reference to the British Museum: inner façades and footways are on the museum side of the road: outer ones are on the opposite side. Left and right hand sides of a façade are as viewed from the road. Reflectivities of various gorge surfaces are shown in Table 6.3.

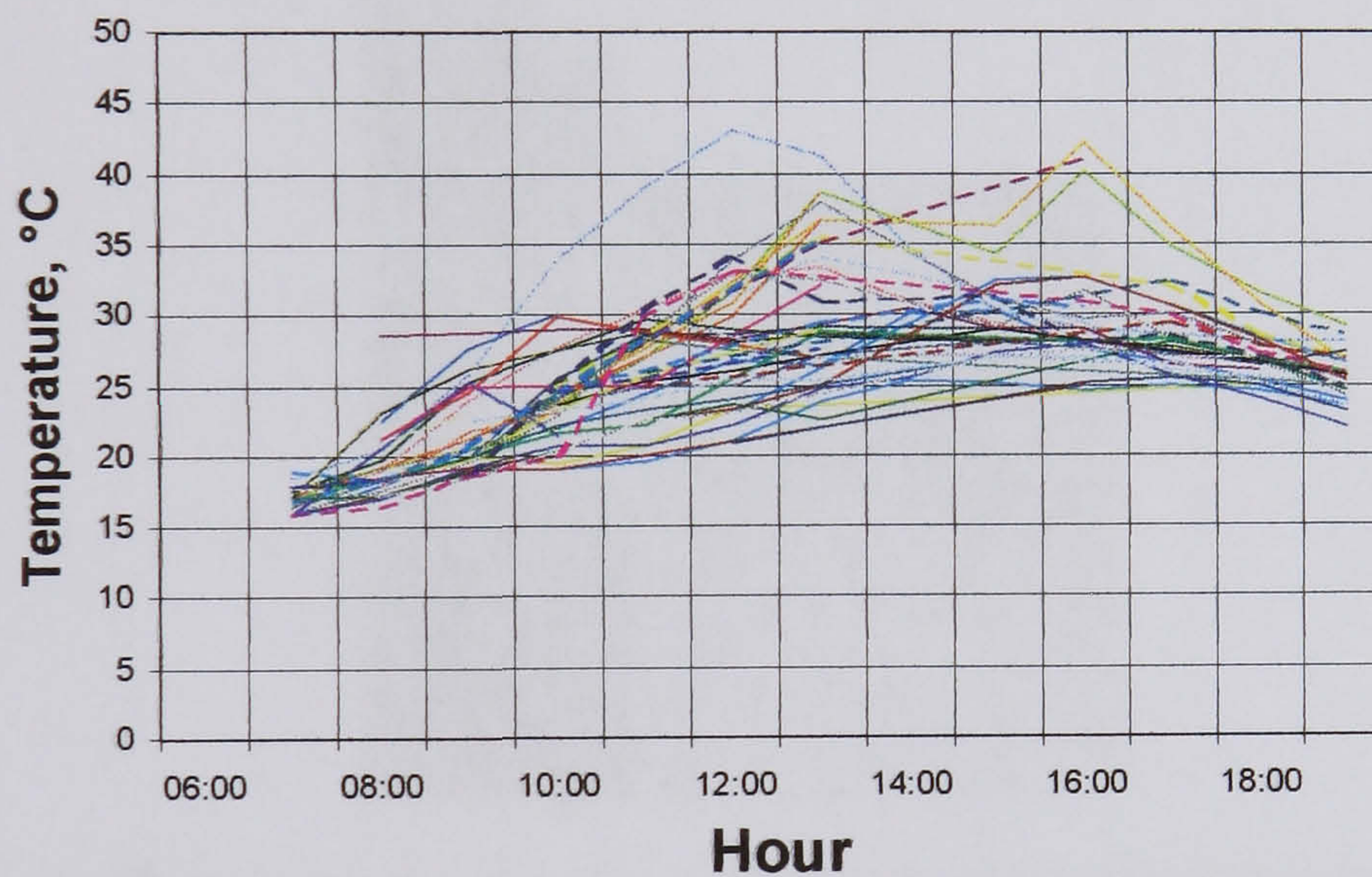
Table 6.2: An example of the surface temperature data, air temperature and speed measurements in Montague Place on a sunny day

Time	Air in gorge (m/s)      (°C)		Surface temperature, °C					
			INNER FAÇADE Centre		ROAD		OUTER FAÇADE Centre	
			Lower	Upper	Inner	Outer	Lower	Upper
7:00 am	0.18	17.6	17.2	16.0	15.9	15.9	18.4	16.5
8:00 am	0.24	18.5	18.5	17.2	17.1	17.9	20.6	19.0
9:00 am	0.35	22.0	20.0	19.0	19.2	20.5	25.8	24.1
10:00 am	0.28	23.3	19.4	19.0	20.7	22.1	33.8	27.7
11:00 am	0.50	24.9	20.7	19.6	20.6	24.4	39.0	30.5
12:00 pm	0.74	27.1	23.2	21.1	22.1	26.7	43.0	32.8
1:00 pm	0.84	28.5	—	23.9	24.7	26.4	41.3	33.4
2:00 pm	0.81	28.1	—	25.2	25.5	30.0	34.8	30.9
3:00 pm	0.74	27.4	—	25.1	27.3	30.3	30.1	29.3
4:00 pm	0.70	27.4	—	24.5	27.9	27.5	29.0	28.1
5:00 pm	0.82	26.7	—	25.0	25.7	26.5	28.5	27.0
6:00 pm	0.58	26.3	24.9	24.5	23.9	25.2	28.0	26.5
7:00 pm	0.12	25.3	23.1	23.5	22.1	23.8	28.0	25.5

Table 6.3: Reflectivity to daylight of various surfaces in the streets

No.	Location	Surface	Reflectivity
1	Montague Place	Upper white outer façade	42%
2	Montague Place	Lower darker outer façade	36%
3	Montague Street	Upper dark inner façade	8%
4	Montague Street	Lower white inner façade	50%
5	Montague Place	Outer road	6%
6	Montague Place	Outer footway	16%
7	Bloomsbury	Dark inner footway	9%
8	Bloomsbury	Red brick outer façade	9%
9	Bloomsbury	Dark inner façade	3%

Hourly surface temperatures - Sunny



Hourly surface temperatures - Cloudy

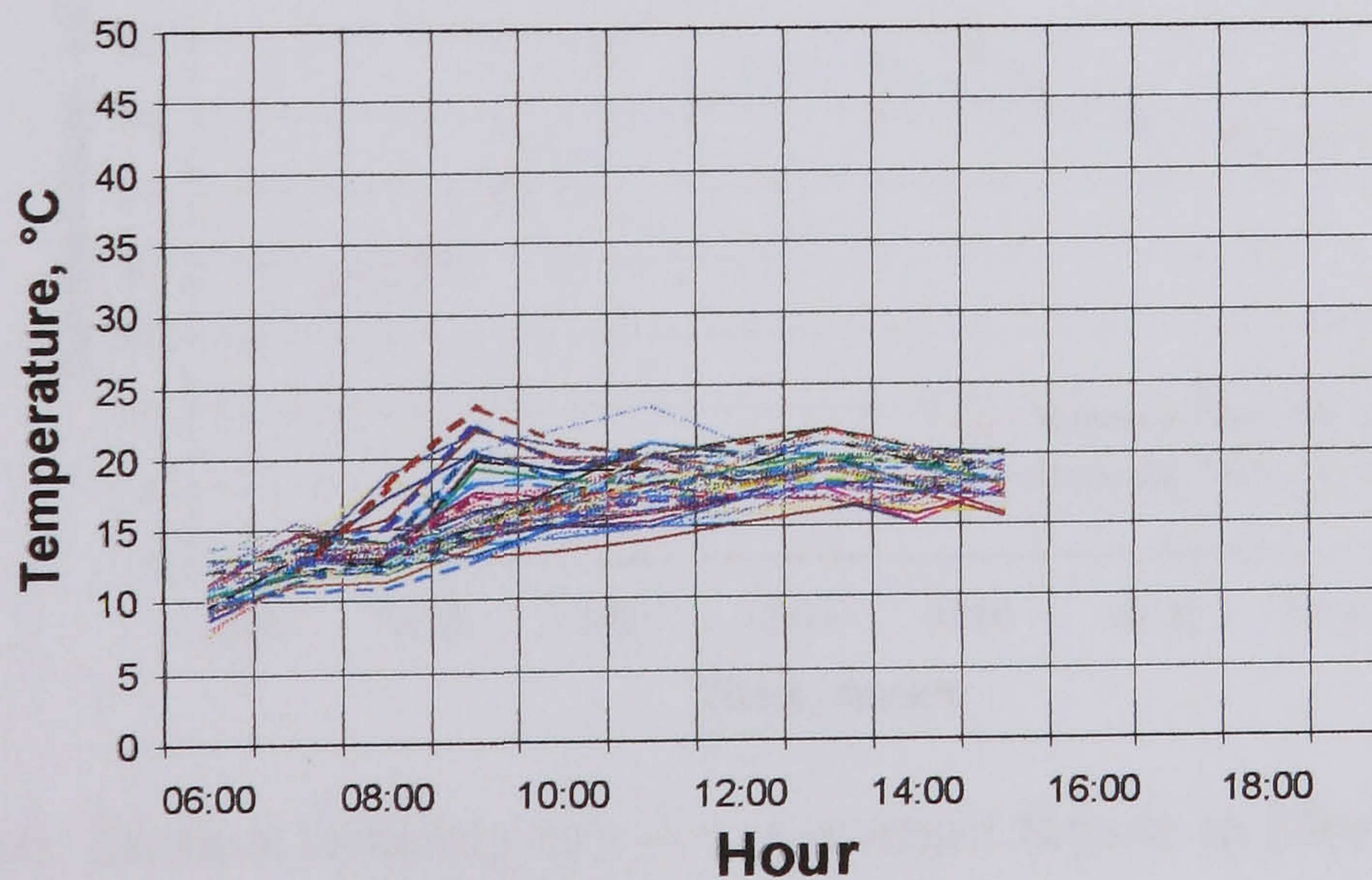


Figure 6.5: The variation of surface temperatures on the two days. Up to 64 surfaces (16 in each gorge) were measured each hour

### 6.3.2.1 Variation of surface temperature - overall

Figure 6.5 shows all the hourly surface data (up to 64 values/hour). It illustrates the wide difference in temperature to be found within adjacent streets. On the sunny day the range across the data reached a maximum of 22°C at midday, but a 5-10°C spread of temperature was more typical.

On the cloudy day, the maximum difference was much lower, 11°C, and a 5°C range more typical. This maximum occurred early, at 9am, but this was a time when the sky was actually relatively clear, with low angle bright sun. It clouded over immediately after this.

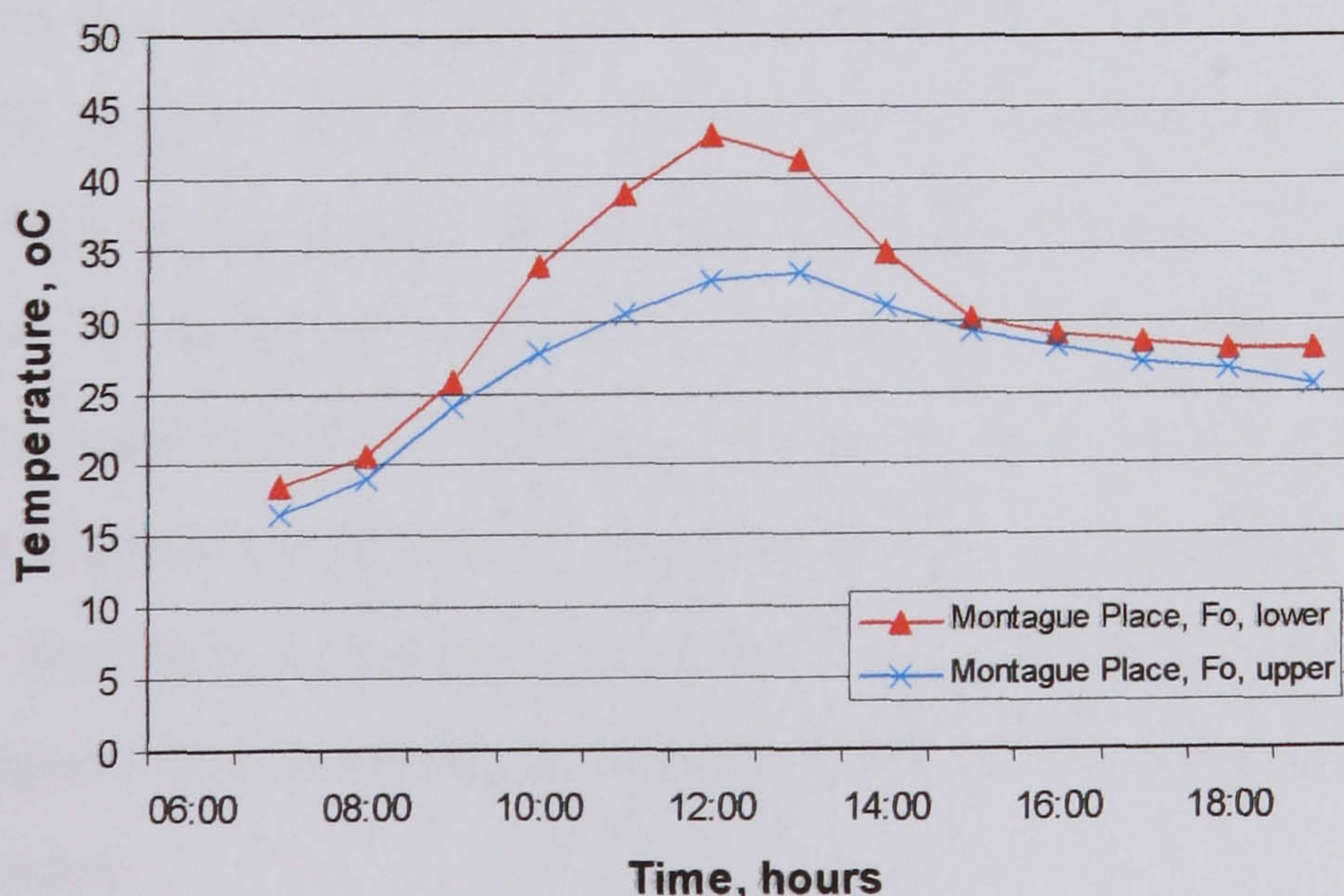


Figure 6.6: Surface temperature of a re-entrant façade in Montague Place: a light upper surface contrasted with a ground floor darker section set back one metre

The highest surface temperature, 43°C, occurred at midday on the sunny day for a building in Montague Place with a re-entrant façade – the upper floors oversail the ground floor by one metre. See Figure 6.6. The combination of a slightly darker colour for the ground floor wall with overhang above (reducing convection) and reflected radiation from the ground (light-coloured hard paving) are likely to be responsible for the lower façade being up to 10.2°C warmer (at midday) than the upper façade. The mean difference from 7am to 7pm was 3.8°C. The 6% difference in reflectivity of the two sections (36% and 42% from Table 3) would be too small to account for such a large temperature difference.

#### *6.3.2.2 Comparison of parallel streets with contrasting façades*

To test the effect of façade colour on surface temperature, two parallel streets with contrasting façade colours were selected. The inner façade at Bloomsbury (Fi) is brick painted very dark all over (reflectivity 3%); the outer one (Fo) at Montague Street is rendered brick with a matt white paint finish at lower level, with dark brick above (reflectivities 50% lower and 8% upper). See Figure 6.7. These values for reflectivity are only indicative of the way solar radiation is absorbed on the different surfaces as they do not measure the absorption of infra-red radiation (or UV) – a significant component of solar radiation.

Figure 6.7 shows that the three dark parts of both façades had similar temperatures, but that the light surface was 6-10°C cooler. The Bloomsbury street gorge has the same width as that of Montague Street, but it has some taller buildings (7 stories, rather than 4) on the south west side that increase the over-shadowing of the inner façade there (Bloomsbury Fi). Conversely, there are also some road junctions and wider spaces that improve solar access along the street. It is probable that overall the façades receive similar solar radiation, and that the reduced temperature of the white façade in Montague Street is mainly as a result of the colour difference with the other three darker façades.

Figure 6.7 also shows the divergence of temperature between the four surfaces started at around 10 or 11am (BST). This is the time when the façades came out of shadow and started to receive direct sun. Before that time, the façades would have received only diffuse solar radiation, and radiation from the opposite façades. After

13.30, overshadowing by the opposite façades rendered further comparison of the gorges invalid.



Bloomsbury – inner façade, Fi

Montague Street – outer façade, Fo

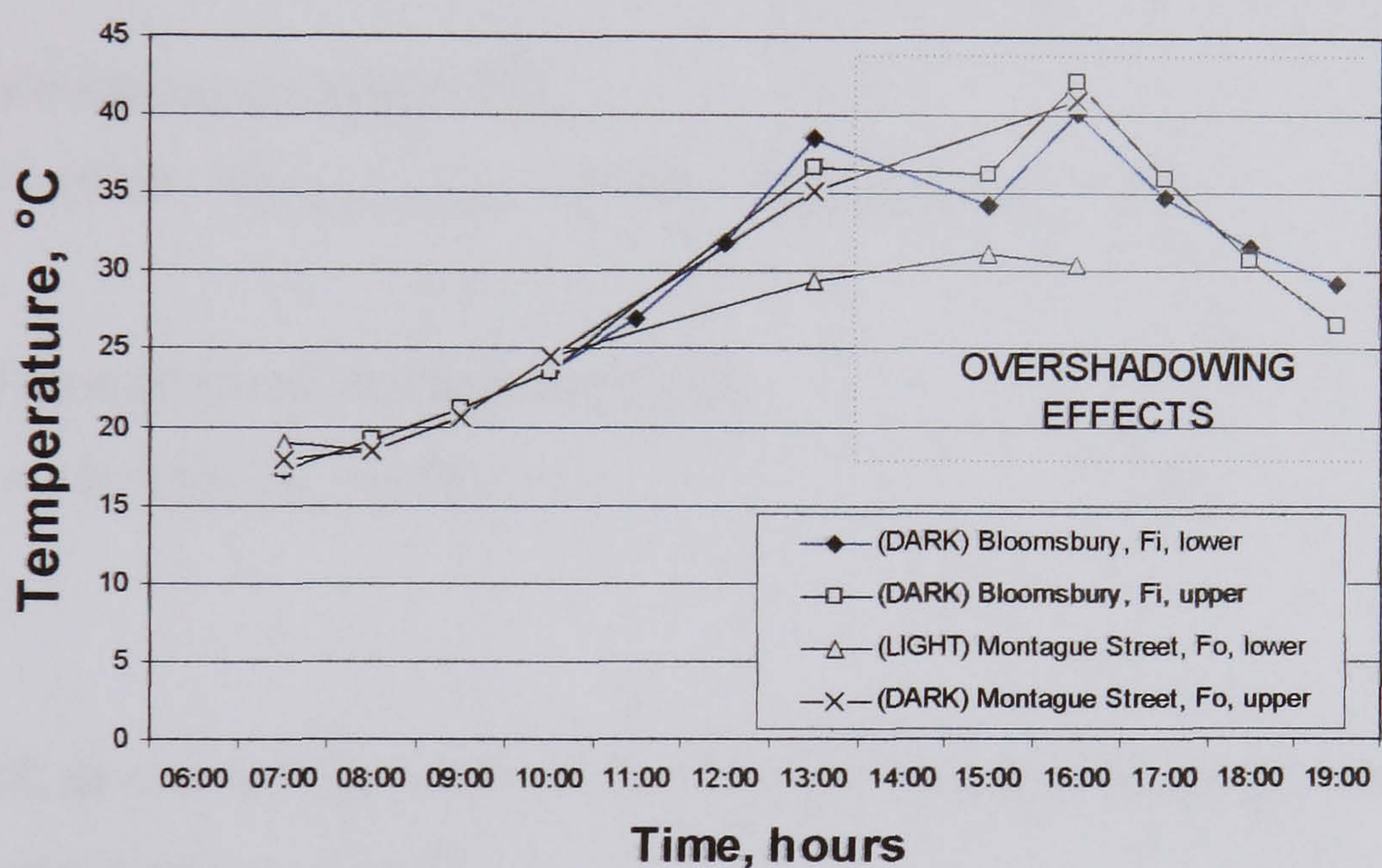


Figure 6.7: Surface temperature ( $T_s$ ) at ground level & high level on an all dark façade (Bloomsbury), contrasted with one that is light at low level and dark above (Montague St.). Sunny day

### 6.3.2.3 Relationship between façade temperature and gorge air temperature

The main way in which the temperature of air is raised is by contact with warmer surfaces. To investigate the effect of the warmer façades on the air passing through the street gorge, a mean gorge surface temperature has been calculated.

#### Mean gorge surface temperature

Each façade was divided up and categorized according to colour, and the closest temperature data available ascribed to it. Footways and roads were treated similarly. The main dimensions of Montague Street gorge are shown in Figure 6.8.

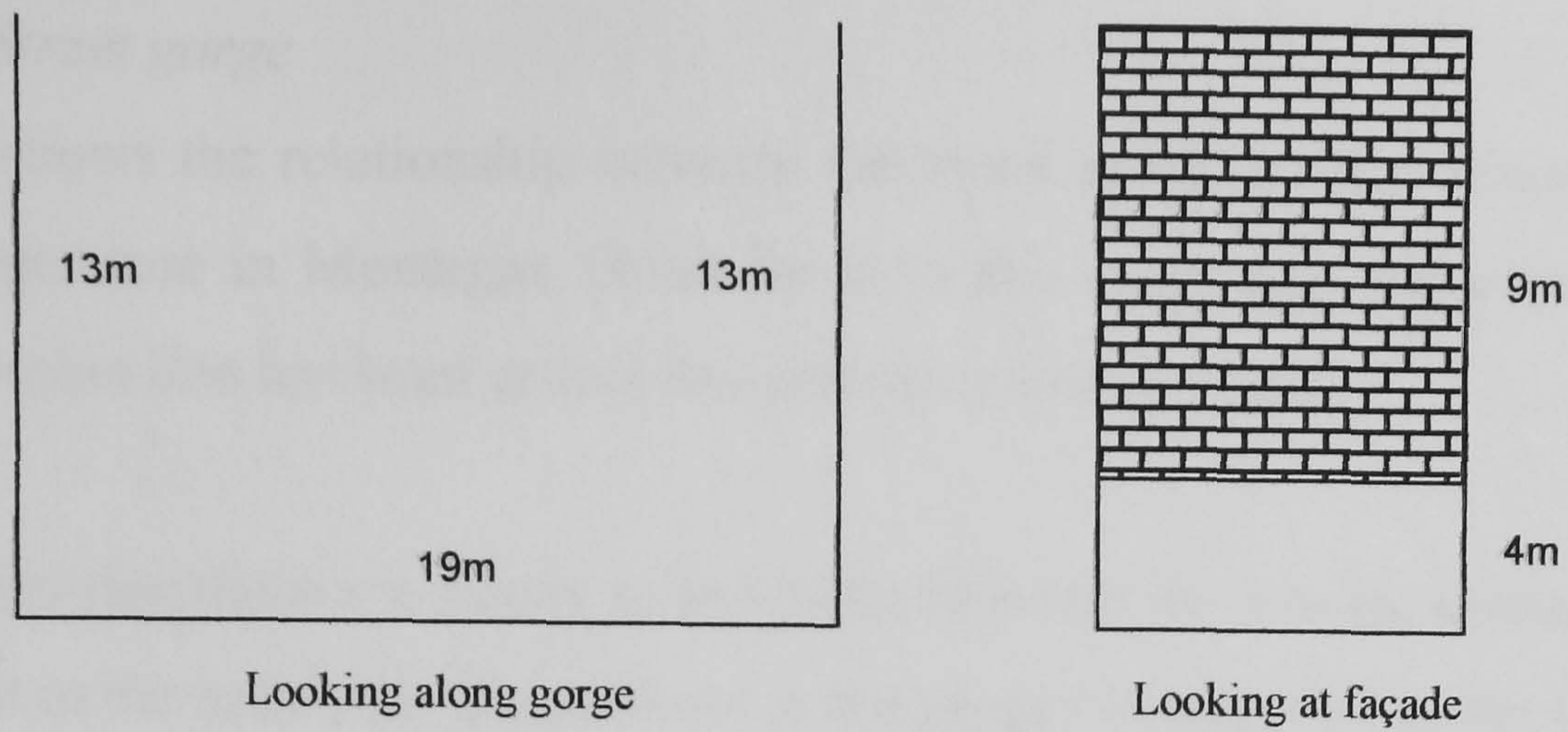


Figure 6.8: Principal dimensions of Montague Street gorge

The mean surface temperature of the outer façade ( $F_o$ ),

$$T_{F_o} = (9/13) \cdot T_{F_o\text{Upper}}(L,C,R) + (4/13) \cdot T_{F_o\text{Lower}}(L,C,R) \quad (1)$$

Similarly, for the inner façade ( $F_i$ ),

$$T_{F_i} = (9/13) \cdot T_{F_i\text{Upper}}(L,C,R) + (4/13) \cdot T_{F_i\text{Lower}}(L,C,R) \quad (2)$$

and for the ground (road and footways) ( $G$ ),

$$T_G = (10/19) \cdot T_R + (9/19) \cdot T_F \quad (3)$$

where:

$L,C,R$  is left, centre or right parts of the façade (Montague St. gorge is uniform).

$T_R$  = the mean road temperature

$T_F$  = the mean footway temperature

This process yielded three mean values for the inner façade, ground, and outer façade temperatures. These were combined, weighting the terms according to the ratio of the height (façades) or width (road or footways) to produce a final mean gorge surface temperature,  $\overline{T}_{\text{gorge}}$ .

$$\overline{T}_{\text{gorge}} = (13/45) \cdot T_{F_o} + (13/45) \cdot T_{F_i} + (19/45) \cdot T_G \quad (4)$$

Glazing and roofs were ignored.



### Montague Street gorge

Figure 6.9 shows the relationship between the mean gorge surface temperature and the air temperature in Montague Street for both the sunny day and cloudy day. A linear regression line has been drawn through the combined data.

It can be seen that there is a strong relationship between the two parameters; 98% of the variance in the hourly air temperature in the gorge is explained by the variation in hourly mean gorge surface temperature. The gradient of the regression line is 0.83 showing that air temperature increases more gradually than surface temperature.

It is perhaps surprising that the relationship is so strong, as advection from adjacent areas with different characteristics might be expected to introduce variation. However, the gorge chosen is quite long, and uniform, and air speeds were low (a mean of 0.6m/s for both days). The relationship holds for both cloudy and sunny conditions, although it is stronger for the sunny and warmer day ( $r^2 = 0.94$  – sunny, and 0.87 – cloudy).

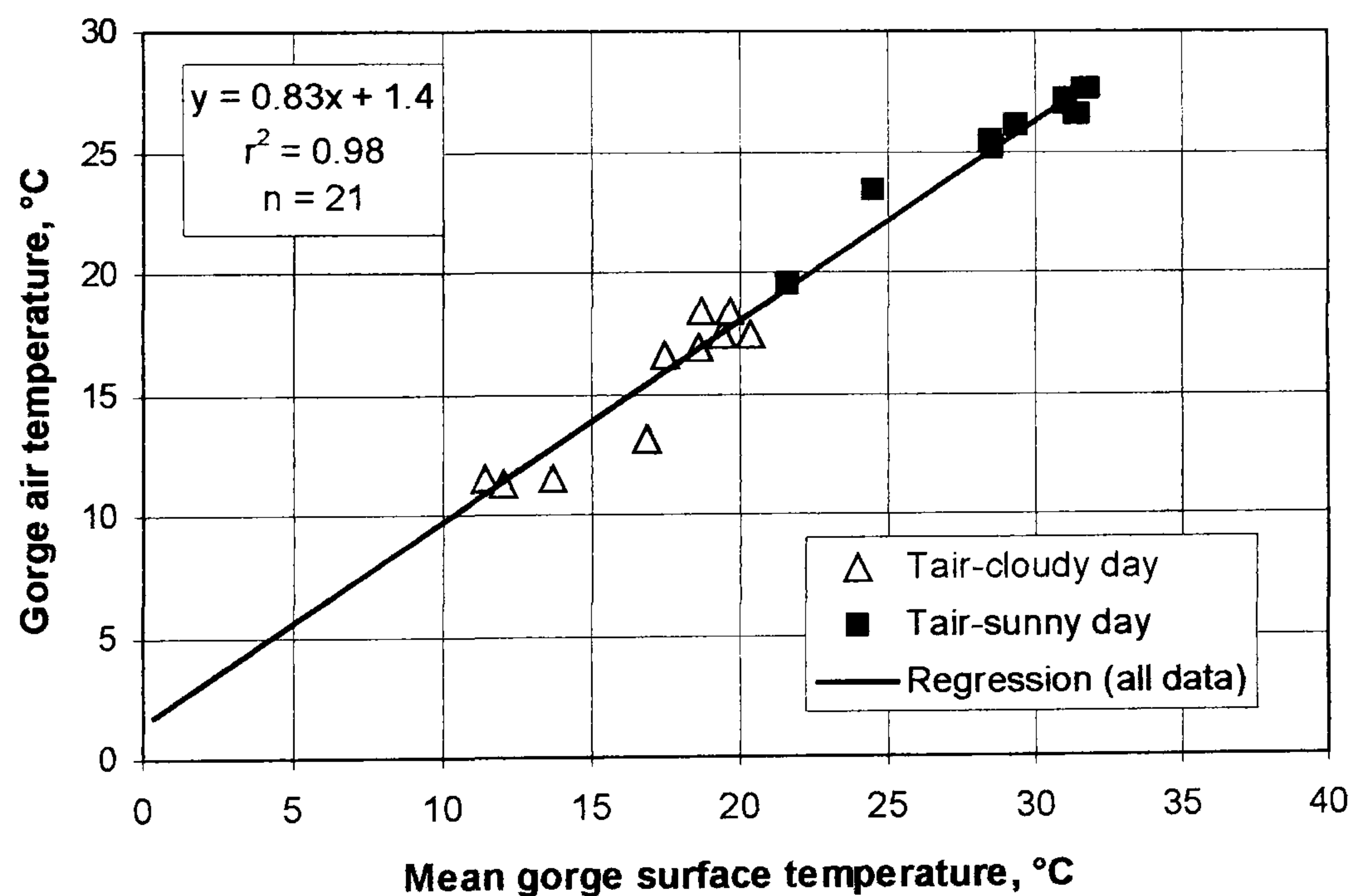


Figure 6.9: The hourly variation in gorge air temperature with mean gorge surface temperature.

#### 6.3.2.4 Comparison of air temperature in the street gorges and a small park

Table 6.4 compares the mean air temperature in the small park adjacent to the British Museum and the four street gorges nearby. On the sunny day, the variation in the means from street to street was small – within 0.4°C. The park was the coolest, but was only 0.2°C cooler than the adjacent Montague Street, from which air travelled mostly towards the park.

The spread of temperatures for the cloudy day was similar, but in contrast the park was the warmest of all five sites, by 0.1°C (not significant).

A similar contrast for the two days is evident for the maximum temperatures reached. On the sunny, warmer day, the park was the coolest; on the cloudy day the park temperature was close (within 0.1°C) to the maximum values found in the streets.

For both days the park started the day warmer than the streets. This temperature difference was greater on the cloudy day, but the sky had in fact been clear overnight, so that differentiation by sky view (radiative cooling) would still favour the park being warmer, with its mature tree canopy inhibiting heat loss.

Table 6.4: Mean air temperatures over the test period, °C

	<b>Park</b>	<b>Montague Place</b>	<b>Bloomsbury</b>	<b>Great Russell St.</b>	<b>Montague St.</b>
<i>Sunny day</i>					
Means:	24.3	24.9	24.8	24.6	24.5
Maxima:	27.2	28.5	28.4	29.1	27.6
Minima:	17.9	17.6	17.7	17.4	17.4
<i>Cloudy day</i>					
Means:	15.5	15.4	15.4	15.0	15.2
Maxima:	18.2	17.9	18.3	18.0	18.3
Minima:	12.1	11.1	11.7	11.2	11.2

Table 6.4 shows that on both days the air temperature in the park varied less than outside; its range of temperature on the sunny day being 2.4°C *less* than that of the warmest streets. (1°C less on the cloudy day.) The general temperature range for the two days was about 11°C and 7°C respectively.

At the warmest time of the day, around 3-4pm, the coolest location was in the park. The difference was about 0.4-0.6°C compared to the coolest streets adjacent to the park.

## 6.4 Chapter 6 Conclusions

### *Primrose Hill Park*

Air temperature was measured at five places inside and five places outside a park on a sunny day. Taking the mean values of these two groups of measurements, the air in the park was found to be cooler than air outside by an average of 0.6°C over the test period of twelve hours. The difference reached a peak of 1.1°C at 15:00. Cooler average, and cooler maximum temperatures were associated with the park. In a test in 1963, Chandler compared the air temperature in Hyde Park with its surroundings north and south on a sunny day and found a maximum contrast of 1.3°C (Chandler 1965). Local wind speed was not measured, but reached 6.7 m/s at 18:00 at Heathrow, which is close to the speeds measured in this test (6.0 m/s at 18:00) at the highest point of Primrose Hill Park. The maximum temperature depressions recorded are similar for both tests.

Considering individual measurement sites, an area in the main shopping street, unshaded by trees, was the warmest, and was 3°C warmer than the centre of the park at 14:00. A mostly residential street with little shading was the next warmest site. Warmer temperatures were associated with unshaded streets.

Air passing out from the park and along a street gorge appeared to extend the park's cooler environment along the gorge. The street was uniform in tree cover and buildings, but temperature rose with increasing distance from the park. The park's influence apparently extended between 200-400 metres along the gorge from the park.

These results suggest that both peak and average air temperatures can be reduced by the presence of a park, and by the use of trees. Both these use part of the incident solar energy to evaporate water, and hence make less available for heating of the air. Trees also intercept solar energy above the ground and thus aid the dispersal of solar heat to upper layers of air.

### *Gorges*

The air temperature in a street gorge (measured at approximately half gorge height) is strongly related ( $r^2 = 0.98$ ,  $n=21$ ) to the mean surface temperature of the gorge, computed from the ground and façade temperatures. This is true for hourly simultaneous data, in either sunny or cloudy conditions, although the relationship is slightly weaker for the latter.

The colour of a building surface has a strong effect on the temperature that a surface reaches when exposed to the sun. A white painted brick wall can be around 10°C cooler than a dark one under the same solar exposure. Higher radiant temperatures, and lower air speeds, can be responsible for reducing the comfort level of pedestrians in street gorges. These two results suggest that the local air temperature in a gorge may be amenable to manipulation, up or down, through the alteration of the façade or ground characteristics

The small park exhibited a smaller range of temperature variation than in the street gorges. This is probably a result of the tree canopy in the park reducing the radiative cooling at night, and ground level solar access in the daytime.

It should be noted that the air speeds measured in the streets were low on both test days. This may have allowed the temperatures in the streets to develop more according to their individual characteristics than on days with greater displacement and mixing with air from adjacent areas. The relationship between daytime surface and air temperature is much stronger here than that reported for streets in housing estates in Singapore ( $r^2 = 0.49-0.70$ ,  $n > 485$ ) (Nichol 1996). Eliasson, using night-time data over a wider area, concluded that the surface and air temperature patterns within a city are very different (Eliasson 1996).

This concludes the reporting of the measured data showing the variation of the London heat island across the city and at local level. The following chapter introduces the work on modelling the impact of this variation on cooling demand.

## **CHAPTER 7**

### **Modelling the impact of the London heat island**

# CHAPTER 7 – Modelling the impact of the London heat island

## 7.1 Introduction

The urban environment has been found often to be warmer than the surrounding rural area, but not always. Moreover, the diurnal temperature pattern is different, with peak temperatures being reached at different times of the day. The density of buildings in urban areas also offers opportunities for reducing solar gain through mutual shading, thereby offsetting to some extent a warmer environment.

Because of the complexity of the interactions, it has been convenient to use simulation software to model the performance of a building and, in particular, the energy needed for air-conditioning it. By siting a standard building at different measurement sites it is possible to predict the change in energy use with location within the heat island, and address the following general objectives, to:

- model the energy performance of an example building in urban contexts
- determine the factors important to the variation of energy used for cooling
- determine the annual balance of the effect of the urban environment on energy used for heating and cooling

## 7.2 Modelling methodology

The purpose of the modelling work was to generate predictions indicative of the impact of the urban environment on the energy needed for cooling in air conditioned buildings. The work involved choosing a building to simulate, a simulation model to use, urban locations and appropriate weather data, before running the simulations. Predictions of heating and cooling load within the building spaces were then converted to the energy input to the plant by allowing for its efficiency.

The modelling proceeded in two phases. A *Pilot phase* modelled the performance of the notional building at 7 sites for one summer month (August) looking at cooling load alone. The *Main phase* used 24 sites and modelled for 12 months looking at total load.

### 7.2.1 Choice of building

Buildings vary greatly in their age, insulation, and design. To enable an easy comparison from site to site, and with other work, a design of building was selected from a well-known set of notional buildings that are used for providing guidelines on energy efficiency. The Energy Consumption Guide 19 (BRECSU 1999) lists four types of offices: naturally ventilated (open plan or cellular), and air-conditioned (standard or prestige). From these types, type 3 (air-conditioned, standard) was chosen as best representing a typical office building with air-conditioning. This is referred to here as ECON 19/3.

This building is associated with a type of construction and operation rather than being defined uniquely. However, details of a typical design, and U-values, have been developed (Saporito 1997). To enable a complete definition of the building to be formulated for this modelling, it was necessary to make further reasonable judgements in some of the details of the design. Detailing internal zoning was considered unnecessary for this work. Automatic window systems for daylight control were thought to be atypical of most offices and not modelled.

#### 7.2.1.1 Building description

Figure 7.1 shows the ECON 19/3 office building modelled. It is a three storey building, 9m high, 30m long and 15m wide orientated with the longer sides facing north:south, with 60% glazing on the north and south façades. There is clear double glazing with no shading. The end walls are unglazed. Walls and roof are concrete with insulation. Intermediate floors are of concrete with false ceilings. The ground floor is uninsulated. The building is open plan.

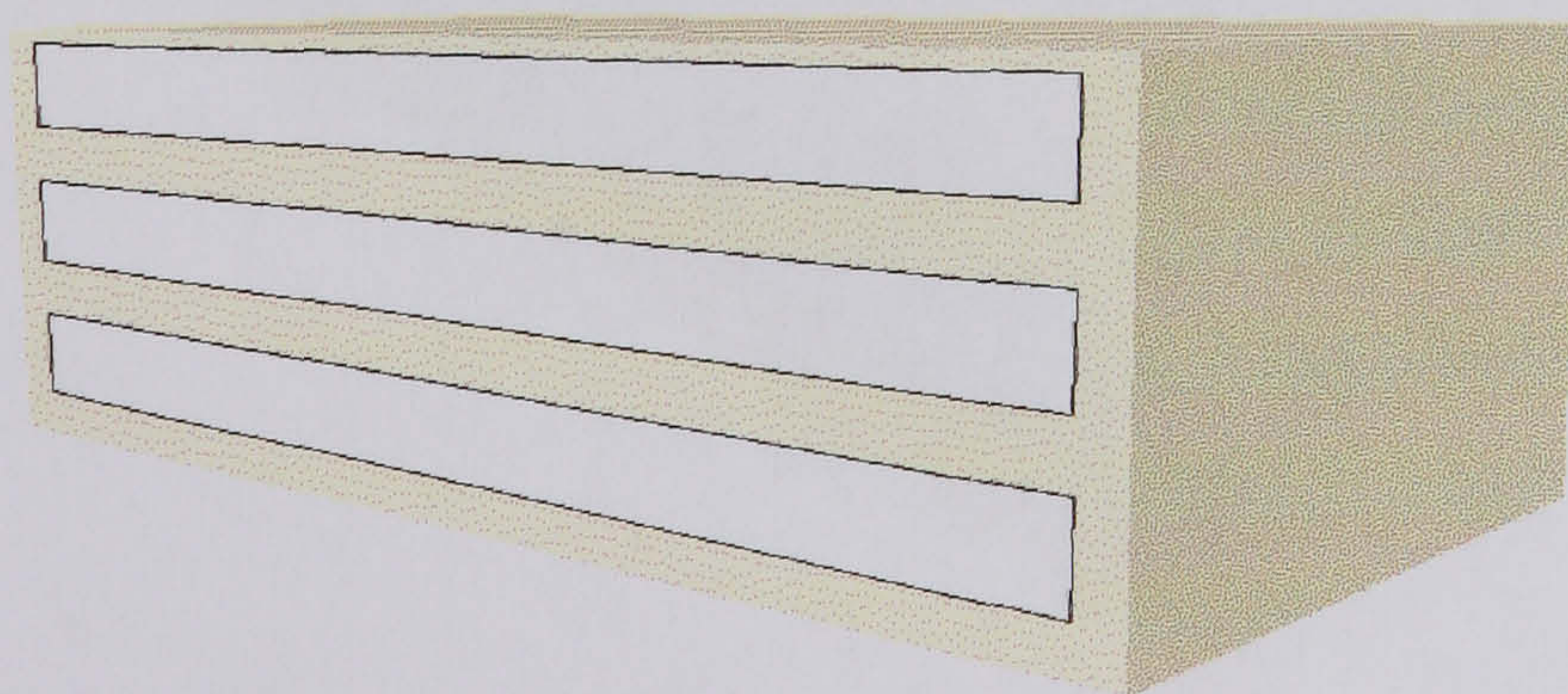


Figure 7.1: The ECON 19/3 building as modelled



The surrounding land is set to have 20% ground reflectance to solar radiation. A reflectance of 20% is “usually regarded as representative of typical conditions at higher latitudes” (CIBSE 1999). This is the ground reflectance for the entire solar radiation spectrum.

An air-conditioning system and heating system operates from 06:00 to 18:00 maintaining the internal air temperature between 20° and 24°C. Fresh air is supplied during occupied hours with a total air change rate of 1.1 ach/hour. This includes infiltration of 0.5 ach/hour at all times.

Allowance is made for heat gains from lights, occupants, plant and the sun. The walls have a solar absorptance of 40% and the roof 65%.

A detailed description appears in Appendix 6.

The above building was also modelled with overshadowing, i.e. surrounded by other buildings, as in an urban context. It was decided to make the context annular and symmetrical. These adjacent buildings were given the same height, 9m, as the test building, and spaced either 9m away (pilot modelling) or a variable distance away (main modelling). See Figure 7.2.

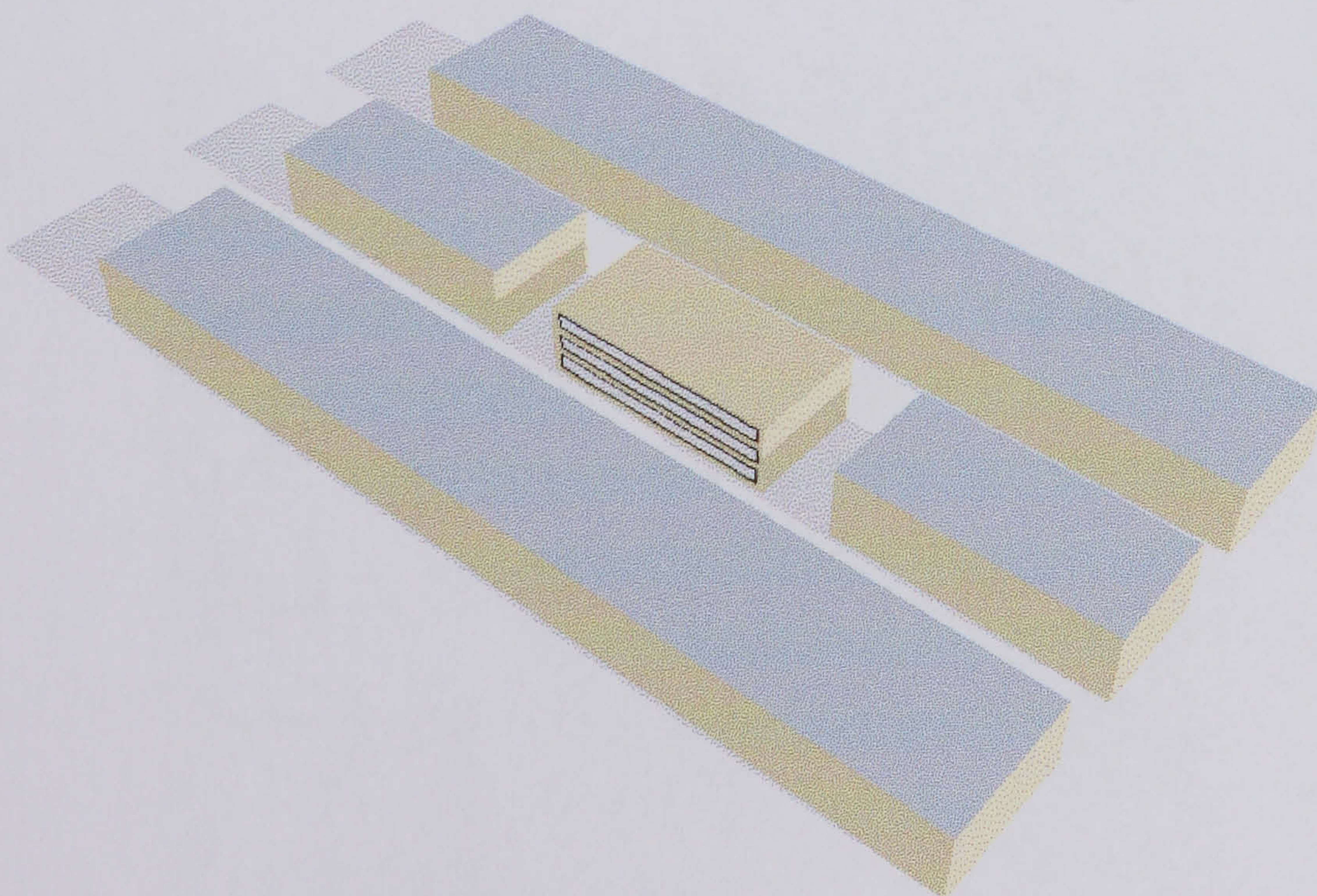


Figure 7.2: The ECON 19/3 building in an urban context

In the main modelling, for each of the seven site categories previously defined (Chapter 4, and shown again in Table 7.2), a context was modelled to represent that urban setting. Categories 1 to 3 are open – there is no over-shadowing. Numbers 4 to 7 have buildings surrounding them at an increasingly closer spacing.

The categories had been defined using bands of street height:width ratios. For modelling the context, the upper end of each band was arbitrarily chosen. Table 7.1 shows the ratios used for simulation. Figure 7.3 shows an example of the test building surrounded by context buildings, for a category 7 site.

Table 7.1: Street contexts used in the model for each site category

Site category	H/W ratio of streets in the model
1	open
2	open
3	open
4	0.3
5	0.5
6	1
7	2

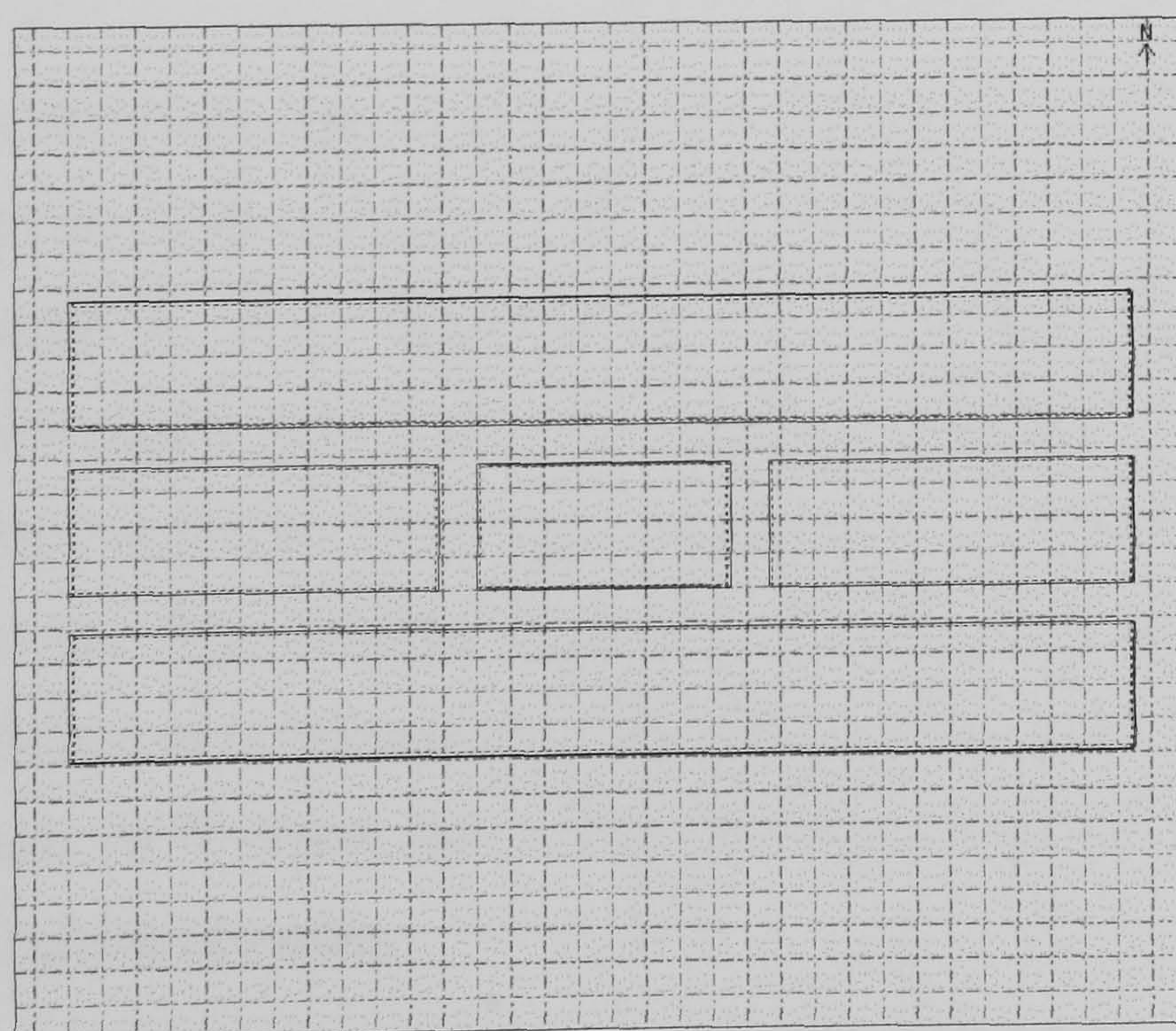


Figure 7.3: A category 7 context shown in plan, drawn on a 4m grid

### 7.2.2 Location of modelling sites

For the Pilot phase, to assess the variation of cooling demand a sample of six sites was chosen within the urban heat island together with the reference station beyond it. The six sites were chosen to be within a few miles of the centre of London and covering a range of dense and open sites, with or without vegetation.

The sites of all the monitoring stations in the project were previously categorized (shown again in Table 7.2) according to two main criteria: the nature of the surfaces in the area and sky view (height to width ratio of street).

Table 7.2: Criteria used for categorizing sites

Site category	H/W ratio of street, x	Surface	Example site, or description
1	$x=0$	Grass, etc.	Rural fields, or large park, or trees
2	$x=0$	Hard and grass	Housing near park or field
3	$x=0$	Hard	Urban derelict or unbuilt area or car park
4	$0 \leq x < 0.3$	Hard, very wide gorge	Low density residential area
5	$0.3 \leq x < 0.5$	Hard, wide gorge	Medium density urban area
6	$0.5 \leq x < 1$	Hard, wide gorge	High density urban area; around focus
7	$1 \leq x < 2$	Hard, medium gorge	Liverpool Street station site

The categories of the seven sites chosen for the pilot modelling are shown in Table 7.3. The sample of six urban sites and rural reference covers six of the seven defined site categories, and 85% of the monitored sites. (An additional eighth category has very little data associated with it and has not been used here, or for most of the analysis.) The first two letters of the site name refer to the compass direction from the centre of London. The number afterwards denotes the number of miles away from the British Museum in Bloomsbury (the focus of the radial array of monitoring stations.) (EE=East, WW=West, etc.) Thus SE03 refers to a location three miles south east of the British Museum.

Table 7.3: Pilot modelling: the seven sites and their categorizations

Site	Site category
EE02	7
NE02	4
NN01	3
NW02	2
SE03	4
SS05	5
WW11	1

The hourly temperature profiles for these sites represent the most important determinant of cooling load. To simplify the modelling for the pilot phase, the height:width ratio of the surrounding streets, the context, was not modelled site by site, but fixed at a ratio of 1:1. This ratio is associated with site category 6 and above, i.e. with relatively deep street gorges. The use of a fixed ratio is an approximation.

Table 7.4: Main modelling: the 24 sites and their categorizations

Site	Site category	Site	Site category
FS00	6	SE05	2
NN02	4	SE06	4
NN03	6	SE09	4
NE02	4	SW08	1
NE05	5	WW04	2
EE02	7	WW05	3
EE04	2	WW06	4
EE06	4	WW09	4
EE07	3	NW01	6
EE08	3	NW02	2
SE02	5	NW03	4
SE04	5	WW11	1

In the Main Phase of modelling the sample was increased to 24 sites (and the simulation run for a year) and the surrounding streets were made site-category specific. It was necessary to replace three of the pilot phase sites as there was not a complete year's data for them. See Table 7.4.

### 7.2.3 Simulation models

This section discusses the choice of a building simulation model and gives an indication of the likely accuracy of its predictions.

#### 7.2.3.1 Choice of model

A simulation model was required that would adequately predict the impact of different external temperature profiles on air-conditioning energy demand. In addition, it was necessary for solar gain and overshadowing to be taken into account. One approach to choosing a model might be to identify the most accurate one and use that. However (see Validation in the next section), gauging the accuracy of models is difficult, and in practice, the choice of model is constrained in other ways:

- usability
- the availability of support, e.g. a model may be in the public domain, but the inevitable questions about the operation of the model can then be difficult to answer
- hardware requirements and cost, e.g. some models have unusually high demands on hardware.

Initially some simplified models were considered, but very quickly it became apparent that more detailed thermal simulations were needed in order to take into account specific building geometry and operation as well as the effect of external weather and surroundings. Three models *Apache*, *Tas*, and *ESP* were considered. These are similar in their capabilities although *ESP* requires more detailed and complex input data. *Tas* (EDSL 2001) was eventually chosen as it was available.

#### 7.2.3.2 The validity of the predictions of a simulation model

It is quite difficult to test the accuracy of building simulation models. Inter-model comparisons can be useful and it has been suggested that this may be a more fruitful approach (Strachan 1994), but for most users, the crucial test of confidence is to compare predicted values against measured data.

Validation exercises have to work with very simple buildings, or test cells, but even so, there are difficulties in the testing because of uncertainties,

on the measurement side in:

- the measured performance of the test cell (where should measurements be made, how accurate is the energy measurement)
- the measured data (weather data, site characteristics' data, test-cell construction data) used as input to the simulation models

and on the modelling side in:

- a user's interpretation of building plans

Inaccuracies in the ability of a model to realistically simulate a given building's operation are part of the error of the model being tested. There are many ways in which a model can lose accuracy, for example:

- the model does not cater for a particular physical characteristic, e.g. the convective/radiant split of a heating source
- the need for data that are difficult to obtain, e.g. night-time cloud cover, which may be assumed to be the same as daytime cover
- algorithmic errors
- coding errors of the algorithms

An important International Energy Agency study (Lomas 1994) was conducted in 1993 which sought to reduce these uncertainties and “assess the ability of a number of DSPs [Detailed Simulation Programmes] to predict the performance of a few simple buildings under conditions reflecting those which exist when used to model a real building.”

17 different simulation programmes were compared. Each was used to predict the heating energy needed in a test-room in one October week, as well as the maximum and minimum temperatures. Predictions of temperature for an unheated May week were also made. The test cells were either opaque, single or double-glazed.

The different models gave energy predictions of around  $\pm 20\%$  of the mean of all the 25. The predicted change in energy consumption from an opaque test-room to a double-glazed one varied from 13% to 40%, a factor of three. Predicted peak temperatures varied by 11°C, (3-11°C above the set-point temperature). Some models lay further from the average results than others. The results from a selection of models are shown in Table 7.5, below. Those from *Tas* are highlighted. The table shows the energy used (MJ), and the maximum and minimum temperatures, in the test-room for one week in October when the room was either opaque or with double-glazing. The temperatures for an unheated period in May are also shown.

Table 7.5: Measured and modelled results of the energy use and temperatures reached in a test cell (Lomas, Eppel et al. 1994)

Programme	Heated, October period						Free-floating, May period			
	Double glazed			Opaque			Dbl glazed		Opaque	
	Energy	Tmax	Tmin	Energy	Tmax	Tmin	Tmax	Tmin	Tmax	Tmin
DOE2.1E	65.6	40.8	11.7	100.7	30.2	11.5	30.3	11.5	16.1	7.6
<b>Tas 7.54</b>	<b>83.3</b>	<b>36.5</b>	<b>10.8</b>	<b>109.4</b>	<b>30.0</b>	<b>12.9</b>	<b>28.5</b>	<b>11.6</b>	<b>16.1</b>	<b>8.3</b>
Apache 6.52	86.1	36.3	12.6	118.6	30.1	14.8	26.9	12.1	15.8	8.9
HTB2 1.10	94.4	33.3	9.8	108.2	30.1	13.0	26.4	10.8	16.6	8.3
Seri-Res 1.2	82.2	36.8	11.1	103.8	30.0	13.2	28.9	11.8	16.7	9.2
ESP-r 7.7a	69.5	40.3	12.4	100.3	30.3	12.8	28.9	11.7	15.4	7.9
Mean of 25	74.6	38.0	11.6	102.4	30.0	13.1	29.6	12.2	16.6	9.1
Measured	<b>89.3</b>	<b>37.8</b>	<b>11.9</b>	<b>117.1</b>	<b>29.8</b>	<b>14.6</b>	<b>31.0</b>	<b>12.2</b>	<b>16.8</b>	<b>9.2</b>
" upper bound	92.7	40.5	13.9	122.3	30.2	16.4	33.4	13.6	17.5	10.0
" lower bound	78.1	36.5	11.5	105.3	29.4	14.0	29.6	11.6	15.7	8.6



Figure 7.4: Predicted heating energy used in the double-glazed test room compared to the measured value, for Tas 7.54 (Lomas, Eppel et al. 1994)

In Table 7.5, the average for all 25 models tested is given (not just the mean of the six shown), together with the measured values and the upper and lower confidence (99%) levels.

It can be seen that *Tas*'s predicted temperatures are usually about one degree lower than the measured values, and lower than the mean of all 25 models. They are within the error bounds for 4 out of the 8 results. In the appendices of the report (Lomas, Eppel et al. 1994) on this validation exercise, the authors of *Tas* suggest that the primary reason for the lower temperatures is because long wave radiation from the sky was under-estimated. The sky radiation model was subsequently refined.

The predictions of heating energy for the double-glazed and opaque rooms are both within the error bounds of the measured data. Figure 7.4 illustrates the double-glazed results. The predicted *change* in heating energy is closer in agreement than the absolute values: 26.1MJ (predicted) and 27.8MJ (measured), i.e. the prediction is 6% lower than the measured value.

These results seem sufficiently accurate for this work and it is not obvious that other models would be significantly better. The version of *Tas* used in the empirical validation exercise was 7.54, in 1993. The version used for this work is 8.3.

#### 7.2.3.3 Operation of *Tas*

For calculating the conduction of heat within a building, *Tas* uses a method based on a response factor technique (Mitalas 1967) (Florides 2001) (EDSL 2000). This uses the history of a surface's temperatures to predict the flow of heat within a component. This is a fast procedure and overall the model runs quickly on a standard PC. There are many other algorithms needed to model the energy fluxes from the sky, walls and ventilation.

*Tas* takes into account the hourly changing air temperature, humidity and solar radiation together with the internal gains from equipment and people. An hourly schedule is used to state the required internal conditions, and occupancy periods (which affect gains from lighting, etc.). The flow of energy through the building fabric is modelled in detail.



Direct solar radiation impinging on the walls is partially reflected according to the surface specification of the fabric. Blocking of this direct solar radiation by adjacent buildings is modelled. Diffuse radiation from the sun may also be blocked by overshadowing, but the model does not take this into account. Diffuse and direct solar radiation incident on the ground will be partially reflected and the amount captured by the building is calculated.

Long wave radiation from the sky depends on cloud cover and this is taken into account. Long wave radiation emitted from the ground is calculated assuming the ground surface is at the same temperature as the air. Sky radiation is also reflected from the ground and this is calculated.

In this modelling exercise, the air change rate for the building has been scheduled rather than calculated. This is more acceptable for an air-conditioned building, than a naturally ventilated one, as the former is designed to be more constantly and predictably ventilated.

#### **7.2.4 Weather data**

The simulation model runs with data from a weather file. Hourly weather data were therefore acquired from the Meteorological Office for a site in central London (the London Weather Centre, LWC) and for a site 15 miles SW of London (Heathrow Airport). For the pilot modelling one month's data were used, and at the time of the main modelling it was possible to acquire 15 months' data as necessary.

The parameters included cloud cover, relative humidity, and global and diffuse solar radiation, wind speed and direction. It was thought that the airport wind data would be more applicable to a variety of sites in the study region than urban measurements taken in one place. For this reason, the wind data from Heathrow were combined with the non-wind data from the LWC.

It is realized that Heathrow wind data could be higher than in urban areas, but conversely urban form at each of the modelled sites could also result in locally higher speeds depending on wind direction and other factors. Variations in wind speed can affect the calculation of heating and cooling in two ways: through

modifying ventilation/infiltration rates, and external convective heat transfer. In this study, of an air-conditioned building, both ventilation and infiltration have been *scheduled* rather than calculated. Such scheduling is more appropriate for a relatively sealed building but the effect of *local* wind speed on the convective heat transfer coefficient is not taken into account. Convective heat transfer is varied with wind speed, but this is the Heathrow wind speed, and is the same for all sites.

These weather data were then assembled together with the project's hourly measured air temperature data for seven sites (pilot phase) and seven new weather files were produced from these. The same procedure was followed for the main phase.

For sites within a few miles of London, the solar radiation data from the LWC are appropriate. For other sites, including the rural reference site 18 miles west of London, it is possible that there is a different solar input from that of central London – but this is not known. The assumption in this work is that the difference is not significant – and that the air temperatures experienced in different places are not significantly different because of regional insolation differences, but different for other reasons.

### **7.2.5 Efficiency**

The *Tas* model used in this study predicts the space heating and cooling load. This load may be met by a variety of plant and distribution schemes, and the efficiency of the system will vary according to plant type, load, temperature, humidity and controls. Chapter 8 (section 8.6.1) discusses this further.

In order to estimate the power input required to meet the demand for cooling a simplifying assumption has been made. It has been assumed that a vapour compression system is used and that this provides chilling with a COP of approximately 3, and that the compressor is electrically driven. Electrical input has therefore been derived by dividing the chilling demand in kWh by 3. More details are given in Chapter 8.

The heating system is assumed to be based on a gas-fired boiler with an annual efficiency of 0.75.

### **7.3 Chapter 7 Conclusions**

Two samples of 7 and 24 sites have been selected that cover the range of site-categories from urban to rural. A simulation model has been selected which will allow modelling of the urban context and its accuracy has been checked against other models and measured results from a major empirical validation exercise. The accuracy of the model *Tas* in predicting an energy change in a test room when solar energy was increased was within 6% of the measured value.

The next chapter describes the predicted impact of the heat island on cooling load , and also considers how the heat island affects the balance of heating and cooling load over a year.

## **CHAPTER 8**

### **Modelling results**

# CHAPTER 8 – Modelling results

## 8.1 Introduction

Thermal simulations of the ECON 19/3 (BRECSU 1999) building were run using the measured external air temperature data for different locations, as described in Chapter 7. The Pilot modelling results (7 locations, 1 month) are presented first, followed by the Main modelling results (24 locations, for the whole year). The annual balance of heating and cooling load is then presented followed by work on the sensitivity of the balance to internal gains. Load and energy use are shown as totals for the ECON 19/3 building, rather than being normalized to kWh/m<sup>2</sup>; all comparisons are made to itself rather than to other buildings.

## 8.2 Pilot modelling results

Each run of the model simulated the 31 days of August 1999 preceded by 10 days in July to pre-condition the model.

### 8.2.1 Cooling load and site

Table 8.1 shows the predicted total amount of cooling required to maintain the internal temperature within set limits during August 1999. For each site there are two predictions: the cooling load for the building in the open, and the load if the building experiences some over-shadowing from adjacent buildings.

Table 8.1: The cooling load for the ECON 19/3 building in 7 locations

Site	Cooling load, kWh	
	Open	Shaded
EE02	8230	8147
NE02	8143	8100
NN01	7983	7940
NW02	7711	7669
SE03	8405	8363
SS05	8260	8218
WW11	7128	7045

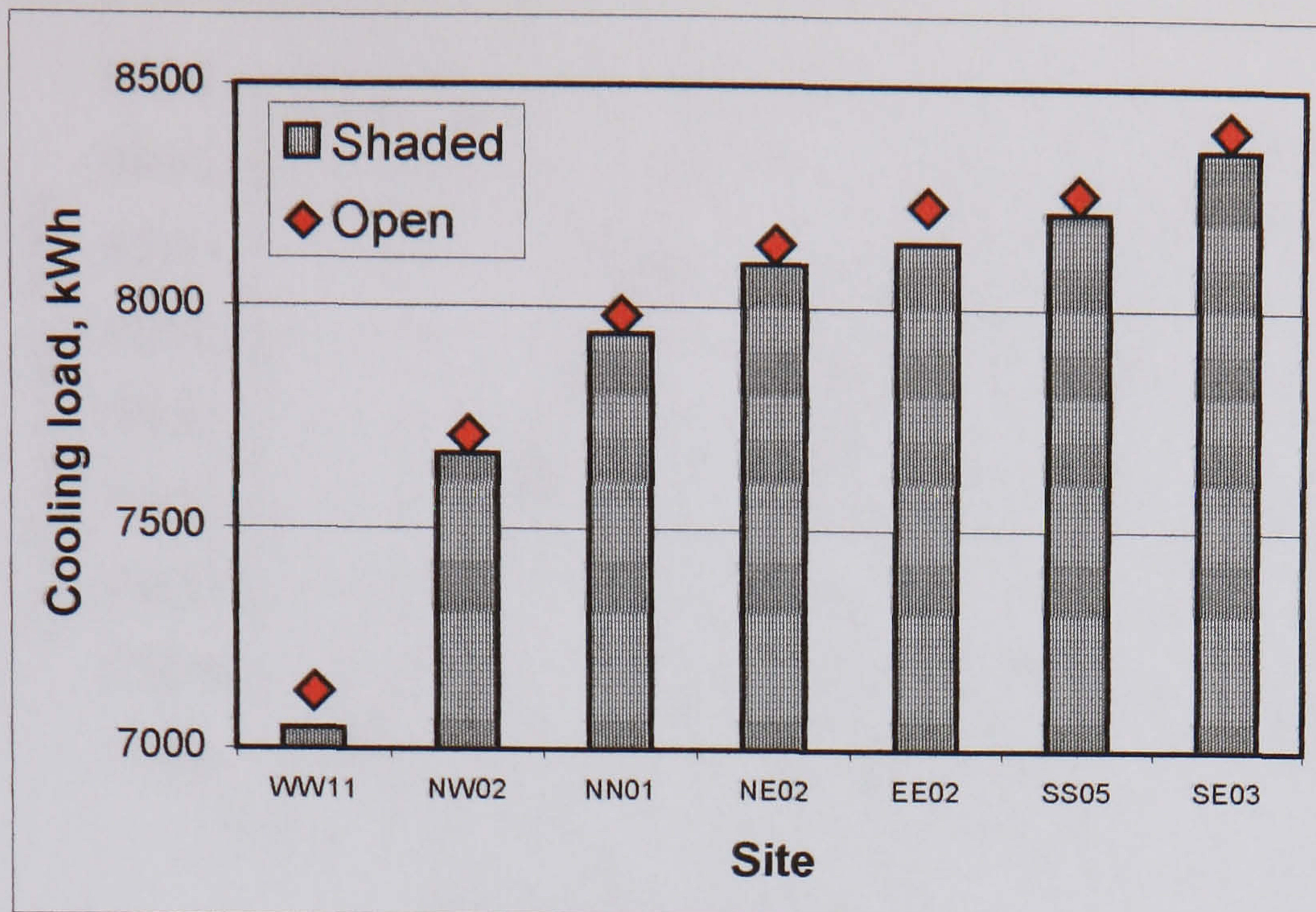


Figure 8.1: The cooling load for the ECON 19/3 building in 7 locations

The data are shown ordered in Figure 8.1. A number of points may be made:

- The lowest load is at the rural site (WW11) (with the lowest mean temperature).
- The highest load is at a site 3 miles SE of the focus, 18% more than at the rural site.
- Shading from adjacent buildings reduces the cooling load slightly, e.g. the SE03 site's load reduces from 18% more than the rural site to 17%, and at each site the load reduces by between 0.6-1.0 of a percentage point.
- There is a relatively high cooling load at a site 5 miles from central London.

### 8.2.2 Cooling load and mean temperature

The average temperature of a location will have an impact on the cooling load during occupied hours. Figure 8.2 shows the relationship between the measured mean temperature of each site in August and the cooling load for the month. Two temperatures are plotted: the mean 24 hour temperature and the mean daytime temperature. These cooling loads allow for shading.

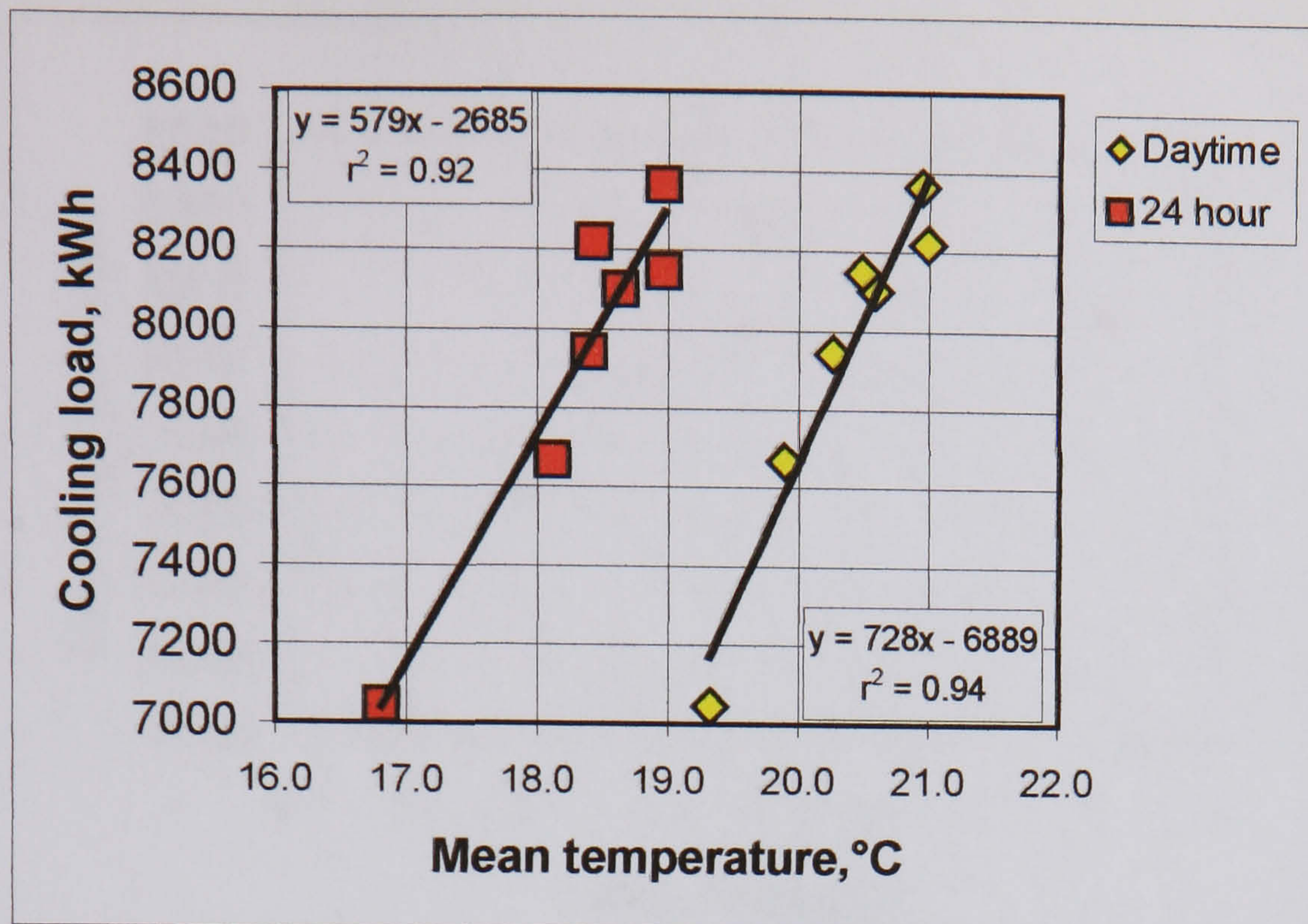


Figure 8.2: The relationship between mean temperature in August and cooling load

It can be seen that there is a good relationship between the measured mean air temperature for the month and the predicted cooling load. As might be expected, the relationship with daytime temperature, rather than 24 hour temperature, is somewhat stronger.

### 8.2.3 Cooling load and site category

As explained earlier, each monitoring station has been categorized according to the nature of its surfaces, and sky view. Figure 8.3 shows the relationship between (shaded) cooling load and type of site.

Cooling load is seen to increase broadly with increasing site category value. This might be expected as although site category is a non-interval parameter, the range from 1 to 7 does essentially represent a scale of increasing urbanization. It can be seen that after category 4, there is little change in the cooling load. It is interesting that there is a small reduction in demand at the most urban site, category 7. This could be associated with the presence of very tall buildings, thereby increasing the heat capacity/unit urban area (which acts as a thermal buffer), and providing interception of solar energy high above the street where the air temperature was measured.

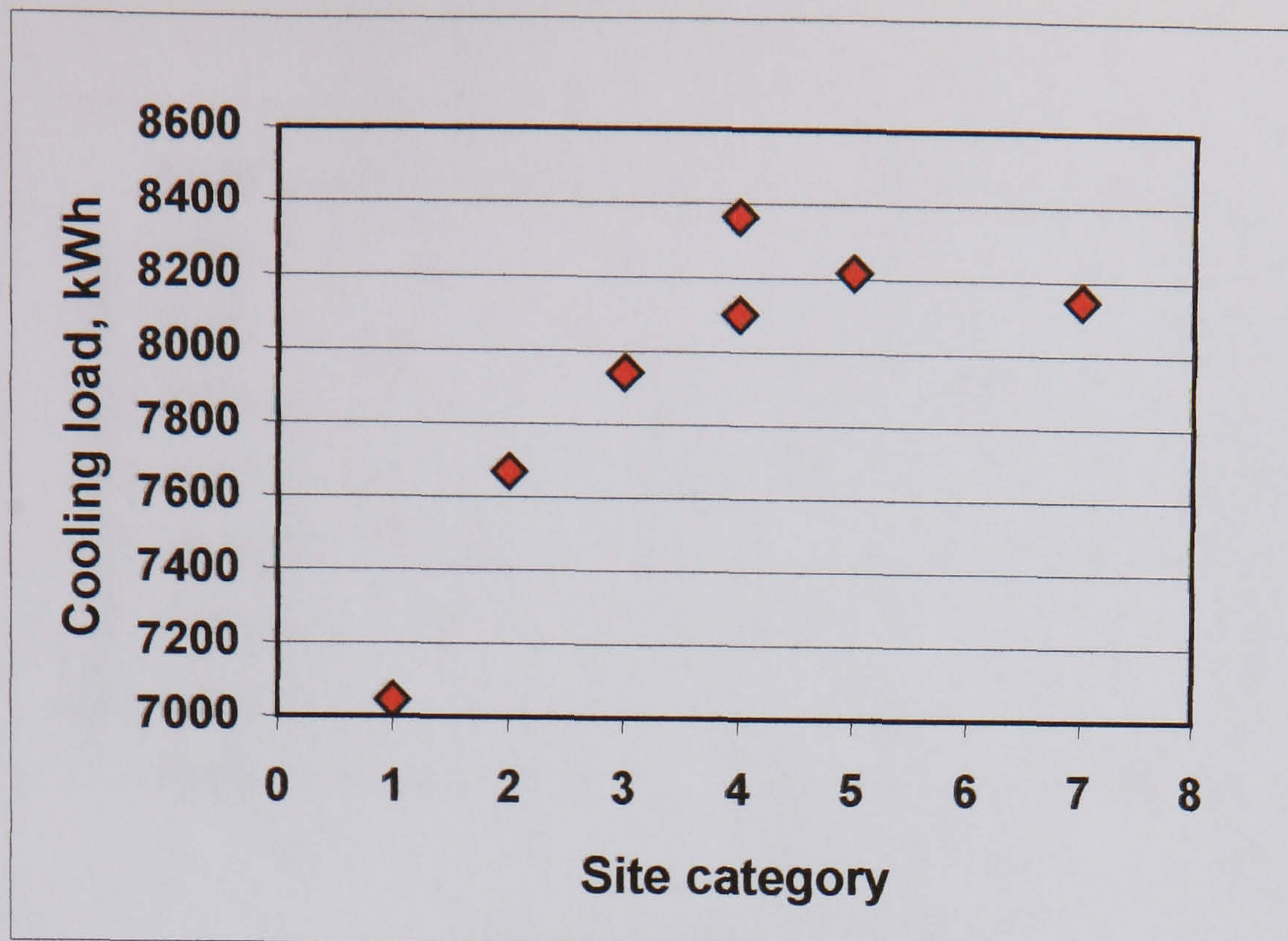


Figure 8.3: The relationship between site category and cooling load

#### 8.2.4 Cooling load and radial distance

In Chapter 4 it was found that the mean temperature of each site was strongly related (about 70% of variance explained) to the distance that site was from London (the radial distance). This was true for the mean night-time and 24 hour temperatures, but not the daytime mean. It was also shown that site category was related to radial distance (more open sites tend to be found further away from the city centre).

Figure 8.4 shows the relationship between predicted cooling load and the radial distance from London for each site. Radial distance is measured from the focus of the monitoring array, at the British Museum.

Apart from the lowest load at the rural site, radial distance appears to be a poor indicator of cooling load, and site category is more useful. Given that mean temperature is strongly related to cooling load (Figure 8.2) and that mean temperature was found to be strongly related to radial distance, it may seem surprising that cooling load is poorly related to radial distance. However, although a strong relationship was found between radial distance and mean temperature, about one third of the variance was left unexplained. This particular sample of six urban sites, all within 5 miles of the centre, may be atypical in their relationship with radial distance, or, as seems likely, site categorization (indicative of the heat capacity and sky view of a location) is indeed an important determinant of cooling load.



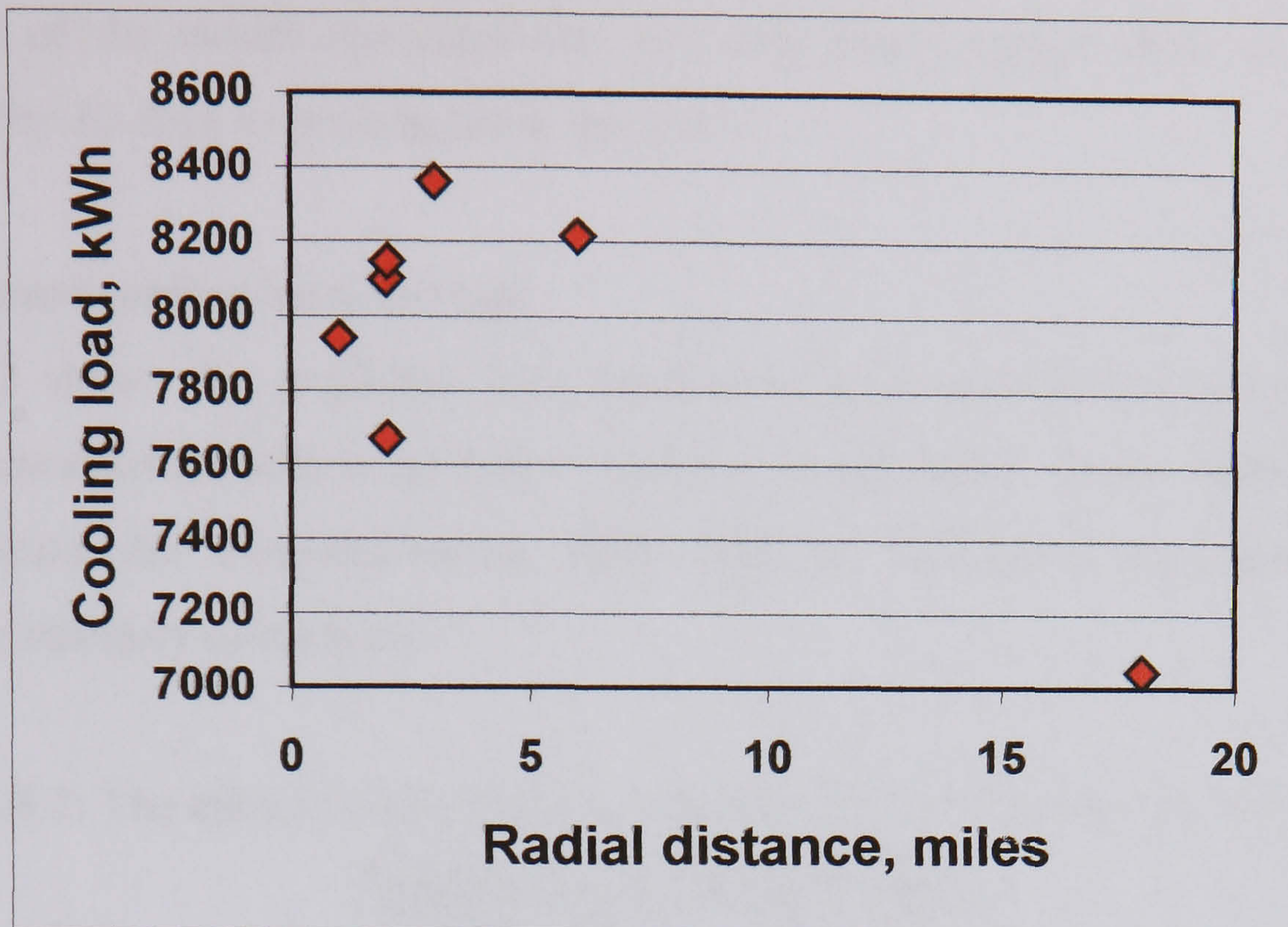


Figure 8.4: The relationship between cooling load and distance from the city centre

### 8.2.5 Conclusions from pilot modelling

The initial modelling shows that increased cooling load in August is related to increasing urbanization. In particular, there is an encouraging relationship between site category and cooling load. This relationship is stronger than that with radial distance for this sample of sites. Overshadowing reduces cooling load but by only about 1%. However, for this pilot modelling the overshadowing context is fixed to be the same for all six urban sites, and has a spacing (height:width of street) of 1:1. For south facing façades, over-shadowing in August at this spacing is small.

### 8.3 Main modelling results

Each run of the model simulated the 365 days from August 1999 to July 2000 preceded by 10 days to pre-condition the model.

#### 8.3.1 Annual cooling load and site

Table 8.2 shows the predicted total amount of cooling required to maintain the internal temperature within set limits during the year 99/00. These predictions take into account the over-shadowing from adjacent buildings, depending on the particular category of each site.

Table 8.2: The annual cooling load for the ECON 19/3 building in 24 locations

Site name	Cooling load, kWh
FS00	38714
NN02	36643
NN03	38602
NE02	38316
NE05	38245
EE02	36328
EE04	37494
EE06	38103
EE07	36897
EE08	37757
SE02	40181
SE04	38791
SE05	36274
SE06	35812
SE09	34564
SW08	35287
WW04	38020
WW05	36464
WW06	36836
WW09	35641
NW01	34769
NW02	35792
NW03	35154
WW11	32103

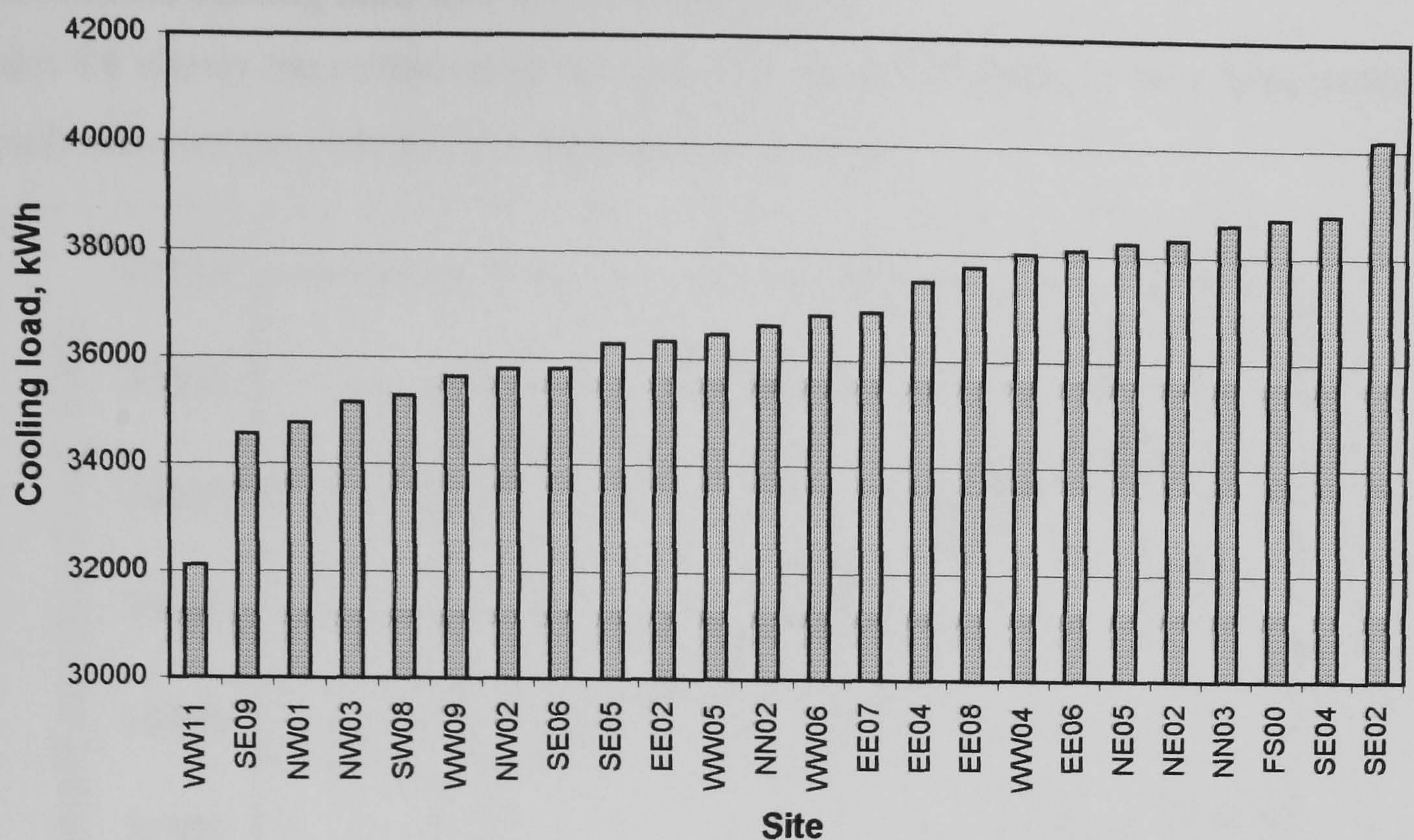


Figure 8.5: The annual cooling load for the ECON 19/3 building in 24 locations

The simulation results are shown ordered in Figure 8.5. A number of points may be made:

- The lowest load is at the rural site (WW11) (with the lowest mean temperature).
- There is a stepwise increase from the rural site WW11 to SE09 (a suburban site) and to WW09 four miles towards London from the rural site.
- The highest load is at a site 2 miles SE of the focus, 25% more than at the rural site.
- There is a relatively high cooling load at a site (EE08 at Ford Dagenham Works) 12 miles from central London.
- There is a relatively low cooling load at some sites within three miles of London (NW01 near Regent's Park) (NW03 towards Hampstead) (NW02 adjacent to Primrose Hill Park). The short-term test (Chapter 6) showed that on a sunny afternoon, air at Primrose Hill Park was up to 1.1°C cooler than air in the High Street nearby.

### 8.3.2 Annual cooling load and mean temperature

Figure 8.6 shows the relationship between the measured mean 24 hour temperature of each site over the year and the annual cooling load.

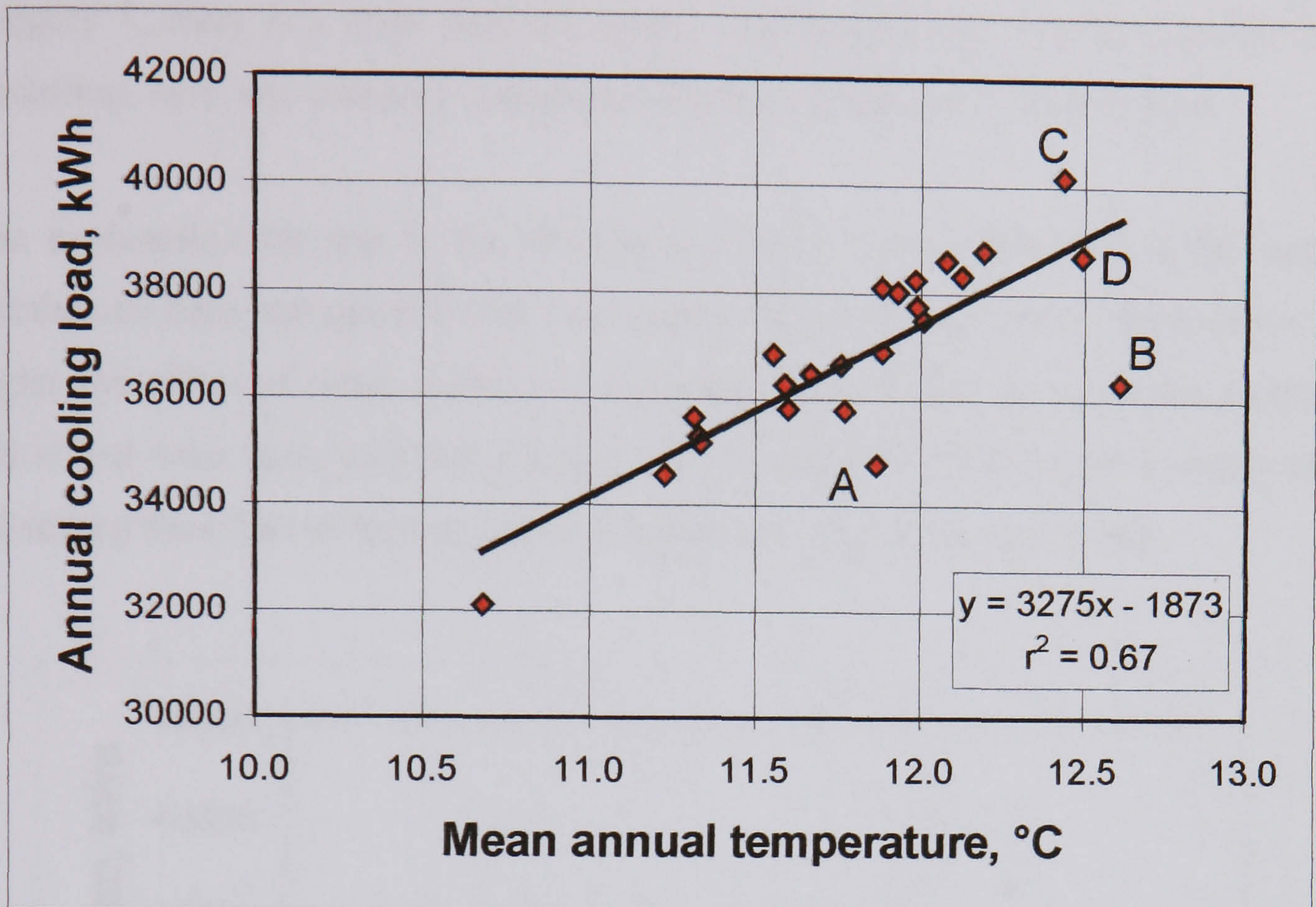


Figure 8.6: The relationship between annual mean temperature and cooling load

Approximately two thirds of the variance in cooling load is associated with varying mean temperature. The cooling loads at three sites are at some distance from the regression line. Site A is one mile from the focus, has over-shadowing (category 6) and is 250m from a large park. Site B is in the city of London and warmer, but has heavy over-shadowing (category 7). Both these sites have particularly low cooling loads for their mean temperatures. Site C is 2 miles from London in the centre of the heat island, warm, but in a more open site (category 5), and has a high cooling load for its temperature. Site D is at the focus, warm and has over-shadowing (category 6). Thus at the three warmest sites (B, C and D) the order of *decreasing* cooling load follows the order of *increasing* urbanization, i.e. categories 5, 6 and 7. Another reason for the increased scatter in Figure 8.6, compared to looking at August alone (Figure 8.2), is the inclusion of temperatures outside the main cooling season. In the model there is a cooling load, albeit small (less than 100 kWh/month), in every month of the year apart from January and December.

### 8.3.3 Annual cooling load and site category

Figure 8.7 shows the relationship between annual cooling load and type of site. Although cooling load does tend to increase with the more urban categories, up to category 5, there is a great deal of scatter. Compared to the results from the pilot modelling, here, site category appears to be a poor predictor of cooling load.

One explanation for this is the increased effect of over-shadowing in the annual simulations here compared to the pilot modelling in August alone. With lower sun angles the effect of urban context is more pronounced, and an important aspect of this is that solar gain, and thus cooling load, is reduced in the higher category sites, off-setting the effect of higher urban temperatures. This is explored later.

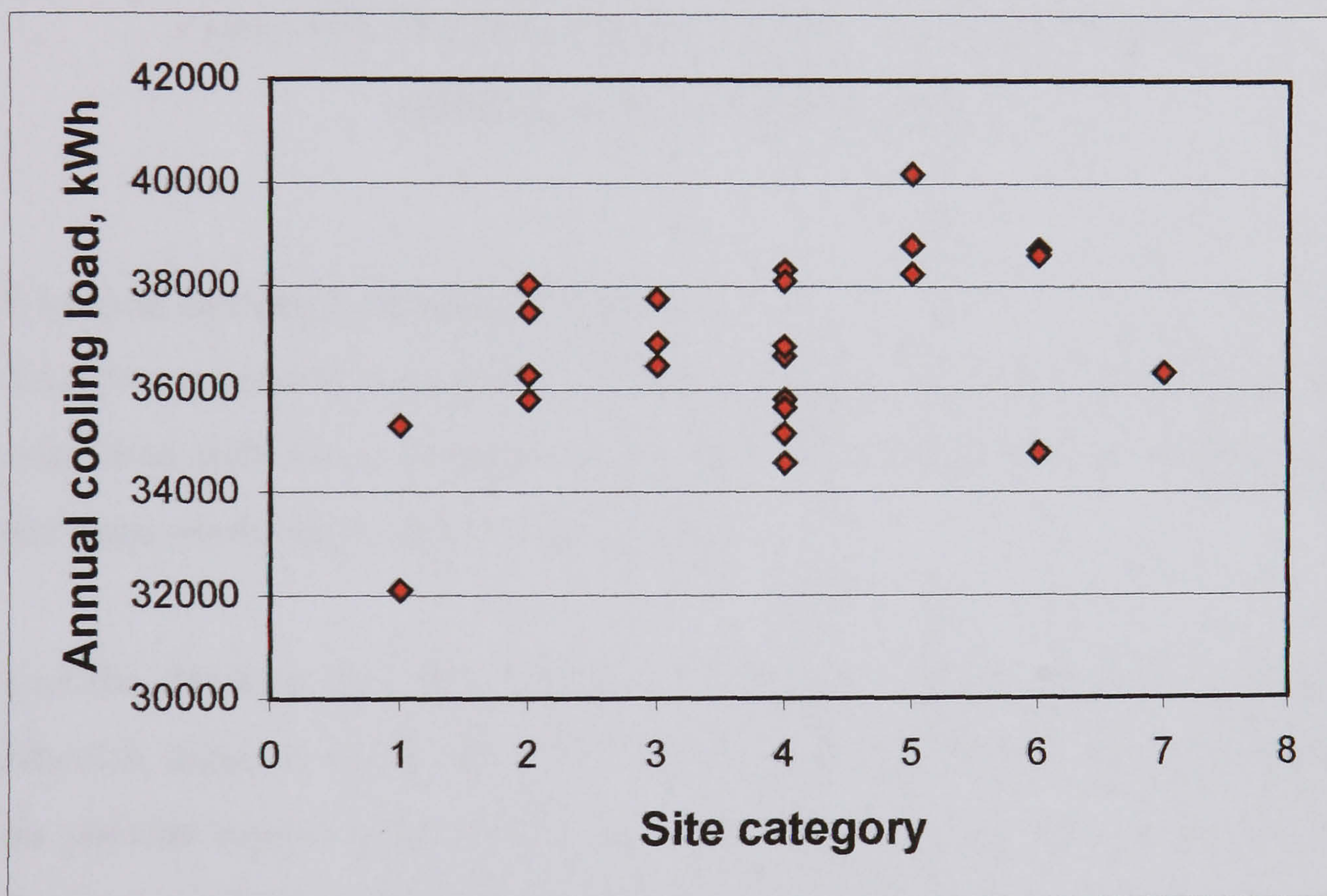


Figure 8.7: The relationship between site category and annual cooling load

### 8.3.4 Annual cooling load and radial distance

Figure 8.8 shows the relationship between predicted cooling load and the radial distance from London for each site. Radial distance is measured from the focus of the monitoring array, at the British Museum. Cooling load is seen to increase progressively from the rural site at 18 miles towards the centre. However, closer than four miles, radial distance does not predict the cooling load well.

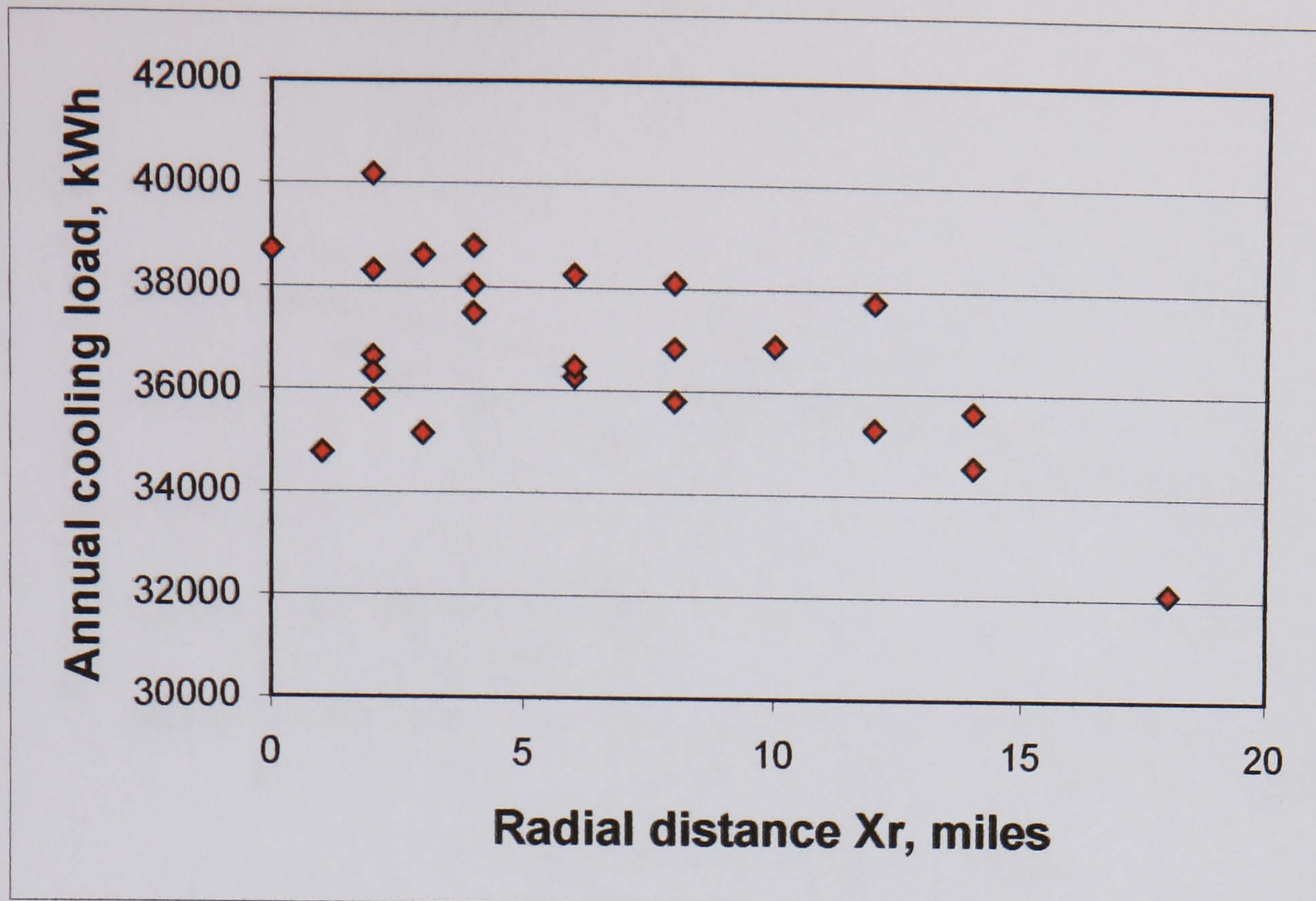


Figure 8.8: The relationship between annual cooling load and distance from the city centre

### 8.3.5 Annual cooling load and greenness

The field investigations described in Chapter 6 showed that green urban areas tend to be associated with lower daytime temperatures. It would therefore be expected that greener sites would have a lower cooling load.

Each of the 24 sites has been assessed from aerial photographs for its greenness, described in detail in Appendix 4. An inner circle around each site of 125m radius and an annulus beyond up to 500m were assessed separately. Each area was divided into 8 sectors and assessed separately for upwind studies, but here only the mean area greenness is used, termed inner and outer % greenness.

Figures 8.9 and 8.10 show the relationship between predicted cooling load and the inner and outer percentage greenness at each site. In both cases cooling load tends to be higher at sites with less greenness. Linear regression lines are shown, but an asymptote to 100% greenness would be expected. The lines are indicative of the strength of the relationship, with the outer greenness of a site explaining more of the variance (47%) in cooling load compared to inner greenness (34%).

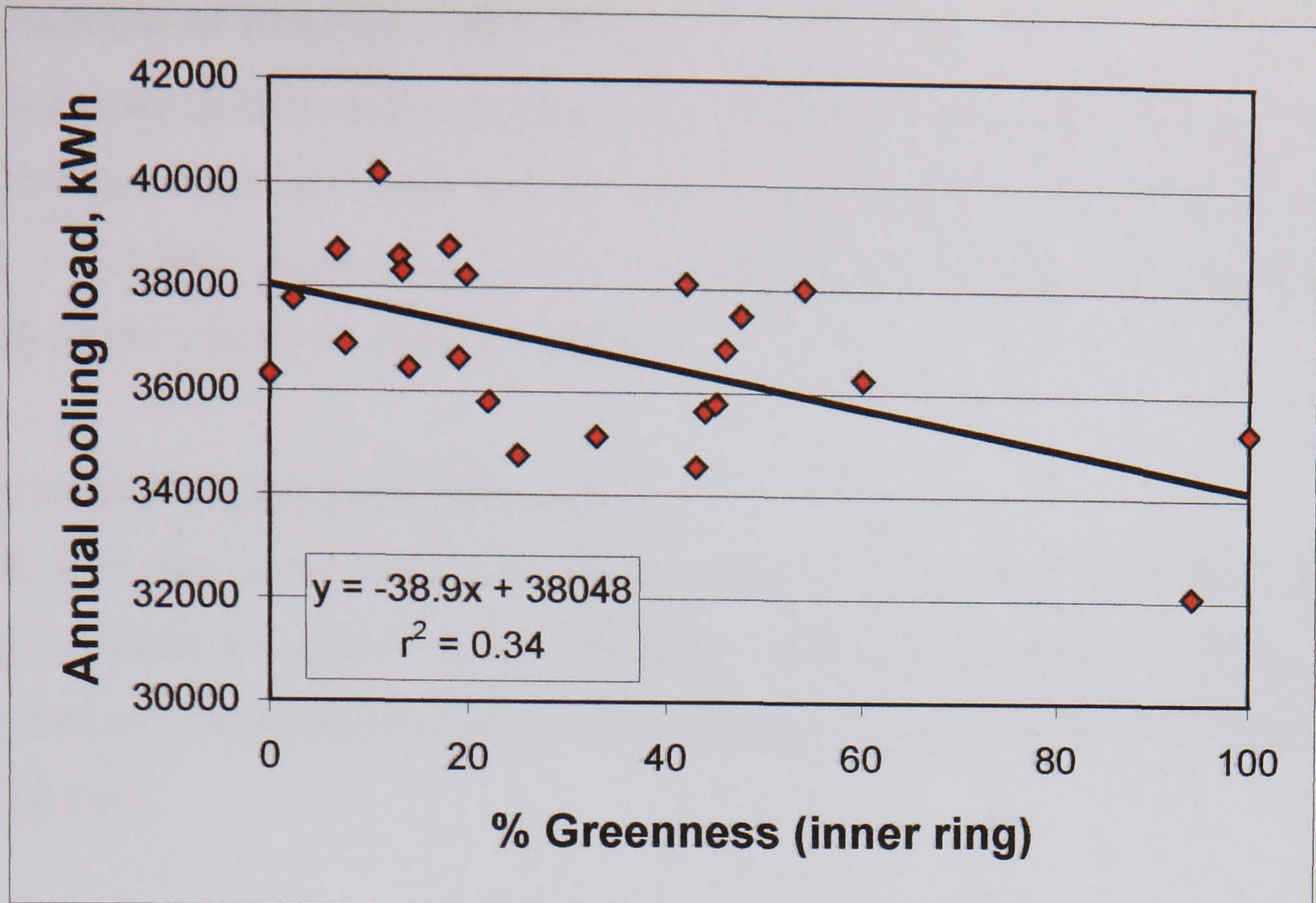


Figure 8.9: The relationship between annual cooling load and % inner greenness (0-125m) of each site

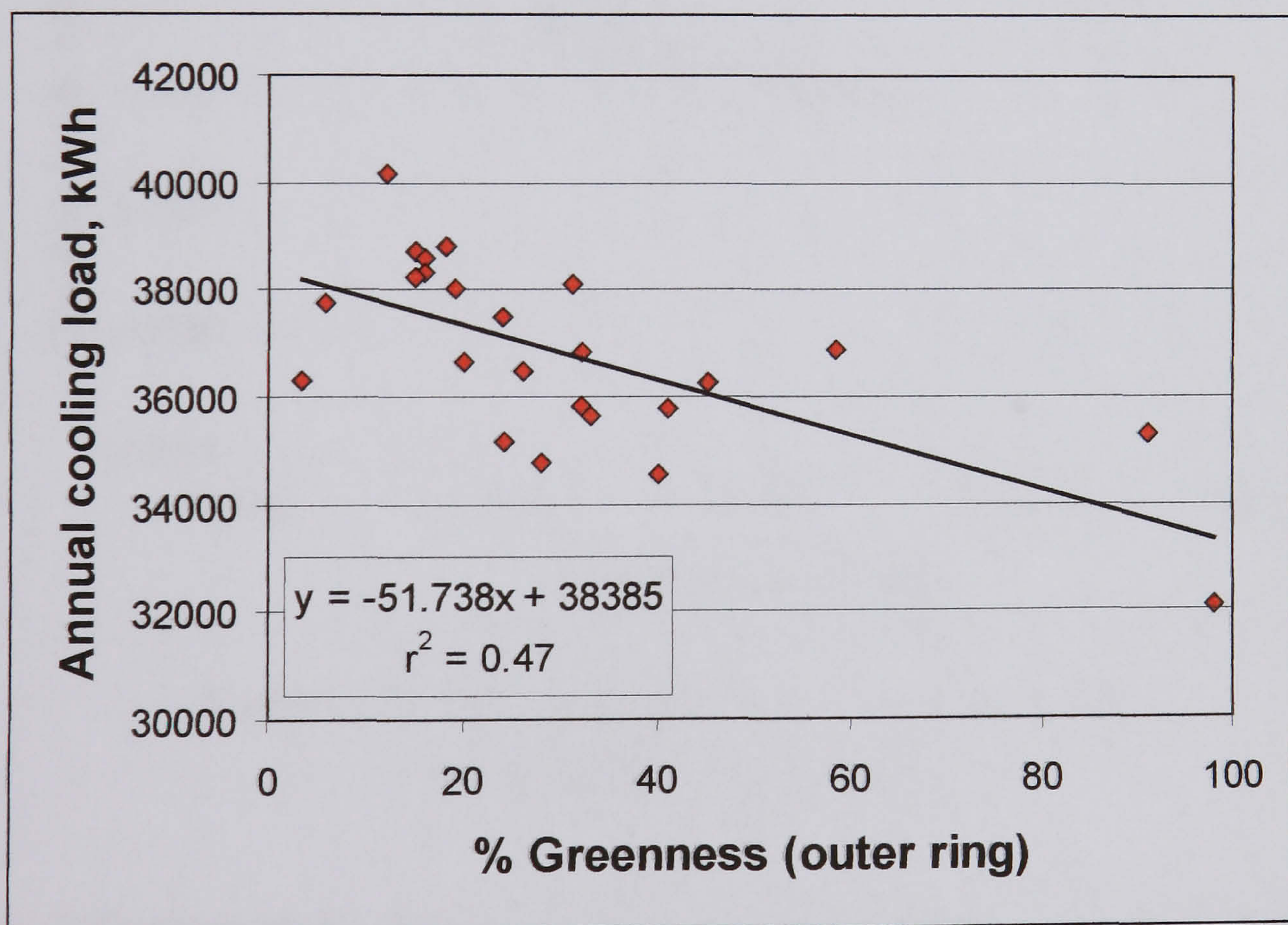


Figure 8.10: The relationship between annual cooling load and % outer greenness (125-500m) of each site

## 8.4 Balance of heating and cooling

In a temperate climate neither heating nor cooling load necessarily dominate fuel use in a building. Although higher urban temperatures are associated with higher cooling loads, it is highly pertinent to ask if this is offset by a saving in heating load. On balance is the urban heat island beneficial?

### 8.4.1 Annual heating and cooling loads

Figure 8.11 shows how sites with higher cooling loads tend to have lower heating loads. A reason for scatter in the relationship is that some sites with higher mean temperatures (increasing cooling load), experience over-shadowing which reduces cooling load.

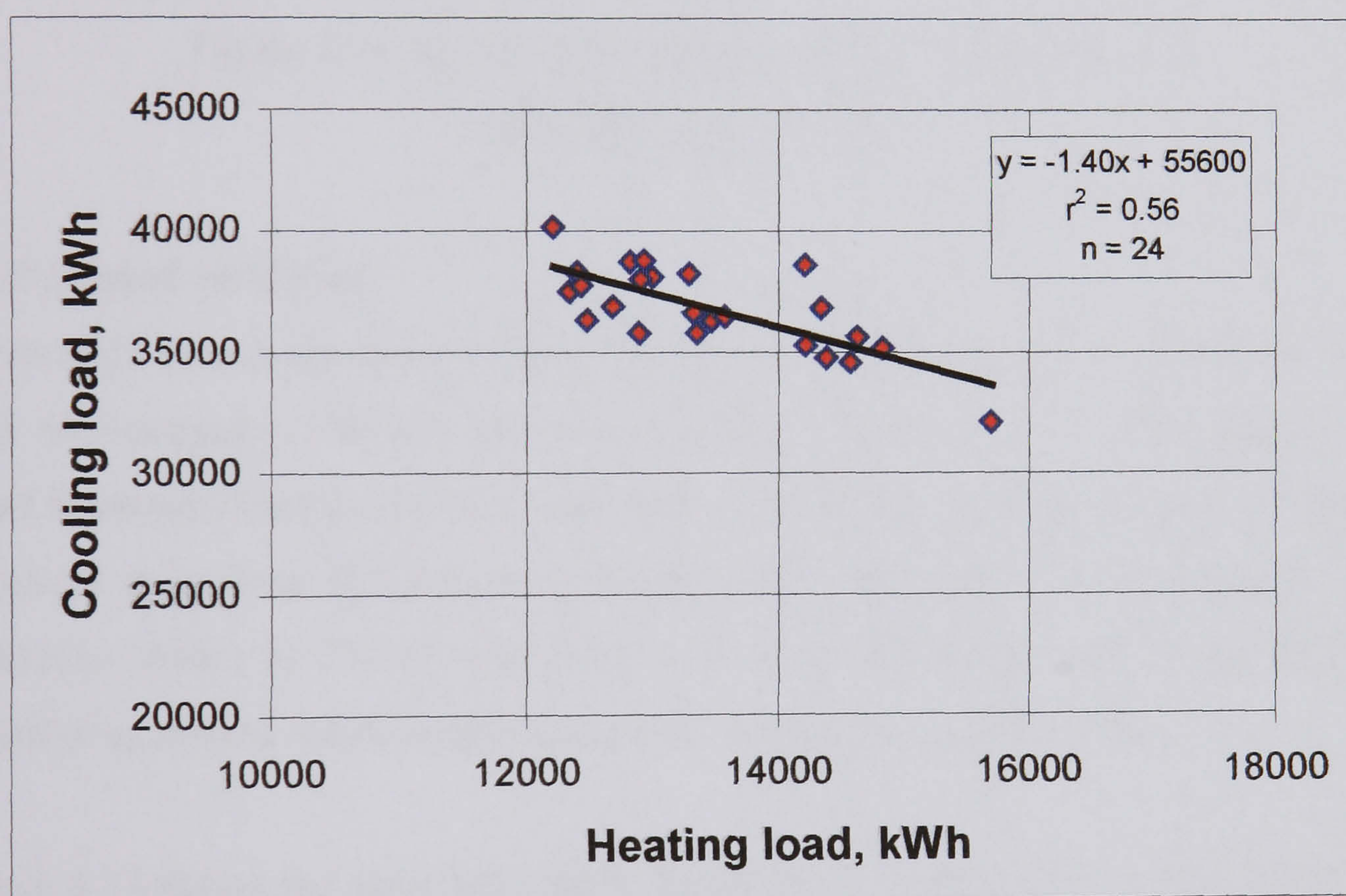


Figure 8.11: The relationship between annual heating and cooling load at each site

Figure 8.12 shows more clearly the relative contributions to load of heating and cooling requirements, and shows the relatively flat relationship of heating load with site category apart from category 1 (green sites).



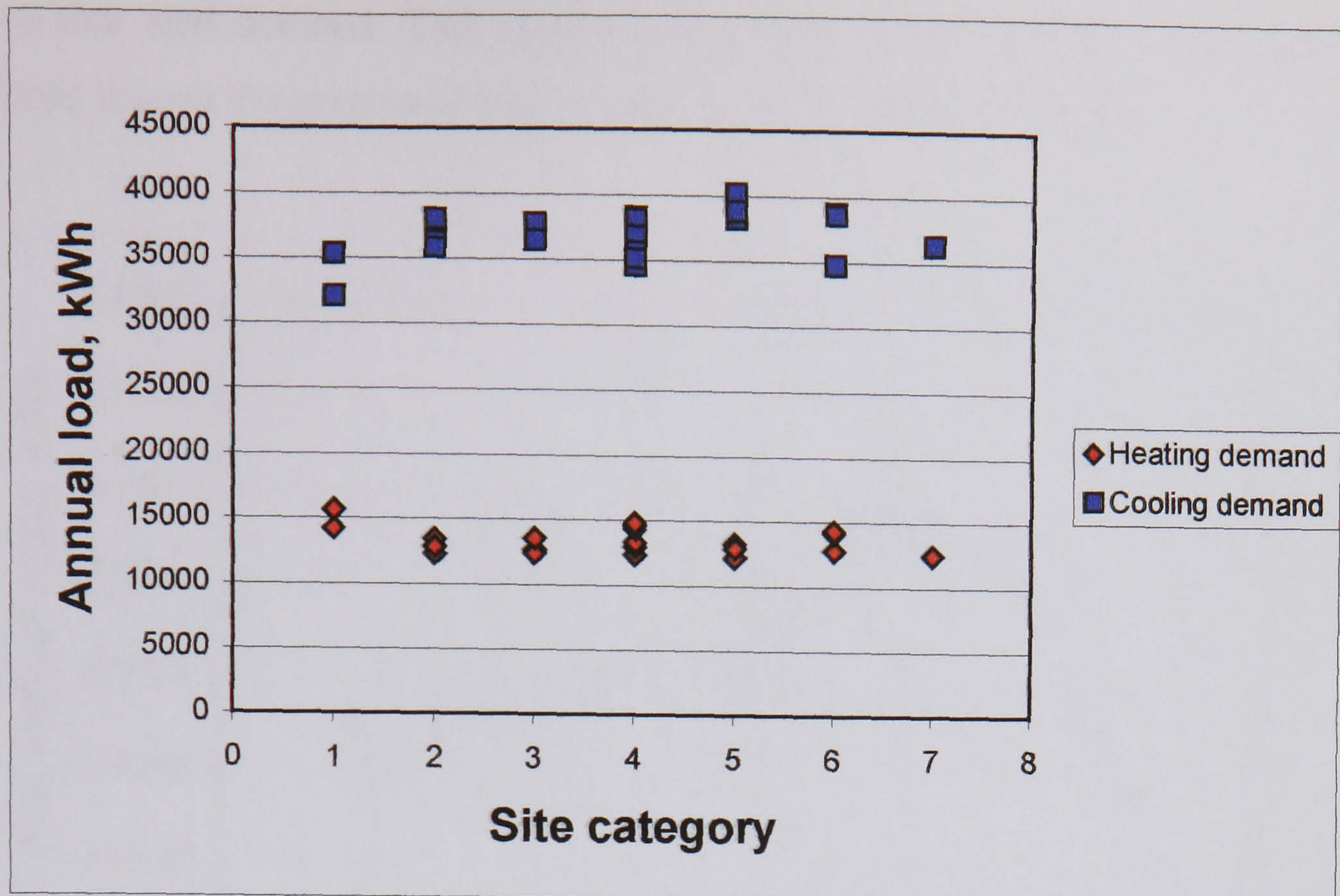


Figure 8.12: Annual heating and cooling load at each site, separated by site category

#### 8.4.2 Annual total load

Figure 8.13 shows the total (heating + cooling) load at each site and how this varies with site category. The line shows the mean of the values for each category. The trend is for total load to increase with increasing urbanization, at least to site category 5 (where it is about 8.5% higher than the total rural load). There appears to be a reduction (down to 2% of total rural load) after this point, with increasing over-shadowing, but the small sample makes this speculative at this stage.

Figure 8.14 shows the same total loads, but how these vary with the distance of each site from the city centre. The line shows the mean of the values at each distance. Total load tends to increase closer to the city, but the range of scatter also increases. This may be associated with the increasing contrast in environments as one approaches a city centre: hard surfaces (open, or heavily over-shadowed) on the one hand, contrasted with large parks. At a radial distance of two miles ( $X_r=2$ ), the *highest* total demand is from a hard surfaced site (SE02) that has the highest annual cooling load of all sites. The *lowest* total demands at  $X_r=2$  are at a site next to a park (NW02) and a site in a hard area of the City of London but heavily over-shadowed (EE02). At a radial distance of one mile the site is near Regent's Park (NW01) and

has a low total demand. This point is responsible for the sudden fall in the mean demand line on the graph and may be atypical of load at this distance.

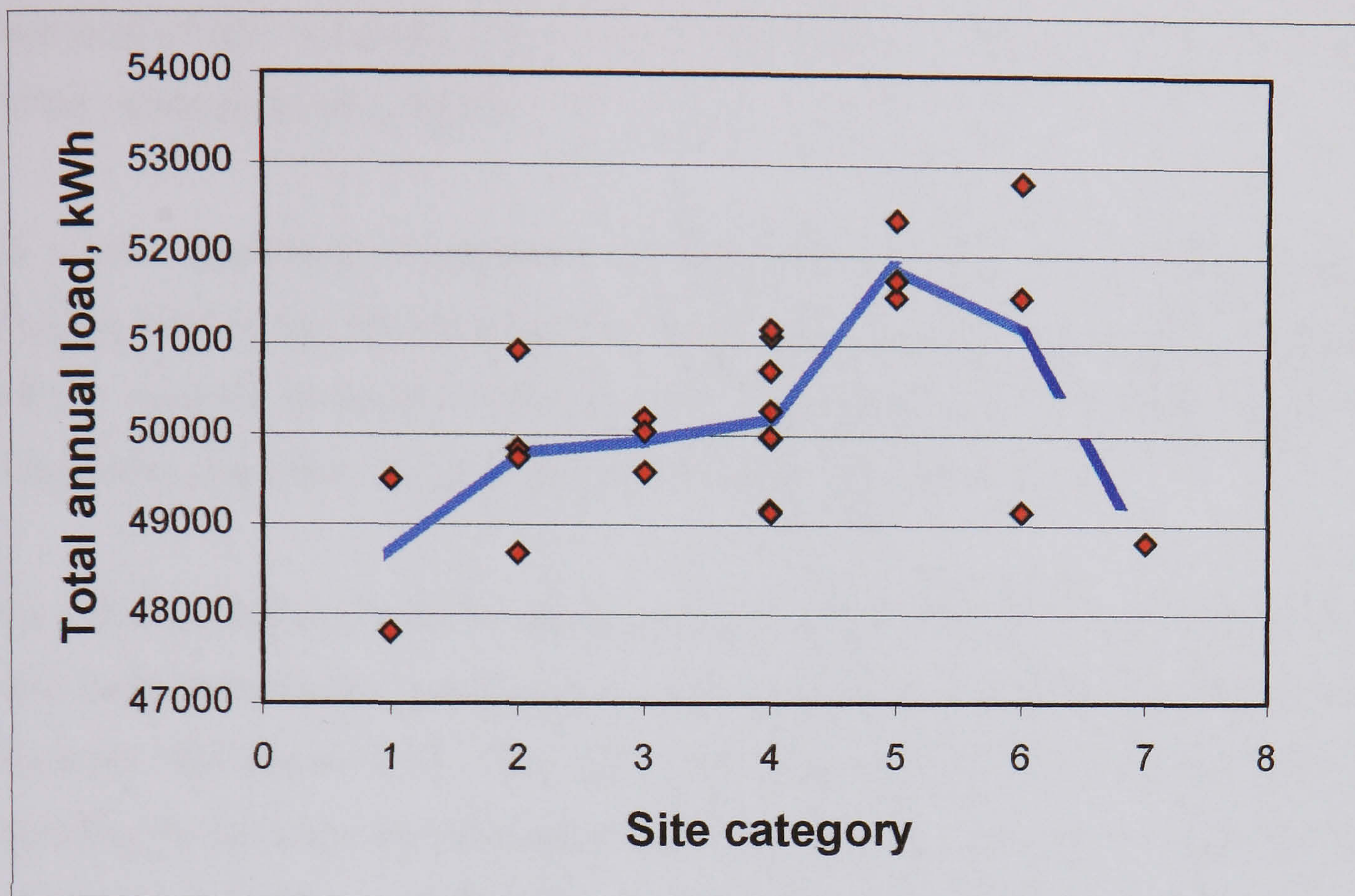


Figure 8.13: Annual total load at each site, separated by site category

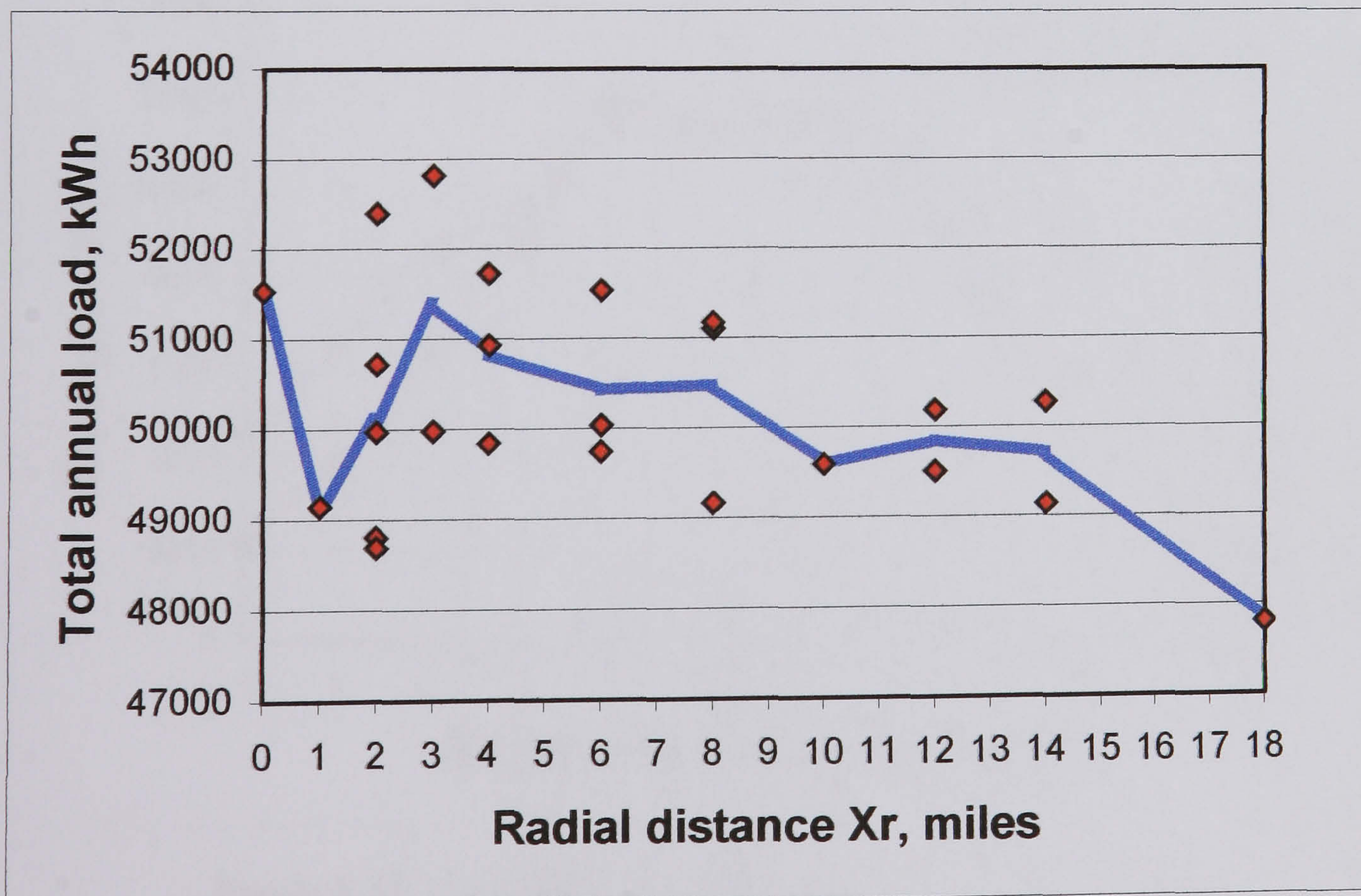


Figure 8.14: Annual total load at each site, separated by distance from the city centre

## 8.5 Separation of the temperature and context effects

There appear to be two main factors affecting load: higher urban temperatures increase cooling load, and higher over-shadowing decreases it. They have the opposite effect on heating load. This section determines the size of these effects when operating independently.

It is also important to appreciate that if a building has, for example, negligible heating load, it can be advantageous for it to be positioned near other buildings so that it receives protection from the sun. If cooling load is negligible, then over-shadowing decreases the solar gain and increases the heating load.

Over-shadowing is greater in the heating season and the difference between shaded and unshaded monthly solar gain is much greater in the heating season than in the summer. See Figure 8.15. This shows the solar gain received by the ECON 19/3 building for an open site (category-1) and an urban site (category-7). There is little difference from May to July inclusive, but significant differences for the rest of the year.

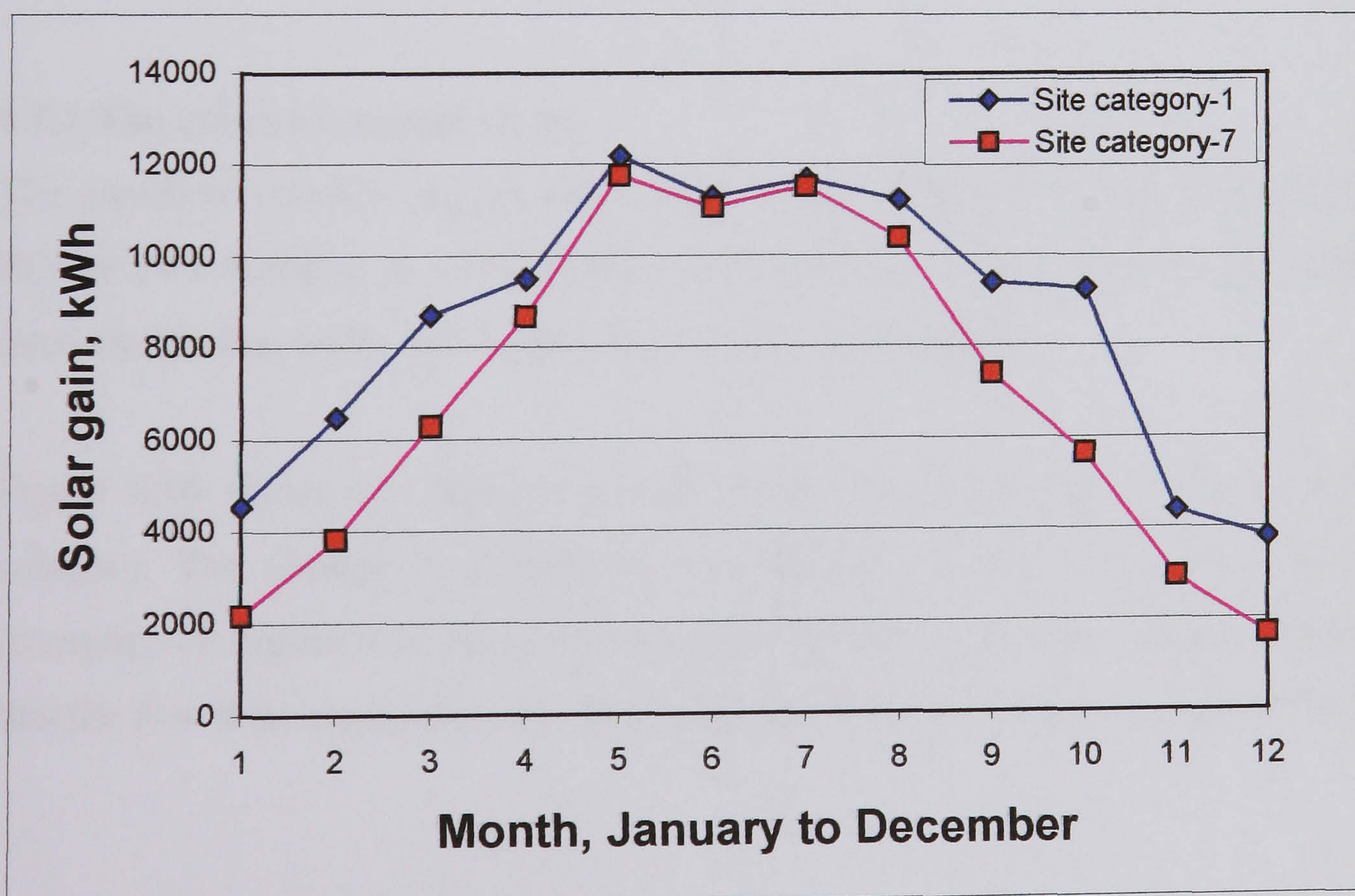


Figure 8.15: Solar gain received by the ECON 19/3 building for an open site and a heavily over-shadowed one

The relative size of the heating and cooling loads for an air-conditioned building depends on many factors. However, given the fixed design and orientation of the ECON 19/3 building, an important factor is the size of the internal gain; the higher the internal gain, the more the annual load shifts from heating to cooling. From the results presented so far, it appears that the relative need for heating and cooling is important in determining the net effect of the heat island, viz. beneficial or not.

For this reason, the results to be presented next were determined for the ECON 19/3 building operating with higher and lower gains than the standard ones used. Table 8.3 shows the gains used so far, in the BASE model (43 W/m<sup>2</sup>), and the variations to be introduced. These higher and lower gains are not artificial and are quite likely to be found in practice. Occupancy gains have not been changed.

Table 8.3: The internal gains used in the ECON 19/3 building

Model	Lighting gain, W/m <sup>2</sup>	Occupancy Sensible, W/m <sup>2</sup>	Occupancy Latent, W/m <sup>2</sup>	Equipment gain, W/m <sup>2</sup>	TOTAL, W/m <sup>2</sup>
Base	15	8	5	15	43
+25%	20	8	5	21	54
+50%	25	8	5	27	65
-25%	8	8	5	11	32

### 8.5.1 The effect of context alone

The simulation model has been run using rural weather (site WW11) acting on the ECON 19/3 building in each of the seven contexts. This introduces the effects of over-shadowing, while controlling for external temperature.

Figure 8.16 shows the change in total annual load (heating + cooling) with site category. The change is plotted as a percentage of the load in a rural setting (category-1). Figure 8.17 shows the absolute changes with respect to rural load. Note that the first three categories are open sites and there is therefore no change for these.

The following observations can be made:

- The effect of site category depends on the level of internal gain
- For a low internal gain building, increasing over-shadowing leads to an increase in total annual load, even at the densest urban category-7.
- For the BASE gain building, greater overshadowing leads to an increase in total load, but starts to fall for the most urban site type.
- Higher gain buildings have a reduced total load with any level of over-shadowing.
- The BASE gain building's total load increases by about 2% (about 1000 kWh) at the urban site (category 6), before falling to almost the same as in a rural context, at the most over-shadowed site (category 7).

As noted above, for the BASE and low gain buildings, increasing context density leads initially to an increase in total annual load, and then a reduction. This is probably because of the angle of the sun being higher during the cooling season compared to the heating season. Applying a wide context affects gain during the heating season much more than in the cooling season.

The trend of reducing total annual load with increasing site-category is apparent as early as category 4 for the high gain building. This suggests that this effect, first observed in Figure 8.13 where temperature was uncontrolled, and for just one site and therefore speculative, is in fact a real effect and not an anomaly.

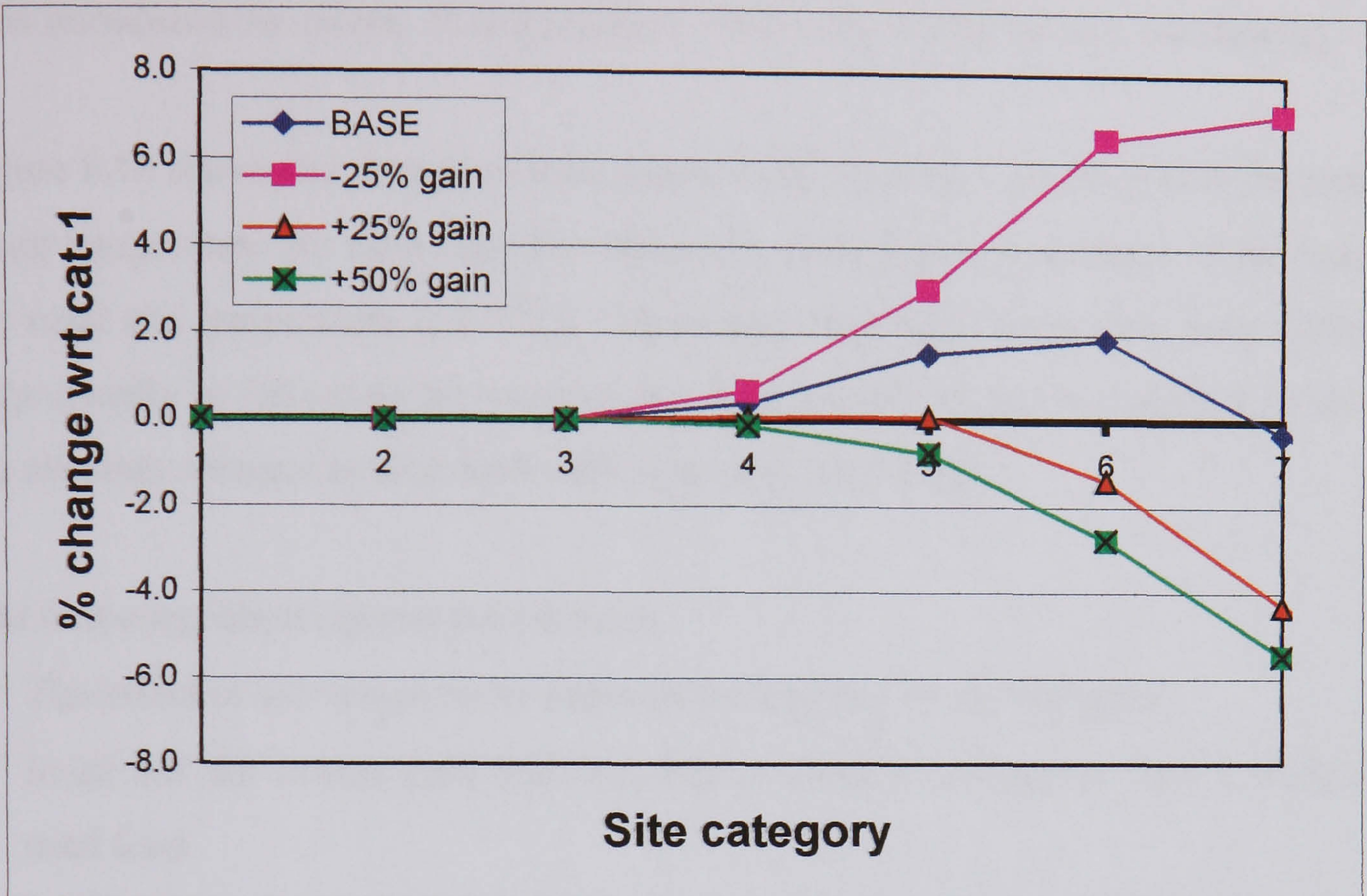


Figure 8.16: Percentage change in total annual load with site category alone for different internal gains. Rural weather

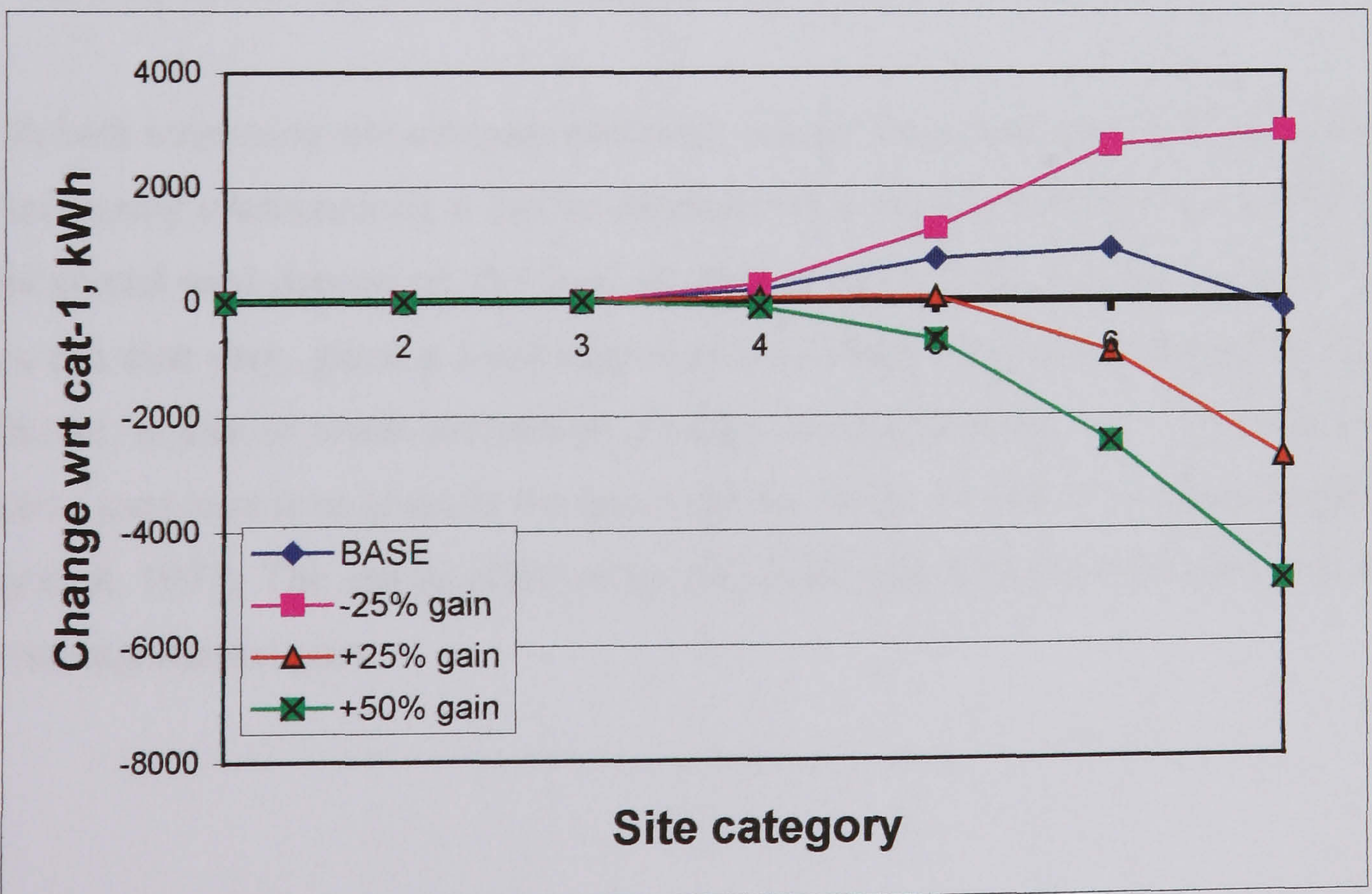


Figure 8.17: Change in total annual load with site category alone for different internal gains. Rural weather

### 8.5.2 The effect of temperature alone

The simulation model has also been run using the measured hourly temperatures at each site, but keeping the ECON 19/3 building in the open, as if in a rural context. This introduces the effects of temperature, while controlling for over-shadowing.

Figure 8.18 shows the change in total annual load (heating + cooling) with the annual mean temperature for each site. The change is plotted as a percentage of the load at the rural site temperature (10.7°C). Polynomial regression lines have been fitted to help visually in following the trend of the different sets of points. Figure 8.19 shows the absolute changes in total load with respect to rural load.

The following observations can be made:

- The effect of site temperature depends on the level of internal gain
- In all but the lowest gain building, higher mean temperatures lead to increased total load
- In the low gain building, higher temperatures have only a small effect on total load and at the highest temperatures total load decreases.
- The BASE gain building's total load increases by about 7% (4000 kWh) at the warmest site in the heat island compared to the load at rural temperatures.

With both increasing site category and mean temperature (both general concomitants of increasing urbanization), it can be concluded that the size and sign of the effect on total annual load depend on the level of internal gains. Note that the level of solar gain can also vary, given a fixed degree of over-shadowing, if the façade design is different: higher or lower percentage glazing, shading features, etc. The percentage glazing used here is as given in the specification for the ECON 19/3 office (Saporito, Day et al. 1997). The annual effect of varying solar gain is likely to be similar to that of varying internal gain.

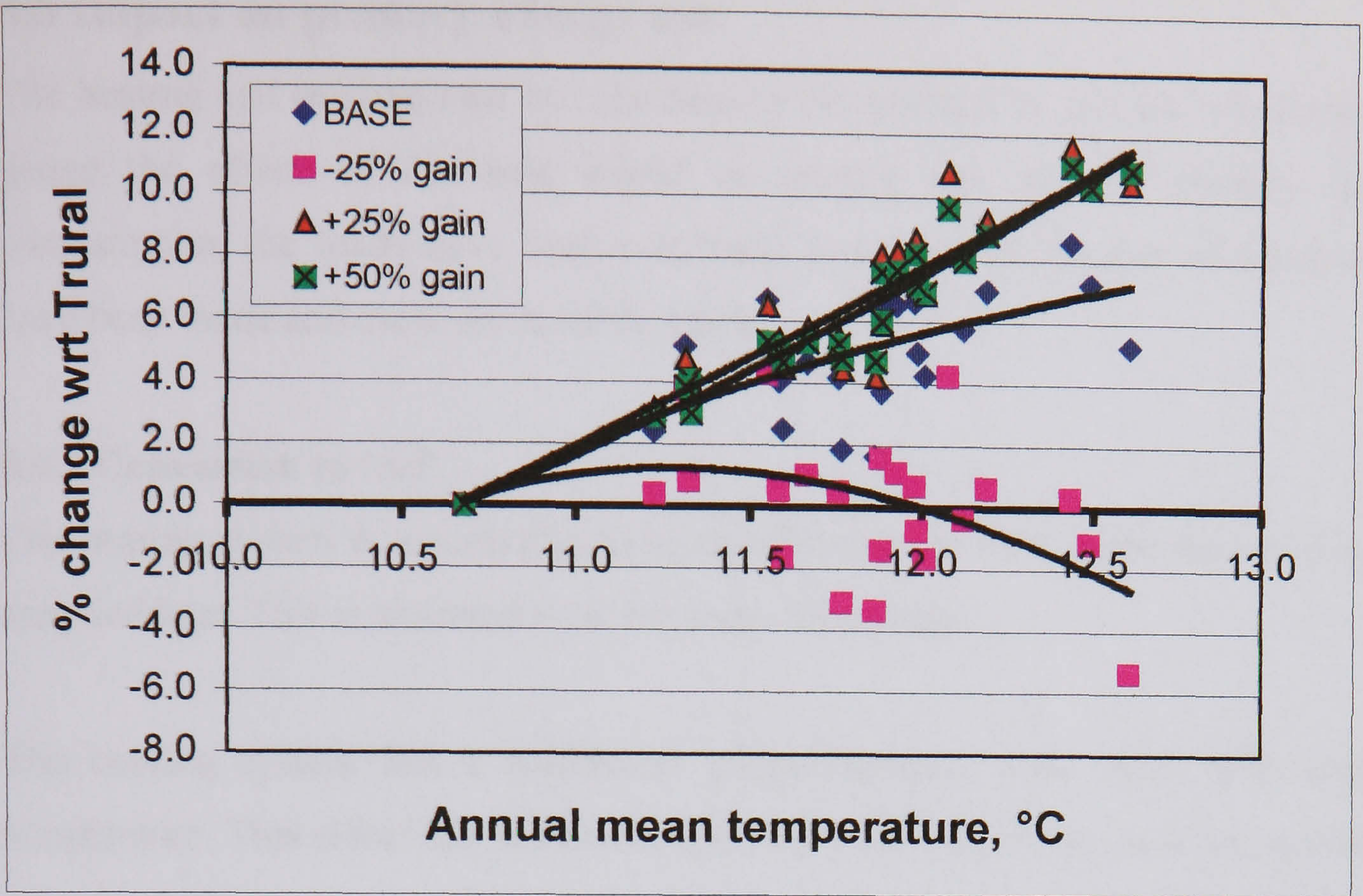


Figure 8.18: Percentage change in total annual load with mean temperature alone for different internal gains. Rural site category

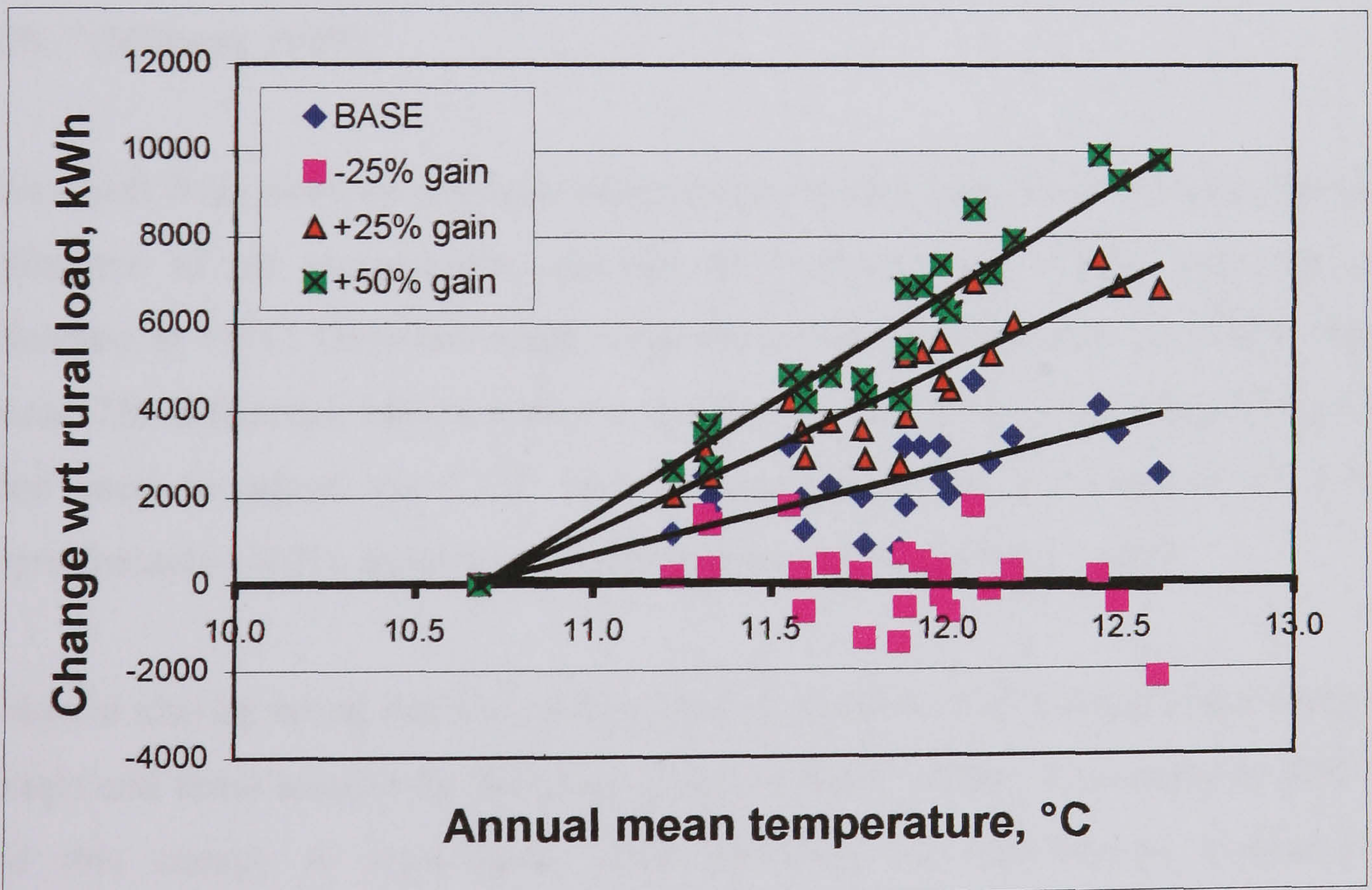


Figure 8.19: Change in total annual load with mean temperature alone for different internal gains. Rural site category



## **8.6 Impact on primary energy use**

The heating and cooling load are assumed to be serviced by gas and electricity. To gauge the effect of the heat island on energy use, i.e. on primary energy consumption, the loads have been converted to energy. A number of assumptions have been made and these are described first.

### **8.6.1 Conversion to fuel**

The heating system is assumed to have an efficiency of 75%, from delivered gas to supplied heat. This is assumed to be the same for all sites.

The cooling system has a coefficient of performance that varies with external temperature. This effect has not been explicitly modelled, for instance on an hour by hour basis. Instead, an existing published estimate has been used: “The changes in energy use [for providing air-conditioning] are almost proportional to climatic changes. At the top end of the range, an increase of 4.5°C [in the mean air temperature] would effectively reduce refrigeration efficiency by about 10%.” (Milbank 1989)

This result from work on climate change has been used here. Over the year, the mean difference in air temperature between the warmest site (EE06) and the rural reference, is 1.9°C. Over this small range the effect of temperature on COP is almost linear. The difference between the rural reference and each of the other 23 sites has been used to adjust the COP from a base of 3.0 to a minimum of 2.87 – approximately a 4.5% reduction for the warmest site in the heat island.

It should also be noted that the energy used to distribute the heating and cooling (by pumps and fans) around the building is not included in this assessment of fuel use, and this energy is significant. Data published in the Energy Consumption Guide (BRECSU 1999) suggest that for the ECON 19/3 type buildings, delivered energy consumption for fans, pumps and controls is approximately twice the delivered energy used for cooling.

Other plant effects not included are, e.g. the dependency of boiler efficiency on operating conditions (load-factor, sequencing, etc.); and the need for terminal re-heat in certain conditions. Heating and cooling are also assumed to operate sensibly only; latent heat gains have not been included. (Note that in the ECON 19/3 building modelled temperature is controlled, but relative humidity is allowed to float.)

The full modelling of plant is quite complex and would have introduced a range of interacting parameters, as listed above, which combined with the impact of control systems may have obscured the main point of this section: to estimate the variation of annual energy use within the heat island. However, it should be born in mind throughout this section that the energy shown to service the cooling load is but one part of the total energy that may be associated with the provision of cooling.

### **8.6.2 Conversion to primary energy**

The energy required to provide and deliver gas is assumed to add 6% to the delivered energy, i.e. a primary energy ratio of 1.06 (UEA 2002).

Electricity is not a primary fuel, and the cost of provision depends on the mix of fuels used, time of day, etc. In the last ten years the introduction of combined cycle gas turbine power stations has reduced the primary energy ratio for electricity supply from about 3.20 to 2.68 (DEFRA 1999). A figure of 3.2 has been taken here, given that cooling demand is in the daytime when less efficient power stations will be operating.

### **8.6.3 Primary energy use**

Figure 8.20 shows the primary energy used by the ECON 19/3 building when internal gain is at BASE level. Primary heating energy is approximately half the primary cooling energy. The total primary energy used varies by site, and as shown here, by distance from the city centre.

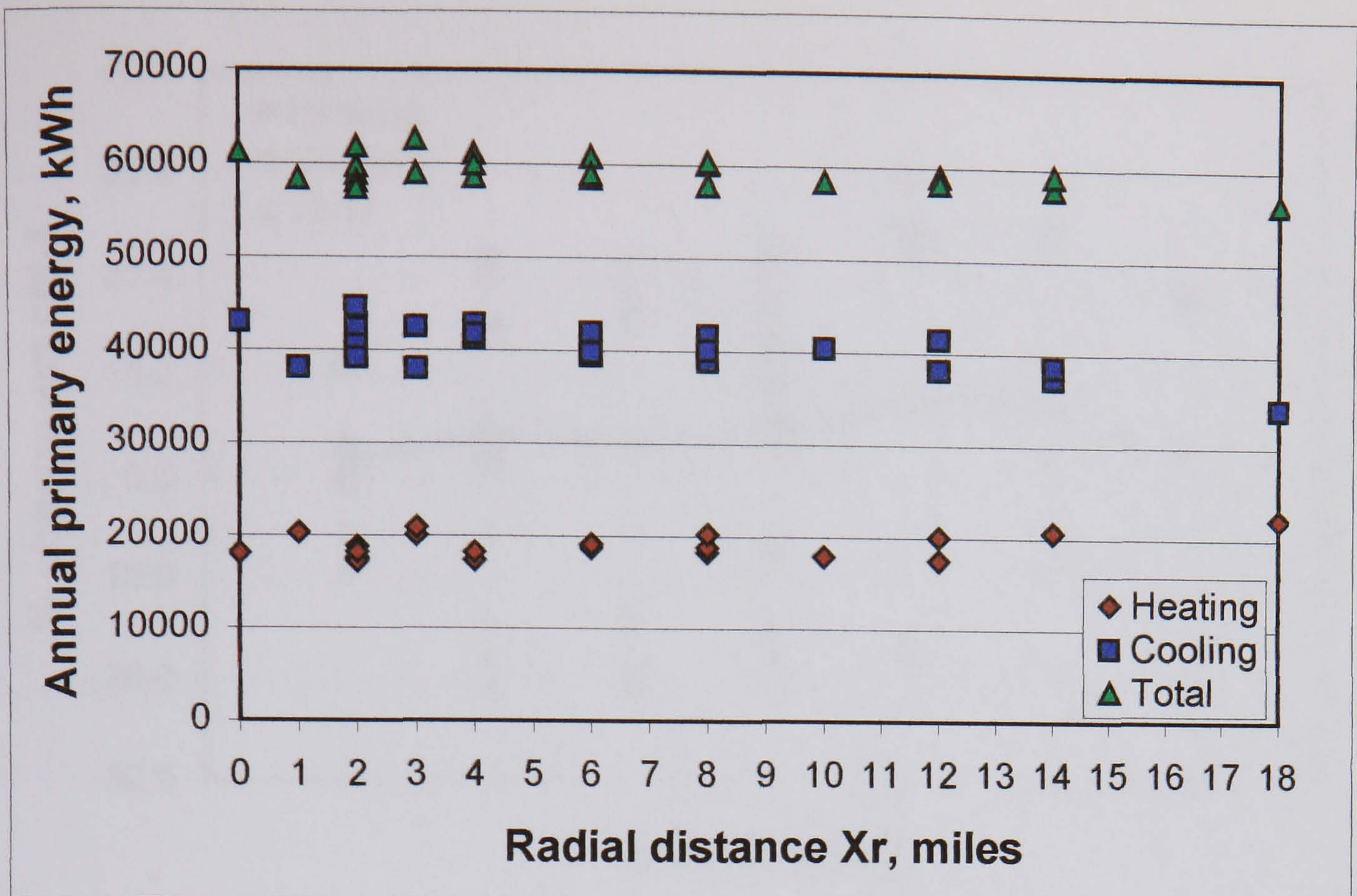


Figure 8.20: Annual primary energy use at each site, separated by distance from the city centre. BASE gain

Figure 8.21 shows the change in primary energy use as a percentage of the energy used at the rural site. The line links the averages for total primary energy change within each site-category. Cooling primary energy increases by up to 30% and heating primary energy decreases by up to 22% as urbanization increases. Although these largely balance each other, there is still a net change.

Total primary energy use can be seen to increase with urbanization to category-5 and then decrease on average. Category-7 has only one site and therefore the value here is less certain. On average, total primary energy increases by 8.5% at the category-5 sites, with respect to the rural energy use at category-1. There is no site where the total primary energy use for heating and cooling is lower than at the rural site.

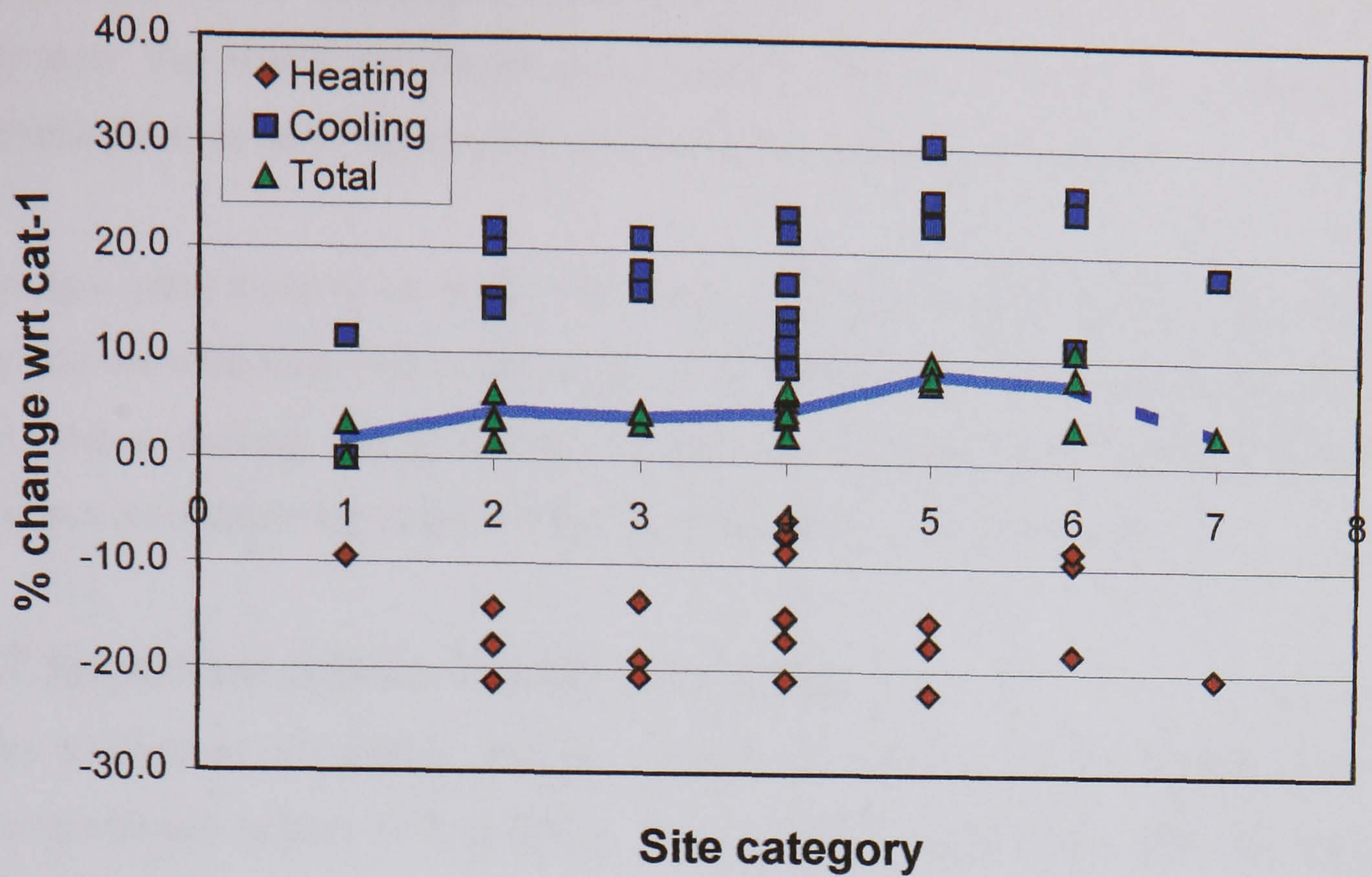


Figure 8.21: The relationship between site category and annual primary energy use. BASE gain

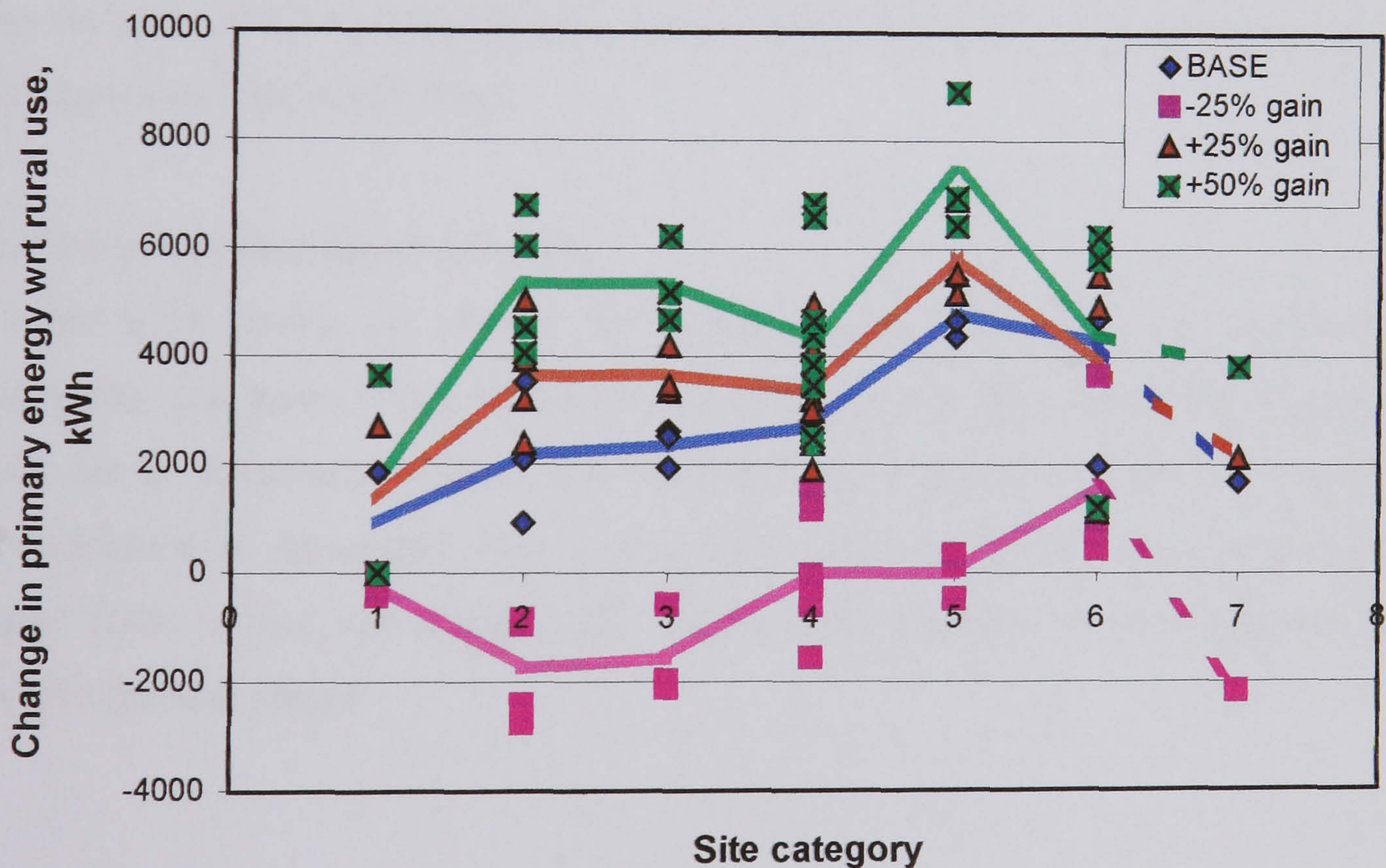


Figure 8.22: The relationship between site category and change in annual total primary energy use, for different internal gains

Figure 8.22 shows how primary energy changes with site category for the ECON 19/3 building for different levels of internal gain. The changes are plotted

with respect to the consumption at the rural site. The lines join the averages of each category. For BASE and higher gain, primary energy use generally increases with urbanization, as far as category-5, when it falls to categories-6 and 7.

For low gain, there is an initial fall which is probably attributable to the effect of warmer surroundings reducing energy use in a heating dominated building, followed by a rise as cooling energy starts to become more significant and followed by a final fall as over-shadowing reduces solar gain and therefore cooling load.

## **8.7 Impact on carbon dioxide production**

The production of carbon dioxide through energy use is one indicator of the environmental impact of a building. This section describes the effect of the heat island on CO<sub>2</sub> release.

### **8.7.1 Calculating carbon dioxide production**

The delivered fuel, derived earlier, has been converted to carbon dioxide production on the basis of 0.2 kg CO<sub>2</sub>/kWh for the use of gas, and 0.52 kg CO<sub>2</sub>/kWh for the use of electricity (BRECSU 1999).

### **8.7.2 Carbon dioxide production**

Figure 8.23 shows the change in carbon dioxide production for different site categories and gains. The profiles are almost identical to those of primary energy and will not be described in detail. For the low gain building, compared to a rural site urbanization is associated with a reduction in average carbon dioxide generation apart from in one site category (6). Higher gain buildings always generate more within the heat island.

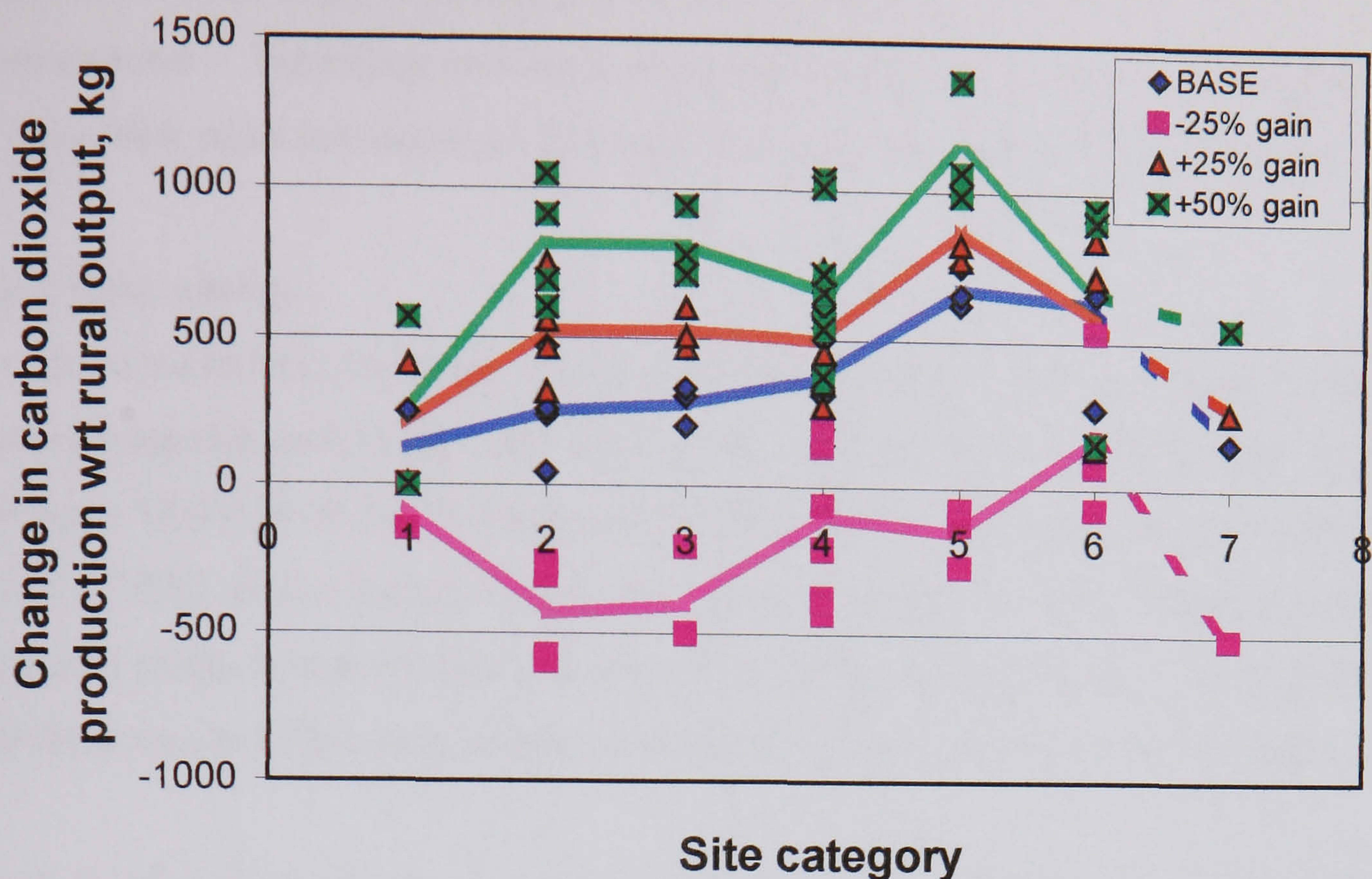


Figure 8.23: The relationship between site category and change in annual total production of carbon dioxide, for different internal gains

## 8.8 Peak energy consumption

Peak loads are important in that they can determine the size of plant specified to service the heating or cooling need. They also have an impact on generating needs and overall generating performance as lower efficiency plant is brought on-line at times of higher demand.

### 8.8.1 Calculation of peak energy

*Tas* has been run on each of the 24 sites to locate the day, time and size of the peak heating and cooling loads. The cooling loads have then been converted to delivered energy as before. The temperature difference between the site and the rural reference has been used to allow for the fall in efficiency of providing cooling – again using the same method as before. It is an approximation that the peak cooling energy consumption coincides with the peak cooling load, but it is likely to be a reasonable one.

Peak delivered energy is shown, rather than peak load, so that the effects of higher temperatures – increasing cooling load but decreasing the efficiency of providing for it – are both taken into account. The peak energy is assessed for BASE gain only.

### **8.8.2 Peak energy**

In the simulations, for most of the 24 sites the peak *cooling* demand occurred between midday and 15:00 GMT on one day, 19 June 2000, with four sites peaking between 15:00-16:00 on 2 August 1999. Both these days were very hot (reaching over 32-33°C at the focus). One of the reasons peaks occur at different times in different places is that the heat island shifts with the wind direction. The wind speeds for these two hot days were similar, but the wind direction was about 45° apart.

Peak *heating* demand occurred for all sites between 07:00-08:00 on the morning of 20 December 1999 when there had been a cold clear night (dropping to -1°C at the focus). Wind speed was very low at 0-1 m/s.

At the time of peak cooling load, temperature differences between each site and the rural reference varied, reaching 4.2°C but averaging 1.7°C. It is these differences that have been used in adjusting the efficiency of providing the cooling. Figure 8.24 shows the change in peak electricity (i.e. delivered energy) use with site category. The upper line joins the averages of each category. The lower line, similarly, but this shows the percentage increase of peak demand with respect to the mean of the category-1 sites.

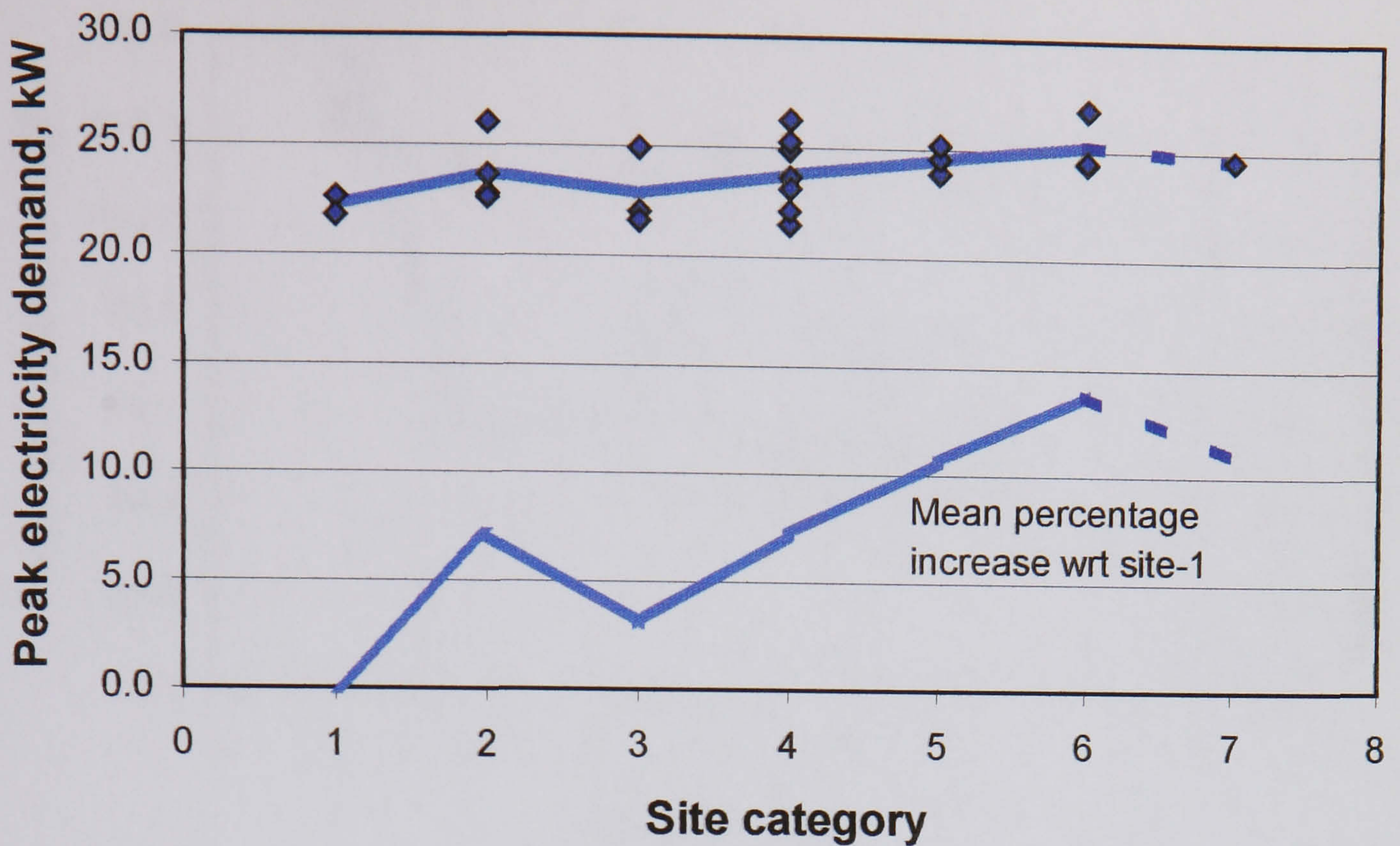


Figure 8.24: The relationship between site category and peak electricity demand for cooling

Peak electricity demand tends to increase with site category up to 13.8% more than the rural category peak, before falling at the (single) most urban site. Peak demand also tends to increase with decreasing radial distance, but the relationship is poor (14% variance is explained by  $X_r$ ).

Figure 8.25 shows the tendency for peak heating fuel use to decrease with increasing urbanization. The most urban site (category-7) has a peak 10% lower than at the rural category. However, there is considerable scatter in the data.

Figure 8.26 shows how peak gas demand reduces with radial distance from the city. The rate of reduction, taken from the regression line, is approximately 0.6kW/mile.



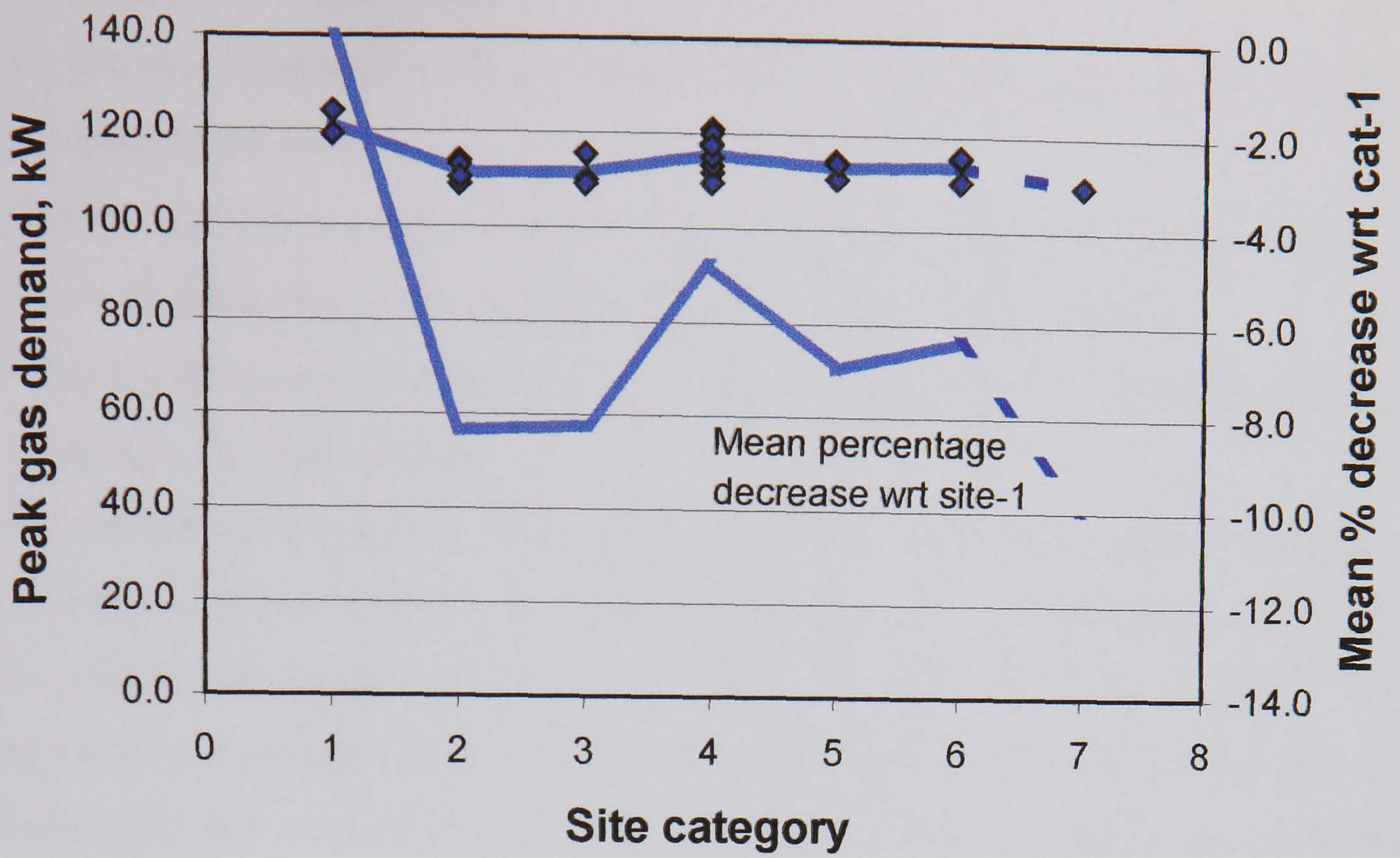


Figure 8.25: The relationship between site category and peak gas demand for heating

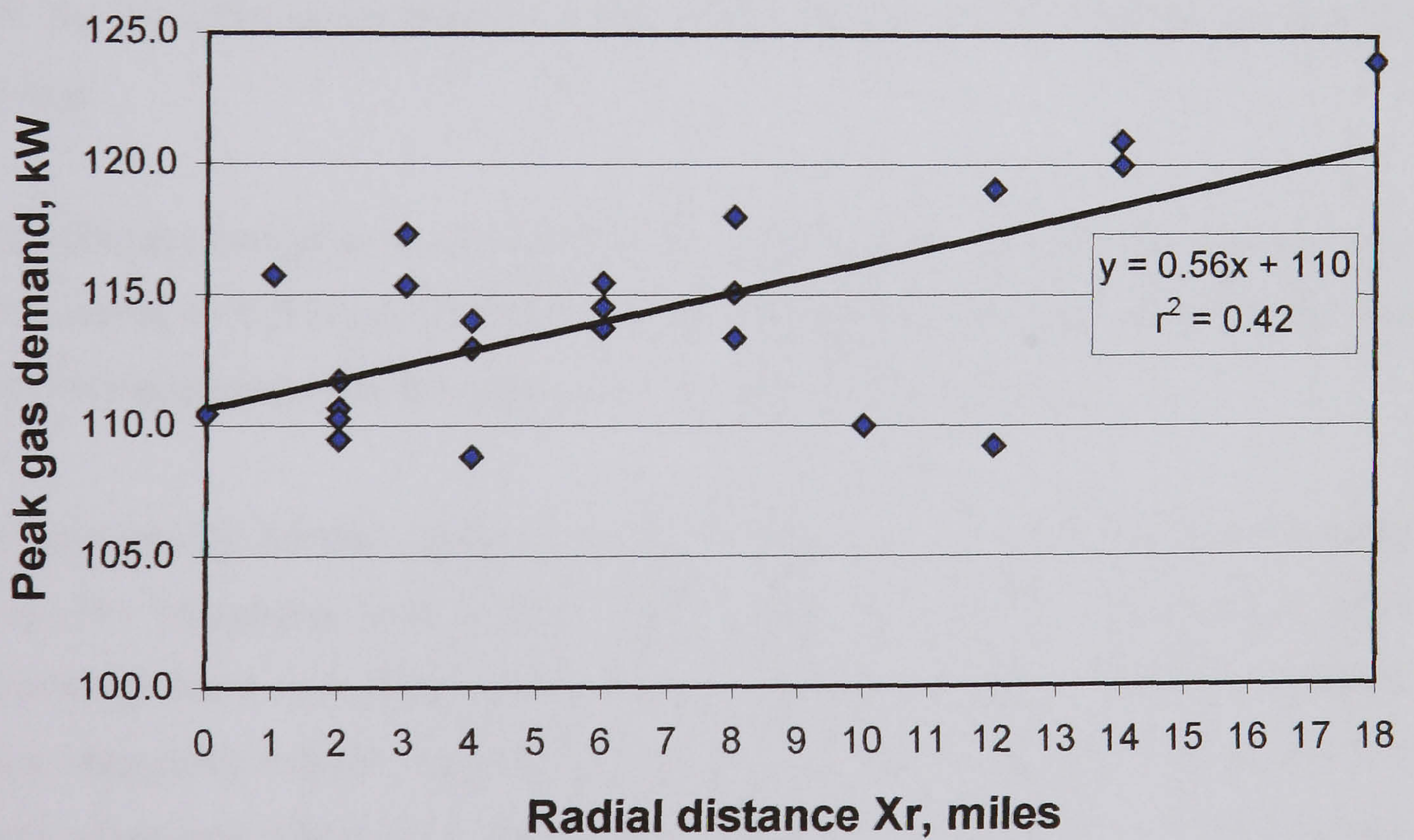


Figure 8.26: The relationship between radial distance and peak gas demand for heating

## 8.9 Chapter 8 Conclusions

There are three important external factors operating to affect energy use in buildings in the urban environment:

- Warmer urban temperatures increase cooling load, but decrease heating load.
- Warmer temperatures decrease the efficiency of providing cooling.
- Direct solar gain to buildings is reduced and this increases the heating load and decreases the cooling load.

The net effect can be seen in Figure 8.20 which shows that the primary energy used for cooling increases towards the centre of the city. The innermost site uses 25% more cooling energy than the rural site (43027 kWh and 34243 kWh). (N.B. This energy does not include the distribution energy (pumps and fans) associated with air-conditioning. See section 8.6.1) When the same data are related to increasing urbanization of the site (Figure 8.21), again the cooling energy increases. However, an effect revealed by the modelling is that over-shadowing starts to have a significant effect at the more urban sites. At the most over-shadowed site (category-7) the primary cooling energy is now 18% greater than the rural site. It can therefore be said that the urban environment is associated with an increase in the energy used for cooling.

Total primary energy used (for heating and cooling) also increases, on average, with urbanization to 8.5% greater than the rural energy use. Use falls again at the two most over-shadowed site categories to 7.5%, and 3% at category-7.

The relationship between energy use and site category is indicative of an average trend. For categories with a high street gorge ratio (and therefore more over-shadowing) there is a downward trend in cooling load which would be expected. Other categories exhibit considerable scatter. One reason for this is that there is a broad urban heat island field that applies to all sites: the smaller the radial distance from the city centre, the warmer it *tends* to be. Superimposed on this is the nature of a site. This was shown for instance in the short term tests reported earlier where greener areas were often cooler, and in Figure 8.10 where almost 50% of the variance in cooling load was associated with the degree of surrounding greenness. It

is therefore not surprising that a relatively simple categorization based on a surrogate for sky view and immediate surface nature gives only approximate predictions.

Another aspect revealed by the modelling is the effect of internal gain. The above conclusions relate to the BASE gain example, and in broad terms also apply to the higher gain examples. However, for a low gain building, Figure 8.22 shows that urbanization initially leads to a decrease in total primary energy use compared to rural use. When category 4 is reached the energy use has risen again to the rural use and then it essentially follows the trend of the higher gain buildings, except that it finishes at category-7 using less energy than at a rural site. In general, as revealed in Figure 8.17 and 8.18, and 8.22, increasing urbanization can lead to an increase or decrease in total annual load and primary energy, depending on whether a building is heating dominated or cooling dominated, i.e. depending on the internal gains.

Peak demand for electricity for cooling increases up to about 14% more than the rural peak before falling again to 11% more, for the most urban category. Peak heating demand for gas conversely falls to around 6-8% less than the rural peak with a fall to 10% less at the most urban site. The extra summertime load on electricity generation is a negative aspect of the heat island that would tend to be associated with higher generating costs and for higher capacity plant to have to be installed in a building. The reduced peak demand for gas is beneficial but it is easier to service changing gas demand than electricity and there are not the same efficiency penalties.

## **CHAPTER 9**

### **Conclusions**

## CHAPTER 9 – Conclusions

This study has looked at the impact of the urban environment on the amount of energy used for cooling buildings in London. Intuitively energy used for air-conditioning increases with rising air-temperature, but urban areas are not simply associated with higher temperatures and moreover the urban fabric is not homogeneous. To assess the impact the study has proceeded in three parts.

First, eighty measurement stations were established along radiating lines from the centre of London as far as rural areas. These measured the air temperature simultaneously at hourly intervals for over a year and allowed the spatial and temporal variation of London's urban heat island to be determined. Second, the impact of the measured temperature variation on energy use and peak load was determined by using simulation to model an air-conditioned office building in different urban contexts. Third, experiments within central London looked at specific aspects of the urban environment that affect air temperature: the effects of vegetation in parks, and façade colour and surface temperature in streets.

The main findings of this work fall into two broad categories: the characteristics of the London heat island, and the impact these and urban form have on energy consumption. The main results are listed below:

### 9.1 Main results

#### Intensity through time in the summer

In the summertime, the London heat island intensity varied widely from a maximum of +8°C down to a cool island of -4°C:

- The mean 24 hour heat island intensity was 2.1°C in 1999 and 1.9°C in 2000.
- In the day, the mean heat island intensity peaks at 1.3°C soon after midday with mean minima at around 10am (0.6°C) and again in the afternoon at 3pm (about 0.8°C). For 10% of the daytime the heat island intensity was more than 2.7°C.
- At night, the mean heat island intensity is greater and rise to 3.2°C on average. For 10% of the night-time the heat island intensity was more than 5.1°C.
- For 6% of the summertime, there was a cool island.

- The general pattern of intensity distribution was very similar for both summers (1999 & 2000), and the intensities the same to within 0.5°C.

### **Intensity through space in the summer**

The heat island intensity varied spatially in several ways:

- It reduced with increasing distance from London. This effect was much stronger at night than in the daytime.
- Using an eight point scale of urbanization (see Chapter 5, Table 5.3), the mean heat island intensity increased progressively the more urbanized sites became. There was evidence that this peaked at category 5 (a wide street gorge typical of medium density urban areas) in the daytime and at more urban categories still, the intensity was lower.
- *For any given distance from the centre* (up to about 10 miles), the mean heat island intensity tended to decrease with decreasing levels of urbanization as defined on the eight point scale. This was particularly so for daytime data.
- At night, the location of the peak intensity in central London could be seen to move up to 2-3 miles downwind and its location could be predicted from the wind direction data in the previous 2-3 hours. In the daytime, the pattern of isotherms was less clear and there were often many peaks.

### **Temperature and cooling factors**

- In the summer, greener sites were associated with lower air temperatures and when sites were re-assessed on the basis of their upwind greenness, computed on an hourly basis, the separation in temperature between the green and less-green sites increased.
- Daytime air temperatures at a small park in the centre, and a large park outside the centre, were between 0.6-1.1°C cooler than temperatures in nearby streets.
- On a sunny summer's day, lighter-coloured surfaces in streets were 6-10°C cooler than darker ones for similar material and solar exposure. (Mean surface temperatures in a street gorge were found to be well-correlated with the air temperature at mid-gorge height on both sunny and cloudy days.)

### **Impact on cooling load**

- The annual cooling load (40181 kWh) for the ECON 19/3 building chosen as a typical building (see chapter 7) at an inner London site was 25% higher than the rural load (32103 kWh).
- There are examples of relatively *low* cooling loads at some sites *close* to central London (NW01 near Regent's Park, and NW02 adjacent to Primrose Hill Park; green areas). Conversely, there is an example of a relatively *high* cooling load at a site *distant* from central London (EE08 at Ford Dagenham Works, 12 miles away; a hard-surfaced industrial area).
- Annual cooling load ( $y$ ) for the ECON 19/3 building at a site was related to its annual mean air temperature ( $T$ ), thus:  $y = 3275.T - 1873$  kWh ( $r^2 = 0.67$ ,  $n=24$ )
- Annual cooling load was related to site category, but with much scatter evident. Load increased with urbanization to category-5 and then tended to fall.
- Annual cooling load increased progressively from the rural site at 18 miles towards the centre. However, closer than four miles, radial distance did not predict the cooling load well.

### **Impact on total load**

- The increase in cooling load with increasing urbanization was mostly offset by a decrease in heating load.
- The trend was for total load to increase with increasing urbanization, at least to site category 5 (where it was about 8.5% higher than the total rural load). There appeared to be a reduction (down to 2% higher than total rural load) after this point, but this was uncertain.
- Total load tended to increase closer to the city, but the range of scatter in the relationship of load and distance also increased.

### **Total load and site category – isolated effect**

- The effect of site category on total annual load depended on the level of internal gain in the ECON 19/3 building and was assessed by using rural weather and adjusting the internal gain from -25% to +50% BASE level.

- For a low internal gain building, increasing over-shadowing at higher (more urban) categories led to an increase in total annual load, even at the densest urban category-7.
- For the BASE gain building, greater overshadowing led to an increase in total load, but started to fall for the most urban site type.
- Higher gain buildings had a reduced total load with any level of over-shadowing.
- The BASE gain building's total load increased by about 2% (about 1000 kWh) at the urban site (category 6), before falling to almost the same as in a rural context, at the most over-shadowed site (category 7).

#### **Total load and site temperature – isolated effect**

- The effect of site temperature on total annual load depended on the level of internal gain in the ECON 19/3 building and was assessed by using a rural open site and adjusting the internal gain from -25% to +50% BASE level.
- For a low internal gain building, higher temperatures had only a small effect on total load and at the highest temperatures total load decreased.
- For buildings with higher gain, higher mean temperatures led to an increased total load.
- The BASE gain building's total load increased by about 7% (i.e. 4000 kWh) at the warmest site in the heat island compared to the load at rural temperatures.

#### **Impact on total primary energy use**

- For the ECON 19/3 building, with BASE level internal gain, the annual primary heating energy is approximately half the primary cooling energy.
- Cooling primary energy increased with respect to the rural use by up to 30% and heating primary energy decreased by up to 22% as urbanization increased.
- Total primary energy use increased with urbanization up to category-5 (8.5% more than rural use) and then decreased on average. This was true for BASE and higher levels of internal gain.
- There was no site where the total primary energy used for heating and cooling was lower than at the rural site.

*Note that the above do not include the primary energy used for the distribution of heating and cooling.*



### **Impact on carbon dioxide production**

- The profiles of change in carbon dioxide production with urbanization were almost identical to those of primary energy.
- For the low gain ECON 19/3 building, compared to a rural site, urbanization was associated with a *reduction* in average carbon dioxide generation apart from in one site category (6). Higher gain buildings always generated more carbon dioxide within the heat island.

### **Impact on peak energy consumption**

- For the BASE gain ECON 19/3 building, peak electricity demand tended to increase with site category up to about 14% more than the rural category peak, before falling at the (single example of the) most urban site.
- Peak gas use tended to decrease with increasing urbanization. The most urban site (category-7) had a peak 10% lower than at the rural category. However, there was considerable scatter in the data.

## 9.2 Conclusions

### *The urban environment*

London has been found to be warmer in the summer than a rural reference site. This difference is greatest overnight and at a minimum in the afternoon. This suggests that the main reason for the existence of the heat island in London is the nature of the urban form – higher heat capacity, more effective absorption of solar energy, reduced dissipation efficiency. Anthropogenic heat release in the city is less likely to be important and no evidence was found that supported it having a major role.

The mean heat island intensity at a location tends to reduce with increasing distance from London, or with decreasing levels of urbanization. An eight level site-categorization based on sky-views and surface nature has been found useful in characterizing the variation of temperature between sites. There is in essence a broad urban heat island field that applies to any site, characterized by its radial distance from the centre of London, and superimposed on this is the nature of a site, characterized by its particular degree of urbanization – its site category.

One aspect of low urbanization – greenness – was found to be associated with cooler temperatures. Air in parks in the daytime was found to be about 0.6-1°C cooler than air in street gorges near by. Tests indicated that downwind of a park, the streets were also cooler. As the mean daytime heat island intensity of London is around 2°C, this indicates that cooling loads can be significantly reduced by keeping or introducing vegetation into the urban environment.

### *The impact of the urban environment*

Three important external factors operate to affect energy use in buildings in the urban environment:

- Warmer urban temperatures increase cooling load, but decrease heating load.
- Warmer temperatures decrease the efficiency of providing cooling.
- Direct solar gain to buildings is reduced and this increases the heating load and decreases the cooling load.

The net effect of these factors was assessed by simulating the performance of a standard air-conditioned office building ECON 19/3 using the measured air temperature data.

The annual primary energy used for cooling (see italicized paragraph at end of this section) increases towards the centre of the city. Of 24 sites across London, the ECON 19/3 building at the innermost site uses 25% more cooling energy than at the rural site (43027 kWh and 34243 kWh). When the same data are related to increasing urbanization of the site, again the cooling energy increases. However, the advantage of over-shadowing starts to have a significant effect at the more urban sites. At the most over-shadowed site the primary cooling energy is now 18% greater than the rural site.

Heating energy use tends to decrease towards the centre, but on balance, the total annual primary energy used (for heating and cooling) increases, on average, with urbanization to 8.5% greater than the rural energy use. Use tends to fall again at the two most over-shadowed site categories to 7.5%, and then 3%.

It should be noted that in general, increasing urbanization can lead to an increase or decrease in total annual load and primary energy, depending on whether a building is heating dominated or cooling dominated, i.e. depending on the internal gains. The conclusions above relate to the BASE gain example, and in broad terms also apply to higher gain examples. However, for a low gain building urbanization initially leads to a decrease in total primary energy use compared to rural use.

Peak demand for electricity for cooling generally increases with urbanization, and peak demand for gas decreases. The extra summertime load on electricity generation is a negative aspect of the heat island that would tend to be associated with higher generating costs and for higher capacity plant to have to be installed in a building. The reduced peak demand for gas is beneficial but it is easier to service changing gas demand than electricity and there are not the same efficiency penalties.

*The energy quoted above does not include the energy for distribution which has not been assessed in this work, and which is dependent on the system design.*

*Distribution energy is significant, and, in all-air systems, can be two thirds of the total energy used by plant associated with providing ventilation and cooling. The variation of energy used for cooling, quoted in the text, should therefore be seen in the context of the total energy used which includes the relatively fixed energy, i.e. insensitive to the heat-island, used for distribution. See section 8.6.1.*

### 9.3 Recommendations for further work

The study has identified a number of uncertainties, and opportunities for further research, as well as areas where application of the results could be useful. Some possibilities are given here:

1. The convective heat loss coefficient that is used in the simulation of the energy performance of buildings varies with wind speed and turbulence. Given that most buildings are in urban areas, there is a need for more information on the appropriate value to use within street gorges and how it varies with gorge characteristics (H/W ratio, orientation, surface temperature distribution) and the relationship with regional wind speed. Simulation models could usefully then incorporate such information.
2. There is a need for the development of more detailed modelling of urban contexts, which involve long-wave exchange, and solar reflection and shadowing. This could then be used to enhance the accuracy of urban building simulation.
3. In a street of brick buildings, gorge air temperature was shown to be well-related to mean gorge ground and façade temperature. The impact of different façade constructions on local peak air temperature may be significant, particularly in the case of modern insulated over-cladding and rainscreens. With their low heat capacity and poor coupling to the building mass, high surface temperatures may develop, and heat the gorge air accordingly.
4. The depth of the urban heat island may be of the order of 100m. Mechanically ventilated high rise offices may therefore benefit in the cooling season by drawing in air at high level, and vice versa in the heating season. The net effect will have an impact on design calculations. There are few data on actual air inlet temperatures at high and low level.
5. Trees in streets affect the wind flow, the building convective heat loss coefficient, and intercept long and short wave radiation. They also provide

evaporative cooling. They are often advocated for mitigating heat island impacts, but their overall impact on building energy use is not clear.

6. The study suggests that daytime temperatures and energy used for cooling are reduced with either more open or closer spacing of buildings, i.e. for energy issues alone, there is a peak spacing to avoid. This knowledge could usefully be included in building design advice, and should be applicable across the UK. Other aspects of the work are more particular to the London heat island, e.g. maps of heating and cooling degree days across London. However, at present, the position of a site within a city's heat island is rarely taken into account when sizing plant for a building, and advice could be developed to rectify this.
7. The large database of hourly air temperature data across London could provide opportunities for further study, e.g. in developing existing urban temperature prediction models.
8. Relative humidity affects comfort and, in fully air-conditioned buildings, the energy used for conditioning the internal environment. Selected stations in the existing monitoring array could be used for assessing the humidity field across London.
9. The detailed behaviour of plant and controls and their impact could be modelled in order to improve the assessment of the overall energy used for heating and cooling.
10. The results are derived from a study of 80 discrete locations in London, with site characteristics being assessed in 24 sites using digital aerial photographs. A geographically more complete assessment and prediction of temperature and loads could be obtained if GIS data on land cover and an urban DEM were used to allow an automatic analysis of urban terrain. The results could also be compared in detail for the first time with satellite-based surface temperature data.

## **REFERENCES**

## REFERENCES

- Aida (1982). Urban albedo as a function of the urban structure - a model experiment (part 1). *Boundary Layer Meteorology* **23**: 405-414.
- Akbari, H., S. Bretz, D. Kurn and J. Hanford (1997). Peak power and cooling energy savings of high-albedo roofs. *Energy and Buildings* **25**: 117-126.
- Akbari, H., S. Konopacki and M. Pomerantz (1999). Cooling energy savings potential of reflective roofs for residential and commercial buildings in the United States. *Energy* **24**: 391-407.
- Akbari, H., D. Kurn, S. Bretz and J. Hanford (1997). Peak power and cooling energy savings of shade trees. *Energy and Buildings* **25**: 139-148.
- Asaeda, T. and V. T. Ca (2000). Characteristics of permeable pavement during hot summer weather and impact on the thermal environment. *Building and Environment* **35**: 363-375.
- Asaeda, T., V. T. Ca and A. Wake (1996). Heat storage of pavement and its effect on the lower atmosphere. *Atmospheric Environment* **30**(3): 413-427.
- Atkinson, B. W. (1985). *Update: The Urban Atmosphere*, Press Syndicate of the University of Cambridge.
- Barlag, A. B. and W. Kuttler (1991). The Significance of Country Breezes for Urban-Planning. *Energy and Buildings* **15**(3-4): 291-297.
- Bärring, L., J. Mattsson and S. Lindqvist (1985). Canyon geometry, street temperatures and urban heat-island in Malmo, Sweden. *Journal of Climatology* **5**(4): 433-444.
- Barry, R. G. and R. J. Chorley (1968). *Atmosphere, Weather and Climate*, Methuen.
- Böhm, R. (1998). Urban bias in temperature time series - A case study for the city of Vienna, Austria. *Climatic Change* **38**(1): 113-128.
- BRECSU (1999). Energy use in offices (Energy consumption guide 19), BRECSU.
- Brundl, W. and P. Hoppe (1984). Advantages and disadvantages of the urban heat-island - an evaluation according to the hygro-thermic effects. *Archives for Meteorology Geophysics and Bioclimatology Series B - Theoretical and Applied Climatology* **35**(1-2): 55-66.
- Chandler, T. J. (1962). London's urban climate. *Geographical journal* **128**: 279-302.
- Chandler, T. J. (1964). City growth and urban climates. *Weather* **19**(6): 170-171.



- Chandler, T. J. (1965). *The Climate of London*, Hutchinson & Co (Publishers) Ltd.
- Chandler, T. J. (1968). *Urban climatology - inventory and prospect*. Symposium on urban climates and building climatology, Brussels, World Meteorological Organization.
- Chandler, T. J. and S. Gregory, Eds. (1976). The Climate of the British Isles, Longman Group.
- Chow, T. T., Z. Lin and Q. W. Wang (2000). Effect of building re-entrant shape on performance of air-cooled condensing units. *Energy and Buildings* **32**: 143-152.
- CIBSE (1999). *Environmental design, Guide A*, CIBSE.
- CIBSE (2002). *Weather, Solar and Illuminance Data, Guide J*, CIBSE.
- Coronel, J. F., S. Álvarez, A. Quijano, F. J. Sánchez and C. Prieto (1997). Extended case study - Santa Cruz District, Final report (Draft), University of Seville.
- Deacon, A. R. (1990). The Changing Intensity and Spatial Extent of London's Urban Heat Island. Environmental Studies. London, Southlands College: 26.
- DEFRA (1999). "Conversion factors and procedures" for the Climate Change Levy. **2002**.
- EDSL (2000). *A-Tas Theory Manual*, Environmental Design Solutions Limited.
- EDSL (2001). *Tas Lite version 8.19*, Environmental Design Solutions Limited.
- Eliasson, I. (1994). Urban-suburban-rural air-temperature differences related to street geometry. *Physical Geography* **15**(1): 1-22.
- Eliasson, I. (1996). Urban nocturnal temperatures, street geometry and land use. *Atmospheric Environment* **30**(3): 379-392.
- Eliasson, I. and H. Upmanis (2000). Nocturnal airflow from urban-parks - implications for city ventilation. *Theoretical Applied Climatology* **66**: 95-107.
- Florides, G. (2001). Investigations into the effectiveness of measures to reduce the energy requirements of domestic dwellings in Cyprus. Department of Mechanical Engineering. London, Brunel University: 280.
- Givoni, B., Ed. (1971). Architectural and Urban Planning in Relation to Weather and Climate. Progress in Biometeorology A.
- Givoni, B. (1998). *Climate considerations in building and urban design*, Van Nostrand Reinhold.
- Golany, G. S. (1996). Urban design morphology and thermal performance. *Atmospheric Environment* **30**(3): 455-465.

- Haeger-Eugensson, M. and B. Holmer (1999). Advection caused by the urban heat island circulation as a regulating factor on the nocturnal urban heat island. *International Journal of Climatology* **19**: 975-988.
- Hannel, F. G. (1976). Some features of the heat island in an equatorial city. *Geografiska Annaler* **58(A)**: 95-110.
- Harrison, R., B. McGoldrick and C. G. B. Williams (1984). Artificial heat release from Greater London 1971-1976. *Atmospheric environment* **18(11)**: 2291-1304.
- Haselden, R. F. and M. P. Huggins (1997). *Energy consumption in the United Kingdom*, Government Statistical Services.
- Herring, H., R. Hardcastle and R. Phillipson (1988). *Energy use and energy efficiency in UK commercial and public buildings up to the year 2000*, HMSO.
- Hildebrandt, E. W. and M. Sarkovich (1998). Assessing the cost-effectiveness of SMUD's shade tree program. *Atmospheric Environment* **32(1)**: 85-94.
- Honjo, T. and T. Takakura (1990/91). Simulation of thermal effects of urban green areas on their surrounding areas. *Energy and Buildings* **15-16**: 443-446.
- Hoyano, A., A. Iino, M. Ono and S. Tanighchi (1999). Analysis of the influence of urban form and materials on sensible heat flux - a case study of Japan's largest housing development "Tama New Town". *Atmospheric Environment* **33**: 3931-3939.
- Ichinose, T., K. Shimodozono and K. Hanaki (1999). Impact of anthropogenic heat on urban climate in Tokyo. *Atmospheric Environment* **33**: 3897-3909.
- Jauregui, E. (1991). Influence of a Large Urban Park on Temperature and Convective Precipitation in a Tropical City. *Energy and Buildings* **15(3-4)**: 457-463.
- Jauregui, E. (1997). Heat island development in Mexico City. *Atmospheric Environment* **31(22)**: 3821-3831.
- Jones, W. P. (1967). *Air conditioning engineering*, Edward Arnold.
- Kawashima, A. (1990/91). Effect of vegetation on surface temperature in urban and suburban areas in winter. *Energy and Buildings* **15-16**: 465-469.
- Kawashima, S., T. Ishida, M. Minomura and T. Miwa (2000). Relations between surface temperature and air temperature on a local scale during winter nights. *Journal of Applied Meteorology* **39**: 1570-1579.
- Lam, J. C. (2000). Shading effects due to nearby buildings and energy implications. *Energy Conversion & Management* **41**: 647-659.
- Landsberg, H. (1981). *The Urban Climate*, Academic Press.

- Lee, D. O. (1991). Urban rural humidity differences in London. *International Journal of Climatology* **11**(5): 577-582.
- Lee, D. O. (1992). Urban warming? - An analysis of recent trends in London's heat island. *Weather* **47**(2): 50-56.
- Levermore, G. and E. Keeble (1997). New weather data for the Guide. *Building Services Journal*(December): 39-40.
- Littlefair, P. J., M. Santamouris, S. Alvarez, A. Depagne, D. Hall, J. Teller, J. F. Coronel and N. Papanikolaou (2000). *Environmental site layout planning: solar access, microclimate and passive cooling in urban areas*. London, Construction Research Communications Ltd.
- Lomas, K. J., H. Eppel, C. Martin and D. Bloomfield (1994). Empirical validation of thermal building simulation programs using test room data. Volume 1: Final Report. London, Building Research Establishment: 150.
- Ludwig, F. L. (1968). *Urban temperature fields*. Symposium on urban climates and building climatology, Brussels, World Meteorological Organization.
- Lyall, I. T. (1977). The London heat-island in June-July 1976. *Weather* **32**(8): 296-302.
- Meier, A. K. (1991). Strategic Landscaping and Air-Conditioning Savings - A Literature-Review. *Energy and Buildings* **15**(3-4): 479-486.
- Met.Office (1981). *Measurement of temperature*. London, HMSO.
- Milbank, N. (1989). Building design and use - response to climate change. *Architect's Journal* **196**(2 August): 59-63.
- Mills, G. (1997). The radiative effects of building groups on single structures. *Energy and Buildings* **25**: 51-61.
- Mitalas, G. P. and D. G. Stephenson (1967). Room thermal response factors. *ASHRAE Transactions* **73**: 2.1-2.10.
- Moreno-Garcia, M. C. (1994). Intensity and form of the urban heat-island in Barcelona. *International journal of climatology* **14**(6): 705-710.
- Nichol, J. E. (1996). High-resolution surface temperature patterns related to urban morphology in a tropical city: A satellite-based study. *Journal of Applied Meteorology* **35**(1): 135-146.
- Oke, T. R. (1973). City size and the urban heat island. *Atmospheric Environment* **7**: 769-779.

- Oke, T. R. (1982). The energetic basis of the urban heat-island. *Quarterly Journal of the Royal Meteorological Society* **108**(455): 1-24.
- Oke, T. R. (1987). *Boundary Layer Climates*, Routledge.
- Oke, T. R. (1988). The urban energy balance. *Progress in physical geography* **12**(4): 471-508.
- Papadopoulos (2001). The influence of street canyons on the cooling loads of buildings and the performance of air conditioning systems. *Energy and Buildings* **33**: 601-607.
- Parker, D. and S. J. Barkaszi (1997). Roof solar reflectance and cooling energy use: field research results from Florida. *Energy and Buildings* **25**: 105-115.
- Parry, M. L., J. F. Skea, P. Bullock and M. G. R. Cannell (1991). *The potential effects of climate change in the United Kingdom*, HMSO.
- Pout, C. H., S. A. Moss, P. J. Davidson, J. P. Steadman, H. Bruhns, N. Mortimer and J. Rix (1998). *Non-domestic building energy fact file*, Construction Research Communications Ltd.
- Raeissi, S. and M. Taheri (1999). Energy saving by proper tree plantation. *Building and Environment* **34**: 565-570.
- Rosenfeld, A. H., H. Akbari, S. Bretz, B. L. Fishman, D. M. Kurn, D. Sailor and H. Taha (1995). Mitigation of urban heat islands - materials, utility programs, updates. *Energy and buildings* **22**(3): 255-265.
- Rosenfeld, A. H., H. Akbari, J. J. Romm and M. Pomerantz (1998). Cool communities: strategies for heat island mitigation and smog reduction. *Energy and Buildings* **28**(1): 51-62.
- Runnalls, K. E. and T. R. Oke (2000). Dynamics and controls of the near-surface heat island of Vancouver, British Columbia. *Physical Geography* **21**: 283-304.
- Saito, I., O. Ishihara and T. Katayama (1990/91). Study of the effect of green areas on the thermal environment in an urban area. *Energy and Buildings* **15-16**: 493-498.
- Sakakibara, Y. (1996). A numerical study of the effect of urban geometry upon the surface energy budget. *Atmospheric Environment* **30**(3): 487-496.
- Sánchez, F. J. and S. Álvarez (1996). Impact of vegetation and mass of water on urban climate II. Seville, University of Seville: 9.
- Sánchez, F. J., S. Álvarez and J. Zambonino (1998). Impact of vegetation and mass of water on urban climate III: Volumetric cooling. Seville, University of Seville: 9.

- Santamouris, M. (1990). *Natural cooling techniques*. Proceedings of Conference on Passive Cooling,, Ispra, EEC, DGXII.
- Santamouris, M. and P. Littlefair (1997). Urban layout guidelines for the wind pattern over built-up regions, channelling of air flow over and around buildings, solar exposure of buildings, and building form, University of Athens & BRE.
- Santamouris, M., N. Papanikolaou and I. Koronaki (1998). Urban canyon experiments in Athens Part A: Temperature distribution. Athens, University of Athens: 49.
- Santamouris, M., N. Papanikolaou, I. Koronaki, I. Tselepidaki, D. N. Assimakopoulos and T. Makrogiannis (1998). The Athens urban climate experiment - temperature distribution. Athens, University of Athens & Aristotle University of Thessaloniki: 10.
- Saporito, A., A. Day, T. Karayiannis, F. Parand and K. Davies (1997). A sensitivity analysis on the effect of comfort dead-bands on energy use in office buildings. London, South Bank University and BRE.
- Shashua-Bar, L. and M. E. Hoffman (2000). Vegetation as a climatic component in the design of an urban street. An empirical model for predicting the cooling effect of urban green areas with trees. *Energy and Buildings* **31**: 221-235.
- Simpson, J. R. and E. G. McPherson (1997). The effects of roof albedo modification on cooling loads of scale model residences in Tucson, Arizona. *Energy and Buildings* **25**: 127-137.
- Stanhill, G. and J. D. Kalma (1995). Solar dimming and urban heating at Hong Kong. *International Journal of Climatology* **15**: 933-941.
- Strachan, P. A. and J. A. Clarke (1994). *Experiences with validating simulation programs*. BEPAC conference BEP'94, York, BEPAC.
- Taesler, R. (1991). The Bioclimate in Temperate and Northern Cities. *International Journal of Biometeorology* **35**(3): 161-168.
- Taha, H. (1997). Urban climates and heat islands: albedo, evapotranspiration, and anthropogenic heat. *Energy and Buildings* **25**: 99-103.
- Taha, H., H. Akbari, A. Rosenfeld and J. Huang (1988). Residential cooling loads and the urban heat-island - the effects of albedo. *Building and Environment* **23**(4): 271-283.

- Taha, H., H. Akbari and A. Rosenfield (1991). Heat-Island and oasis effects of vegetative canopies - micro-meteorological field-measurements. *Theoretical and Applied Climatology* **44**(2): 123-138.
- Taha, H., S. Douglas and J. Haney (1997). Mesoscale meteorological and air quality impacts of increased urban albedo and vegetation. *Energy and Buildings* **25**: 169-177.
- Tévar, R. G., J. Guerra and F. Sánchez de la Flor (1996). Impact of vegetation and mass of water on urban climate. Seville, University of Seville: 9.
- Torok, S., C. Morris, C. Skinner and N. Plummer (2001). Urban heat island features of southeast Australian towns. *Australian Meteorological Magazine* **50**: 1-13.
- Tsinonis, A., Koutsogiannakis, M. Santamouris and I. Tselepidaki (1993). Statistical analysis of summer comfort conditions in Athens, Greece. *Energy and Buildings* **19**: 285-290.
- UEA (2002). Introduction to Energy (Course Handout), Department of Environmental Sciences, University of East Anglia.
- Unwin, D. J. (1980). The synoptic climatology of Birmingham's urban heat island. *Weather* **35**(2): 43-50.
- Upmanis, H. and D. Chen (1999). Influence of geographical factors and meteorological variables on nocturnal urban-park temperature differences - a case study of summer 1995 in Göteborg, Sweden. *Climate Research* **13**: 125-139.
- Vu, T. C., T. Asaeda and E. Abu (1998). Reductions in air conditioning energy caused by a nearby park. *Energy and buildings* **29**: 83-92.
- Wheeler, D. and J. Mayes, Eds. (1997). Regional climates of the British Isles, Routledge.
- Willis, S., M. Fordham and B. Bordass (1995). *Avoiding or minimizing the use of air-conditioning - a research report from the EnREI programme. General Information Report 31*, BRECSU.
- Wilmers, F. (1990/91). Effects of vegetation on urban climate and buildings. *Energy and Buildings* **15-16**: 507-514.
- Yannas, S. (1998). *Living with the city: urban design and environmental sustainability*. PLEA '98, Lisbon, James & James Science Publishers Ltd.

## **BIBLIOGRAPHY**

## BIBLIOGRAPHY

- Akbari, H. and H. Taha (1992). The Impact of Trees and White Surfaces on Residential Heating and Cooling Energy Use in 4 Canadian Cities. *Energy* **17**(2): 141-149.
- Al-Rabghi, O. M., M. H. Al-Beirutty and K. A. Fathalah (1999). Estimation and measurement of electric energy consumption due to air conditioning cooling load. *Energy Conversion & Management* **40**: 1527-1542.
- Al-Turki, A. M., H. N. Gari and G. M. Zaki (1997). Comparative study on reduction of cooling loads by roof gravel cover. *Energy and Buildings* **25**: 1-5.
- Ashie, Y., V. T. Ca and T. Asaeda (1999). Building canopy model for the analysis of urban climate. *Journal of Wind Engineering and Industrial Aerodynamics* **81**: 237-248.
- Bacci, P. and M. Maugeri (1992). The Urban Heat-Island of Milan. *Nuovo Cimento Della Societa Italiana Di Fisica C-Geophysics And Space Physics* **15**(4): 417-424.
- Balling, R. C. and R. S. Cerveny (1987). Long-term associations between wind speeds and the urban heat - island of Phoenix, Arizona. *Journal of Climate and Applied Meteorology* **26**(6): 712-716.
- Balling, R. C. and R. S. Cerveny (1988). Comment on long-term associations between wind speeds and the urban heat-island of Phoenix, Arizona - reply. *Journal of Applied Meteorology* **27**(7): 881.
- Barradas, V. L. (1991). Air-Temperature and Humidity and Human Comfort Index of some City Parks of Mexico-City. *International Journal of Biometeorology* **35**(1): 24-28.
- Benn, D. (1998). Human impact on the atmosphere. Lecture 8: Human impact on climate: heat islands and global warming, Aberdeen University, Geography Department. 1998.
- Bennett, M. and M. Newborough (2001). Auditing energy use in cities. *Energy Policy* **29**: 125-134.
- Berdahl, P. and S. Bretz (1997). Preliminary survey of the solar reflectance of cool roof materials. *Energy and Buildings* **25**: 149-158.
- Borghesi, S., G. Corbetta and L. De Biase (2000). A heat island model for large urban areas and its application to Milan. *Nuovo Cimento* **23**(5): 547-566.



- Bretz, S. and H. Akbari (1997). Long-term performance of high-albedo roof coatings. *Energy and Buildings* **25**: 159-167.
- Bretz, S., H. Akbari and A. Rosenfeld (1988). Practical issues for using solar-reflective materials to mitigate urban heat islands. *Atmospheric Environment* **32**(1): 95-101.
- Camilloni, I. and V. Barros (1997). On the urban heat island effect dependence on temperature trends. *Climatic Change* **37**(4): 665-681.
- Caselles, V., M. J. L. Garcia, J. Melia and A. J. P. Cueva (1991). Analysis of the Heat-Island Effect of the City of Valencia, Spain, through Air-Temperature Transects and NOAA Satellite Data. *Theoretical and Applied Climatology* **43**(4): 195-203.
- Cermak, J. E. (1996). Thermal effects on flow and dispersion over urban areas: Capabilities for prediction by physical modeling. *Atmospheric Environment* **30**(3): 393-401.
- Cherry, N. J. (1988). Comment on long-term associations between wind speeds and the urban heat-island of Phoenix, Arizona. *Journal of Applied Meteorology* **27**(7): 878-880.
- Chow, S. D. (1992). The Urban Climate of Shanghai. *Atmospheric Environment Part B-Urban Atmosphere* **26**(1): 9-15.
- Chow, S. D., J. C. Zheng and L. Wu (1994). Solar-Radiation and Surface-Temperature in Shanghai City and their Relation to Urban Heat-Island Intensity. *Atmospheric Environment* **28**(12): 2119-2127.
- Christy, J. R. and J. D. Goodridge (1995). Precision Global Temperatures from Satellites and Urban Warming Effects Of Non-Satellite Data. *Atmospheric Environment* **29**(16): 1957-1961.
- Cionco, R. M. and R. Ellefsen (1998). High resolution urban morphology data for urban wind flow modeling. *Atmospheric Environment* **32**(1): 7-17.
- Coronel, J. F., S. Álvarez and R. Velázquez (1996). Energy and Climatic impact due to urbanization, University of Seville.
- Deaves, D. M. and I. G. Lines (1998). *On the persistence of low wind speed conditions*. 4th UK Conference on wind engineering, Wind Engineering Society.
- Eliasson, I. (1990/91). Urban geometry, surface temperature and air temperature. *Energy and Buildings* **15-16**: 141-145.

- Eliasson, I. and B. Holmer (1990). Urban heat-island circulation in Goteborg, Sweden. *Theoretical and Applied Climatology* **42**(3): 187-196.
- Elnahas, M. M. and J. Williamson (1997). An improvement of the CTTC model for predicting urban air temperatures. *Energy and Buildings* **25**: 41-49.
- Finch, C. R. (1980). Summer and winter temperatures in London 1763-1980 and in Central England 1659-1980. *Weather* **6**(54): 309-313.
- Glass, J. (1998). Keeping the lid on urban overheating. *Concrete quarterly* **1998**(Winter): 2-3.
- Goldreich, Y. (1985). The structure of the ground-level heat-island in a central business district. *Journal of Climate and Applied Meteorology* **24**(11): 1237-1244.
- Gomez, F., E. Gaja and A. Reig (1998). Vegetation and climatic changes in a city. *Ecological Engineering* **10**(4): 355-360.
- Graves, H. and M. Phillipson (2000). *Potential implications of climate change in the built environment*. London, Construction Research Communications Ltd.
- Graves, H., R. Watkins, P. Westbury and P. Littlefair (2001). Cooling buildings in London - overcoming the heat island, Construction Research Communications Ltd.: 32.
- Green, N. E., D. W. Etheridge and S. B. Riffat (2001). Location of air intakes to avoid contamination of indoor air: a wind tunnel investigation. *Building and Environment* **36**: 1-14.
- Hadley, D. L. (1993). Daily variations in HVAC system electrical energy consumption in response to different weather conditions. *Energy and Buildings* **19**: 235-247.
- Hall, D. C. (1998). Albedo and vegetation demand-side management options for warm climates. *Ecological Economics* **24**(1): 31-45.
- Hassid, S., M. Santamouris, N. Papanikolaou, A. Linardi and N. Klitsikas (2000). The effect of the Athens heat island on air conditioning load. *Energy and Buildings* **32**(131-141).
- Heilman, J. L. and R. W. Gesch (1991). Effects of Turfgrass Evaporation on External Temperatures of Buildings. *Theoretical and Applied Climatology* **43**(4): 185-194.
- Jauregui, E. (1990/91). Effects of revegetation and new artificial water bodies on the climate of Northeast Mexico City. *Energy and Buildings* **15-16**: 447-455.
- Jauregui, E., J. Cervantes and A. Tejeda (1997). Bioclimatic conditions in Mexico City - An assessment. *International Journal of Biometeorology* **40**(3): 166-177.

- Jauregui, E., L. Godinez and F. Cruz (1992). Aspects of Heat-Island Development in Guadalajara, Mexico. *Atmospheric Environment Part B-Urban Atmosphere* **26**(3): 391-396.
- Jauregui, E. and E. Luyando (1998). Long-term association between pan evaporation and the urban heat island in Mexico City. *ATMOSFERA* **11**(1): 45-60.
- Johnson, G. T., T. R. Oke, T. J. Lyons, D. G. Steyn, I. D. Watson and J. A. Voogt (1991). Simulation of Surface Urban Heat Islands under Ideal Conditions at Night .1. Theory and Tests Against Field Data. *Boundary-Layer Meteorology* **56**(3): 275-294.
- Katsoulis, B. D. and G. A. Theoharatos (1985). Indications of the urban heat-island in Athens, Greece. *Journal of Climate and Applied Meteorology* **24**(12): 1296-1302.
- Kimura, F. and S. Takahashi (1991). The Effects of Land-Use and Anthropogenic Heating on the Surface-Temperature in the Tokyo Metropolitan-Area - A Numerical Experiment. *Atmospheric Environment Part B-Urban Atmosphere* **25**(2): 155-164.
- Koronaki, I., M. Santamouris and N. Papanikolaou (1998). Thermal modelling of an urban canyon, University of Athens.
- Lee, D. O. (1975). Rural atmospheric stability and the intensity of London's heat island. *Weather* **30**(4): 102-109.
- Lee, D. O. (1977). Urban influence on wind directions over London. *Weather* **32**(5): 162-170.
- Lee, D. O. (1979). Contrasts in warming and cooling rates at an urban and a rural site. *Weather* **34**(2): 60-66.
- Lee, D. O. (1984). Urban climates. *Progress in geography* **8**(1): 1-31.
- Lyons, T. J. (1983). Canyon geometry and the nocturnal urban heat-island - comparisons of scale model and field observations - comments. *Journal of Climatology* **3**(1): 95-97.
- Macdonald, R. W., D. J. Hall and R. F. Griffiths (1998). *Measurements of velocity profiles within scale model urban arrays*. 4th UK Conference on Wind Engineering (WES 98), Bristol, England.
- Melhuish, E. and M. Pedder (1998). Observing an urban heat island by bicycle. *Weather* **53**(4): 121-128.

- Moffitt, B. J. (1972). The effect of urbanization on mean temperatures at Kew Observatory. *Weather* **1972**(March): 121-125.
- Myrup, L. O., C. E. McGinn and R. G. Flocchini (1993). An Analysis of Microclimatic Variation in a Suburban Environment. *Atmospheric Environment Part B-Urban Atmosphere* **27**(2): 129-156.
- Ojima, T. (1991). Changing Tokyo Metropolitan-Area and its Heat-Island Model. *Energy and Buildings* **15**(1-2): 191-203.
- Oke, T. R. (1981). Canyon geometry and the nocturnal urban heat-island - comparison of scale model and field observations. *Journal of Climatology* **1**(3): 237 et seq.
- Oke, T. R. (1983). Canyon geometry and the nocturnal urban heat-island - comparisons of scale model and field observations - reply. *Journal of Climatology* **3**(1): 97.
- Oke, T. R., G. T. Johnson, D. G. Steyn and I. D. Watson (1991). Simulation of Surface Urban Heat Islands under Ideal Conditions at Night .2. Diagnosis of Causation. *Boundary-Layer Meteorology* **56**(4): 339-358.
- Oke, T. R., G. Zeuner and E. Jauregui (1992). The Surface-Energy Balance in Mexico-City. *Atmospheric Environment Part B-Urban Atmosphere* **26**(4): 433-444.
- Palmer, J., P. Littlefair, R. Watkins and M. Kolokotroni (2000). Urban heat islands. *Building Services Journal*(May): 55-56.
- Pearlmutter, D., A. Bitan and P. Berliner (1999). Microclimatic analysis of "compact" urban canyons in an arid zone. *Atmospheric Environment* **33**: 4143-4150.
- Poreh, M. (1996). Investigation of heat islands using small scale models. *Atmospheric Environment* **30**(3): 467-474.
- Potchter, O. (1990/91). Climatic aspects in the building of ancient urban settlements in Israel. *Energy and Buildings* **15-16**: 93-104.
- Saitoh, T. S. and N. Yamada (2001). Evaluation of effective temperature scale under urban heat island formation. *JSME International Journal Series B* **44**(1): 111-118.
- Sánchez, F. J. and S. Álvarez (1996). Impact of vegetation and mass of water on urban climate II. Seville, University of Seville: 9.
- Sánchez, F. J., S. Álvarez and J. Zambonino (1998). Impact of vegetation and mass of water on urban climate III: Volumetric cooling. Seville, University of Seville: 9.

- Santamouris, M. (1990). *Natural cooling techniques*. Proceedings of Conference on Passive Cooling,, Ispra, EEC, DGXII.
- Santamouris, M. (1998). *The Athens Urban Climate Experiment*. PLEA '98, Lisbon, James & James Science Publishers Ltd.
- Santamouris, M. and A. Argiriou (1996). Air flow in urban canyons: Theoretical developments and measurements - A literature review. Athens, University of Athens & National Observatory of Athens: 11.
- Santamouris, M., N. Papanikolaou, I. Koronakis, I. Livada and D. Asimakopoulos (1999). Thermal and air flow characteristics in a deep pedestrian canyon under hot weather conditions. *Atmospheric Environment* **33**(27).
- Sarkar, A., R. S. Saraswat and A. Chandrasekar (1998). Numerical study of the effects of urban heat island on the characteristic features of the sea breeze circulation. *Proceedings of the Indian Academy of Science - Earth and Planetary Sciences* **107**(2): 127-137.
- Schmidlin, T. W. (1989). The urban heat-island at Toledo, Ohio. *Ohio Journal of Science* **89**(3): 38-41.
- Segal, M., R. Turner and D. Todey (2000). Using radiosonde meteorological data to better assess air conditioning loads in tall buildings. *Energy and Buildings* **31**: 243-250.
- Shafir, H. and P. Alpert (1990). On the urban orographic rainfall anomaly in Jerusalem - a numerical study. *Atmospheric Environment Part B-Urban Atmosphere* **24**(3): 365-375.
- Shahgedanova, M., T. P. Burt and T. D. Davies (1997). Some aspects of the three-dimensional heat island in Moscow. *International Journal of Climatology* **17**(13): 1451-1465.
- Shih, N.-J. and Y.-S. Huang (2001). An analysis and simulation of curtain wall reflection glare. *Building and Environment* **36**: 619-626.
- Shudo, H., J. Sugiyama, N. Yokoo and T. Oka (1997). A study on temperature distribution influenced by various land uses. *Energy and Buildings* **26**: 199-205.
- Stemmers, K., N. Baker, D. Crowther, J. Dubiel and M. Nikolopoulou (1998). Radiation absorption and urban texture. *Building Research and Information* **26**(2): 103-112.
- Stoll, M. J. and A. J. Brazel (1992). Surface-air temperature relationships in the urban environment of Phoenix, Arizona. *Physical Geography* **13**(2): 160-179.

- Swaid\_H (1991). Nocturnal Variation of Air Surface-Temperature Gradients for Typical Urban and Rural Surfaces. *Atmospheric Environment Part B-Urban Atmosphere* **25**(3): 333-341.
- Swaid\_H (1993). Numerical Investigation into the Influence of Geometry and Construction Materials on Urban Street Climate. *Physical Geography* **14**(4): 342-358.
- Takakura, T., S. Kitade and E. Goto (2000). Cooling effect of greenery cover over a building. *Energy and Buildings* **31**: 1-6.
- Terjung, W. H. and a. Collaborators (1970). The Energy balance climatology of a city-man system. *Energy Balance Climatology*(September): 466-492.
- Theurer, W. (1999). Typical building arrangements for urban air pollution modelling. *Atmospheric Environment* **33**: 4057-4066.
- Unger, J. (1996). Heat island intensity with different meteorological conditions in a medium-sized town: Szeged, Hungary. *Theoretical and Applied Climatology* **54**(3-4): 147-151.
- Watson, R. T., M. C. Zinyowera and R. H. Moss (1995). *Climate change, 1995. [Vol.2], Impacts, adaptations and mitigation of climate change: scientific-technical analyses*, Cambridge University Press.
- Webster, F. B. (1984). The climatological station at London's Heathrow airport. *Weather* **39**(10): 311-315.
- Winkler, J. A., R. H. Skaggs and D. G. Baker (1981). Effect of temperature adjustments on the Minneapolis-St-Paul urban heat-island. *Journal of Applied Meteorology* **20**(11): 1295-1300.
- Yague, C., E. Zurita and A. Martinez (1991). Statistical-Analysis of the Madrid Urban Heat-Island. *Atmospheric Environment Part B-Urban Atmosphere* **25**(3): 327-332.
- Yamashita, S. (1996). Detailed structure of heat island phenomena from moving observations from electric tram-cars in Metropolitan Tokyo. *Atmospheric Environment* **30**(3): 429-435.
- Yamashita, S. and K. Sekine (1991). Some Studies on the Earths Surface Conditions Relating to the Urban Heat-Island. *Energy and Buildings* **15**(1-2): 279-288.
- Yik, F. W. H., J. Burnett and I. Prescott (2001). Predicting air-conditioning energy consumption of a group of buildings using different heat rejection methods. *Energy and Buildings* **33**: 151-166.

Yoshikado, H. (1994). Interaction of the Sea-Breeze with Urban Heat Islands of Different Sizes and Locations. *Journal of the Meteorological Society of Japan* **72**(1): 139-143.

Yoshino, M. (1990/91). Development of urban climatology and problems today. *Energy and Buildings* **15-16**: 1-10.

## **APPENDIX 1**

### **Calibration of loggers**



# APPENDIX 1 – Calibration of loggers

## 1.1 Calibration

Abbreviation: TT = *Tinytalk*

1. 119 TTs were put in a filing cabinet, which was sealed with tape, and then left for 3 days. (From 13:00 on Tuesday 13.4.99 until 11:00 on Friday 16.4.99)
2. No absolute (correct) temperature comparison was made.
3. Apart from the first two hours, all the data were used in one block.
4. The mean values over the period for all 119 were calculated. The maximum deviation of these from the grand mean was  $-0.375^{\circ}\text{C}$  and  $+0.304^{\circ}\text{C}$ . This is rather higher than the quoted accuracy of  $\pm 0.2^{\circ}\text{C}$ . It was hoped that the effects of the limited resolution of the TTs ( $0.25^{\circ}\text{C}$ ) would have been eliminated by conducting the test over a range of temperatures ( $18\text{-}22^{\circ}\text{C}$ ).
5. To see if the test conditions presented a uniform thermal environment to the TTs, two checks were made. (The TTs had been laid out with one batch at the front, and two at the back, one above the other. The rear upper layer were upside down so that the sensors were facing each other – all 119 sensors within 2cm height of each other.)
  - a. The front layer (A), the rear lower layer (B) and the rear upper layer (C) were analysed separately to see if there were any significant differences.
  - b. The TTs along the edges in all layers were compared with those in the core areas in all layers.

The results showed that the differences were very small.

a.		Group A	Group B	Group C
	<b>Mean</b>	19.74	19.75	19.67
	<b>Max</b>	21.80	21.80	21.80
	<b>Min</b>	18.00	18.00	17.70
	<b>S.Dev</b>	0.91	0.90	0.89

Comments:

-means are very close (within 0.08°C)

-maxima are identical

-minima are within 0.3°C

-spread is almost identical

b.		Edge	Core
	<b>Mean</b>	19.71	19.73
	<b>Max</b>	21.80	21.80
	<b>Min</b>	18.00	18.00
	<b>S.Dev</b>	0.90	0.90

Comments:

-means are very close (within 0.02°C)

-maxima are identical

-minima identical

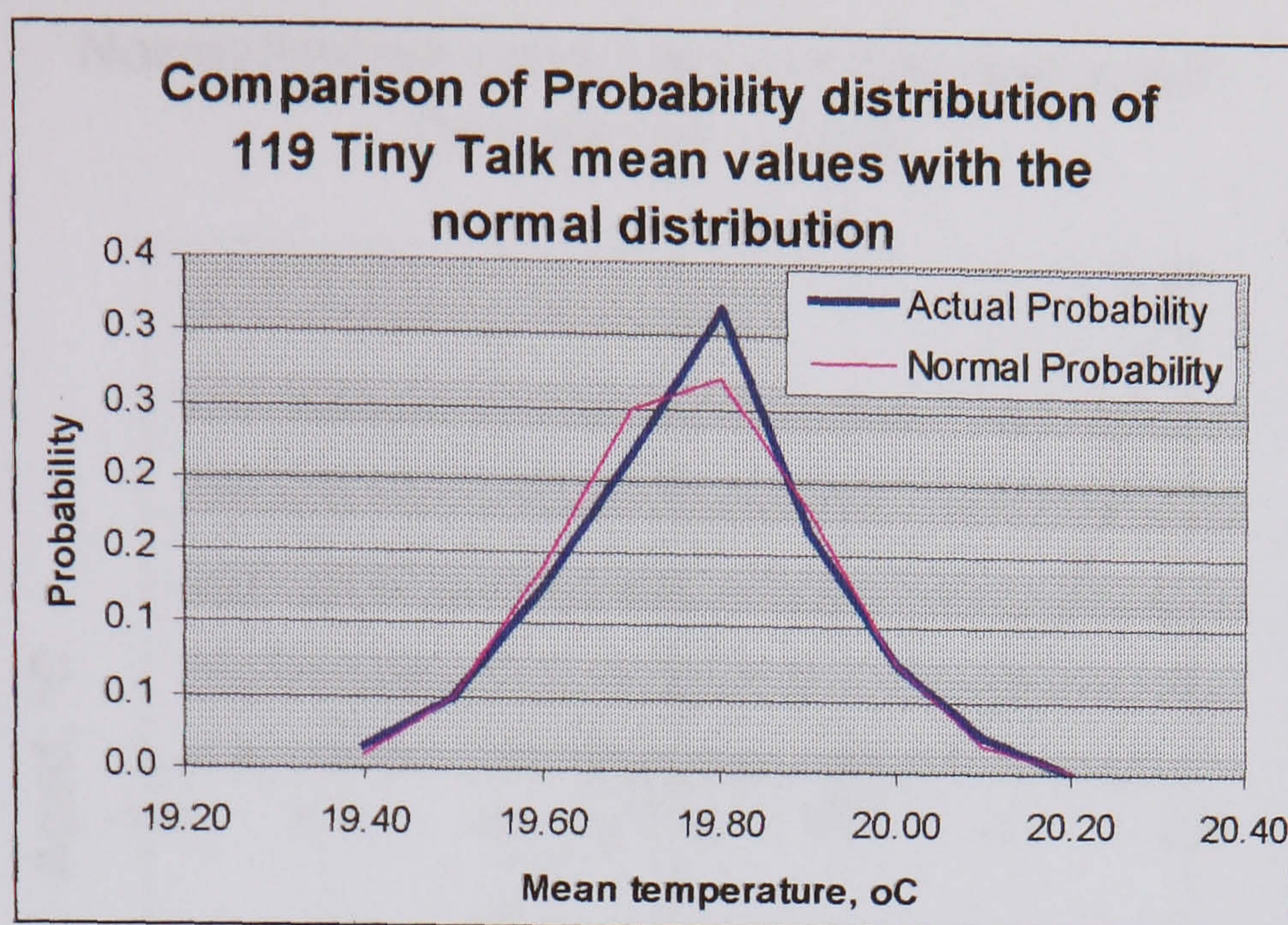
-spread is identical

6. The distribution of the 119 mean temperatures was analysed to see if it was normal. The means were slotted into 0.1°C bands between 19.3 and 20.2°C. The Kolmogorov-Smirnov statistic gave:

0.0360

which compared with the critical value at the 1% level: 0.1494

and thus the distribution of measurement errors was considered normal.



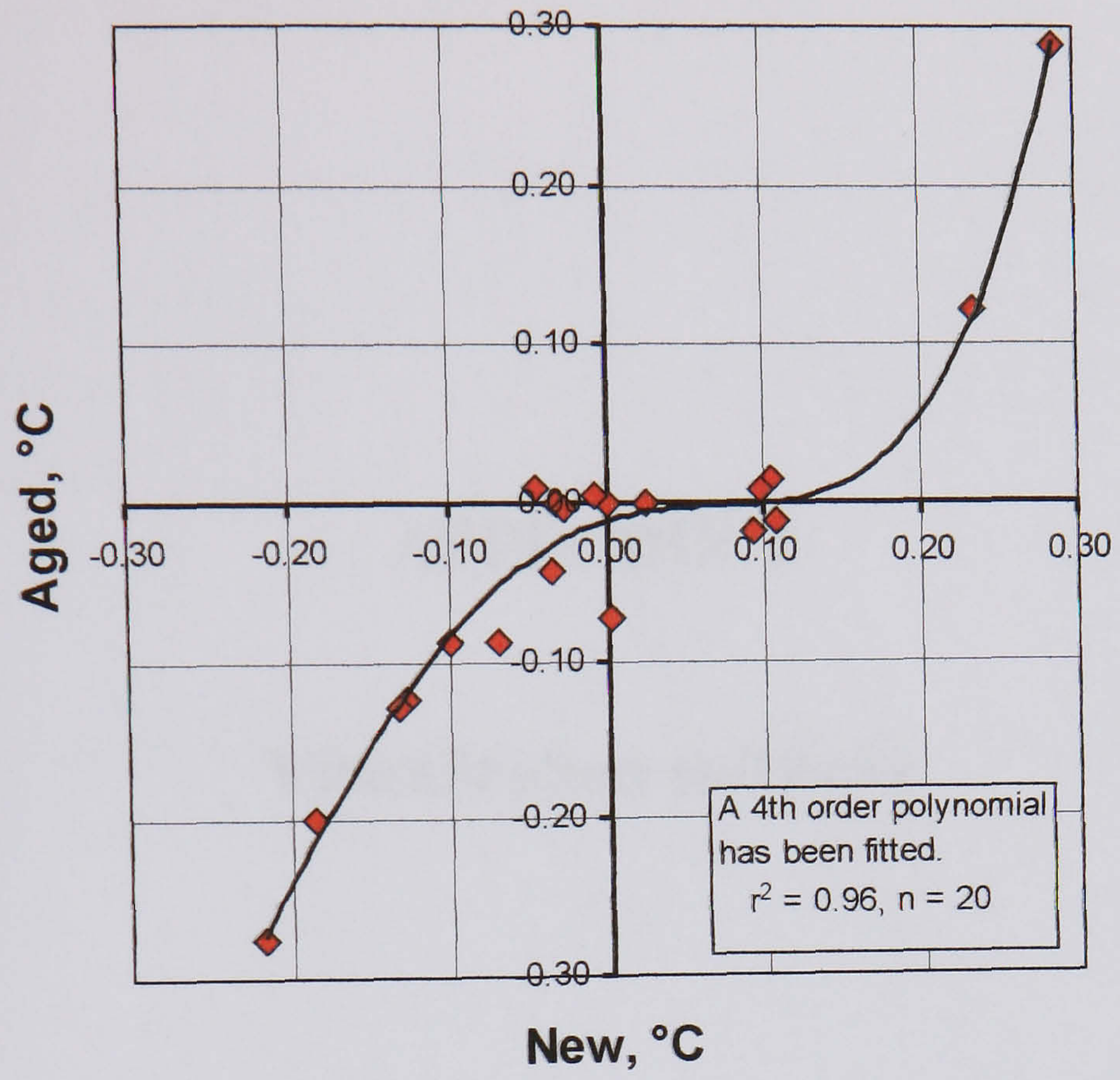
7. The mean value of the 119 TTs was taken as indicating the true temperature, and adjustment constants established for all the loggers to normalize them to this standard. A logger that required essentially zero normalization has been preserved (a “master” logger) and used to calibrate further Tinytalks, so that all Tinytalks are referenced to the same standard one.

## 1.2 Post-monitoring calibration checks

To check for sensor and logger drift, a sample of Tinytalks (approximately 15%) was re-calibrated towards the end of the work. 20 loggers including the master were tested for five days in a sealed box in a sealed drawer. New normalization constants were computed (with respect to the master logger) and compared with the ones determined two years before. The figure overleaf shows that the accuracy of the sample of 19 loggers with respect to the master logger has been maintained.

The normalization constants have changed very little. The maximum error introduced because of drifting is  $0.12^{\circ}\text{C}$ , with a standard deviation of  $0.05^{\circ}\text{C}$ .

### Normalization constants for new and aged Tynytalks (2 years)



## **APPENDIX 2**

### **Visualization software**

## **APPENDIX 2 – Visualization software**

Over the summer of 1999, the monitoring array was expanded from 18 pilot stations to 63 around London, with more planned. It became clear that it would be advantageous to be able to view the large amount of hourly spatial data being collected en masse, so that a picture could more easily be formed of how temperature changed in time and in space. To this end, software was written to produce an investigative tool that proved very useful.

### **Structure**

In essence, two programmes are controlled simultaneously under Visual Basic, each programme accessing separate data files. All information is then brought into one programme and displayed on the screen. Microsoft's **Excel** is used to gain access to a database of hourly weather information (wind speed, wind direction, solar radiation) and Golden Software's **Surfer** is used to generate contour maps of temperature.

### **Software and data preparation**

For Surfer to generate contour plots, a co-ordinate system was ascribed to the London measurement area. The origin is the British Museum and the x,y co-ordinates are measured from this to each station (negative for stations to the west or south). Surfer works in two stages to produce a contour map. The data associated with specific x,y co-ordinates are first interpolated to generate a new dataset on a fixed grid across London. The grid data is then used to generate isopleths.

Early work on the software showed that

- the time taken for a grid file to be interpolated and then a map generated was at least five seconds which was unacceptably long. It is visually difficult to retain a picture with such time gaps.
- isopleths could change quite dramatically from hour to hour making it difficult to follow their development.

To address these issues, it was decided to use Excel to interpolate 10 minute data from the hourly measured data, giving smoother changes, and pre-prepare all the Surfer grid files (some 4000 for one month) to speed up viewing.

Visual Basic routines were written to control Surfer (through its ActiveX facilities) and generate the interpolated grid files. Grids of temperature and temperature difference (local heat island intensity) were produced. It takes about three hours to generate and save 4000 grid files (200 Mbytes), from one month of hourly Excel data.

To allow easy visualization of the key weather parameters (wind and sun) and their development, data were mapped to bar charts (wind speed and solar radiation) and wind direction arrows were automatically rotated. It was arranged that the current hour and the preceding five hours' values were displayed side by side. A cross hair is overlaid over the contour map centred on the origin with a scale in miles at the axes.

### **Running the software**

The software was written to operate on the 31 days of August 1999. A simple interface was written to allow the user to time-step forwards or backwards by either one hour, or ten minute intervals. Days of the month can be jumped to or approached sequentially. Either temperature, or heat island intensity can be displayed across London and the contours can be colour shaded or left open.

An example of the output of the software is given in Chapter 4, e.g. Figure 4.21.

(Note: At the time of the development of the software, the weather data available were taken from the Building Research Establishment, and this is the reason that solar radiation on a vertical south-facing surface, rather than global horizontal, is shown on all the visualization figures. This is adequate for this qualitative work tool.)

## **APPENDIX 3**

### **Site categorizations of urbanization for all sites**



## APPENDIX 3 – Site categorizations of urbanization for all sites

The 79 monitoring stations are listed here showing their position in the monitoring array (shown as the radial distance from the focus in London) and the categorization of the site (1 to 8). A key to the categories is given.

Radial distance, miles	N	NE	E	SE	S	SW	W	NW
1	3	5	4	4	6	8	6	6
2	4	4	7	5	4	6	2	2
3	6	6	6	4	4	5	3	4
4	6	5	2	5	4	5	2	5
6	3	5	4	2	5	5	3	2
8	4	1	4	4	5	1	5	4
10	1	4	3		4	4	5	2
12	1	2	3	2	4	1	5	1
14		1	2	4	3	2	4	
16				1			1	
18			2				1 & 1	
20						1		

Focus N	5
Focus E	6
Focus S	6
Focus W	6

### Key:

Category No.	Height/Width ratio of street, x	Surface	Example site
1	$x=0$	Grass, etc.	Rural fields, or large park, or trees
2	$x=0$	Hard and grass	Housing near park or field
3	$x=0$	Hard	Urban derelict or unbuilt area or car park
4	$0 \leq x < 0.3$	Hard, very wide gorge	Low density residential area
5	$0.3 \leq x < 0.5$	Hard, wide gorge	Medium density urban area
6	$0.5 \leq x < 1$	Hard, wide gorge	High density urban area; around focus
7	$1 \leq x < 2$	Hard, medium gorge	Liverpool Street station site
8	$x \geq 2$	Hard, narrow gorge	Grafton Street

## **APPENDIX 4**

### **Site categorization from aerial photographs**

## **APPENDIX 4 – Site categorization from aerial photographs**

To provide an additional and important descriptor of a measurement site, the percentage greenness was determined by reference to aerial images. Vegetation is known to have a cooling effect and the extent to which this influences a neighbouring area varies. However, a literature review suggested that a few hundred metres was a typical limit of influence. It was decided that the area within 500 metres of a site would be assessed. It was also decided to divide the assessment circle up into sectors to enable analysis by wind direction. An inner circle to 125 m radius, and outer annulus were also defined. Each of 24 sites was assessed, as used in the modelling work, with the percentage greenness measured in 16 places (8 sectors; inner and outer).

### **Measurement**

For each site, nine aerial photographs were obtained from the internet (Cities Revealed – images from Geoinformation Systems) and joined together to cover a 1.5km square. Using Golden Software's Surfer programme, a sector reticule was drawn and this was embedded in the 1.5km image after centring on the measurement site. This was exported as a single JPEG image and then converted to a TIFF image.

Image analysis software, Scion Image, was used to measure the area of all green areas, after scaling. Scion Image can measure only 8-bit colour images, and it was necessary to convert the 24-bit images to 8-bit first. Because a good deal of colour information is lost in the process, the measurement work was done with a 24-bit image loaded in a separate programme and registered with the Scion image window, so that in cases of ambiguity, the clearer picture could be consulted. Area measurement data were transferred directly to Excel from Scion Image.

See image below for an example of measurement for the NW01 site. Green areas, dashed, are shown ready for measurement in the NW to N sector.



Measurement of green areas: example for the NW01 site (NW to N sector annulus)

## **APPENDIX 5**

### **Short-term tests**

# APPENDIX 5 – Short-term tests

## 5.1 PARK test pictures



Primrose Hill, park and measurement sites

Key to pictures

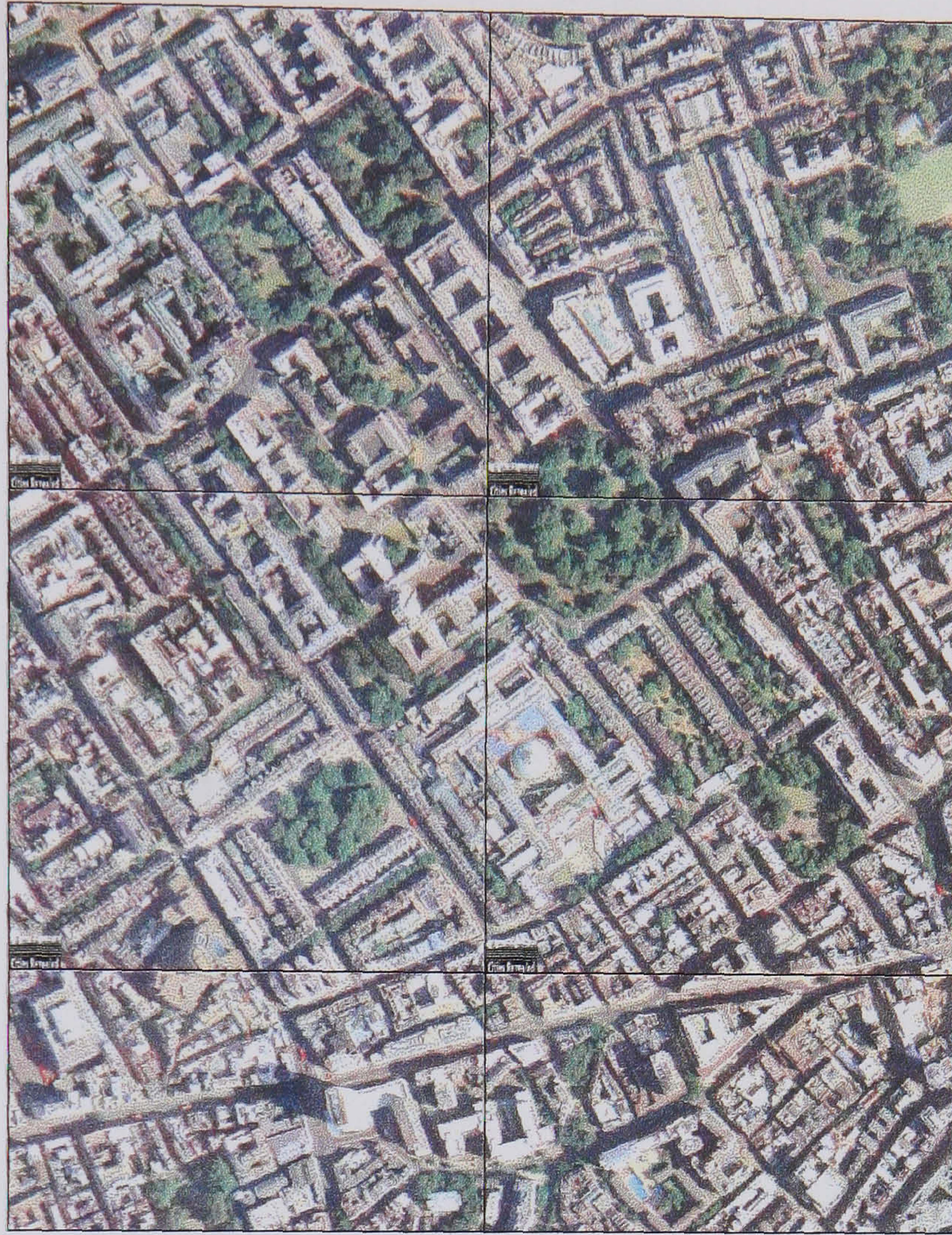


The ten measurement sites

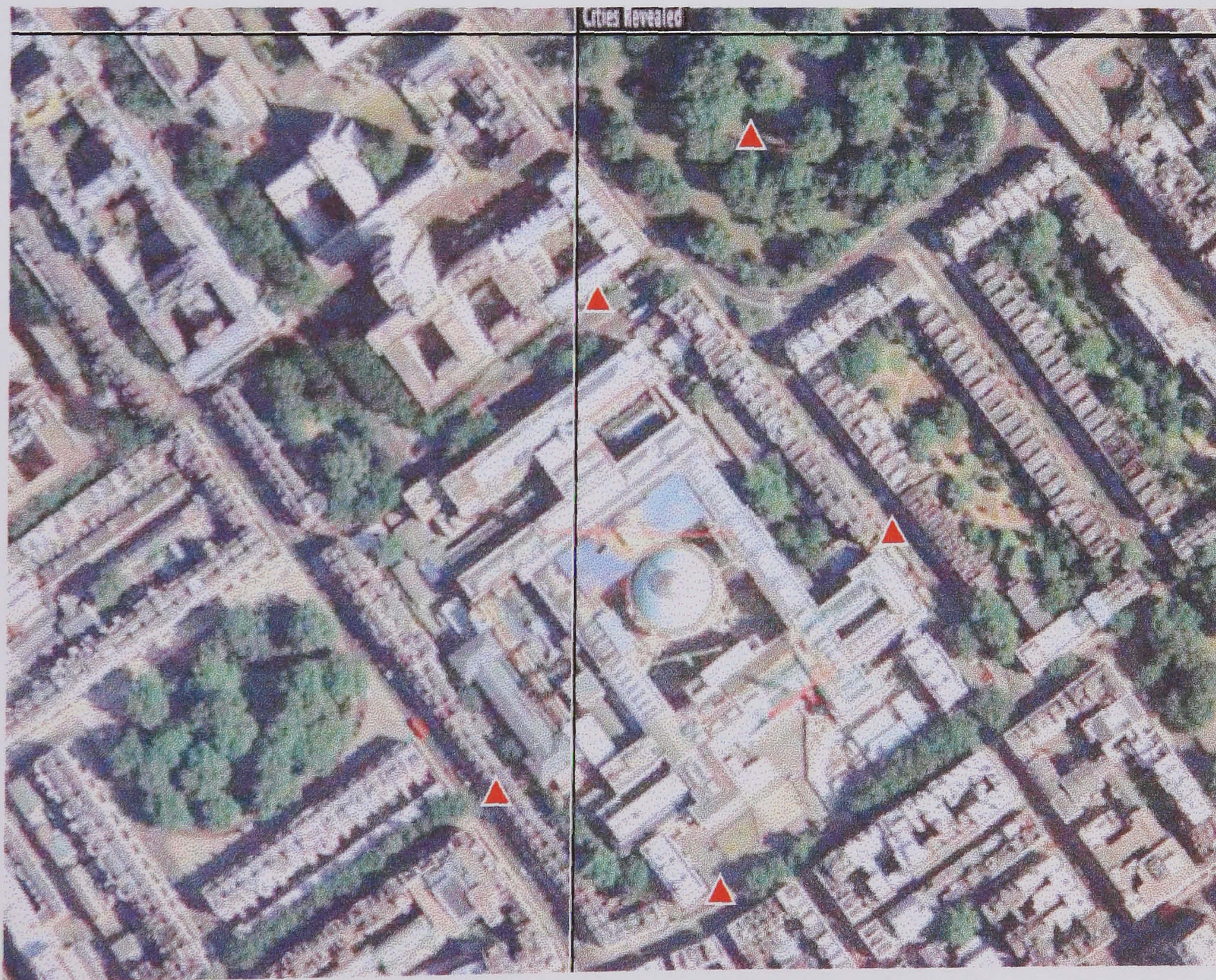
**Key to pictures:**

Site 1	Site 2	Site 3
Site 4	Site 5	Site 7
Site 8	Site 9	Site 10
<b>Panorama from Site 6 looking SE (downhill)</b>		
<b>Looking uphill to Site 6</b>		

## 5.2 GORGE test pictures



The British Museum and context



The British Museum and the main measurement sites



## **APPENDIX 6**

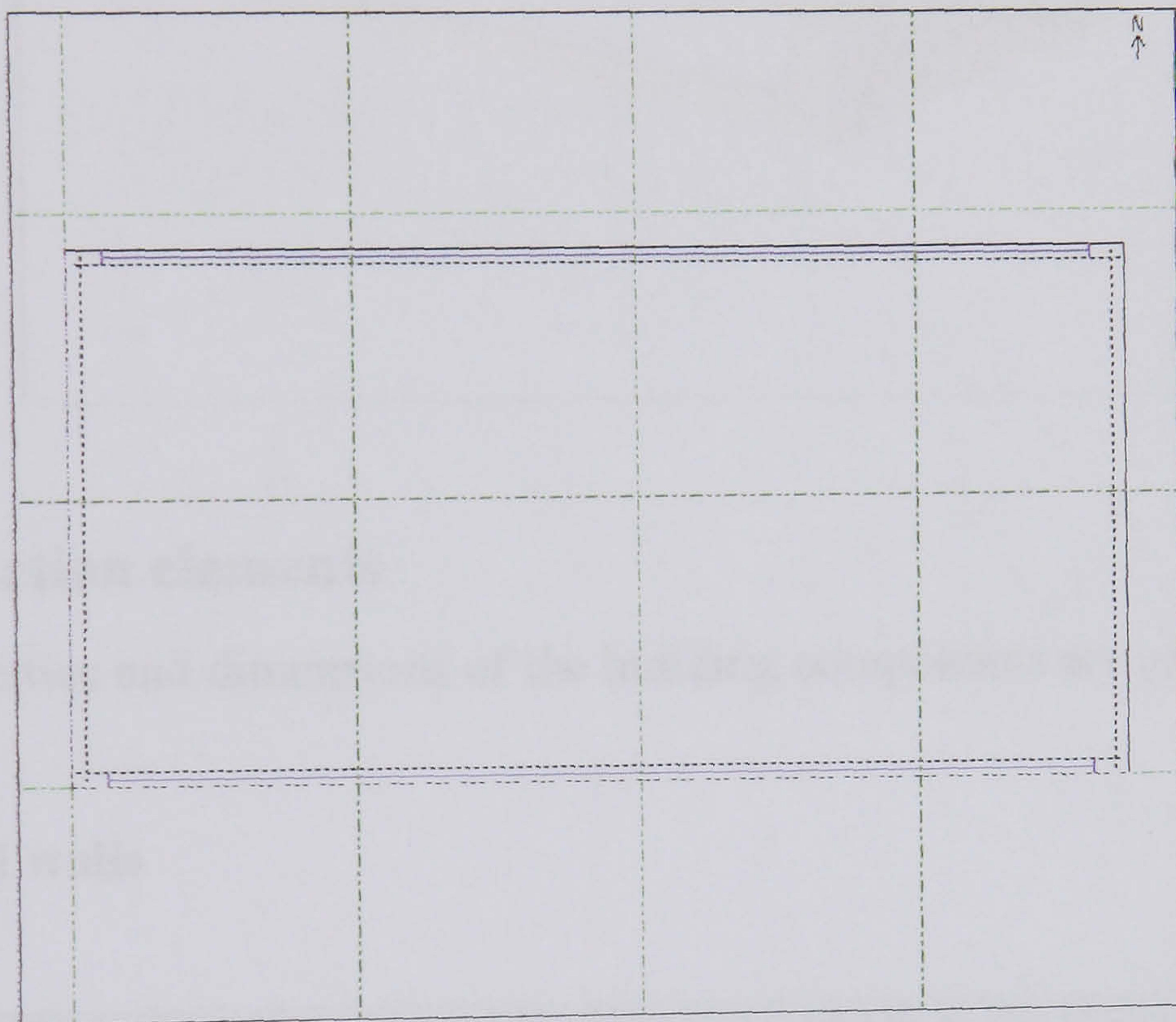
### **Building description for model**

## APPENDIX 6 – Building description for model

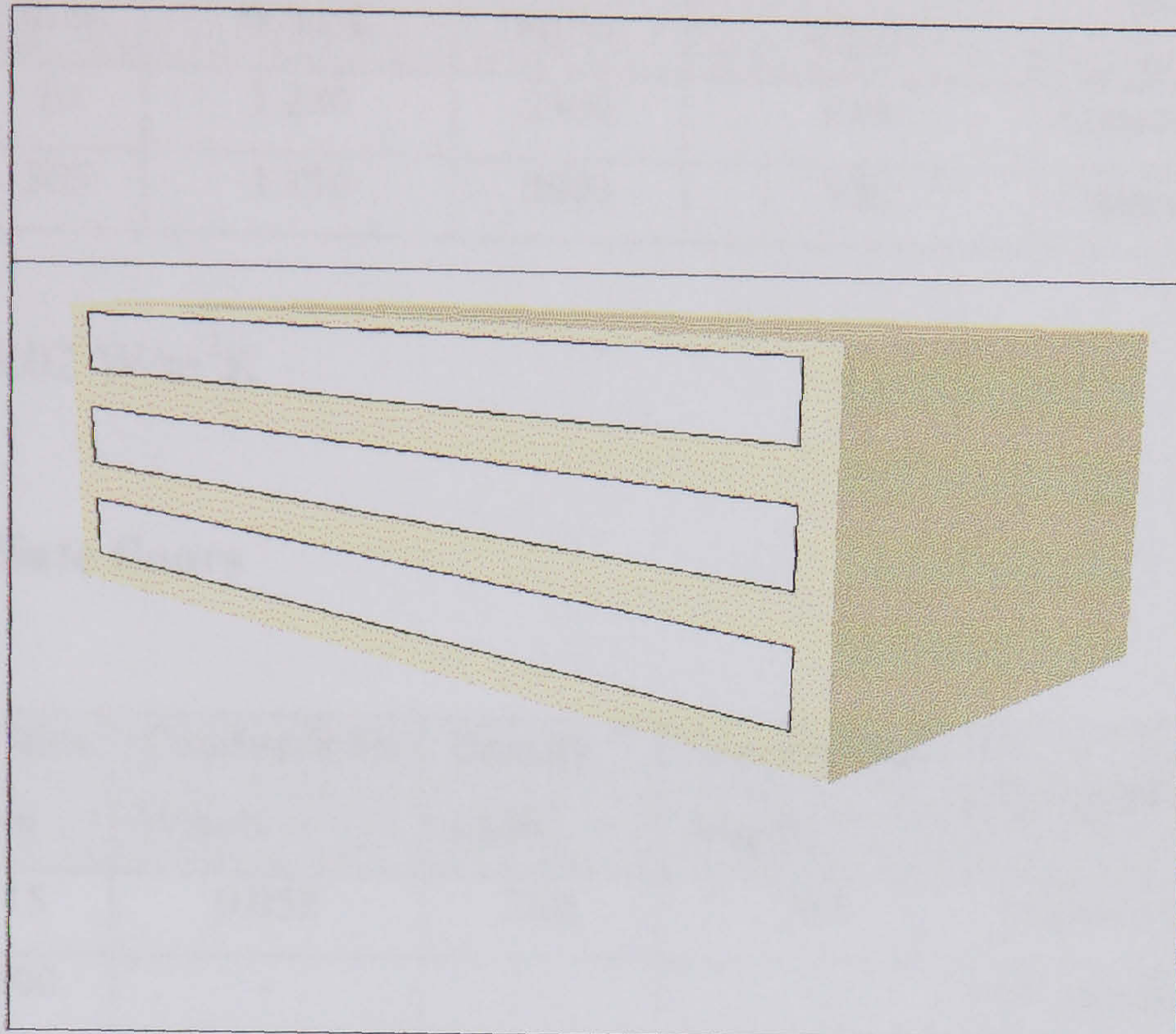
A detailed description follows of the ECON 19/3 building as modelled in this project.

### 6.1 Floor plan

A plan of the building is shown below on a grid of 8m squares. The building is 30m long by 15 wide by 9m high.



## 6.2 Perspective



## 6.3 Construction elements

Thermal properties and dimensions of the building components are given below.

### 6.3.1 External walls

Layer	Width mm	Conductivity W/mK	Density kg/m <sup>3</sup>	Specific heat J/kgK	Material
1	13	0.577	1860	837	Plaster
2	100	1.100	2300	1070	Concrete
3	50	0.033	25	1200	Expanded polystyrene
4	80	1.100	2300	1070	Concrete
5	19	1.730	1890	780	Cement rendering

Conductance: 1.27 W/m<sup>2</sup>K

External solar absorptance: 40%

External emissivity: 90%

### 6.3.2 Ground floor

Layer	Width mm	Conductivity W/mK	Density kg/m <sup>3</sup>	Specific heat J/kgK	Material
1	10	1.280	2100	1000	Concrete screed
2	365	1.130	2000	920	Concrete

Conductance: 3.02 W/m<sup>2</sup>K

### 6.3.3 Intermediate floors

Layer	Width mm	Conductivity W/mK	Density kg/m <sup>3</sup>	Specific heat J/kgK	Material
1	15	0.058	288	586	Acoustic tile
2	100	-	-	-	Air gap (upward flow)
3	150	1.100	2300	1070	Concrete
4	50	1.280	2100	1000	Concrete screed
5	10	0.060	186	1360	Carpet

Conductance: 1.27 W/m<sup>2</sup>K

### 6.3.4 Roof

Layer	Width mm	Conductivity W/mK	Density kg/m <sup>3</sup>	Specific heat J/kgK	Material
1	13	0.500	1300	837	Plaster
2	150	1.100	2300	1070	Concrete
3	75	1.280	2100	1000	Concrete screed
4	1.5	0.160	1055	1000	Bitumen
5	50	0.030	140	1380	Expanded polystyrene
6	50	1.400	2100	840	Concrete

Conductance: 0.52 W/m<sup>2</sup>K

External solar absorptance: 65%

External emissivity: 90%

### 6.3.5 Glazing

Layer	Width mm	Solar transmission	Solar reflection ext	Solar reflection int	Emissivity ext	Emissivity int	Convection coefficient, W/m <sup>2</sup> K	Conductivity W/mK	Material
1	6	0.78	0.70	0.70	0.85	0.85	-	1.00	6mm clear float glass
2	12	-	-	-	-	-	2.08	-	12mm air gap (horiz. flow)
3	6	0.78	0.70	0.70	0.85	0.85	-	1.00	6mm clear float glass

Conductance: 5.46 W/m<sup>2</sup>K

Solar transmittance: 61%

Light transmittance: 76%

### 6.4 Internal gains

Internal gains are entered into the model in terms of a rate of heat input per square metre of floor area. The modelling assumptions are shown below.

#### *Occupants*

Occupants occupy 10m<sup>2</sup> of floor space, and generate 130 W each. Heat gain is set to 13 W/m<sup>2</sup>.

#### *Lighting*

Fluorescent triphosphor lighting is used to provide 500 lux. Heat gain is set to 15 W/m<sup>2</sup>.

#### *Equipment*

Photocopiers, computers, etc. release heat. Heat gain is set to 15 W/m<sup>2</sup>.

## **6.5 Scheduling**

The building is assumed to be unoccupied at weekends. On weekdays, the above gains are applied from 08:00 to 18:00. Outside this time gains are set to zero. Infiltration is set to 0.5 ac/h at all times, with an additional 0.6 ac/h of ventilation air during occupied times. The plant are enabled at 06:00 and switched off at 18:00 on weekdays only. Both cooling and heating capacity of the plant are set to 100 kW maximum output. During occupied periods the internal temperature is maintained between 20 and 24°C.

